UFRGS
UNIVERSIDADE FEDERAL
DO RIO GRANDE DO SUL

PPGBAN
PROGRAMA DE PÓS-GRADUAÇÃO EM BIOLOGIA ANIMAL

INSTITUTO DE BIOCIÊNCIAS

PROGRAMA DE PÓS-GRADUAÇÃO EM BIOLOGIA ANIMAL

DARIO RUBEN FAUSTINO FUSTER

ANÁLISE FILOGENÉTICA DE HEPTAPTERIDAE GILL, 1861 E TAXONOMIA INTEGRATIVA DE *Heptapterus* BLEEKER, 1858 (HEPTAPTERINAE: HEPTAPTERINI)

PORTO ALEGRE

2022

DARIO RUBEN FAUSTINO FUSTER

ANÁLISE FILOGENÉTICA DE HEPTAPTERIDAE GILL, 1861 E TAXONOMIA INTEGRATIVA DE *Heptapterus* BLEEKER, 1858 (HEPTAPTERINAE: HEPTAPTERINI)

Tese apresentada ao Programa de Pós-Graduação em Biologia Animal, Instituto de Biociências da Universidade Federal do Rio Grande do Sul, como requisito parcial à obtenção do título de Doutor em Biologia Animal.

Área de concentração: Biologia Comparada

Orientador: Prof. Dr. Luiz R. Malabarba

PORTO ALEGRE

2022

DARIO RUBEN FAUSTINO FUSTER

ANÁLISE FILOGENÉTICA DE HEPTAPTERIDAE GILL, 1861 E TAXONOMIA INTEGRATIVA DE *Heptapterus* BLEEKER, 1858 (HEPTAPTERINAE: HEPTAPTERINI)

Aprovada em 25 de abril de 2022.

BANCA EXAMINADORA

_____

Dr. Hernan Lopez-Fernandez

_____

Dr. Paulo Buckup

_____

Dr. Tiago Cravalho

AGRADECIMENTOS

Agradeço muito a meu orientador, Dr. Luiz R. Malabarba, pela oportunidade e apoio de realizar o doutorado; assim como também pelas sugestões, recomendações, correções, opiniões e comentários na realização tese. Pela grande amizade e incentivo para participar, realizar e continuar trabalhando nas grandes descobertas dentro do grupo.

Ao Dr. Nathan Lujan, pelo apoio e a confiança para iniciar uma larga caminhada que passei visitando as principais coleções de peixes da América do Norte. Além dos comentários, correções e sugestões das propostas de pesquisa para conseguir o apoio econômico para visitar as principais coleções e instituições internacionais e assim complementar o desenvolvimento da tese.

A Vanessa Meza parceira, amiga e cúmplice pelo seu carinho e por sempre estar presente apoiando-me e incentivando-me incondicionalmente para ariscar em novas metas e logros durante o todo o tempo.

Aos professores e colegas do Programa de Pós-graduação em Biologia Animal por tornarem as disciplinas e minha pesquisa amenas e à Coordenação de Aperfeiçoamento de Pessoal de Nível Superior (CAPES) pela bolsa de doutorado, que apesar do corte da verba e pandemia lograram apoiar até o final desta etapa.

Aos curadores e técnicos das coleções ictiológicas nacionais e internacionais pela disponibilidade do material examinado que está sob seus cuidados quando visitei ou quando enviaram para o estudo. Ao Jonathan W. Armbruster e David C. Werneke (AUM); Mark Sabaj e Mariangeles Arce (ANSP); Dave Catania (CAS); Gastón Aguilera, Juan Marcos Mirante e Guillermo Teran (CI-FML); Susan Mochel, Caleb McMahan e Kevin Swagel (FMNH); Carlos DoNacimento (IAvH); Ivan Mojica e Henry Agudelo Zamora (ICN-MHN); Claudio Oliveira (LBP); Carlos Lucena, Margarete Lucena e Roberto Reis (MCP); Hernán Ortega, Max Hidalgo

e Carla Muñoz (MUSM); Mario de Pinna, Aléssio Datovo e Oswaldo Oyakawa (MZUSP); Paulo Buckup e Marcelo Brito (MNRJ); Mary Burridge, Erling Holm e Marg Zur (ROM); Luiz Malabarba e Juliana Wingert (UFRGS); Hernán Lopez-Fernandez e Douglas Nelson (UMMZ); Lynne Parenti, Jeff Clayton e Sandra Raredon (USNM); Nathan Lovejoy (UofT); Marcelo Loureiro (ZVC).

Aos meus colegas do Laboratório de Ictiologia, pela acolhida, convivência e troca de experiência durante estes seis anos desde o mestrado que fizeram meus dias fáceis com suas recomendações, sugestões e apoio na UFRGS e Porto Alegre. Ao Junior meu amigo e Vanessa parceiros da vida Ictiológica, obrigado pela ajuda, sugestões, críticas, intercâmbio de informações e largas conversas sobre peixes neotropicais e do Peru. A Juliana e Juliano pela assistência na coleção, as caronas para ir a casa e o auxílio e orientação durante minha estadia em Porto Alegre. Aos amigos do laboratório de peixes do MCP, pela acolhida e convivência durante minha estadia no Rio Grande do Sul, visita. Aos colegas e amigos do departamento de Ictiologia do Museo de História Nacional de San Marcos-Lima, que durante minha visita curta continuamos com novos projetos e pesquisas para conhecer a diversidade de peixes de água doce do Peru. Aos professores Hernán Ortega e Max Hidalgo pelos conselhos e apoio incondicional para obter material do Peru e acesso ao material da coleção do MUSM.

Agradecer também áquelas pessoas e instituições que tornaram este trabalho possível para visitar coleções ictiológicas e trabalhar nos laboratórios do exterior, durante os estágios: Ao Hernán Lopez-Fernandez e Karen Alofs por me receberem em sua casa durante minha visita para revisar material do Museum of Zoology University of Michigan, em Ann Arbor durante o verão de 2018. A Mariangeles Arce e Mark Sabaj pela ajuda e recebimento durante minha vista a The Academy of Natural Sciences of Drexel University na Filadélfia durante o inverno de 2018. Ao Erling Holm, Mary Burridge, Nathan Lujan e Bernardette Chung, que tornaram minha visita ao Royal Ontario Museum in Toronto agradável e acolhedor durante o inverno de

2019. Ao Jonathan Armbruster, David Werneke, Cori Black, Malorie Hayes e Kerry Cobb, pelo apoio e hospedagem durante minha visita ao Auburn University Museum of Natural History in Alabama durante o 'inverno' de 2019. Agradeço muito a Lynne Parenty por aceitar ser minha orientadora para ganhar o Fellowship Smithsonian Visiting Student durante minha vista ao National Museum of Natural History no Whasintong e tudo o pessoal do NMNH, especialmente ao Jeff Clayton por tudo a ajuda administrativa e curatorial durante minha estadia no NMNH. A Susan Mochel, Caleb McMahan e Kevin Swagel (FMNH)

À minha família, pela compreensão durante minha ausência e que mesmo sem entender o que eu faço me deu o apoio incondicional durante todos estes anos.

Agradeço também as seguintes instituições pelo apoio financeiro para as coletas e as análises moleculares para completar minha pesquisa: Böhlke Award from the Academy of Natural Science of Drexel University, em Filadélfia. Smithsonian Visiting Student (Fellowship) at the National Museum of Natural History (NMNH), Washington. Grainger Bioinformatics Center at the Field Museum of Natural History em Chicago. Royal Ontario Museum E.J. Crossman Endowment Fund em Toronto. National Science Foundation via NSF DEB-0315963 (All Catfish Species Inventory), Estados Unidos. Coypu Foundation em New Orleans. Aquatic Critter Inc., em Nashville. Systematics Research Fund, Londres. Society of Systematic Biologists. Catfish Study Group, Inglaterra.

SUMARIO

RESUMO

A família Heptapteridae contém 23 gêneros e 231 espécies válidas que são encontradas em uma ampla gama de habitats de água doce do sul do México ao norte da Argentina. A sistemática filogenética atual de Heptapteridae é significativamente moldada por uma análise baseada em morfologia da maioria dos gêneros existentes, realizada há mais de 20 anos e não publicada. Nós fornecemos uma nova hipótese filogenética molecular abrangendo 19 dos 23 gêneros válidos em Heptapteridae, incluindo todos os gêneros válidos de Brachyglaniini (4 de 4), 11 dos 14 gêneros válidos de Heptapterini e 66% de todas as espécies válidas de Heptapterini (58 de 88; além de muitas espécies não descritas). A amostragem inclui 15 espécies tipo dos 23 gêneros válidos de Heptapteridae. O presente trabalho, baseado em uma análise multilocus de cinco marcadores moleculares, 3 marcadores mitocondriais (COI, cytochrome oxidase subunit I; Cyt b: cytochrome b e ND2: NADH dehydrogenase subunit 2), e dois marcadores nuclear (RAG2: recombination activating 2, e Glyt: glycosyltransferase), produziu filogenias geralmente consistentes, bem resolvidas e fortemente suportadas. Com base nesses resultados, fornecemos uma nova classificação supragenérica dentro de Heptapteridae subdividida em: Heptapterinae (contendo Brachyglaniini e Heptapterini) e Rhamdiinae (contendo Rhamdiini e Goeldiellini); dentro de Heptapterini foram reconhecidas cinco subtribos novas. O trabalho inclui uma análise integrativa do gênero *Heptapterus* espécie tipo da família onde o gênero foi redefinido e limitado a 4 quatro espécies validas, com a descrição de um gênero novo irmão de *Heptapterus* contendo duas espécies novas. Finalmente apresentamos descrições de novas espécies de Heptapteridae.

ABSTRACT

The Heptapteridae family contains 23 genera and 231 valid species that are specific in a wide range of freshwater habitats from southern Mexico to northern Argentina. A current phylogenetic systematics of Heptapteridae is significantly shaped by an unpublished morphology-based analysis of most extant genera carried out over 20 years ago. We provide a new multilocus molecular phylogenetic hypothesis encompassing 19 of 23 valid genera in Heptapteridae, including all valid genera of Brachyglaniini (4 of 4), 11 of 14 valid genera of Heptapterini and 66% of all valid species of Heptapterini (58 of 88, plus many new species). The analysis includes 15 type species from the 23 valid genera of Heptapteridae. The present work is based on a multilocus analysis of five molecular markers, being three mitochondrial markers (COI, cytochrome oxidase subunit I; Cyt b: cytochrome be ND2: NADH dehydrogenase subunit 2) and two nuclear markers (RAG2: recombination activating 2, and Glyt: glycosyltransferase), and have recovered generally well-resolved and consistently supported phylogenies. Based on these results, we provide a new suprageneric classification within Heptapteridae, subdivided into: Heptapterinae (comprising Brachyglaniini and Heptapterini) and Rhamdiinae (containing Rhamdiini and Goeldiellini); five new subtribes were recovered within Heptapterini. This work includes an integrative analysis of the genus *Heptapterus*, type genus of the family, that is redefined and limited to four valid species. It includes the description of a new genus sister of *Heptapterus* and containing two new species. Finally, we present the description of new species within Heptapteridae.

ESTRUTURA DA TESE

Este trabalho está estruturado em formato de artigos, composta por três capítulos:

CAPÍTULO I

Capítulo publicado na revista Molecular Phylogenetics and Evolution. Neste artigo é apresentada a primeira hipótese filogenética molecular de 16 dos 23 gêneros da família Heptapteridae, baseado numa análise multilocus (três genes mitocondriais e dois nucleares). O estudo apresenta uma densa amostragem dos gêneros e espécies da tribo Brachyglaniini, distribuídas ao redor do escudo das Guianas, propondo uma nova classificação supragenérica para a família Heptapteridae com base em dados moleculares e estudos prévios disponíveis de morfologia.

CAPÍTULO II

Capítulo a ser submetido na revista Journal of Zoological Systematics and Evolutionary Research, neste capítulo são apresentadas as relações filogenéticas, mas abrangentes da família Heptapteridae baseadas em uma análise multilocus (três genes mitocondriais e dois nucleares). Os conjuntos de dados foram gerados para os 19 dos 24 gêneros validos de Heptapteridae, com uma densa amostragem das espécies da tribo Heptapterini, contendo 9 espécies-tipo dos 14 gêneros da tribo. Nós propusemos novos clados e discutimos as relações filogenéticas ao nível genérico dentro de Heptapterini.

CAPÍTULO III

Capítulo a ser submetido na revista Neotropical Ichthyology. Neste artigo apresenta-se a revisão taxonômica de *Heptapterus*, baseada numa análise integrativa. Nós exploramos caracteres da morfologia externa e interna para ajudar a delimitar as espécies, assim como fornecemos informações sobre sua distribuição, realocamos as espécies que não pertenceriam ao gênero *Heptapterus* nos gêneros correspondentes e apresentamos uma chave ao nível de espécie. Além disso, se descreve um novo gênero, com as descrições de duas espécies novas baseadas em dados morfológicos e moleculares.

CAPÍTULO IV

Artigos publicados nas revistas Zootaxa e Journal of Fish Biology. Este capítulo mostra a diversidade que se encontrava escondida para a ciência de espécies dos gêneros *Mastiglanis* e *Cetopsorhamdia*, produto de grandes esforços realizados nos inventários biológicos ao longo da Amazonia Peruana, cujo objetivo foi a criação de áreas naturais protegidas.

CAPÍTULO I. MULTI-LOCUS PHYLOGENY WITH DENSE GUIANA SHIELD SAMPLING SUPPORTS NEW SUPRAGENERIC CLASSIFICATION OF THE NEOTROPICAL THREE-BARBELED CATFISHES (SILURIFORMES: HEPTAPTERIDAE)

Faustino-Fuster et al., 2021. Multi-locus phylogeny with dense Guiana Shield sampling supports new suprageneric classification of the Neotropical three-barbeled catfishes (Siluriformes: Heptapteridae). Molecular Phylogenetics and Evolution, 162, 107186.

https://doi.org/10.1016/j.ympev.2021.107186

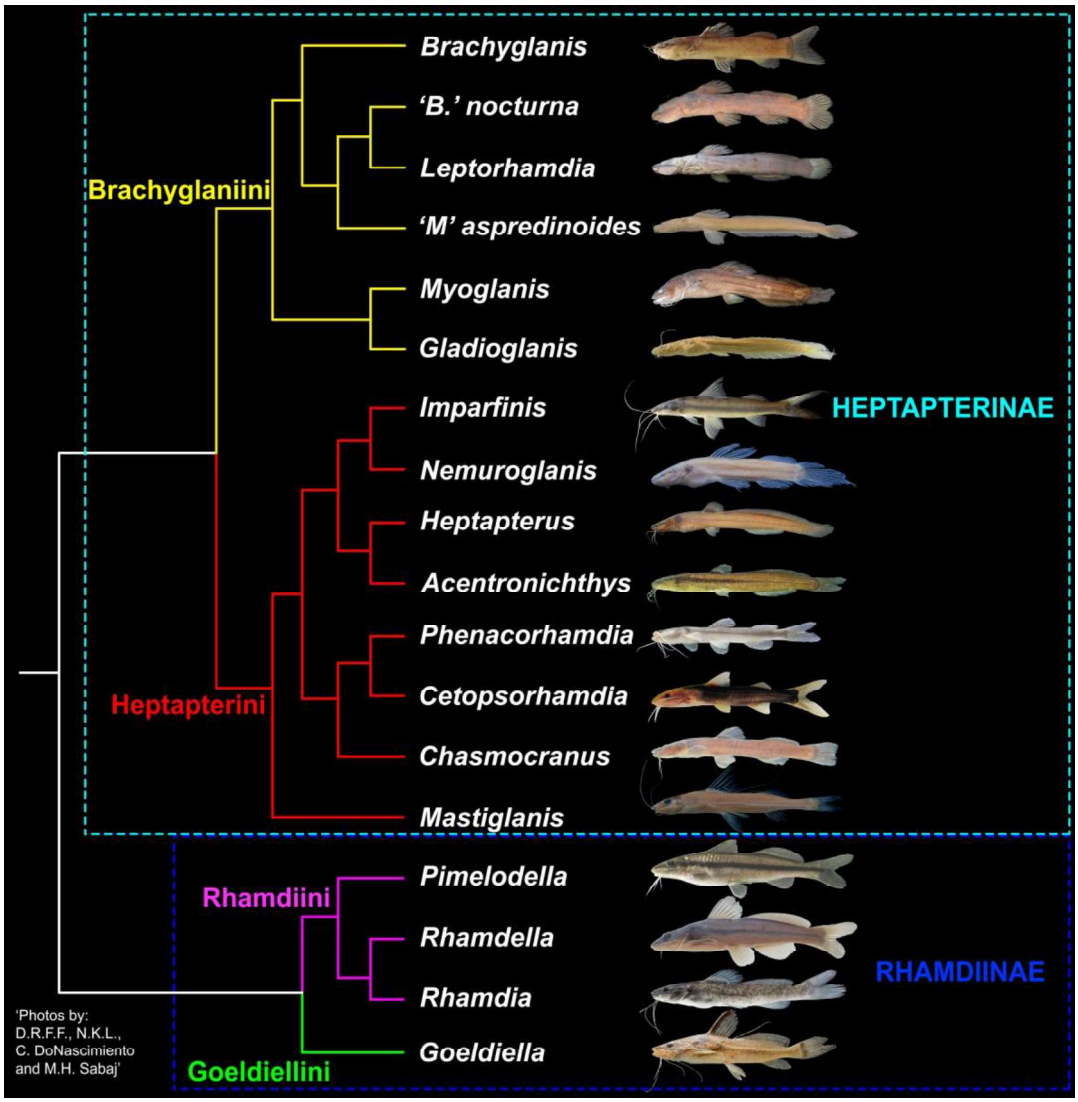

Molecular Phylogenetics and Evolution 162 (2021) 107186

Contents lists available at ScienceDirect

Molecular Phylogenetics and Evolution

journal homepage: www.elsevier.com/locate/ympev

Multi-locus phylogeny with dense Guiana Shield sampling supports new suprageneric classification of the neotropical three-barbeled catfishes (Siluriformes: Heptapteridae)

Dario R. Faustino-Fuster [a,b,*], Vanessa Meza-Vargas [a,c], Nathan R. Lovejoy [d], Nathan K. Lujan [e]

[a] Departamento de Ictiología, Museo de Historia Natural, Universidad Nacional Mayor de San Marcos, Avenida Arenales 1256, Lima 14, Peru
[b] Departamento de Zoologia, Universidade Federal do Rio Grande do Sul, Programa de Pós-Graduação em Biologia Animal, Av. Bento Gonçalves, 9500, Bloco IV, Prédio 43433, Campus do Vale, 91509-900 Porto Alegre, RS, Brazil
[c] Laboratório de Sistemática de Vertebrados, Pontifícia Universidade Católica do Rio Grande do Sul., Av. Ipiranga, 6681, 90619-900 Porto Alegre, RS, Brazil
[d] Department of Biological Sciences, University of Toronto Scarborough, Toronto M1C 1A4, Canada
[e] Department of Ichthyology, American Museum of Natural History, New York, NY 10024, USA

ARTICLE INFO

Keywords:
Biogeography
Brachyglanis
Brazilian shield
Classification
Molecular systematics
trans-Andean

ABSTRACT

The catfish family Heptapteridae is ubiquitous across a range of freshwater habitats from southern Mexico to northern Argentina and contains 23 genera and 228 valid species. After a century of mostly morphology-based systematic analyses of these fishes, we provide the first molecular phylogenetic hypothesis spanning most valid Heptapteridae genera (16 of 23). We examined eight of 14 valid genera in the *Nemuroglanis*-subclade (Heptapterini), all valid genera in the *Brachyglanis*-subclade (Brachyglaniini) and most valid Brachyglaniini species (11 of 15). Maximum likelihood and Bayesian analyses of a 4156-base alignment of five gene regions (three mitochondrial: COI, Cyt *b*, and ND2; two nuclear: RAG2, Glyt) yielded thoroughly resolved and statistically robust phylogenies that were largely congruent with each other and with previous morphology-based hypotheses. We propose a revised phylogenetic classification consisting of two subfamilies (Rhamdiinae, Heptapterinae) each with two tribes. Dense taxonomic sampling of Brachyglaniini, including type species of *Brachyglanis*, *Gladioglanis*, *Leptorhamdia*, and *Myoglanis*, revealed widespread paraphyly. Newly recovered clades within Brachyglaniini are closely associated with either the upper Orinoco or the Essequibo suggesting repeated dispersals and/or range expansions/contractions across the western Guiana Shield highlands and from there to the upper Amazon and Brazilian Shield. These biogeographical processes appear to have been an important driver of allopatric diversification in the clade.

1. Introduction

The three-barbeled catfish family Heptapteridae contains 23 genera and 228 valid species (Fricke et al., 2020), most of which are small-sized (< 20 mm SL) with a generalized catfish body shape and appearance. The family occupies a wide range of freshwater habitats from southern Mexico to northern Argentina, but is especially characteristic of small streams and headwaters. In such habitats the widespread, large-bodied genus *Rhamdia* (≤70 cm TL; Machacek, 2019) is often among the largest fishes present and is harvested as a food fish throughout its range (DRFF, NKL pers. obs.). *Rhamdia* is also commercially cultivated in both temperate and tropical areas of Argentina, Brazil, and Uruguay, where it is marketed under the common names 'black catfish,' 'silver catfish,' and 'jundiá' (Grigio and Meurer, 2020; DRFF pers. obs.). Some smaller genera sporadically enter the ornamental aquarium fish trade, but most Heptapteridae have no specific social or economic value. Given the historical absence of a well-resolved species-level phylogeny, the three-barbeled catfish radiation has made no major contributions to macro-evolutionary theory, yet the considerable taxonomic diversity of the family and its broad geographic range make the clade a potentially valuable model for testing biogeographical hypotheses. Fin shapes, sizes, and modifications such as soft *vs.* pungent fin rays, serration number and shape, and filament length are also highly variable across Heptapteridae, suggesting the family could be an important model for

* Corresponding author at: Departamento de Ictiología, Museo de Historia Natural, Universidad Nacional Mayor de San Marcos, Avenida Arenales 1256, Lima 14, Peru.
E-mail address: dariorff36@gmail.com (D.R. Faustino-Fuster).

https://doi.org/10.1016/j.ympev.2021.107186
Received 2 August 2020; Received in revised form 7 April 2021; Accepted 26 April 2021
Available online 29 April 2021

understanding fin evolution.

Heptapteridae was first erected by Gill (1861) as a subfamily within the strictly Neotropical long-barbeled catfish family Pimelodidae containing only the species *Heptapterus mustelinus* (Valenciennes 1835). Although no unique characters define Heptapteridae, Bockmann and Guazzelli (2003) proposed a combination of 10 homoplastic external characteristics that distinguish Heptapteridae from other fishes (Supplementary Table 1). Internally, three osteological synapomorphies were proposed by Lundberg and McDade (1986) to support the monophyly of 13 genera now placed in Heptapteridae (Table 1). Rhamdiinae Bleeker 1862 was the original name given by Lundberg et al. (1991) to the clade defined by these characters, and this name was elevated to Rhamdiidae in the unpublished thesis of de Pinna (1993) and the cytogenetic analysis of Swarça et al. (2000). However, Heptapterinae Gill 1861 had priority over Rhamdiinae Bleeker 1862, thus cementing the former for the family-level clade (de Pinna, 1993; Silfvergrip, 1996). Historically, the phylogenetic position of Heptapteridae within Siluriformes has greatly varied across studies (Mo, 1991; Arratia, 1992; Pinna, 1993; Bockmann and Guazzelli, 2003). However, the only phylogenetic hypothesis consistently supported by both morphological and molecular data places Heptapteridae as sister to Pimelodidae + Pseudopimelodidae (Lundberg and McDade, 1986; Lundberg et al., 1991; Sullivan et al., 2006, 2013; Arcila et al., 2017; Betancur et al., 2017).

Heptapteridae intergeneric relationships and generic diagnoses have been iteratively revised by studies ranging from descriptions and identification keys to phylogenetic syntheses based almost exclusively on morphological data. Eigenmann (1912) developed an identification key to ten genera while also erecting four. Gosline (1941) reworked Eigenmann's key with a focus on taxa lacking a free orbital rim, which mostly comprised 12 genera now in Heptapteridae. Lundberg and McDade (1986) not only proposed three synapomorphies for Heptapteridae (Supplemental Table 1), but also diagnosed a *Brachyrhamdia* subgroup containing six genera and an unnamed subgroup containing two (Table 1). Ferraris (1988), in his description of *Nemuroglanis paucimaculatus*, diagnosed a newly labeled *Nemuroglanis*-subclade containing nine genera united by four synapomorphies (Supplemental Table 1; Table 1). Lundberg et al. (1991) again focused on the free orbital rim and diagnosed an unnamed clade 1 for 15 genera with a reduced or absent orbital rim, and unnamed clade 2 for the genus *Brachyrhamdia*, which retains the orbital rim (Table 1, Supplemental Table 1). The unnamed clade 1 comprised an expanded *Nemuroglanis*-subclade containing 11 genera plus an unnamed group of four genera outside the *Nemuroglanis*-subclade (Table 1, Supplemental Table 1). These authors also suggested that the three genera we focus on in this study – *Brachyglanis* Eigenmann 1912, *Leptorhamdia* Eigenmann 1918, and *Myoglanis* Eigenmann 1912 – form a distinct clade supported by the shared dorsal expansion of a superficial layer of the adductor mandibulae muscles over the hyomandibular articulation nearly to the midline of the skull roof. In a broad morphological analysis, Bockmann (1994) expanded Heptapteridae to include 21 genera, rediagnosed the *Nemuroglanis*-subclade with 12 additional osteological synapomorphies (Supplemental Table 1), and defined two unnamed clades within the *Nemuroglanis*-subclade based on aspects of the complex centrum.

The first taxonomically comprehensive cladistic analysis of Heptapteridae was by Bockmann (1998), who analyzed 278 morphological characters from 72 ingroup species (Bockmann 1998: fig. 216). This analysis yielded a monophyletic Heptapteridae, inclusive of *Phreatobius* Goeldi 1905, based largely on characters highlighted in previous studies. Bockmann (1998) generated a partially resolved hypothesis of phylogenetic relationships within Heptapteridae, which is the primary alternative hypothesis discussed herein (Fig. 1, Table 1).

Despite the generic richness of Heptapteridae and the attention previously given to resolving intergeneric relationships, less than half of heptapterid genera have undergone species-level taxonomic revisions. These include *Brachyrhamdia* Myers 1927 (Lundberg and McDade, 1986), *Heptapterus* Bleeker 1858 (Buckup, 1998; Faustino-Fuster et al., 2019), *Gladioglanis* Ferraris and Mago-Leccia 1989 (Lundberg et al., 1991), *Mastiglanis* Bockmann 1994 (Bockmann, 1994), *Nemuroglanis* Eigenmann and Eigenmann 1889 (Ferraris, 1988; Bockmann and

Table 1
Historically significant classification proposals for Heptapteridae genera. Genus names in bold not originally examined but were inserted by us based on characters proposed in previous studies.

Lundberg and McDade 1986	Ferraris 1988	Lundberg et al. 1991	Bockmann 1998	This study
Brachyrhamdia subgroup	*Nemuroglanis*-subclade	*Nemuroglanis*-subclade	Clade 129	Heptapterinae
Brachyrhamdia	*Acentronichthys*	*Acentronichthys*	Clade 119	Heptapterini
Cetopsorhamdia	*Cetopsorhamdia*	*Cetopsorhamdia*	*Acentronichthys*	*Acentronichthys*
Goeldiella	*Chasmocranus*	*Chasmocranus*	*Cetopsorhamdia*	*Cetopsorhamdia*
Pimelodella	*Heptapterus*	*Heptapterus*	*Chasmocranus*	*Chasmocranus*
Rhamdella	*Imparfinis*	*Horiomyzon*	*Heptapterus*	*Heptapterus*
Rhamdia	*Nannorhamdia*	*Imparfinis*	*Horiomyzon*	***Horiomyzon***
Unnamed Group	*Nemuroglanis*	*Nemuroglanis*	*Imparfinis*	*Imparfinis*
Heptapterus	*Pariolius*	*Pariolius*	*Mastiglanis*	*Mastiglanis*
Nannorhamdia	*Rhamdiopsis*	*Phenacorhamdia*	*Nannoglanis*	***Nannoglanis***
		Phreatobius	*Nemuroglanis*	*Nemuroglanis*
		Rhamdiopsis	*Pariolius*	***Pariolius***
		Unnamed Group	*Phenacorhamdia*	*Phenacorhamdia*
		Brachyglanis	*Rhamdioglanis*	***Rhamdioglanis***
		Gladioglanis	*Rhamdiopsis*	***Rhamdiopsis***
		Leptorhamdia	*Phreatobius*	
		Myoglanis	*Tanaqyia*	***Tanaqyia***
		Unnamed Group	Clade 128	Brachyglaniini
		Brachyrhamdia	*Brachyglanis*	*Brachyglanis*
		Goeldiella	*Gladioglanis*	*Gladioglanis*
		Pimelodella	*Leptorhamdia*	*Leptorhamdia*
		Rhamdella	*Myoglanis*	*Myoglanis*
		Rhamdia	*Brachyrhamdia*	Rhamdiinae
			Goeldiella	Goeldiellini
			Pimelodella	*Goeldiella*
			Rhamdella	Rhamdiini
			Rhamdia	***Brachyrhamdia***
				Pimelodella
				Rhamdella
				Rhamdia

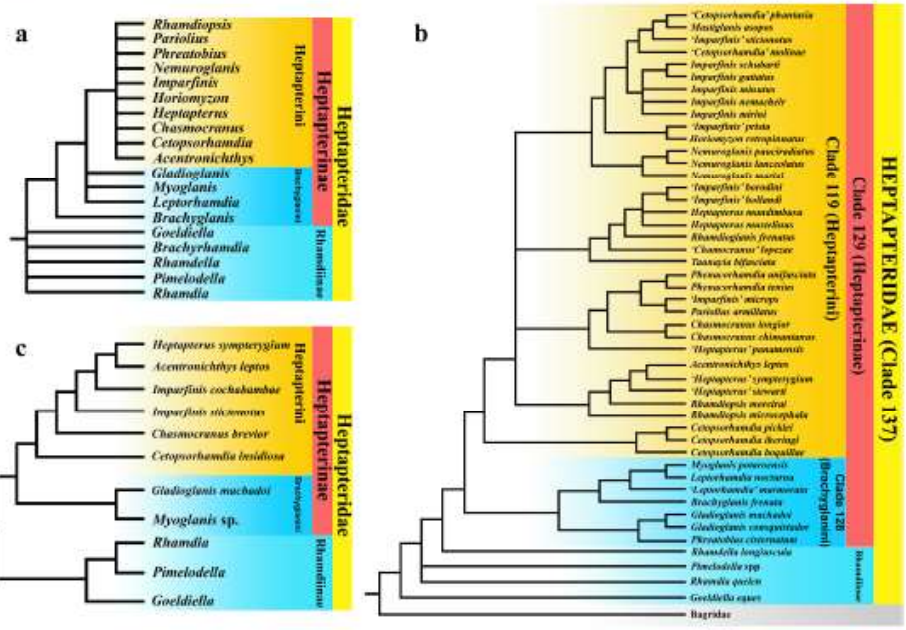

Fig. 1. Previous phylogenetic hypotheses for Heptapteridae modified from Lundberg et al. 1991: fig. 10 (a), Bockmann, 1998: fig. 216 (b) and Sullivan et al., 2013: fig. 6 (c). Quotation marks ('') indicate new genera according to Bockmann's (1998) hypothesis.

Ferraris, 2005), *Phenacorhamdia* Dahl 1961 -(DoNascimiento and Milani, 2008), *Tauroglanis* Miranda Ribeiro 1918 (Oliveira and Britski, 2000), *Rhamdella* Eigenmann and Eigenmann 1888 (Bockmann and Miquelarena, 2008), *Rhamdia* Bleeker 1858 (Silfvergrip, 1996), and *Rhamdiopsis* Haseman 1911 (Bockmann and Castro, 2010). All of these except (Faustino-Fuster et al., 2019) have been based exclusively on morphological data.

In this study we examine phylogenetic relationships throughout the Heptapteridae using a multi-locus molecular phylogenetic approach. We especially focus on the *Nemuroglanis*-subclade (Clade 119; Bockmann, 1998), its putative sister group the *Gladioglanis*-subclade (Clade 128; Bockmann, 1998), and within the latter the *Brachyglanis*-subclade first diagnosed by Lundberg et al. (1991). We also use the results of our phylogenetic analysis in conjunction with previously proposed morphological characters as the basis for a new suprageneric classification for Heptapteridae. Finally, we discuss the major biogeographical patterns apparent from our dense phylogenetic sampling of Heptapteridae genera associated with the western Guiana Shield.

2. Material and methods

2.1. Taxon sampling

We generated novel sequence data for 14 genera, 39 species, and 62 samples collected from Colombia, Brazil, Ecuador, Guyana, Peru, Suriname, Uruguay and Venezuela between the years 1992 and 2017. Novel data were combined with GenBank reposited data for four mostly outgroup genera and seven species so that sampled taxa encompassed 70% of all valid Heptapteridae genera (16 of 23), 57% of all valid Heptapterini (*Nemuroglanis*-subclade) genera (8 of 14), 100% of all valid genera in the *Brachyglanis* subclade (4 of 4), and 73% of all valid species in the *Brachyglanis* subclade (11 of 15; plus several undescribed species) (Table 1). Nine of the Heptapteridae genera examined in this study are represented by type species, although two of these species were collected far from the type locality, suggesting that a more thorough taxonomic analysis may reveal them to be undescribed species (denoted by 'cf.').

Specimens examined in this study are cataloged at the following eight ichthyological collections: American Museum of Natural History, New York (AMNH), Academy of Natural Sciences of Drexel University, Philadelphia (ANSP), Auburn University Museum of Natural History, Auburn (AUM), Universidade Federal do Rio Grande do Sul, Porto Alegre (UFRGS), Museu de Ciências e Tecnologia, Pontifícia Universidade Católica do Rio Grande do Sul, Porto Alegre (MCP), Museu de Zoologia da Universidade de São Paulo, São Paulo (MZUSP), Museu Nacional, Universidade Federal do Rio de Janeiro, Rio de Janeiro (MNRJ), Royal Ontario Museum, Toronto (ROM). Institutional abbreviations follow Sabaj (2019).

2.2. Molecular markers, DNA extraction, amplification, and sequencing

We sequenced fragments of three mitochondrial (COI: cytochrome oxidase subunit I, Cyt *b*: cytochrome *b*, and ND2: NADH dehydrogenase subunit 2), and two nuclear markers (RAG2: recombination activating genes 2, and Glyt: glycosyltransferase). Markers were selected based on their ease of unambiguous amplification in Heptapteridae and how they might enhance phylogenetic resolution at various depths of the tree, with most having been used in previous phylogenetic studies of catfishes (Sullivan et al. 2006, 2013; Smith et al., 2016; Supplementary Table 2).

Whole genomic DNA was extracted from fin or muscle tissues

following a standard salt extraction protocol (Lujan et al., 2020a). Fragments were amplified using a reaction mix with 25 µL total volume, comprising 18.8 µL dH_2O, 2.5 µL Erika Hagelberg (EH) buffer (Hagelberg, 1994; 10 mM), 0.1 µL Platinum Taq polymerase (LTI: Life Technologies Inc., Carlsbad, CA), 1 µL forward primer (10 mM), 1 µL reverse primer (10 mM), 0.6 µL deoxyribonucleotide triphosphate (dNTP, 10 mM), and 1 µL extracted genomic DNA (gDNA). Genes were amplified via standard polymerase chain reaction (PCR) using an Eppendorf Mastercycler pro S thermocycler (Eppendorf Ltd., Hamburg, Germany). A 636 bp fragment of the COI gene was amplified with an initial denaturation step of 1 min at 94 °C followed by 35 cycles of 94 °C for 30 s, annealing at 52 °C for 40 s, extension at 72 °C for 1 min, and final extension at 72 °C for 10 min. An 845 bp fragment of the Cyt *b* gene was amplified by denaturing at 95 °C for 2 min followed by 35 cycles of 95 °C for 30 s, annealing at 48 °C for 1 min, extension at 72 °C for 1 min 30 s, and final extension at 72 °C for 5 min. An 862 bp fragment of the ND2 gene was amplified by denaturing at 94 °C for 2 min, followed 35 cycles of 95 °C for 1 min, annealing at 58 °C for 1 min, extension at 72 °C for 2 min, and final extension at 72 °C for 10 min. An 856 bp fragment of the Glyt gene was amplified by denaturing at 95 °C for 2 min followed by 40 cycles of 95 °C for 30 s, annealing at 56 °C for 1 min, extension at 72 °C for 1 min 30 s, and final extension at 72 °C for 5 min. A 979 bp fragment of the RAG2 gene was amplified by denaturing at 94 °C for 2 min followed by 31 cycles of 94 °C for 30 s, annealing at 58 °C for 45 s, extension at 72 °C for 1 min, and final extension at 72 °C for 5 min. Products of each amplification were visualized by running 3 µL of amplicon on a 1% agarose gel. Remaining PCR product was purified using exonuclease I and calf intestine alkaline phosphatase (ExoCIAP). Successful amplifications were bidirectionally sequenced using the dye termination method of Sanger et al. (1977).

2.3. Sequence editing, alignment, and phylogeny inference

Bidirectional sequences were assembled into contigs and manually edited using the software Geneious v6.1.7 (Biomatters Ltd., Auckland, New Zealand). Sequences for contigs having many ambiguities were reamplified and resequenced. Contigs for each gene region were aligned using the MUSCLE algorithm Edgar (2004), with the alignments being manually edited and evaluated based on amino acid translations of consensus sequences. Individual gene alignments were concatenated to create a single matrix comprising 4156 bp × 69 individuals (see Table 2).

Maximum likelihood (ML) phylogenetic analyses of each unpartitioned gene alignment were conducted using RAxML v8.0.0 (Stamatakis, 2014), to check for consistency in phylogenetic signal across markers. Phylogenetic analyses of the concatenated alignment were partitioned by both gene and codon position resulting in 15 data partitions (Supplementary Table 3). The optimal model of molecular evolution for each partition was determined using the software Partition Finder v1.1.1 (Lanfear et al., 2012), which was programmed to select from models respectively available in MrBayes v3.2.6 (Ronquist and Huelsenbeck, 2003; Supplementary Table 3) or RAxML using the 'greedy' algorithm and the Bayesian information criterion (BIC). For the RAxML analysis a GTRCAT model was selected for all 15 data partitions.

All phylogenetic analyses were conducted on the CIPRES supercomputing cluster (Miller et al., 2010). The clade of Pimelodidae (*Pimelodus ornatus* Kner 1858) + Phreatobiidae (*Phreatobius cisternarum* Goeldi 1905, *Phreatobius dracunculus* Shibatta, Muriel-Cunha, and de Pinna 2007 and *Phreatobius* sp.) was designated the outgroup based on previous molecular studies finding that Heptapteridae is closely related to Pimelodidae and Phreatobiidae (Sullivan et al., 2013). Maximum likelihood analysis of the concatenated alignment was conducted using RAxML programmed with workflow bootstrap and consensus, based on a 1000 generation search of tree space. A Bayesian analysis of the concatenated alignment was conducted using a Markov chain Monte Carlo search of tree space implemented in the program MrBayes. MrBayes was programmed to run for 10 million generations using four chains (nchain = 4), two parallel runs; sampling every 1000 trees and discarding the first 10% of trees as burn-in. Tracer v1.6 (Rambaut et al., 2013) was used to ensure that effective sample sizes (ESS) for all metrics exceeded 200 and that parameter estimates were fluctuating within a stable range.

2.4. Presentation of phylogenetic results

Results of maximum likelihood phylogenetic analyses of each gene alignment are presented as supplemental Figs. 1–5. Results of maximum likelihood and Bayesian analyses of the concatenated data matrices are presented in a single merged figure using the Bayesian topology. Bayesian posterior probability (Bayesian inference = BI) and maximum likelihood (ML) bootstrap support values for each node are discussed in the text. Support values are described throughout the manuscript as either strong (ML: 95–100%, BI: 0.95–1), moderate (75–94%, BI: 0.75–0.94) or weak (ML: < 74%, BI: < 0.74).

2.5. Undescribed taxa

Samples of putatively undescribed species are designated by sequential numbers, in accordance with a separate and ongoing taxonomic revision, and by the river drainage from which they were collected. In cases where genera were found to be paraphyletic, genus epithets of species found to be more closely related to alternate genera than to the type species of the currently valid genus are denoted by single quotation marks.

3. Results

3.1. Major clades and tribe-level classification

Results of our phylogenetic analyses of the concatenated multi-locus dataset are presented in Fig. 2, which places node support values from both maximum likelihood and Bayesian inference analyses on a tree topology from the maximum likelihood analysis. Both analyses yielded moderate support for the monophyly and interrelationships of two geographically widespread clades that we describe as subfamilies: (Rhamdiinae + Heptapterinae) (see Discussion).

Within Rhamdiinae, two individuals of the monotypic genus and species *Goeldiella eques* (Müller and Troschel 1849) from the Essequibo River, near the type locality of the species, represented the new tribe Goeldiellini. Goeldiellini was sister to a strongly supported clade containing the three genera *Pimelodella* Eigenmann and Eigenmann 1888, *Rhamdella*, and *Rhamdia*, with this clade forming the new tribe Rhamdiini. Within Rhamdiini, *Pimelodella* was strongly supported, distributed east and west of the Andes, and sister to the clade of *Rhamdia* + *Rhamdella*. Monophyly and interrelationships of these taxa were all strongly supported (ML: ≥99, BI: 1). All remaining Heptapteridae species formed a moderately supported (ML: 84 and BI: 0.75), widespread, and taxonomically diverse clade that is described below as the newly recircumscribed subfamily Heptapterinae.

3.2. Heptapterinae major clade interrelationships and composition

Genera within Heptapterinae were divided into two widespread and strongly supported (ML: ≥99, BI: 1) sister clades that are described below as tribes: Heptapterini contained the genera *Acentronichthys* Eigenmann and Eigenmann 1889, *Cetopsorhamdia* Eigenmann and Fisher 1916, *Chasmocranus* Eigenmann 1912, *Heptapterus*, *Imparfinis* Eigenmann and Norris 1900, *Mastiglanis*, and *Phenacorhamdia*. Brachyglaniini contained *Brachyglanis*, *Gladioglanis*, *Leptorhamdia*, and *Myoglanis*. With the exception of '*Myoglanis*' *koepkei* Chang 1999 from the Ucayali River in Peru, examined species of Brachyglaniini were entirely restricted to drainages of the western Guiana Shield in Guyana and

Table 2
Loci sequenced, voucher code, catalog number, country, and drainages of origin for tissues analyzed in this study. Taxa grouped according to the family, subfamily, and tribe classification defined in this study.

Taxa	Tissue number	Loci	*col*	*cytb*	*nd2*	glyt	rag2	Catalog Number	Country	Drainage
Pimelodidae										
Pimelodus ornatus	Genbank	3	KP294265	JF898524			DQ492363	Genbank	Guyana	Demerara
Phreatobiidae										
Phreatobius cisternarum	Genbank	1					JX899764	Genbank	Brazil	Amazon
Phreatobius dracunculus	Genbank	1					JX899763	Genbank	Brazil	Madeira
Phreatobius sp.	Genbank	1					JX899762	Genbank	Brazil	Rio Negro
Heptapteridae										
Rhamdiinae										
Goeldiellini										
Goeldiella eques	AUPT3164	4	MWS30083		MW877383	MW877435	MW877459	AUM44843	Guyana	Rupununi
Goeldiella eques	AUPT3168	4	MWS30084		MW877384	MW877436	MW877458	AUM47869	Guyana	Rupununi
Rhamdiini										
Pimelodella modesta	T13894	5	MWS30110	MW877541	MW877367	MW877448	MW877501	ROM93790	Ecuador	Santa Rosa
Pimelodella sp.	T09547	4	MWS30111	MW877545	MW877370		MW877502	ROM92396	Venezuela	Orinoco
Pimelodella sp.	T02817	5	MWS30112	MW877543	MW877368	MW877405	MW877451	ROM66436	Guyana	Waini
Pimelodella sp.	T02818	5	MWS30113	MW877544	MW877369	MW877406	MW877450	ROM66436	Guyana	Waini
Rhamdella eriarcha	Genbank	1		KX379765				Genbank		
Rhamdella longiuscula	Genbank	1		KX379764				Genbank		
Rhamdia cf. *quelen*	T12676	5	MWS30114	MW877559	MW877371	MW877407	MW877449	ROM89896	Guyana	Potaro
Heptapterinae										
Heptapterini										
Acentronichthys leptos	TEC8330	4		MW877546	MW877372	MW877430	MW877467	UFRGS24782	Brazil	Ribeira do Iguape
Cetopsorhamdia insidiosa	T24800	3	MWS30078	MW877548	MW877380			ROM107245	Colombia	Orteguaza
Cetopsorhamdia molinae	T24506	5	MWS30079	MW877521	MW877347	MW877434	MW877461	ROM106958	Colombia	Suaza
Cetopsorhamdia molinae	T24508	5	MWS30080	MW877522	MW877348	MW877401	MW877460	ROM106958	Colombia	Suaza
Cetopsorhamdia nasus	T24601	3	MWS30081	MW877549	MW877381			ROM106960	Colombia	Suaza
Chasmocranus longior	AUPT3167	5	MWS30082	MW877550	MW877382	MW877402	MW877462	AUM45279	Guyana	Essequibo
Heptapterus bleekeri	AUPT4772	5	MWS30085	MW877523	MW877349	MW877437	MW877463	AUM50413	Suriname	Marowijne
Heptapterus mustelinus	T23652	3		MW877524	MW877385	MW877438		ROM102813	Uruguay	Laguna dos Patos
Heptapterus mustelinus	T23708	4		MW877525	MW877386	MW877403	MW877464	ROM102813	Uruguay	Laguna dos Patos
Imparfinis hasemani	T14941	5	MWS30087	MW877527	MW877351	MW877441	MW877465	ROM96232	Guyana	Takutu
Imparfinis hasemani	T13325	5	MWS30088	MW877528	MW877352	MW877418	MW877457	ROM97193	Guyana	Berbice
Imparfinis guttatus	T10382	4	MWS30086	MW877526	MW877350	MW877439		AUM57509	Peru	Madre de Dios
Imparfinis timana	T25012	3	MWS30090	MW877552	MW877387			ROM107865	Colombia	Guarapas
Imparfinis piipersi	T22565	3	MWS30089	MW877551	MW877388			ROM101455	Suriname	Saramaca
Imparfinis usmai	T24490	3		MW877553	MW877389	MW877440		ROM106933	Colombia	Cauca
Mastiglanis cf *asopos*	T09910	3	MWS30103			MW877426	MW877454	AUM54198	Venezuela	Cataniapo
Mastiglanis cf *asopos*	T09911	3	MWS30104			MW877404	MW877453	AUM54198	Venezuela	Cataniapo
Nemuroglanis pauciradiatus	AUPT3184	5	MWS30108	MW877540	MW877393	MW877447	MW877452	AUM43876	Venezuela	Soromoni
Phenacorhamdia boliviana	T10136	3	MWS30109	MW877542	MW877394			AUM51212	Peru	Inambari
Brachyglaniini										
Brachyglanis frenata	AUPT2071	5	MWS30064	MW877503	MW877335	MW877395	MW877468	AUM62845	Guyana	Lower Kuribrong
Brachyglanis frenata	T15600	5	MWS30065	MW877504	MW877336	MW877408	MW877469	ROM91440	Guyana	Lower Kuribrong
Brachyglanis microphthalmus	t11380	5	MWS30066	MW877505	MW877373	MW877409	MW877466	ANSP197628	Brazil	Xingu
Brachyglanis microphthalmus	t11497	5	MWS30067	MW877506	MW877374	MW877410	MW877470	ANSP197628	Brazil	Xingu
Brachyglanis nocturna	T09452	5	MWS30098	MW877509	MW877339	MW877411	MW877473	ROM93578	Venezuela	Lower Ventuari
Brachyglanis nocturna	T09302	5	MWS30096	MW877507	MW877337	MW877431	MW877471	ROM94418	Venezuela	Orinoco
Brachyglanis nocturna	T09306	5	MWS30097	MW877508	MW877338	MW877432	MW877472	ROM94418	Venezuela	Orinoco
Brachyglanis phalacra	T15598	4		MW877547	MW877375	MW877396	MW877474	ROM091434	Guyana	Lower Kuribrong
Brachyglanis phalacra	T15599	4		MW877510	MW877340	MW877412	MW877475	ROM91434	Guyana	Lower Kuribrong
Brachyglanis sp. 1	AUPT2043	5	MWS30068	MW877511	MW877341	MW877413	MW877476	AUM62763	Guyana	Upper Kuribrong
Brachyglanis sp. 1	T17250	5	MWS30077	MW877518	MW877376	MW877400	MW877480	ROM94950	Guyana	Upper Kuribrong
Brachyglanis sp. 1	T17164	5	MWS30074	MW877517	MW877346	MW877399	MW877479	ROM95036	Guyana	Upper Potaro
Brachyglanis sp. 2	AUPT3180	5	MWS30069	MW877512	MW877342	MW877433	MW877477	AUM43870	Venezuela	Soromoni
Brachyglanis sp. 2	AUPT3181	5	MWS30070	MW877513	MW877343	MW877397	MW877478	AUM43870	Venezuela	Soromoni

(continued on next page)

Table 2 (*continued*)

Taxa	Tissue number	Loci	col	cytb	nd2	glyt	mgl	Catalog Number	Country	Drainage
Brachyglanis sp. 3	T09674	5	MW830072	MW877515	MW877377	MW877398	MW877465	AUM54283	Venezuela	Upper Ventuari
Brachyglanis sp. 4	t872	5	MW830076	MW877520	MW877379	MW877416	MW877463	ANSP190908	Venezuela	Siapa
Brachyglanis sp. 4	t862	5	MW830075	MW877519	MW877378	MW877415	MW877464	ANSP182832	Venezuela	Siapa
Brachyglanis sp. 5	T09181	5	MW830071	MW877514	MW877344	MW877414	MW877481	ANSP192082	Venezuela	Cuao
Brachyglanis sp. 6	T09914	5	MW830073	MW877516	MW877345	MW877417	MW877462	AUM54284	Venezuela	Cataniapo
Gladioglanis machadoi	LBP4270	1					JQ599765	Gelbank	Brazil	Rio Negro
Leptorhamdia cf. *esequibensis*	T09242	5	MW830093	MW877529	MW877353	MW877419	MW877486	ROM94146	Venezuela	Orinoco
Leptorhamdia cf. *esequibensis*	T09262	5	MW830094	MW877530	MW877390	MW877420	MW877487	ROM94146	Venezuela	Orinoco
Leptorhamdia marmorata	AUF53174	5	MW830095	MW877531	MW877354	MW877423	MW877488	AUM44146	Venezuela	Atabapo
Leptorhamdia schultzi	t3908	4		MW877532	MW877355	MW877421	MW877489	ANSP190037	Brazil	Xingu
Leptorhamdia schultzi	t3907	4		MW877533	MW877356	MW877422	MW877490	ANSP194521	Brazil	Xingu
Leptorhamdia sp. 1	T09642	5	MW830099	MW877554	MW877357	MW877443	MW877455	AUM54484	Venezuela	Upper Ventuari
Leptorhamdia sp. 1	T09653	5	MW830100	MW877534	MW877358	MW877424	MW877491	AUM54484	Venezuela	Upper Ventuari
Leptorhamdia sp. 2	t3666	5	MW830101	MW877535	MW877359	MW877444	MW877492	AUM43544	Venezuela	Siapa
Leptorhamdia sp. 2	t666	5	MW830102	MW877536	MW877360	MW877425	MW877493	AUM43544	Venezuela	Siapa
Myoglanis aspredinoides	t3883	5	MW830092	MW877538	MW877362	MW877427	MW877456	ANSP191198	Venezuela	Orinoco
Myoglanis aspredinoides	T09447	5	MW830091	MW877537	MW877361	MW877442	MW877494	ROM93125	Venezuela	Ventuari
Myoglanis koepckei	GH14201	4	MW830105	MW877555	MW877391		MW877495	ROM95207	Peru	Ucayali
Myoglanis koepckei	GH14202	5	MW830106	MW877539	MW877392	MW877428	MW877496	ROM95207	Peru	Ucayali
Myoglanis potaroensis	T15593	5	MW830107	MW877556	MW877363	SW684264	MW877497	ROM91203	Guyana	Lower Kurituong
Myoglanis sp. 1	T17930	4		MW877557	MW877364	MW877429	MW877498	ROM99029	Guyana	Kwakwanik
Myoglanis sp. 1	T20563	4		MW877558	MW877365	MW877445	MW877499	ROM97694	Guyana	Mazaruni
Myoglanis sp. 1	T20576	5			MW877366	MW877446	MW877500		Guyana	Mazaruni

Venezuela and the northern Brazilian Shield in Brazil. The Heptapterini clade was broadly distributed east and west of the Andes (including three *trans*-Andean nodes) and from northern coastal rivers of Guyana south to Uruguay.

3.2.1. *Heptapterini interrelationships*

The genus *Mastiglanis*, represented by two samples of *Mastiglanis* cf. *asopos* from the Cataniapo River in southern Venezuela, formed a lineage sister to all other members of Heptapterini. Remaining members of Heptapterini were divided between a strongly supported (ML: 100, BI: 1), internally well-resolved, and geographically widespread clade containing *Acentronichthys*, *Heptapterus*, *Imparfinis*, and *Nemuroglanis*, and a poorly resolved assemblage of three valid genera (*Cetopsorhamdia*, *Chasmocranus*, and *Phenacorhamdia*) and two species that are generically misplaced ('*Cetopsorhamdia*' *molinae* Miles 1943, and '*Heptapterus*' *bleekeri* Boeseman 1953).

Within the internally well-resolved, geographically widespread clade, a southern Brazilian and Uruguayan clade of *Acentronichthys leptos* Eigenmann and Eigenmann 1889 + *Heptapterus mustelinus* was sister to a northern and western South American, Andean and Guiana Shield clade of *Imparfinis* + *Nemuroglanis pauciradiatus*. *Imparfinis* was strongly supported and contained a clade of *trans*-Andean species (*I. timana* Ortega-Lara et al. 2011 + *I. usmai* Ortega-Lara et al. 2011) sister to a *cis*-Andean clade containing species from the southwestern Amazon (*I. guttatus* (Pearson 1924)) and Guiana Shield (*I. hasemani* Steindachner 1915 + *I. pijpersi* (Hoedeman 1961)).

Although deep relationships among remaining members of Heptapterini were weakly and/or inconsistently resolved, three genus/species pairs were strongly and consistently supported as respectively monophyletic (ML: 100, BI: 1): *Cetopsorhamdia* contained the type species *Ce. nasus* Eigenmann and Fisher 1916 from the Suaza River (Magdalena River drainage) sister to *Ce. invidiosa* (Steindachner 1915) from the Orteguaza River (Amazon River drainage); *Phenacorhamdia* cf. *boliviana* from the Inambari River (southwestern Amazon) was sister to '*Cetopsorhamdia*' *molinae* from the Suaza River (Magdalena River drainage), and *Chasmocranus longior* Eigenmann 1912 from the Essequibo River was sister to '*Heptapterus*' *bleekeri* from the Marowijn River (both draining the northern Guiana Shield).

3.2.2. *Brachyglaniini interrelationships*

Deep interrelationships within Brachyglaniini were generally well-resolved and strongly supported. One exception was the placement of *Gladioglanis machadoi* Ferraris & Mago-Leccia 1989, which was represented in our analyses by a single GenBank sequence of COI. The BI analysis found *G. machadoi* to be weakly supported (BI: 0.39) as sister to *Myoglanis*, whereas the ML analysis placed *G. machadoi* in a polytomy with *Myoglanis sensu stricto* and a strongly supported clade containing all other species.

Myoglanis formed the sister lineage to all other Brachyglaniini species exclusive of *Gladioglanis machadoi*. Within *Myoglanis*, the type species *M. potaroensis* Eigenmann 1912 was sister to the undescribed species *Myoglanis* sp. 1, with distributions of these species overlapping in northwestern tributaries of the Essequibo River. Two additional species currently placed in *Myoglanis* ('*M.*' *aspredinoides* DoNascimiento and Lundberg 2005 and '*M.*' *koepckei*) were more closely related to the genus *Leptorhamdia*.

Two reciprocally monophyletic and strongly supported sister clades were broadly congruent with the genera *Brachyglanis* and *Leptorhamdia*, although both contained some generically misplaced species. The *Brachyglanis* clade contained the type species *B. frenata* Eigenmann 1912 and eight additional species. One nominal *Brachyglanis* species ('*B.*' *nocturna* Myers 1928) was more closely related to *Leptorhamdia*. *Leptorhamdia* was the genus for which our results posed the greatest challenge to existing species-level classification. In addition to the type species '*L.*' cf. *esequibensis* and two other currently valid species (*L. marmorata* Myers 1928 and *L. schultzi* (Miranda Ribeiro 1964)), *Leptorhamdia*

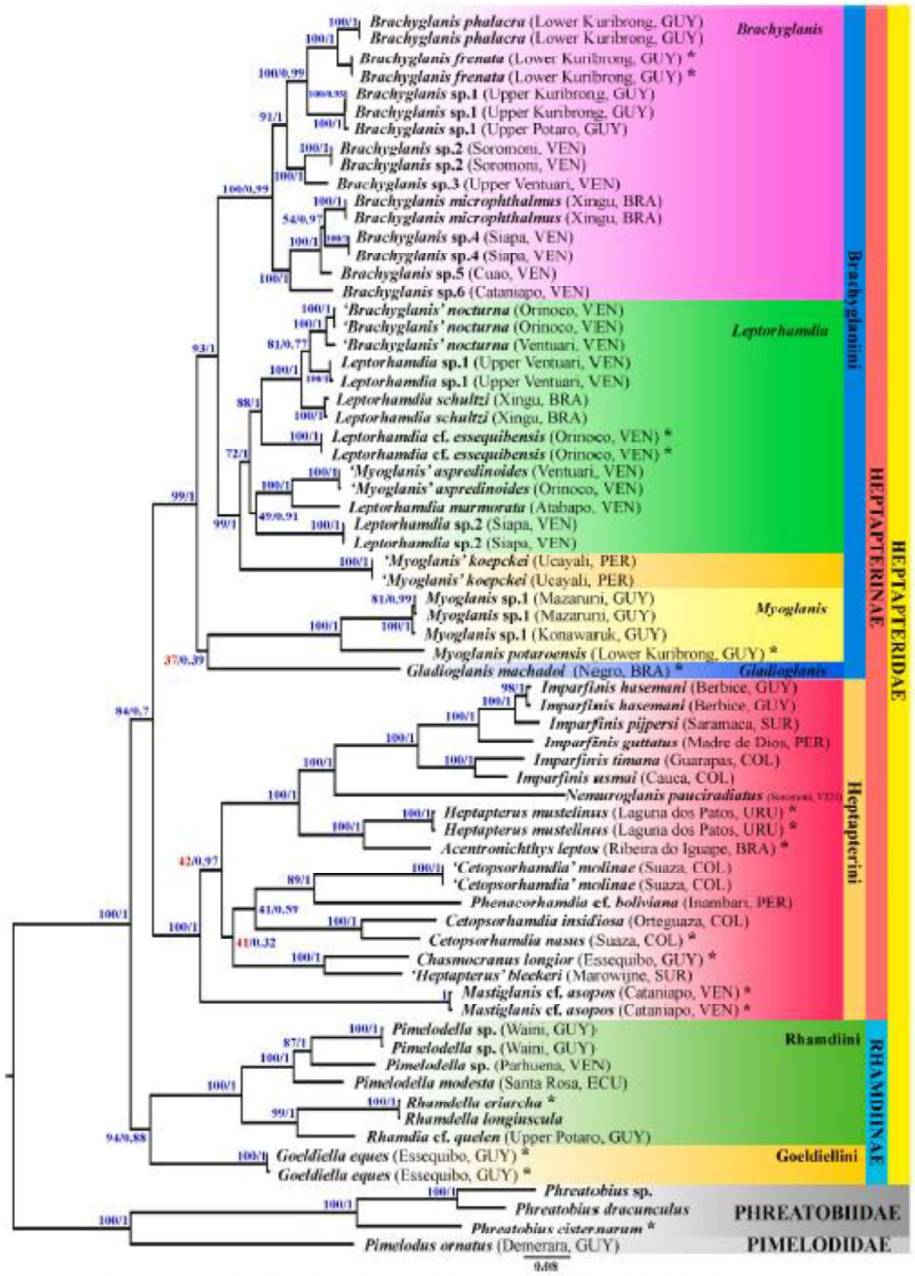

Fig. 2. Phylogenetic hypothesis for Heptapteridae interrelationships produced by maximum likelihood analysis of a 4156 base pair alignment consisting of three mitochondrial (*coI*, *cytb*, *nd2*) and two nuclear (glyt, rag2) gene regions. For each node, the maximum likelihood bootstrap support value is given first, followed by the Bayesian inference posterior probability. Specimens representing species that are types for their genus are indicated by an asterisk (*). BRA = Brazil, COL = Colombia, ECU = Ecuador, GUY = Guyana, PER = Peru, SUR = Suriname, VEN = Venezuela.

contained three species currently placed in other genera ('*B.*' *nocturna*, '*M.*' *aspredinoides*, and '*M.*' *koepckei*) and two undescribed species.

3.2.2.1. Brachyglanis interrelationships. With the exception of one node having ML = 54, interrelationships within *Brachyglanis* were fully and consistently resolved and strongly to moderately supported (all other nodes: ML: ≥91 and BI: ≥0.95). The basal node in *Brachyglanis* produced one clade restricted to eastern and western slopes of the western Guiana Shield in Guyana and Venezuela, and a sister clade spanning upper Orinoco and Negro tributaries draining the western Guiana Shield in Venezuela, and Xingu tributaries draining the northern slope of the Brazilian Shield in Brazil. The basal node in the strictly western Guiana Shield clade produced lineages endemic to opposite (eastern *vs.* western) slopes of the western Guiana Shield highlands in Guyana and Venezuela respectively. The western lineage contained undescribed sister species from disjunct regions of the upper Orinoco watershed: *Brachyglanis* sp. 2 from the Soromoni River near Esmeraldas, and *Brachyglanis* sp. 3 from the upper Ventuari River, ~60 river km upstream of Salto Tencua. The eastern lineage contained five examined species, with the basal node in this lineage giving rise to clades respectively endemic to habitats above *vs.* below the Guiana Shield escarpment separated by Amaila and Kaieteur waterfalls. Samples of the sister species *B. frenata* and *B. phalaera* Eigenmann 1912 were from the Kuribrong River below the escarpment, whereas samples of the undescribed species *Brachyglanis* sp. 1 were from upper reaches of the Kuribrong and Potaro rivers above the escarpment. In the *trans*-shield clade, the first two lineages to branch were for undescribed species from nearby right-bank tributaries of the upper Orinoco south of Puerto Ayacucho: *Brachyglanis* sp. 6 from the Cataniapo River and *Brachyglanis* sp. 5 from the Cuao River. Nested within this clade were the sister species *Brachyglanis* sp. 4 from the Siapa River (a tributary of the Casiquiare-Negro drainage) and *B. microphthalmus* Biserril 1991 from the lower (northern) Xingu River drainage. Although this sister relationship was strongly supported in the Bayesian analysis (BI:0.97), it received weaker support in the maximum likelihood analysis (ML: 54).

3.2.2.2. Leptorhamdia interrelationships. Interrelationships within the *Leptorhamdia sensu lato* clade were fully and consistently resolved and moderately to strongly supported. With the exception of four nodes having ML: 49–88 and one node having BI: 0.77, all other nodes had ML: ≥99 and BI: ≥0.91. The first lineage to branch within this clade produced the sole Andean/upper Amazon species '*Myoglanis*' *koepckei* from the Ucayali River in Peru. All remaining species formed a *Leptorhamdia sensu stricto* clade. The basal node of this clade produced a strictly Guiana Shield lineage restricted to southern Venezuela, and a *trans*-shield lineage distributed across southern Venezuela and the lower Xingu River in northern Brazil. The basal node within the strictly Guiana Shield lineage produced an undescribed species (*Leptorhamdia* sp. 2) from the Siapa River sister to a clade containing sister species from tributaries to opposite banks of the upper Orinoco River: '*Myoglanis*' *aspredinoides* from the right-bank clearwater Ventuari River and Orinoco River itself and *L. marmorata* from the left-bank blackwater Atabapo River. The only node in *Leptorhamdia* with weak maximum likelihood support (ML: 49) but moderate Bayesian support (BI: 0.91) was this basal node within the strictly Guiana Shield lineage. The first lineage to branch from the basal node in the *trans*-shield clade gave rise to *Leptorhamdia* cf. *essequibensis* from the upper Orinoco. The next lineage to branch was *L. schultzi* from the middle Xingu River, followed by the sister species '*Brachyglanis*' *nocturna* from the lower Ventuari River and *Leptorhamdia* sp. 1 from the upper Ventuari River, ~60 river km upstream of Salto Tencua.

4. Discussion

4.1. Overview

After over a century of mostly morphology-based analyses of the species-rich family Heptapteridae, we provide the first well-resolved, robustly supported molecular phylogenetic hypothesis for 31 valid species, spanning 70% of Heptapteridae genera (16), 57% of Heptapterini (*Nemuroglanis*-clade) genera (8), and 73% of valid species in the *Brachyglanis* subclade (11). Only nine species distributed in eight heptapterid genera have previously been included in molecular phylogenetic analyses (Sullivan et al., 2013, Arcila et al., 2017; Betancur et al., 2017), leaving many morphology-based hypotheses for intrafamilial relationships untested by independent data. Our phylogenetic hypothesis provides a robust basis on which to reevaluate suprageneric classification schemes throughout the family, and we propose six new taxa for intrafamilial clades that have been previously hypothesized based on morphology and which receive additional molecular support here. The classification scheme we propose for Heptapteridae is:

Family Heptapteridae Gill 1861
- Subfamily Rhamdiinae Bleeker 1862, new usage
  - Tribe Goeldiellini, new tribe
  - Tribe Rhamdiini Bleeker 1862, new usage
- Subfamily Heptapterinae Gill 1861
  - Tribe Heptapterini Gill 1861, new usage
  - Tribe Brachyglaniini, Silva & Bockmann 2021

Our results also lend novel insights into the biogeographical history of Heptapteridae. While this is an area of ongoing research, we conclude our discussion with a review of biogeographical patterns revealed by our phylogeny and reinforced by other freshwater taxa.

4.2. Subfamily Rhamdiinae Bleeker 1862, new usage

4.2.1. Rhamdiae Bleeker 1862 (in Bleeker, 1862–63: 11, 60)

Type genus: *Rhamdia* Bleeker 1858.

4.2.2. Included tribes (2)

Goeldiellini and Rhamdiini (see descriptions below).

4.2.3. Diagnosis

Rhamdiinae is distinguished from Heptapterinae by having the free orbital rim well-defined (*vs.* reduced or absent) and having the principal pectoral-fin ray ossified and pungent with anterior margins having antrorse serrations (*vs.* principal pectoral-fin ray segmented and flexible or ossified and pungent with anterior margins having retrorse serrations).

4.2.4. Distribution

Rhamdiinae is the most broadly distributed and ubiquitous Heptapteridae subfamily, being encountered throughout lake and stream habitats from headwaters to large main channels in drainages both west of the Andes (*trans*-Andean) from southern Mexico to northern Peru and east of the Andes (*cis*-Andean) from Colombia and Venezuela, throughout the Guianas, and south to Argentina.

4.2.5. Remarks

Rhamdia Bleeker 1858 is the second oldest genus name in Heptapteridae. Four years after erecting *Rhamdia*, Bleeker (1862) erected the family group name Rhamdiae, in which he placed various members of the modern Akysidae, Claroteidae, Heptapteridae, Pimelodidae, and Pseudopimelodidae. Rhamdiae fell into disuse due to its heterogeneous composition and the superimposition of the constituent family groups. From 1991 (Lundberg et al., 1991) to Silfvergrip's (1996) recognition that Heptapterinae Gill 1861 had priority, Rhamdiae was resurrected as

a name for the subfamily group Rhamdiinae, which was equivalent to the modern Heptapteridae. We resurrect Rhamdiinae again for a more restricted clade that is consistently strongly supported in our molecular phylogeny and is morphologically clearly diagnosed from our other proposed heptapterid subfamily. Some Rhamdiinae species reach the largest body sizes in Heptapteridae, up to approximately 70 cm TL for *Rhamdia quelen* Quoy and Gaimard 1824 (Machacek, 2019).

4.3. Goeldiellini, new tribe

Type genus: *Goeldiella* Eigenmann and Norris 1900.

Included genera (1): *Goeldiella* Eigenmann and Norris 1900.

Diagnosis: Goeldiellini is distinguished from Rhamdiini by having cephalic laterosensory canals dendritic with multiple pores (*vs.* simple with single pores), pectoral-fin spine anterior and posterior margins with well-developed serrations, hypobranchial 1 quadrangular (*vs.* rectangular) and hypobranchial 3 lacking anterolateral projection (*vs.* present) (Bockmann and Miquelarena, 2008; Bockmann and Slobodian, 2017; DRFF pers. obs.).

Interrelationships: Previously, morphological data (Bockmann, 1998; Bockmann and Miquelarena, 2008) and Bayesian analysis of concatenated nuclear and mitochondrial markers (Sullivan et al., 2013) placed *Goeldiella* as sister to all other Heptapteridae. However, sequence data from nuclear markers exclusively (Sullivan et al. 2006) and parsimony analysis of concatenated nuclear and mitochondrial markers (Sullivan et al., 2013) placed *Goeldiella* in a position similar to this study, as sister to *Pimelodella* + *Rhamdia* which together formed a clade sister to all other Heptapteridae. Our analyses consistently found *Goeldiella* to be sister to a more inclusive clade containing *Rhamdella*, *Rhamdia*, and *Pimelodella* (Fig. 2), which comprise our newly recircumscribed tribe Rhamdiini.

Distribution: Although *Goeldiella* currently contains only the species *G. eques*, this species is broadly distributed across northern *cis*-Andean South America, from the lower courses of right-bank (southern) tributaries of the Amazon River northward to the Orinoco and Essequibo.

Remarks: In the cladistic analysis of Bockmann (1998) (Fig. 1), *Goeldiella eques* was diagnosed by 15 autapomorphies. Of these characters, the following five are unique (numbered as in Bockmann, 1998): character 115: pharyngobranchial 1 absent; character 179: pectoral-fin spine anterior and posterior margins with well-defined serrations; character 219: number of branched caudal-fin rays on ventral lobe nine; character 228: ventral caudal-fin lobe longer than dorsal lobe; character 237: epiphyseal branch opening of the supraorbital canal large.

4.4. Rhamdiini Bleeker 1962, new usage

Diagnosis: Rhamdiini is distinguished from Goeldiellini by having cranial laterosensory canals simple, terminating in single pores (*vs.* dendritic, terminating in multiple pores), and pectoral-fin spine anterior margin having only weakly developed serrations (*vs.* anterior and posterior margins with well-developed serrations) (Bockmann and Miquelarena, 2008; Bockmann and Slobodian, 2017; Ferraris, 1988; Lundberg et al., 1991; Lundberg and McDade, 1986; DRFF pers. obs.).

Included genera (4): *Brachyrhamdia* Myers 1927; *Pimelodella* Eigenmann and Eigenmann 1888; *Rhamdella* Eigenmann and Eigenmann 1888; and *Rhamdia* Bleeker 1858.

Distribution: As described for Rhamdiinae.

Remarks: The cladistic analysis of Bockmann and Miquelarena (2008) identified two putative synapomorphies that place *Rhamdella* as sister to a clade containing *Brachyglanis*, *Gladioglanis*, *Leptorhamdia*, and *Myoglanis* plus the *Nemuroglanis* sub-clade: pharyngobranchial 1 absent, and tip of transverse process of vertebra 5 simple. However, ours and previous molecular analyses (Sullivan et al, 2006; Arcila et al., 2017; Betancur et al., 2017) find *Rhamdella* to be strongly supported as sister to *Rhamdia* (Fig. 2). In addition to the genera *Pimelodella*, *Rhamdella*, and *Rhamdia*, which we directly examined, previous studies have found that *Brachyrhamdia* is closely related to *Pimelodella* (Bockmann and Miquelarena, 2008; Ferraris, 1988; Lundberg and McDade, 1986; Slobodian and Bockmann, 2013). Thus, we also include *Brachyrhamdia* as part of this subfamily.

4.5. Subfamily Heptapterinae Gill 1861

Heptapterinae Gill 1861: 54. **Type genus:** *Heptapterus* Bleeker 1858.

Included tribes: Brachyglaniini and Heptapterini (see definitions below).

Diagnosis: Heptapterinae is distinguished from Rhamdiinae by having free orbital rim reduced or absent (*vs.* well-defined) and having principal pectoral-fin ray segmented and flexible or ossified and pungent with anterior margins having retrorse serrations (*vs.* principal pectoral-fin ray ossified and pungent with anterior margins having antrorse serrations) (Lundberg et al., 1991; Bockmann and Slobodian, 2017; DRFF pers. obs.).

Distribution: Heptapterinae is distributed in drainages west of the Andes (*trans*-Andean) from Panama to northern Peru, and in drainages east of the Andes (*cis*-Andean) from Colombia and Venezuela, throughout the Guianas, south to central Argentina. Species of Heptapterinae are generally more characteristic of headwater streams than of large main river channels.

Remarks: Heptapterinae was originally proposed by Gill (1861) for the then monotypic genus and species *Heptapterus mustelinus*. Our subfamily Heptapterinae is closest in composition to an unnamed clade proposed by Lundberg et al. (1991) and Clade 129 in Bockmann (1998) (Fig. 1). In the latter cladistic analysis, Clade 129 was diagnosed by 19 synapomorphies, the following seven of which were unique (numbered as in Bockmann, 1998): character 108: lateral profile of cartilaginous head of ceratobranchial 4 straight; character 110: length of distal cartilage of ceratobranchial 5 short; character 113: base of uncinate process of epibranchial 3 wide; character 130: arborescent portion of posterior branch of transverse process of vertebra 4 undivided; character 141: distal end of transverse process of vertebra 5 simple; character 188: mesial cartilages of basipterygia fused along midline; character 276: orbital margin poorly defined, with shallow grooves around eye or without grooves. We likewise find strong support for this clade, and find that it comprises two strongly supported subclades for which we erect new tribes.

4.6. Tribe Heptapterini Gill 1861, new usage

4.6.1. Type genus: Heptapterus Bleeker 1858

Included genera (14): *Acentronichthys* Eigenmann and Eigenmann 1889; *Cetopsorhamdia* Eigenmann and Fisher 1916; *Chasmocranus* Eigenmann 1912; *Heptapterus* Bleeker 1858; *Horiomyzon* Stewart 1986; *Imparfinis* Eigenmann and Norris 1900; *Mastiglanis* Bockmann 1994; *Nannoglanis* Boulenger 1887; *Nemuroglanis* Eigenmann and Eigenmann 1889; *Pariolius* Cope 1872; *Phenacorhamdia* Dahl 1961; *Rhamdioglanis* Ihering 1907; *Rhamdiopsis* Haseman 1911; *Taunayia* Miranda Ribeiro 1918.

Diagnosis: Heptapterini is distinguished from Brachyglaniini by having the principal unbranched pectoral- and dorsal-fin rays segmented and flexible (*vs.* ossified and rigid) (Stewart, 1986; Ferraris, 1988; Lundberg et al., 1991; Bockmann, 1994; Bockmann and Slobodian, 2017; DRFF pers. obs.).

Interrelationships: In his description of the genus *Mastiglanis*, Bockmann (1994) described a synapomorphy that united all members of the *Nemuroglanis*-subclade exclusive of *Mastiglanis* and *Nemuroglanis*: triangular posterior lamina of the Weberian transverse process having an additional distal notch. Based on this evidence and one additional distinguishing feature of *Mastiglanis* that distinguishes it from other members of the *Nemuroglanis*-subclade (medial notch separating two symmetrical arms of posterior Weberian limb more attenuated), Bockmann (1994) suggested that *Mastiglanis* may be sister to all other

members of the subclade. However, Bockmann and Ferraris (2005) proposed a different hypothesis: that within the *Nemuroglanis*-subclade, *Mastiglanis* is part of a clade with *Imparfinis*, *Horiomyson* and *Nemuroglanis* based on a single putative synapomorphy: contacting borders between frontals, sphenotics, pterotics, and supraoccipital mostly continuous and smooth. Our molecular analyses consistently supported the hypothesis of Bockmann (1994) that *Mastiglanis* is sister to all other members of the *Nemuroglanis*-subclade (our tribe Heptapterini), but also found some support for the second hypothesis of Bockmann and Ferraris (2005) by finding that *Imparfinis* and *Nemuroglanis* are sister lineages (*Horiomyson* was not examined here). Our results parallel those of other molecular analyses having more limited taxon sampling, such as Sullivan et al. (2013) who also found *Heptapterus* and *Acentronichthys* to form a clade sister to *Imparfinis*, and Arcila et al. (2017) and Betancur-R et al. (2017) who also found *Mastiglanis* to be sister to other Heptapterini.

Bockmann and Slobodian (2017) suggested that '*Cetopsorhamdia*' *molinae* likely belongs to a different genus, which our analyses support by consistently finding this species to be more closely related to *Phenacorhamdia* than to *Cetopsorhamdia* (*Ce. nasus*).

4.6.2. Distributions: As described for Heptapterinae

Remarks: Historical usage of the subfamily and family group name Heptapterinae/Heptapteridae is reviewed above. Our tribe Heptapterini is consistent with the '*Nemuroglanis*-subclade,' which was first proposed by Stewart (1986) as the '*Heptapterus* group' based on the principal unbranched pectoral-fin ray being segmented and flexible (*vs.* ossified and rigid). The group was further expanded and diagnosed by Ferraris (1988) and Bockmann (1994) and by the cladistic analysis of Bockmann (1998; Fig. 1, Clade 119; see Introduction). Bockmann's (1998) cladistic analysis diagnosed clade 119 by 12 synapomorphies, the following eight of which are unique (numbered as in Bockmann, 1998): character 22: nasal bone long; character 94: junction between anterior and posterior ceratohyal synchondral; character 133: neural arch of vertebra 4 approximately straight, not covering neural arch of vertebra 5; character 138: subdivision of arborescent portion of posterior branch of transverse process of vertebra 4 separating two main arms; character 140: laminar portion of Weberian transverse process posterior to branched segment triangular, extending nearly to lateral tip of fifth vertebral transverse process; character 151: first dorsal-fin spine element (=dorsal-fin lock) absent; character 158: post-cleithral process absent or short; character 176: principal unbranched pectoral-fin ray weakly or moderately ossified. Bockmann (1998) circumscribed clade 119 to include the following genera: *Acentronichthys*, *Cetopsorhamdia*, *Chasmocranus*, *Heptapterus*, *Horiomyson*, *Imparfinis*, *Mastiglanis*, *Nemuroglanis*, *Pariolius*, *Phenacorhamdia*, *Rhamdioglanis*, *Rhamdiopsis*, and *Taunayia*. Of the genera examined here, our analyses consistently strongly supported the monophyly of a clade containing *Acentronichthys*, *Cetopsorhamdia*, *Chasmocranus*, *Heptapterus*, *Imparfinis*, *Mastiglanis*, *Nemuroglanis*, and *Phenacorhamdia*. In addition to those genera, which we directly examined, we also include the following genera in this tribe based on previous morphology-based studies: *Horiomyson*, *Nannoglanis*, *Pariolius*, *Rhamdioglanis*, *Rhamdiopsis*, and *Taunayia* (Table 1; Bockmann, 1994; Bockmann and Castro, 2010; Bockmann and Ferraris, 2005; Ferraris, 1988; Lundberg et al., 1991; Bockmann and Slobodian, 2017).

4.7. Tribe Brachyglaniini Silva and Bockmann 2021:

Type genus: *Brachyglanis* Eigenmann 1912.

Included genera (4): *Brachyglanis* Eigenmann 1912, *Gladioglanis* Ferraris and Mago-Leccia 1989, *Leptorhamdia* Eigenmann 1918, *Myoglanis* Eigenmann 1912.

Diagnosis: Brachyglaniini is distinguished from Heptapterini by having the principal unbranched pectoral-fin ray forming an ossified, rigid spine (*vs.* segmented and flexible). Additionally, *Brachyglanis*, *Myoglanis* and *Leptorhamdia* can be distinguished from all other Heptapterini by having the adductor mandibulae muscle extending dorsally to the cranial midline (*vs.* restricted to the cheek) (Lundberg et al., 1991; DoNascimiento and Lundberg, 2005; Bockmann and Slobodian, 2017; this study).

Interrelationships: The first study to suggest a close relationship between *Brachyglanis*, *Leptorhamdia*, and *Myoglanis* was Myers (1928) based on gestalt. In the phylogenetic hypothesis of Lundberg et al. (1991) *Brachyglanis*, *Gladioglanis*, *Leptorhamdia*, and *Myoglanis* formed an unresolved polytomy outside the *Nemuroglanis*-subclade but within the clade having a reduced or absent free orbital rim. Nonetheless, Lundberg et al. (1991) suggested that at least *Brachyglanis*, *Leptorhamdia*, and *Myoglanis* might form a clade based on adductor mandibulae muscle morphology. Although our analyses failed to resolve the position of *Gladioglanis* within Brachyglaniini, this morphological evidence suggests that it is sister to all other members of the tribe. Bockmann (1998) and DoNascimiento and Lundberg (2005) suggested that *Leptorhamdia* and *Myoglanis* might be sister lineages, but our results reject this hypothesis.

***Brachyglanis* composition:** We examined four of six currently valid *Brachyglanis* species plus six new species, all of which will be redescribed or described in a forthcoming species-level taxonomic revision. *Brachyglanis* was recognized as monophyletic with the exclusion of '*Brachyglanis*' *nocturna*, which was more closely related to *Leptorhamdia* cf. *essequibensis*, type species of *Leptorhamdia*, than to *B. frenata*, type species of *Brachyglanis*. '*Brachyglanis*' *nocturna* was considered to be a member of *Leptorhamdia* by Bockmann (1998) and Bockmann and Slobodian (2017) but without a formal taxonomic decision.

***Leptorhamdia* composition:** We examined all three currently valid species of *Leptorhamdia* plus two new species, all of which will be redescribed or described in a forthcoming species-level taxonomic revision. *Leptorhamdia* was found to be monophyletic only with the inclusion of '*Brachyglanis*' *nocturna* and '*Myoglanis*' *aspredinoides*. '*Myoglanis*' *koepckei* was found to be sister to this *Leptorhamdia sensu stricto*, leaving open the possibility that this species either be included in *Leptorhamdia* or be treated as a distinct new genus.

***Myoglanis* composition:** We examined all three currently valid species of *Myoglanis* plus one new species, all of which will be redescribed or described in a forthcoming species-level taxonomic revision. *Myoglanis* was found to be monophyletic only with the exclusion of '*Myoglanis*' *aspredinoides* and '*Myoglanis*' *koepckei*.

Remarks: Bockmann's (1998) cladistic analysis diagnosed clade 128 with 15 synapomorphies, six of which are unique (numbered as in Bockmann, 1998): character 25: posterior portion of lateral ethmoid half as long as anterior portion; character 153: principal unbranched dorsal-fin ray (=spine) flattened; character 180: serrations of anterior margin of principal unbranched pectoral-fin ray (=spine) retrorse; character 189: posterior process of ischial cartilage positioned more medially; character 238: epiphyseal branch of the supraorbital canal positioned dorsally; character 241: parietal branch of the supraorbital sensory canal absent. Bockmann (1998) circumscribed the clade to the following genera: *Brachyglanis*, *Gladioglanis*, *Leptorhamdia*, *Myoglanis*, and *Phreatobius*. However, in the molecular phylogenetic analysis of Sullivan et al. (2013), *Phreatobius* was removed from Heptapteridae and treated as either *incertae sedis* or a new family within the clade containing Heptapteridae, Pimelodidae, and Pseudopimelodidae. Our analyses consistently strongly supported the monophyly of a clade containing *Brachyglanis*, *Gladioglanis*, *Leptorhamdia*, and *Myoglanis*. *Phreatobius* was assigned *a priori* to the outgroup in our analyses.

4.8. Biogeographical inferences

Rhamdiinae and Heptapterini are geographically widespread and/or species-rich clades from which we examined few lineages. It is nonetheless clear from our limited sampling that Rhamdiini contains at least two *trans*-Andean nodes (nodes leading to sister lineages on opposite sides of the Andes Mountains), and Heptapterini contains at least three, highlighting these clades as potential models for understanding the

impacts of Andean uplift on freshwater fish diversification. The primary focus of this study, tribe Brachyglaniini, is entirely restricted to east of the Andes (*cis*-Andean) with most species distributed around the western Guiana Shield highlands of southern Venezuela and western Guyana (Fig. 3), making it a valuable clade for understanding the impacts of Guiana Shield uplift, erosion, and associated hydrogeographic evolution on freshwater fish diversification. Although denser geographic sampling and a time-calibrated phylogeny are needed to strengthen biogeographical inferences, it is nonetheless valuable to review the biogeographical patterns that are clearly supported by our phylogenetic results, the geographic distribution of included lineages, the habitat preferences that characterize entire clades, and parallel historical biogeographical patterns in other codistributed taxa.

The only known Brachyglaniini lineages from outside the Guiana Shield are a single lineage from the northwestern Amazon (*'Myoglanis' koepckei*) and two lineages from the northern Brazilian Shield (*Brachyglanis microphthalmus*, *Leptorhamdia schultzi*) (Fig. 3). Independent nestedness of these lineages within the core Guiana Shield clade indicates that they separately dispersed from western Guiana Shield ancestors. Sister lineages of both the northern Brazilian Shield species *B. microphthalmus* and *L. schultzi* are restricted to the upper Negro River (*Brachyglanis* sp. 4) and nearby upper Orinoco River (*'Brachyglanis' nocturna* + *Leptorhamdia* sp. 1; Fig. 3), suggesting that these Brazilian Shield lineages may share a similar dispersal history from the Guiana Shield. Numerous aquatic taxa are codistributed across the Brazilian and Guiana shields (see summary in Lujan et al., 2020), although few have been investigated using a time-calibrated phylogeny to differentiate between alternative dispersal scenarios. A dated phylogeny for the *trans*-shield distributed loricariid *Pseudolithoxus kinja* suggests that dispersal occurred very recently, since the end of the Pliocene, possibly during a

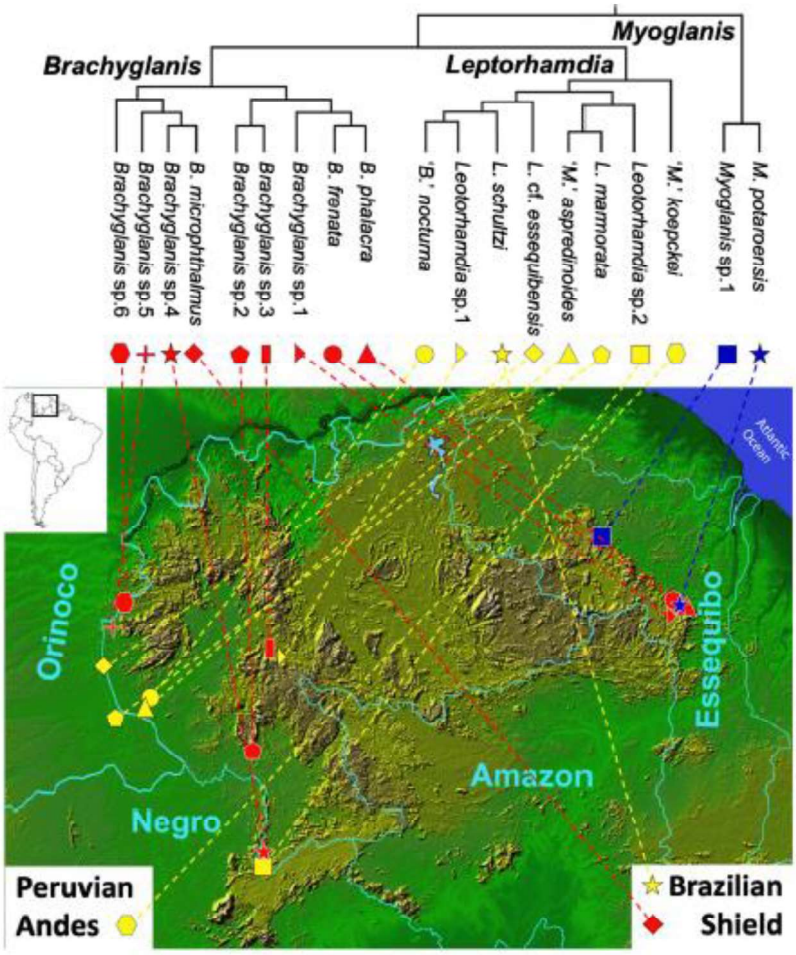

sea-level low (=glacial maximum) when the Negro and Amazon river main channels would have been much shallower (Collins et al., 2018). In contrast, a dated phylogeny for *trans*-shield lineages in the dreissenid bivalve genus *Rheodreissena* supports much earlier dispersal in the early- to mid-Miocene, possibly before formation of the Amazon as a *trans*-continental basin (Geda et al., 2018). The abundance of clades that are endemic to either the Brazilian or Guiana Shield, or that comprise sister lineages in opposite shields, supports the lower Amazon River channel is an important barrier to dispersal, and thus an important driver of cladogenesis after upland lineages disperse across it.

Within Brachyglaniini, the earliest branching lineage exclusive of *Gladioglanis* gave rise to *Myoglanis sensu stricto*, which is entirely restricted to tributaries of the Essequibo River draining the eastern slope of the western Guiana Shield in Guyana (Fig. 3). Most remaining members of the Brachyglaniini, comprising species of *Brachyglanis* and *Leptorhamdia*, occupy tributaries of the upper Orinoco draining the western slope of the western Guiana Shield in Venezuela. Nevertheless, both of these predominantly upper Orinoco clades contain at least one nested lineage present in Guyana (Fig. 3). Thus, it is clear that lineages in this clade have repeatedly dispersed across or around the southern Guiana Shield highlands, or expanded and contracted their range across these highlands leaving disjunct relictual populations. Such biogeographical processes leading to allopatric diversification across the landscape appear to be the predominant mechanism driving diversification in Brachyglaniini; however, differentiating between hypotheses based on active dispersal versus passive range expansion/contraction is challenging in the absence of dense geographic sampling. Habitat preferences, the absence of records from key well-sampled regions, and shared patterns in codistributed taxa can nonetheless provide important clues.

In *Brachyglanis*, the Essequibo clade comprises two sister species from below the escarpment (*Brachyglanis franata* + *B. phalacra*; lower Kuribrong and Potaro rivers) sister to one species from above the escarpment (*Brachyglanis* sp. 1, upper Kuribrong and Potaro rivers). This Essequibo clade is sister to an Orinoco species from the upper Ventuari River above Salto Tencua (*Brachyglanis* sp. 3). A pattern similar to this is observed in *Exastilithoxus*, with *E. fimbriatus* from the upper Caroni River (near Venezuela's border with Guyana) being sister to an undescribed species that co-occurs with *Brachyglanis* sp. 3 in the upper Ventuari River (Lujan et al., 2018). Remarkably, these *Exastilithoxus* sister species have < 2.5% *Cytb* sequence divergence, despite > 450 km linear distance, the Pantepui highlands, and multiple headwaters between them (Lujan et al., 2018). Both *Exastilithoxus* and *Brachyglanis* are headwater endemic taxa not known from intervening lowland river channels. A compelling explanation for such repeated distributions of closely-related headwater endemic fishes across the Guiana Shield highlands, mostly upstream of major waterfalls, is passive geodispersal via headwater capture. However, an alternative 'relictual distribution' hypothesis can be proposed based on the historical existence and relatively recent breakup of the proto-Berbice paleodrainage, which was comparable in size to the modern Orinoco and drained the southern slope of the western Guiana Shield eastward to the Atlantic from the Late Cretaceous to the Pliocene (Lujan and Armbruster, 2011). Headwaters of several north- or west-flowing tributaries of the modern Orinoco, such as the Ventuari, Caura, and Caroni, may have flowed south and east into the proto-Berbice during this period, before tectonic shifts, fault reactivation, and increased Amazon head-cutting divided the proto-Berbice into portions of the modern Orinoco, Branco, Essequibo, and Berbice watersheds (Lujan and Armbruster, 2011). If upland Guiana Shield taxa such as *Exastilithoxus* and *Brachyglanis* were once widely and contiguously distributed across headwaters of the proto-Berbice, then their modern disjunt populations may be relicts left after breakup of the proto-Berbice and the changing drainage affiliation of its headwaters.

In contrast to *Brachyglanis*, the *Leptorhamdia* clade has a predominantly lowland distribution, being locally abundant in rocky shoals of the lower Ventuari, upper Orinoco, and Xingu main river channels. The only member of this clade known from Guyana is the type species *L. essequibensis* (Eigenmann 1912), which has not been collected from the Essequibo since it was first collected by Eigenmann in 1908. Although we were only able to include in this study a sample from the upper Orinoco River identified as *L.* cf. *essequibensis* based on morphological similarity to the nominal species, this morphological similarity indicates a biogeographical connection between the upper Orinoco and Essequibo. There is currently no contiguous, lowland, hydrological corridor between the upper Orinoco and the Essequibo. Hydrologic continuity is disrupted by the 'Rupununi Portal,' which is a seasonally flooded savannah between the Essequibo and upper Branco that lacks suitable habitat for *Leptorhamdia*. Historically, though, the proto-Berbice had a large main river channel that flowed through the Rupununi Savannah region and united the modern upper Branco/Negro with the Essequibo, possibly as late as the Pliocene. The upper portion of the proto-Berbice main river channel is now the main channel of the Uraricoera River, a tributary of the upper Branco in northernmost Brazil. Given the Uraricoera's historical position at the center of the upper proto-Berbice, it is a critical watershed to examine for clues to broader biogeographical patterns across the western Guiana Shield. Unfortunately, we are unaware of any Brachyglaniini having been reported from the Uraricoera. Most of this important drainage remains poorly sampled, making it a high priority for future fieldwork.

5. Conclusions

New well-resolved phylogenetic hypotheses for the neotropical three-barbeled catfish family Heptapteridae are largely consistent with relationships previously hypothesized based on morphological data. Combined morphological and molecular evidence support the recognition of two newly circumscribed subfamilies (Rhamdiinae and Heptapterinae) that are each subdivided into two new tribes (Goeldiellini and Rhamdiini; Heptapterini and Brachyglaniini). Tribe Brachyglaniini is distributed mostly around the western Guiana Shield in southern Venezuela and western Guyana, but contains one upper Amazon lineage and two independent Brazilian Shield lineages. Phylo-distributional patterns in Brachyglaniini across the western Guiana Shield suggest that active dispersal or, more likely, passive range expansions/contractions (driven in part by break-up of the proto-Berbice paleodrainage) have been important drivers of allopatric diversification in this clade. Differentiating hypotheses based on dispersal versus range expansion/contraction will require more dense geographic sampling overall, and especially denser sampling of Brazil's Uraricoera River watershed.

Authorship contribution statement

Conceptualization: DRFF and NKL. Formal Analysis, Data curation and Methodology: DRFF and VMV. Writing – original draft: DRFF and NKL. Writing – review: NRL and VMV. Supervision, Funding acquisition and Validation: NKL and NRL.

Declaration of Competing Interest

The authors declare that they have no known competing financial interests or personal relationships that could have appeared to influence the work reported in this paper.

Acknowledgements

We thank Oscar Leon Mata (*in memorium*) and Donald Taphorn for facilitating fieldwork in Venezuela and the Inter-American Development Bank for facilitating fieldwork in Guyana. We thank Barbara Brown (*in memorium*), Radford Arrindell, Tom Vigliota, and Chloe Lewis (AMNH), Mark Sabaj and Mariangeles Arce (ANSP), Jonathan W. Armbruster and David C. Werneke (AUM), Dave Catania, Jon Fong, and Luiz Rocha (CAS), Don Stacey, Mary Burridge, Erling Holm and Marg Zur (ROM),

Caleb McMahan and Susan Mochel (FMNH), Luiz Malabarba and Juliana Wingert (UFRG), Lynne Parenti, Jeff Clayton, and Sandra Raredon (USNM) for facilitating access to loans of type and non-type specimens and tissues. Research and travel by DRFF and VMV were supported by CAPES (Coordenação de Aperfeiçoamento de Pessoal de Nível Superior; Process number 88881.188697/2018-01 to VMV) and by an award to DRFF from the Royal Ontario Museum E.J. Crossman Endowment Fund. NKL was supported by a Gerstner Fellowship from the Richard Gilder Graduate School at the American Museum of Natural History. NRL was supported by an NSERC Discovery Grant. Fieldwork generating specimens for this study was funded by the National Science Foundation via NSF DEB-0315963 (All Catfish Species Inventory) and NSF OISE-1064578 (International Research Fellowship), grants from the Coypu Foundation of New Orleans, and gifts from Aquatic Critter Inc. in Nashville, TN, via Chris and Wendy Beggin.

Appendix A. Supplementary data

Supplementary data to this article can be found online at https://doi.org/10.1016/j.ympev.2021.107186.

References

Arcila, D., Ortí, G., Vari, R., Armbruster, J.W., Stiassny, M.L., Ko, K.D., Sabaj, M.H., Lundberg, J.L., Revell, L.J., Betancur-R, R., 2017. Genome-wide interrogation advances resolution of recalcitrant groups in the tree of life. Nat. Ecol. Evol. 1 (2), 1–10. https://doi.org/10.1038/s41559-016-0020.

Arratia, G., 1992. Development and variation of the suspensorium of primitive catfishes (Teleostei: Ostariophysi) and their phylogenetic relationships. Bonner Zoologische Monographien 32, 1–149.

Betancur-R, R., Wiley, E.O., Arratia, G., Arturo, A., Bailly, N., Miya, M., Lecointre, G., Ortí, G., 2017. Phylogenetic classification of bony fishes. BMC Evol. Biol. 12, 162. https://doi.org/10.1186/s12862-017-0958-3.

Bleeker, P., 1862. Atlas Ichthyologique des Indes Orientales Néerlandaises, publié sous le auspices du Gouvernement Colonial Néerlandais. Siluroïdes, Characïdes et Hétérobranchoïdes. Amsterdam, De Breuk & Smits, Tome II, p. 112.

Bockmann, F.A., 1994. Description of *Mastiglanis asopos*, a new pimelodid catfish from northern Brazil, with comments on phylogenetic relationships inside the subfamily Rhamdiinae (Siluriformes: Pimelodidae). Proc. Biol. Soc. Wash. 107, 760–777.

Bockmann, F.A., 1998. Análise filogenética da família Heptapteridae (Teleostei: Ostariophysi: Siluriformes) e redefinição de seus gêneros. Universidade de São Paulo, São Paulo. [Tese de doutorado não publicada].

Bockmann, F.A., Guazzelli, G.M., 2003. Heptapteridae (Heptapterids). In: Reis, R.E., Kullander, S.O., Ferraris, C.J. (Eds.), Checklist of the freshwater fishes of South and Central America. Edipucrs, Porto Alegre, Brazil, pp. 406–431.

Bockmann, F.A., Castro, R.M.C., 2010. The blind catfish from the caves of Chapada Diamantina, Bahia, Brazil (Siluriformes: Heptapteridae): description, anatomy, phylogenetic relationships, natural history, and biogeography. Neotrop. Ichthyo. 8, 673–706. https://doi.org/10.1590/S1679-62252010000400001.

Bockmann, F.A., Ferraris Jr., C.J., 2005. Systematics of the Neotropical catfish genera *Nemuroglanis* Eigenmann and Eigenmann 1889, *Imparuriis* Schultz 1944, and *Meleneichthys* Dahl 1961 (Siluriformes: Heptapteridae). Copeia 2005, 124–137. https://doi.org/10.1643/CI-04-019R1.

Bockmann, F.A., Miquelarena, A.M., 2008. Anatomy and phylogenetic relationships of a new catfish species from northeastern Argentina with comments on the phylogenetic relationships of the genus *Rhamdella* Eigenmann and Eigenmann 1888 (Siluriformes, Heptapteridae). Zootaxa 1780, 1–54. https://doi.org/10.11646/zootaxa.1780.1.1.

Bockmann, F.A., Slobodian, V., 2017. Family Heptapteridae – three-barbeled catfishes. In: van der Sleen, P., Albert, J.S. (Eds.), Field Guide to the Fishes of the Amazon, Orinoco & Guianas. Princeton University Press, Princeton, pp. 233–252.

Buckup, P.A., 1988. The genus Heptapterus (Teleostei, Pimelodidae) in southern Brazil and Uruguay, with the description of a new species. Copeia 641–653.

Collins, R.A., Bifi, A.G., de Oliveira, R.R., Ribeiro, R.D., Lujan, N.K., Rapp Py-Daniel, L. H., Hrbek, T., 2018. Biogeography and species delimitation of the rheophilic suckermouth catfish genus *Pseudolithoxus* (Siluriformes: Loricariidae), with the description of a new species from the Brazilian Amazon. Syst. Biodivers. 16 (6), 538–550.

DoNascimiento, C., Lundberg, J.G., 2005. *Myoglanis aspredinoides* (Siluriformes: Heptapteridae), a new catfish from the Río Ventuari, Venezuela. Zootaxa 1009, 37–49. https://doi.org/10.11646/zootaxa.1009.1.4.

DoNascimiento, C., Milani, N., 2008. The Venezuelan species of Phenacorhamdia (Siluriformes: Heptapteridae), with the description of two new species and a remarkable new tooth morphology for siluriforms. Proc. Acad. Natl. Sci. Philadelphia 157 (1), 163–180. https://doi.org/10.1635/0097-3157(2008)157[163:TVSOPS]2.0.CO;2.

Edgar, R.C., 2004. MUSCLE: multiple sequence alignment with high accuracy and high throughput. Nucleic Acids Res. 32, 1792–1797. https://doi.org/10.1093/nar/gkh340.

Eigenmann, C.H., 1912. The freshwater fishes of the British Guiana, including a study of the ecological grouping of species and relation of the fauna of the plateau to that of the lowlands. Mem. Carnegie Mus. 5, 1–578. https://doi.org/10.5962/bhl.title.2174.

Faustino-Fuster, Dario R., Bockmann, Flávio A., Malabarba, Luiz R., 2019. Two new species of *Heptapterus* (Siluriformes: Heptapteridae) from the Uruguay River basin, Brazil. J. Fish Biol. 94 (3), 352–373. https://doi.org/10.1111/jfb.13908.

Ferraris Jr., C.J., 1988. Relationships of the neotropical catfish genus *Nemuroglanis*, with a description of a new species (Ostariophysi: Siluriformes: Pimelodidae). Proc. Biol. Soc. Wash. 101, 509–516.

Fricke, R., Eschmeyer, W.N., Van der Laan, R., (Eds.), 2020. Eschmeyer's catalog of fishes: genera, species, references. http://research.calacademy.org/research/ichthyology/catalog/fishcatmain.asp. Electronic version accessed 06 Apr 2020.

Geda, S.R., Lujan, N.K., Perkins, M., Abernethy, E., Sabaj, M.H., Gangloff, M., 2018. Multilocus phylogeny of the zebra mussel family Dreissenidae (Mollusca: Bivalvia) reveals a fourth Neotropical genus sister to all other genera. Mol. Phyl. Evol. 127, 1020–1033. https://doi.org/10.1016/j.ympev.2018.07.009.

Gill, T., 1861. Synopsis of the genera of the sub-family of Pimelodinae. Abbreviated Proc. Boston Soc. Nat. Hist. 8, 46–55.

Godlee, W.A., 1941. Synopsis of the genera of pimelodid catfishes without a free orbital rim. Stanford Ichthyological Bulletin 2, 83–88.

Grigio, R., Meurer, F., 2020. Alternating Nile tilapia (*Oreochromis niloticus*) and silver catfish (*Rhamdia quelen*) farming in recirculation system: A possibility for aquaculture in Southern Brazil. Brazilian Journal of Development 6, 35338–35356.

Hagelberg, E., 1994. Mitochondrial DNA from ancient bones. In: Hermann, B., Hummel, S. (Eds.), Ancient DNA. Springer-Verlag, New York, NY, pp. 195–204.

Lanfear, R., Calcott, B., Ho, S.Y.W., Guindon, S., 2012. PartitionFinder: combined selection of partitioning schemes and substitution models for phylogenetic analyses. Mol. Biol. Evol. 29, 1695–1701. https://doi.org/10.1093/molbev/mst020.

Lujan, N.K., Armbruster, J.W., 2011. The Guiana Shield. In: Albert, J., Reis, R. (Eds.), Historical Biogeography of Neotropical Freshwater Fishes. University of California Press, Berkeley, pp. 211–224.

Lujan, N.K., Weir, J.T., Noonan, B.P., Lovejoy, N.R., Mandrak, N.E., 2020a. Is Niagara Falls a barrier to gene flow in riverine fishes? A test using genome-wide SNP data from seven native species. Mol. Ecol. 29, 1235–1249. https://doi.org/10.1111/mec.15406.

Lujan, N.K., Armbruster, J.W., Lovejoy, N.R., 2016. Multilocus phylogeny, diagnosis and generic revision of the Guiana Shield endemic suckermouth armored catfish tribe Lithoxini (Loricariidae: Hypostominae). Zool. J. Linnean Soc. 184, 1169–1186.

Lujan, N.K., Armbruster, J.W., Werneke, D.C., Teixeira, T.F., Lovejoy, N.R., 2020b. Phylogeny and biogeography of the Brazilian-Guiana Shield endemic *Corymboplanes* clade of armoured catfishes (Loricariidae). Zool. J. Linnean Soc. 188, 1213–1235. https://doi.org/10.1093/zoolinnean/zlz090.

Lundberg, J.G., McDade, L.A., 1986. On the South American catfish *Brachyrhamdia imitator* Myers (Siluriformes, Pimelodidae), with phylogenetic evidence for a large intrafamilial lineage. Nat. Nat. 463, 1–24.

Lundberg, J.G., Bornbusch, A.H., Mago-Leccia, F., 1991. *Gladioglanis conquistador* n. sp., from Ecuador with diagnoses of the subfamilies Rhamdiinae Bleeker and Pseudopimelodinae n. subf. (Siluriformes, Pimelodidae). Copeia 1991, 190–200.

Machacek, H., 2019. World Records Freshwater Fishing http://www.fishing-worldrecords.com. Accessed 21 January 2021.

Miller, M.A., Pfeiffer, W., Schwartz, T., 2010. Creating the CIPRES Science Gateway for inference of large phylogenetic trees. Gateway Computing Environments Workshop (GCE). Local, Editors.

Myers, G.S., 1928. New fresh-water fishes from Peru, Venezuela, and Brazil. Ann. Mag. nat. Hist. 10, 83–90.

Mo, T., 1991. Anatomy, relationships and systematics of the Bagridae (Teleostei: Siluroidei) with a hypothesis of Siluroid phylogeny. Koeltz Scientific Books, Koenigstein, p. 216.

Oliveira, J.C., Britski, H.A., 2000. Redescrição de *Taunayia bifurciata* (Eigenmann & Norris, 1900), comb. Nova, um bagre endêmico do Estado de São Paulo (Siluriformes, Pimelodidae, Heptapterinae). Pap. Avulsos de Zool. 41, 119–133.

de Pinna, M.C.C., 1993. Higher-level phylogeny of Siluriformes, with a new classification of the order (Teleostei, Ostariophysi). The City University of New York, New York, 482 p. [Tese de doutorado não publicada].

Rambaut, A., Suchard, M., Xie, D., Drummond, A., 2013. Tracer v1.6. Available from http://tree.bio.ed.ac.uk/software/tracer/.

Ronquist, F., Huelsenbeck, J.P., 2003. MrBayes 3: Bayesian phylogenetic inference under mixed models. Bioinformatics 19, 1572–1574. https://doi.org/10.1093/bioinformatics/btg180.

Sabaj, M.H., 2019. Standard symbolic codes for institutional resource collections in herpetology and ichthyology: an online reference. Version 7.1 (21 March 2019). Electronically accessible at http://www.asih.org/. American Society of Ichthyologists and Herpetologists, Washington, DC [Google Scholar].

Sanger, F., Nicklen, S., Coulson, A.R., 1977. DNA sequencing with chain-terminating inhibitors. Proc. Natl. Acad. Sci. U. S. A. 74, 5463–5467. https://doi.org/10.1073/pnas.74.12.5463.

Silfvergip, A.M.C., 1996. A systematic revision of the neotropical catfish genus *Rhamdia*. Department of Vertebrate Zoology, Stockholm, p. 156.

Slobodian, V., Bockmann, F.A., 2013. A new *Brachyrhamdia* (Siluriformes: Heptapteridae) from Rio Japurá basin, Brazil, with comments on its phylogenetic affinities, biogeography and mimicry in the genus. Zootaxa 3717, 1–22. https://doi.org/10.11646/zootaxa.3717.1.1.

Smith, W.L., Stern, J.H., Girard, M.G., Davis, M.P., 2016. Evolution of venomous cartilaginous and ray-finned fishes. Integr. Comp. Biol. 56, 950–961.

Stamatakis, A., 2014. RaxML version 8: a tool for phylogenetic analysis and post-analysis of large phylogenies. Bioinformatics 30, 1312–1313. https://doi.org/10.1093/bioinformatics/btu033.

Stewart, D.J., 1986. A new pimelodid catfish from the deep-river channel of the Río Napo, eastern Ecuador (Pisces: Pimelodidae). Proc. Acad. Nat. Sci. Philadelphia. 38, 46–52.

Sullivan, J.P., Lundberg, J.G., Hardman, M., 2006. A phylogenetic analysis of the major groups of catfishes (Teleostei: Siluriforms) using RAG1 and RAG2 nuclear gene sequences. Mol. Biol. Evol. 41, 636–662. https://doi.org/10.1016/j.ympev.2006.05.044.

Sullivan, J.P., Muriel-Cunha, J., Lundberg, J.G., 2013. Phylogenetic relationships and molecular dating of the major groups of catfishes of the Neotropical superfamily Pimelodoidea (Teleostei, Siluriformes). Proc. Acad. Nat. Sci. Philadelphia 89–110.

Swarça, A.C., Caetano, L.G., Dias, A.L., 2000. Cytogenetics of species of the Pimelodidae and Rhamdiidae (Siluriformes). Genet. Mol. Biol. 23, 589–5 doi.org/10.1590/S1415-47572000000300015.

Further reading

Reckmann, F.A., Slobodian, V., 2013. Heptapteridae. In: Queiroz, L.J., Torre Vilara, G., Ohara, W.M., da Silva Pires, T.H., Zuanon, J., da Costa Doria, Peixes do Rio Madeira. Dialeto, São Paulo, Brazil, pp. 12–71.

Supplementary Material

Supplementary Table 1. Morphological characters list proposed by different authors to support the relationships within Heptapteridae.

Lundberg & McDade 1986	**1. Rhamdiinae:** Posterior limb of the fourth transverse process is laterally expanded above the swimbladder and deeply notched once to several times. **1.1. *Brachyrhamdia* subgroup:** Fifth Weberian transverse process smaller than the fourth, but similarly expanded and notched **1.2. Unnamed Group:** Fifth transverse process simple in form and displaced ventrally to partially enclose the swim bladder from behind
Ferraris 1988	***Nemuroglanis*-subclade:** i) Laminar portion of complex *centrum* transverse process, posterior to branched segment, is triangular and extends nearly to the lateral tip of fifth vertebral transverse process. ii) First dorsal-fin basal pterygiophore is inserted behind Weberian complex, usually above vertebrae 7 to 10. iii) Dorsal-fin spine" is thin and flexible and the dorsal-fin lock is absent. iv) Pectoral-fin "spine" is thin and flexible for its distal half, rather than pungent.
Lundberg et al., 1991	**1. Rhamdiinae:** i) Posterior limb of fourth transverse process laterally expanded above swimbladder and notched once to several rimes. ii) Neural spines of Weberian complex centrum joined by a straight-edged, horizontal or sometimes sloping bony lamina. iii) Process for insertion of levator operculi muscle on posterodorsal corner of hyomandibula greatly expanded. iv) Quadrate with free dorsal margin and bifid shape, its posterior and anterior limbs articulate separately with hyomandibula and metapterygoid. v) Presence of an anteriorly recurved process drawn out from ventrolateral corner of mesethmoid.

	1.1. Unnamed clade 1: Lack or reduction of a free orbital rim. **1.1.1. *Nemuroglanis*-subclade** i)Presence of an expanded, horizontal lamina caudal of branched posterior limb of fourth transverse process. ii) First dorsal-fin pterygiophore associated with neural spine of sixth, or more posterior, vertebra. iii) Loss of first dorsal-fin element (the first spine or "spinelet" that precedes the base of the well-developed dorsal spine of most catfished. iv) Dorsal spine thin and flexible with many distal unfused segments. v) Pectoral spine thin, proximally co-ossified and flexible distally with many unfused segments. **1.1.2. Unnamed Group** Non-segmented and pungent pectoral-spines that bear strong posterior dentitions as in the majority of pimelodids and other catfishes. **1.2. Unnamed Clade 2** Free orbital rim
Bockmann 1994	**1. Rhamdiinae:** **1.1. *Nemuroglanis*-subclade:** i) Laminar portion of complex *centrum* transverse process, posterior to branched segment, is triangular and extends nearly to the lateral tip of fifth vertebral transverse process. ii) First dorsal-fin basal pterygiophore is inserted behind Weberian complex, usually above vertebrae 7 to 10. iii) "Dorsal-fin spine" is thin and flexible; iv) Dorsal-fin lock (= first dorsal-fin spine or spinelet) absent. v) Pectoral-fin "spine" is thin and flexible for its distal half, rather than pungent. vi) Mesocoracoid arch modified into a wide band. vii) Two posterior proximal radials of pectoral fin are enlarged and flattened. viii) pectoral girdle delicate, with a short mesial contact line comprising only three weakly joined scapulo-coracoid dentations. ix) Pointed process projected posteroventrally from the coracoid keel absent. x) Posterior chambers of swimbladder atrophied, conforming a bilobed, transversely aligned structure.

	xi) Nasal bone long and weakly ossified. xii) Ridges of neural arch of the fourth vertebra absent. xiii) Presence of a distinct deep medial notch which divides the posterior limb of the fourth transverse process into two divergent, approximately symmetrical, long arms. xiv) Tips of the parapophyses of anterior free vertebrae distally expanded and ventrally concave. xv) Hemal and neural spines of the caudal vertebrae oriented at about 35° to the vertebral column axis. xvi) Hemal and neural spines of the last free precaudal vertebrae robust. **1.1.1. Unnamed clade 1:** Triangular posterior lamina of the complex centrum transverse process has at its distal angle an additional notch. **1.1.2. Unnamed clade 2:** Triangular posterior lamina of the complex centrum transverse process has at its distal angle without an additional notch.
Bockmann & Guazzelli, 2003	**Heptapteridae** i) skin naked. ii) cutaneous laterosensory canals simple (few species have branched laterosensory canals on the head and anterior trunk). iii) small sized, usually with 20 cm SL or less (species of *Goediella, Rhamdella*, *Pimelodella*, *Rhamdia*, *Rhamdioglanis*, can exceed). iv) nares well separated and lacking barbels. v) 3 pairs of barbels: maxillary, inner and outer mentals. vi) adipose fin well developed. vii) caudal fin deeply forked, emarginate, rounded, or lanceolate. viii) gill membranes free, branchial openings not restricted. ix) orbital rim free or not. x) first dorsal- and pectoral-fin rays varying from having pungent spines to completely flexible or mostly segmented.

Supplementary Table 2. Primers and annealing temperatures (*Ta*) for PCR for all markers.

Gene	Primers	Sequences	Ta (°C)	Reference
coI	FishF1 FishR1	TCA ACC AAC CAC AAA GAC ATT GGC AC TAG ACT TCT GGG TGG CCA AAG AAT CA	52	Ward et al. (2005)
cytb	GLUDG-L CB3-H	TGA CCT GAA RAA CCA YCG TTG GGC AAA TAG GAA RTA TCA TTC	48	Palumbi (1996)
nd2	nd2_f nd2 _r	AGC TTT TGG GCC CAT ACC CCA AGG RAC TAG GAG ATT TTC ACT CCT GCT	58	Arroyave et al. (2013)
glyt	F577 R1464	ACA TGG TAC CAG TAT GGC TTT GT GTA AGG CAT ATA SGT GTT CTC TCC	56	Li et al. (2007)
rag2	MHF1 MHR1	TGy TAT CTC CCA CCT CTG CGy TAC C TCA TCC TCC TCA TCk TCC TCw TTG TA	58	Hardman (2004)

Supplementary Table 3. Summary for each gene partitions and best molecular model of evolution based on Bayesian Information Criterion (BIC).

Subset	Locus	Codon Position	Range in alignment	Length (bp)	Best model
1	*coI*	1		229	GTR+I+G
2	*coI*	2	1 – 686	229	HKY+I
3	*coI*	3		228	GTR+G
4	*cytb*	1		282	SYM+I+G
5	*cytb*	2	687 – 1531	282	GTR+I+G
6	*cytb*	3		281	GTR+G
7	*nd2*	1		287	GTR+I+G
8	*nd2*	2	1532 – 2393	287	HKY+I+G
9	*nd2*	3		288	GTR+G
10	glyt	1		285	K80+G
11	glyt	2	2394 – 3247	285	F81+I
12	glyt	3		284	K80+G
13	rag2	1		303	K80+G
14	rag2	2	3248 – 4156	303	K80+I
15	rag2	3		303	K80+G
Total			4156	4156	

Supplementary Figure 1. Phylogenetic hypothesis for interrelationships of Heptapteridae based on maximum likelihood analysis of 686 bp alignment of the *coI* mitochondrial gene region. Node numbers correspond to bootstrap support values (ML).

Supplementary Figure 2. Phylogenetic hypothesis for interrelationships of Heptapteridae based on maximum likelihood analysis of an 845 bp alignment of the c*ytb* mitochondrial gene region. Node numbers correspond to bootstrap support values (ML).

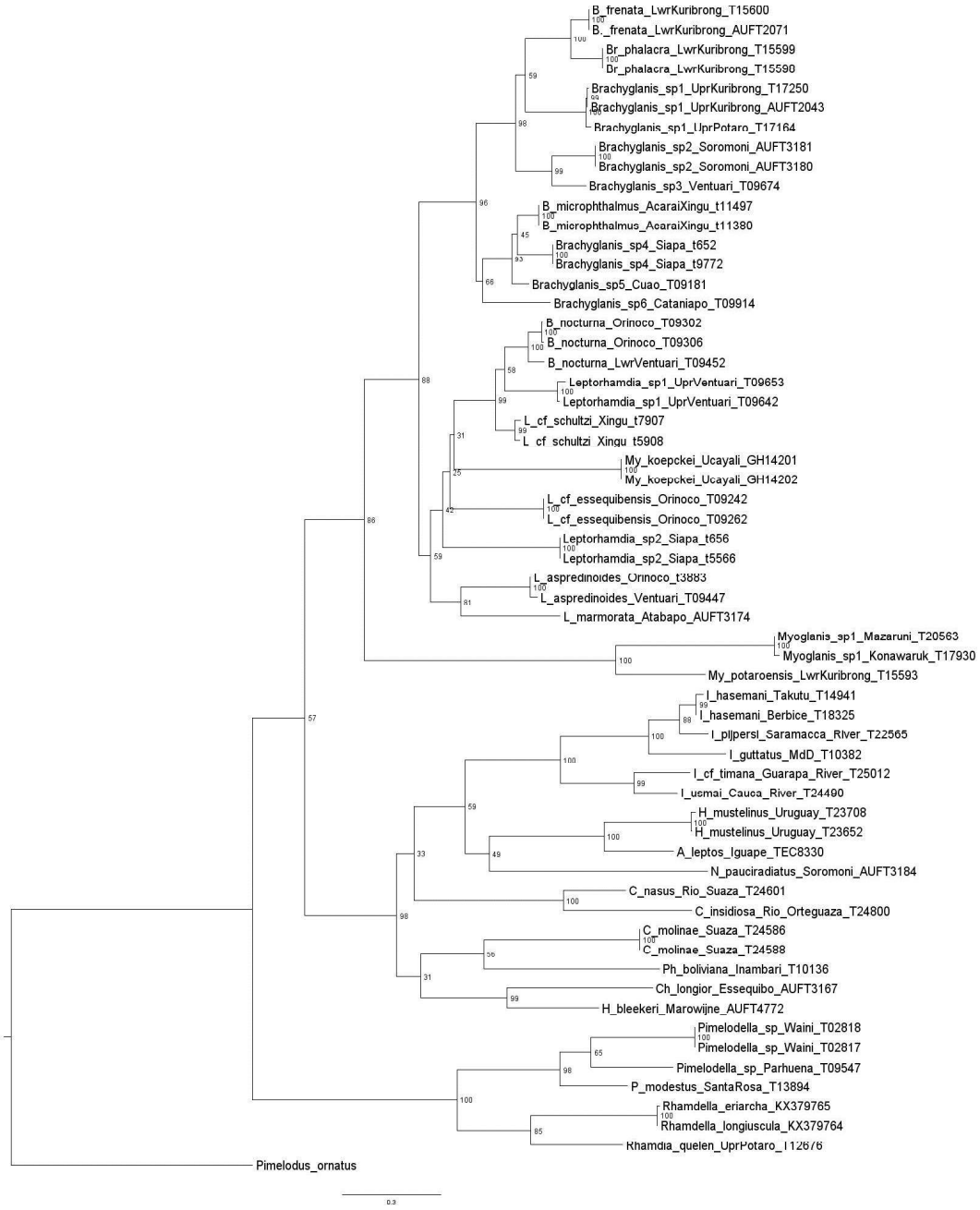

Supplementary Figure 3. Phylogenetic hypothesis for interrelationships of Heptapteridae based on maximum likelihood analysis of an 862 bp alignment of the *nd2* mitochondrial gene region. Node numbers correspond to bootstrap support values (ML).

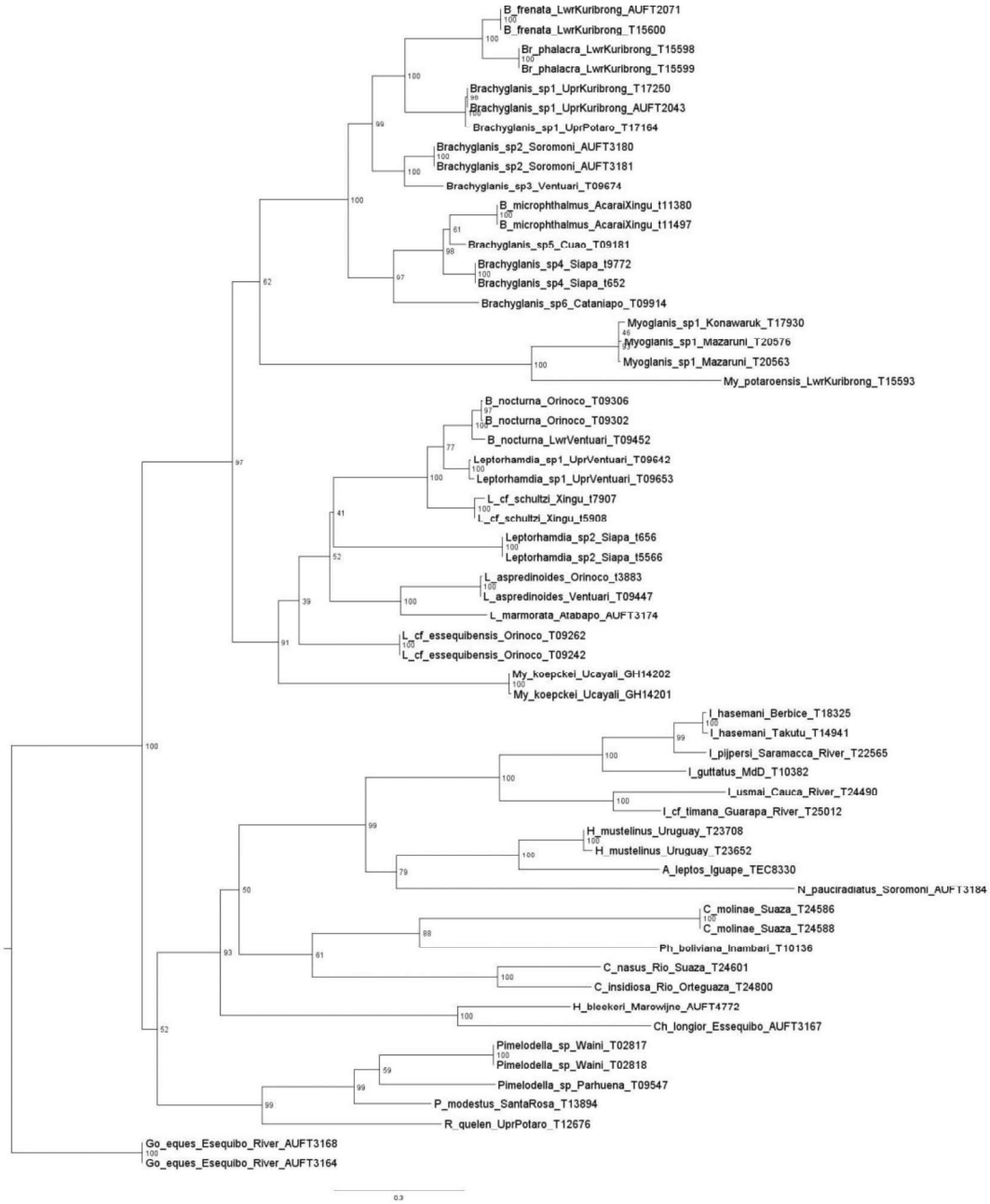

Supplementary Figure 4. Phylogenetic hypothesis for interrelationships of Heptapteridae based on maximum likelihood analysis of 856 bp alignment of the glyt nuclear gene region. Node numbers correspond to bootstrap support values (ML).

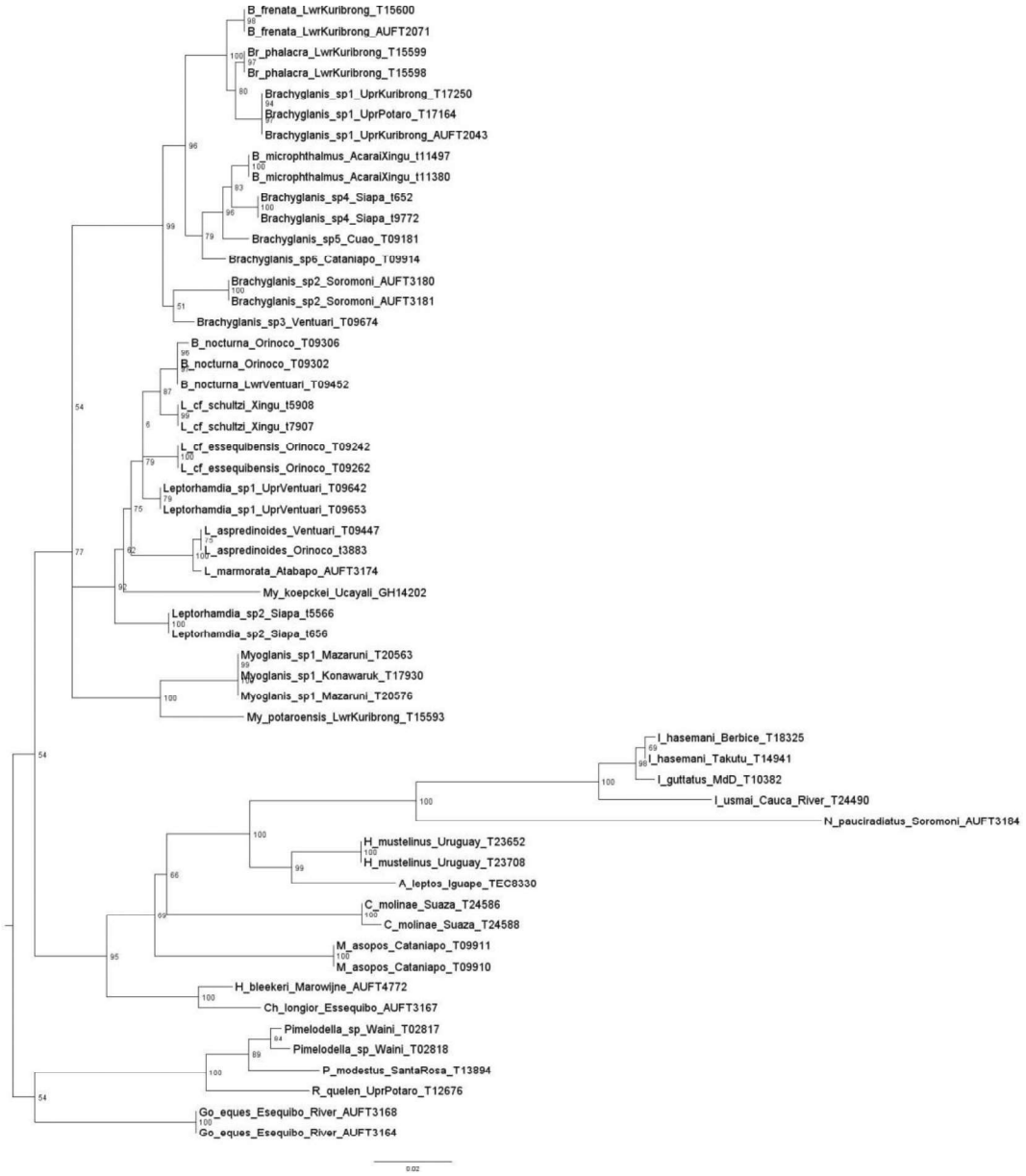

Supplementary Figure 5. Phylogenetic hypothesis for interrelationships of Heptapteridae based on maximum likelihood analysis of 979 bp alignment of the rag2 nuclear gene region. Node numbers correspond to bootstrap support values (ML).

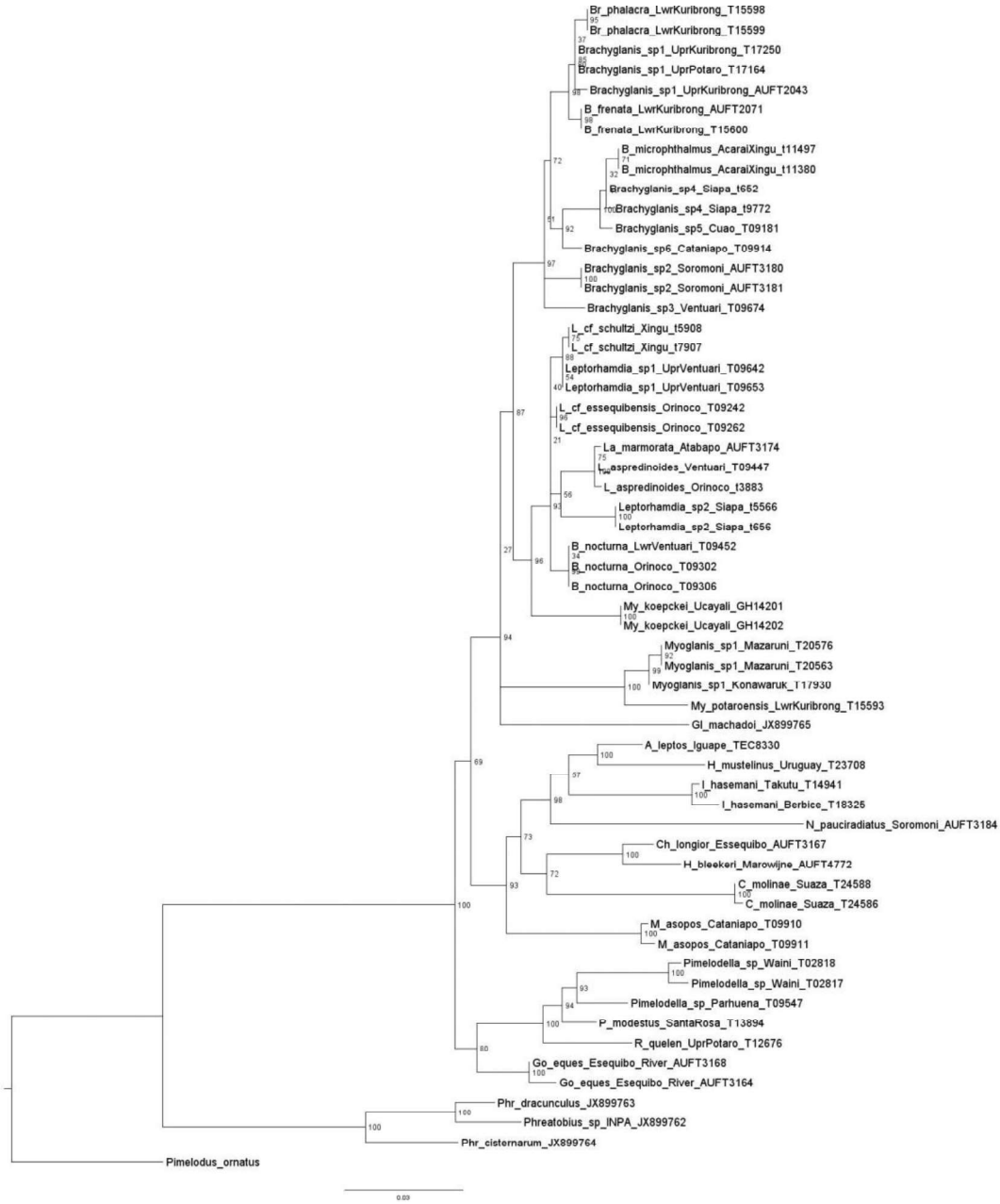

Supplementary Newick tree 1: COI

((((((((((Brachyglanis_sp1_UprKuribrong_AUFT2043:0.0041722851855294785,Brachyglanis_sp1_UprKuribrong_T17250:1.0000005001842283E-6):0.005620451645144797,Brachyglanis_sp1_UprPotaro_T17164:0.020541500253886902):0.08824598399786643,(B_frenata_LwrKuribrong_AUFT2071:1.0000005001842283E-6,B_frenata_LwrKuribrong_T15600:0.003985223334792121):0.14042923547812958):0.07475985883957792,Brachyglanis_sp3_Ventuari_T09674:0.04229310528279395):0.020032437793090274,(Brachyglanis_sp2_Soromoni_AUFT3180:1.0000005001842283E-6,Brachyglanis_sp2_Soromoni_AUFT3181:0.004002684419310842):0.049650216674460346):0.07116298933215814,((((Brachyglanis_sp4_Siapa_t9772:1.0000005001842283E-6,Brachyglanis_sp4_Siapa_t652:1.0000005001842283E-6):0.08695240522865477,(B_microphthalmus_AcaraiXingu_t11380:1.0000005001842283E-6,B_microphthalmus_AcaraiXingu_t11497:1.0000005001842283E-6):0.05882952224149296):0.02181366550155639,Brachyglanis_sp5_Cuao_T09181:0.009037348970199588):0.1118339151228036,Brachyglanis_sp6_Cataniapo_T09914:0.13079242665645419):0.029890602296249735):0.20940068390085553,(((((B_nocturna_Orinoco_T09302:0.0039012511677178896,B_nocturna_Orinoco_T09306:1.0000004999621837E-6):0.02849121216366246,B_nocturna_LwrVentuari_T09452:0.03313134006215823):0.08915599482617709,(Leptorhamdia_sp1_UprVentuari_T09653:0.003950328698954397,Leptorhamdia_sp1_UprVentuari_T09642:1.0000005001842283E-6):0.028115109369305058):0.1932132119059531,(L_cf_essequibensis_Orinoco_T09242:0.002483300737897931,L_cf_essequibensis_Orinoco_T09262:0.005058970546909736):0.23679317219593132):0.05604670574711346,((L_aspredinoides_Ventuari_T09447:0.007550556570168343,L_aspredinoides_Orinoco_t3883:1.0000005001842283E-6):0.23314971589442557,L_marmorata_Atabapo_AUFT3174:0.14239386447685742):0.09223600115746455):0.030756115787326177):0.020049392150870204,((My_koepckei_Ucayali_GH14201:1.0000004999621837E-6,My_koepckei_Ucayali_GH14202:1.0000004999621837E-6):0.3401516040075263,My_potaroensis_LwrKuribrong_T15593:0.47968276206032323):0.15753928999572153):0.052171010277000995,(Leptorhamdia_sp2_Siapa_t5566:1.0000004999621837E-6,Leptorhamdia_sp2_Siapa_t656:1.0000004999621837E-6):0.30586696942763925):0.11890691171485956,(((((((I_pijpersi_Saramacca_River_T22565:0.12269430419556349,I_hasemani_Berbice_T18325:1.0000005001842283E-6):0.008256562161352399,I_hasemani_Takutu_T14941:0.013063103242084484):0.1974532461115288,I_guttatus_MdD_T10382:0.22828404560419768):0.2967545970940102,I_cf_timana_Guarapa_River_T25012:0.15419213621370842):0.19750511883073107,N_pauciradiatus_Soromoni_AUFT3184:0.5861944925513387):0.26378564509267544,(C_nasus_Rio_Suaza_T24601:0.23476836797721012,C_insidiosa_Rio_Orteguaza_T24800:0.22990405649523482):0.257219484320651):0.1574170373073096,(((M_asopos_Cataniapo_T09910:1.0000005001842283E-6,M_asopos_Cataniapo_T09911:1.0000005001842283E-6):1.4486267681745846,Ph_boliviana_Inambari_T10136:0.4614782335508518):0.15556296034564232,(C_molinae_Suaza_T24588:1.0000004999621837E-6,C_molinae_Suaza_T24586:1.0000004999621837E-6):0.3281607351414093):0.14963884034201347):0.06864037916991617,(Ch_longior_Essequibo_AUFT3167:0.19948096490793277,H_bleekeri_Marowijne_AUFT4772:0.3796929458801708):0.24695132335681946):0.11210266439751759):0.09921246292096142,(((((Pimelodella_sp_Waini_T02817:1.0000004999621837E-6,Pimelodella_sp_Waini_T02818:1.0000004999621837E-6):0.22823679566735278,Pimelodella_sp_Parhuena_T09547:0.19637212934832404):0.05933651128189266,P_modestus_SantaRosa_T13894:0.14889509345065366):0.08849246504773278,R_quelen_UprPotaro_T12676:0.41005340035392934):0.2356751786162279,(Go_eques_Esequibo_River_AUFT3168:1.0000004999621837E-6,Go_eques_Esequibo_River_AUFT3164:1.0000004999621837E-6):0.4607074769557966):0.07299677513149838):0.6070211524266373,Pimelodus_ornatus:0.6070211524266376);

Supplementary Newick tree 2: CYTB

((((((((((B_frenata_LwrKuribrong_T15600:1.0000004999621837E-6,'B._frenata_LwrKuribrong_AUFT2071':1.0000004999621837E-
6):0.05573346456041195,(Br_phalacra_LwrKuribrong_T15599:1.0000004999621837E-
6,Br_phalacra_LwrKuribrong_T15598:1.0000004999621837E-
6):0.0976078192145935):0.13751186190748288,((Brachyglanis_sp1_UprKuribrong_T17250:0.0031347375599928284,Brachyglanis_sp1_
UprKuribrong_AUFT2043:1.0000004999621837E-
6):0.004704646272215118,Brachyglanis_sp1_UprPotaro_T17164:0.014741506463450182):0.18357588759778953):0.03055762014985719
,((Brachyglanis_sp2_Soromoni_AUFT3181:1.0000004999621837E-6,Brachyglanis_sp2_Soromoni_AUFT3180:1.0000004999621837E-
6):0.13217632273287627,Brachyglanis_sp3_Ventuari_T09674:0.10314732771594226):0.11093247016407126):0.11953782647108846,((((
B_microphthalmus_AcaraiXingu_t11497:1.0000004999621837E-6,B_microphthalmus_AcaraiXingu_t11380:1.0000004999621837E-
6):0.0646596698023032,(Brachyglanis_sp4_Siapa_t652:1.0000004999621837E-6,Brachyglanis_sp4_Siapa_t9772:1.0000004999621837E-
6):0.10624998929961094):0.017257249056475743,Brachyglanis_sp5_Cuao_T09181:0.0517470364499375):0.0883757684215627,Brachyg
lanis_sp6_Cataniapo_T09914:0.20594858860206933):0.02010988016747084):0.17413874601379575,(((((((B_nocturna_Orinoco_T09302
:0.002823033779609574,B_nocturna_Orinoco_T09306:0.006000461510761612):0.040329975962707376,B_nocturna_LwrVentuari_T0945
2:0.04901342203737569):0.07243113022516168,(Leptorhamdia_sp1_UprVentuari_T09653:0.02454287985486503,Leptorhamdia_sp1_Up
rVentuari_T09642:0.005774733437861945):0.16157842299731007):0.027789671902796353,(L_cf_schultzi_Xingu_t7907:0.01608622116
2067593,L_cf_schultzi_Xingu_t5908:0.013617044168859671):0.06032247544976177):0.12547499272631435,(My_koepckei_Ucayali_GH
14201:1.0000004999621837E-6,My_koepckei_Ucayali_GH14202:1.0000004999621837E-
6):0.5094011401880796):0.012816983489569056,(L_cf_essequibensis_Orinoco_T09242:1.0000004999621837E-
6,L_cf_essequibensis_Orinoco_T09262:1.0000004999621837E-
6):0.2849759133608005):0.022724206462716445,(Leptorhamdia_sp2_Siapa_t656:1.0000004999621837E-
6,Leptorhamdia_sp2_Siapa_t5566:1.0000004999621837E-
6):0.3570800436868089):0.03596432917535197,((L_aspredinoides_Orinoco_t3883:1.0000004999621837E-
6,L_aspredinoides_Ventuari_T09447:0.021006139028476367):0.21195780283601673,L_marmorata_Atabapo_AUFT3174:0.30170631357
434785):0.0917122920433513):0.03577487913859456):0.16644585539687573,((Myoglanis_sp1_Mazaruni_T20563:1.0000005001842283
E-
6,Myoglanis_sp1_Konawaruk_T17930:0.015503764862617508):0.4813492412777802,My_potaroensis_LwrKuribrong_T15593:0.2706501
653219022):0.7661478269161137):0.1806584113419627,(((((((I_hasemani_Takutu_T14941:0.021821204754230328,I_hasemani_Berbice_
T18325:1.0000004999621837E-
6):0.04999227575264853,I_pijpersi_Saramacca_River_T22565:0.08593213331047522):0.09519382234448992,I_guttatus_MdD_T10382:0
.23564886601369595):0.2672525929415923,(I_cf_timana_Guarapa_River_T25012:0.17049734391998284,I_usmai_Cauca_River_T24490:
0.1314934628497384):0.22370203103561748):0.29021697623323783,(((H_mustelinus_Uruguay_T23708:0.013692143617674235,H_must
elinus_Uruguay_T23652:0.002448924600917834 5):0.2643913189964773,A_leptos_Iguape_TEC8330:0.21097490493156323):0.34957832
365573394,N_pauciradiatus_Soromoni_AUFT3184:0.6644681548346041):0.07367011286721858):0.15569317300775953,(C_nasus_Rio_
Suaza_T24601:0.18960036771388555,C_insidiosa_Rio_Orteguaza_T24800:0.39138213307787884):0.4546574891195212):0.0528997105
71770564,(((C_molinae_Suaza_T24586:1.0000004999621837E-6,C_molinae_Suaza_T24588:1.0000004999621837E-
6):0.47468473751117135,Ph_boliviana_Inambari_T10136:0.5343556768626629):0.19227789653189964,(Ch_longior_Essequibo_AUFT31
67:0.4430227083679097,H_bleekeri_Marowijne_AUFT4772:0.2795874094947426):0.26326679651271756):0.07311522167865614):0.279
16543504789737):0.15890488131706548,((((Pimelodella_sp_Waini_T02818:1.0000005001842283E-
6,Pimelodella_sp_Waini_T02817:1.0000005001842283E-
6):0.3146004418870785,Pimelodella_sp_Parhuena_T09547:0.2489368563010661):0.09418521389921741,P_modestus_SantaRosa_T1389
4:0.204540433601494):0.31367860771758216,((Rhamdella_eriarcha_KX379765:0.007114634318261093,Rhamdella_longiuscula_KX379
764:1.0000005001842283E-
6):0.3839826566058764,Rhamdia_quelen_UprPotaro_T12676:0.27891835329633796):0.22473763184732687):0.622248601530142):0.733
645025358856,Pimelodus_ornatus:0.7336450253588562);

Supplementary Newick tree 3: ND2

((((((((B_frenata_LwrKuribrong_AUFT2071:1.0000004999621837E-6,B_frenata_LwrKuribrong_T15600:1.0000004999621837E-
6):0.04130770325138311,(Br_phalacra_LwrKuribrong_T15598:1.0000004999621837E-
6,Br_phalacra_LwrKuribrong_T15599:1.0000004999621837E-
6):0.08261775037834007):0.17948075372388939,((Brachyglanis_sp1_UprKuribrong_T17250:1.0000004999621837E-
6,Brachyglanis_sp1_UprKuribrong_AUFT2043:1.0000004999621837E-
6):0.004625302382119001,Brachyglanis_sp1_UprPotaro_T17164:0.010925100074488547):0.13919897646797597):0.07446535985230285
,((Brachyglanis_sp2_Soromoni_AUFT3180:1.0000004999621837E-6,Brachyglanis_sp2_Soromoni_AUFT3181:1.0000004999621837E-
6):0.06736988248244091,Brachyglanis_sp3_Ventuari_T09674:0.08909055225224627):0.07403338923519809):0.05606285764778818,((((
B_microphthalmus_AcaraiXingu_t11380:1.0000004999621837E-6,B_microphthalmus_AcaraiXingu_t11497:1.0000004999621837E-
6):0.10786545761356492,Brachyglanis_sp5_Cuao_T09181:0.03558062385394778):0.015903778853851636,(Brachyglanis_sp4_Siapa_t97
72:1.0000004999621837E-6,Brachyglanis_sp4_Siapa_t652:1.0000004999621837E-
6):0.07380273041084395):0.11432547281776206,Brachyglanis_sp6_Cataniapo_T09914:0.1962666062840146):0.10408392526853905):0.
20285062984824997,(((Myoglanis_sp1_Konawaruk_T17930:0.013260866013981687,Myoglanis_sp1_Mazaruni_T20576:0.005468760371
748704):1.0000005001842283E-
6,Myoglanis_sp1_Mazaruni_T20563:0.0026807605118310818):0.20102648438057757,My_potaroensis_LwrKuribrong_T15593:0.435724
868394304):0.6244339286856533):0.06275070837222496,((((((((B_nocturna_Orinoco_T09306:0.0026085661839727603,B_nocturna_Ori
noco_T09302:0.002252542660609702):0.020698863733294326,B_nocturna_LwrVentuari_T09452:0.028478721676264085):0.065656154
36760064,(Leptorhamdia_sp1_UprVentuari_T09642:0.0036596040340663993,Leptorhamdia_sp1_UprVentuari_T09653:0.0116454773249
79892):0.057905096788478216):0.03771361885010771,(L_cf_schultzi_Xingu_t7907:0.02233470396216397,L_cf_schultzi_Xingu_t5908:1
.0000004999621837E-6):0.10937074145512993):0.215018046905614,(Leptorhamdia_sp2_Siapa_t656:1.0000004999621837E-
6,Leptorhamdia_sp2_Siapa_t5566:1.0000004999621837E-
6):0.38784105362789223):0.009515952482837875,((L_aspredinoides_Orinoco_t3883:0.00240850633162748,L_aspredinoides_Ventuari_T
09447:1.0000004999621837E-
6):0.18318512000111786,L_marmorata_Atabapo_AUFT3174:0.19734068955775985):0.1639832622615378):0.06982522000426572,(L_cf
_essequibensis_Orinoco_T09262:1.0000004999621837E-6,L_cf_essequibensis_Orinoco_T09242:1.0000004999621837E-
6):0.23046853816388024):0.04828045241177148,(My_koepckei_Ucayali_GH14202:1.0000004999621837E-
6,My_koepckei_Ucayali_GH14201:0.0030000447590556867):0.5313735247001068):0.10539035999891344):0.20678037876601785,((((((
(I_hasemani_Berbice_T18325:0.007229716096989192,I_hasemani_Takutu_T14941:0.010934075850244529):0.06664321717559463,I_pij
persi_Saramacca_River_T22565:0.07446101348326661):0.16453140032350033,I_guttatus_MdD_T10382:0.19220708452315316):0.23672
84345630467,(I_usmai_Cauca_River_T24490:0.2571429917912358,I_cf_timana_Guarapa_River_T25012:0.1082475447065867):0.262399
3153879949):0.30724960345213637,(((H_mustelinus_Uruguay_T23708:1.0000005001842283E-
6,H_mustelinus_Uruguay_T23652:0.01895819187176606):0.14887174044413332,A_leptos_Iguape_TEC8330:0.3224151845756942):0.28
249122502611534,N_pauciradiatus_Soromoni_AUFT3184:0.9155326515280264):0.07037508913722945):0.2906173132390295,(((C_moli
nae_Suaza_T24586:1.0000004999621837E-6,C_molinae_Suaza_T24588:1.0000004999621837E-
6):0.6441123155030408,Ph_boliviana_Inambari_T10136:0.5445977404609199):0.2468858506230338,(C_nasus_Rio_Suaza_T24601:0.23
59065300592198,C_insidiosa_Rio_Orteguaza_T24800:0.2149469286739878):0.4262041163043446):0.16821101427541052):0.043319181
32643864,(H_bleekeri_Marowijne_AUFT4772:0.25867010305764193,Ch_longior_Essequibo_AUFT3167:0.4442367352140373):0.54523
03039870254):0.14531935158142595,((((Pimelodella_sp_Waini_T02817:1.0000004999621837E-
6,Pimelodella_sp_Waini_T02818:1.0000004999621837E-
6):0.26162906199194835,Pimelodella_sp_Parhuena_T09547:0.2650806591629742):0.05891885766141125,P_modestus_SantaRosa_T138
94:0.177237646099474):0.21189130761714492,R_quelen_UprPotaro_T12676:0.41312234836436):0.24077996281849012):0.0337284020
2804195):0.30062970066510303,(Go_eques_Esequibo_River_AUFT3168:1.0000004999621837E-
6,Go_eques_Esequibo_River_AUFT3164:1.0000004999621837E-6):0.30062970066510314);

Supplementary Newick tree 4: GLYT

((((((((((Brachyglanis_sp1_UprKuribrong_T17250:1.0000005000176948E-
6,Brachyglanis_sp1_UprPotaro_T17164:1.0000005000176948E-6):1.0000005000176948E-
6,Brachyglanis_sp1_UprKuribrong_AUFT2043:1.0000005000176948E-
6):0.006750256890865863,(Br_phalacra_LwrKuribrong_T15599:1.0000005000176948E-
6,Br_phalacra_LwrKuribrong_T15598:1.0000005000176948E-
6):0.002230072807720529):0.002263398425639801,(B_frenata_LwrKuribrong_T15600:1.0000005000176948E-
6,B_frenata_LwrKuribrong_AUFT2071:1.0000005000176948E-
6):0.004453487654823202):0.010737569854011877,((((B_microphthalmus_AcaraiXingu_t11497:1.0000005000176948E-
6,B_microphthalmus_AcaraiXingu_t11380:1.0000005000176948E-
6):0.004476473954264898,(Brachyglanis_sp4_Siapa_t652:1.0000005000176948E-
6,Brachyglanis_sp4_Siapa_t9772:1.0000005000176948E-
6):0.006773008878342673):0.002301167843945684,Brachyglanis_sp5_Cuao_T09181:0.006774395086749318 6):0.005274295520935557,
Brachyglanis_sp6_Cataniapo_T09914:0.006042844925153418):0.004330788757507767):0.005836580070050196,((Brachyglanis_sp2_Sor
omoni_AUFT3180:1.0000005000176948E-6,Brachyglanis_sp2_Soromoni_AUFT3181:1.0000005000176948E-
6):0.014177822587340835,Brachyglanis_sp3_Ventuari_T09674:0.005326748249419491):0.002741337151964312 6):0.0235667500588655
2,((((((((B_nocturna_Orinoco_T09306:0.002811751712363853,B_nocturna_Orinoco_T09302:1.0000005000315726E-
6):1.0000005000315726E-6,B_nocturna_LwrVentuari_T09452:1.0000005000315726E-
6):0.004482374444326503 4,(L_cf_schultzi_Xingu_t5908:1.0000005000315726E-6,L_cf_schultzi_Xingu_t7907:1.0000005000315726E-
6):0.004526125645347517):0.004477201277079262,(L_cf_essequibensis_Orinoco_T09242:1.0000005000315726E-
6,L_cf_essequibensis_Orinoco_T09262:1.0000005000315726E-6):0.009025627041347031):1.0000005000315726E-
6,(Leptorhamdia_sp1_UprVentuari_T09642:1.0000005000315726E-6,Leptorhamdia_sp1_UprVentuari_T09653:1.0000005000315726E-
6):0.004482729480112343 5):0.003077131620434076,((L_aspredinoides_Ventuari_T09447:1.0000005000176948E-
6,L_aspredinoides_Orinoco_t3883:1.0000005000176948E-
6):0.002201658325680838 6,L_marmorata_Atabapo_AUFT3174:0.002211823430659426 4):0.01600686988865481):0.00187455045776878
38,My_koepckei_Ucayali_GH14202:0.035260668016163815):0.002320212077817643 3,(Leptorhamdia_sp2_Siapa_t5566:1.000000500031
5726E-6,Leptorhamdia_sp2_Siapa_t656:1.0000005000315726E-
6):0.013929090929918356):0.011079812090562274):1.0000005000315726E-
6,(((Myoglanis_sp1_Mazaruni_T20563:1.0000005000176948E-6,Myoglanis_sp1_Konawaruk_T17930:1.0000005000176948E-
6):1.0000005000176948E-6,Myoglanis_sp1_Mazaruni_T20576:1.0000005000176948E-
6):0.020048292415063 77,My_potaroensis_LwrKuribrong_T15593:0.021588566189260 82):0.022923424422811547):0.0096278718710653
41,((((((((I_hasemani_Berbice_T18325:0.002479020854834868,I_hasemani_Takutu_T14941:1.0000005000176948E-
6):0.002503030183131111,I_guttatus_MdD_T10382:0.004924702987300772):0.009569102085098383,I_usmai_Cauca_River_T24490:0.0
29197514115730586):0.04719184803697653,N_pauciradiatus_Soromoni_AUFT3184:0.104800436843318):0.04309696106056596,((H_m
ustelinus_Uruguay_T23652:1.0000005000176948E-6,H_mustelinus_Uruguay_T23708:1.0000005000176948E-
6):0.017948684133503534,A_leptos_Iguape_TEC8330:0.026868165770461888):0.010816095555290256):0.021582953856182807,(C_mol
inae_Suaza_T24586:1.0000005000315726E-
6,C_molinae_Suaza_T24588:0.005020389354945323):0.05043451405726035):0.003150817144558185,(M_asopos_Cataniapo_T09911:1.0
000005000315726E-6,M_asopos_Cataniapo_T09910:1.0000005000315726E-
6):0.0463023333778903):0.012356370193979407,(H_bleekeri_Marowijne_AUFT4772:0.008664742952822754,Ch_longior_Essequibo_A
UFT3167:0.01606836601843563):0.02378644811991408):0.018646202234736675):0.011250052397990914,(((Pimelodella_sp_Waini_T0
2817:0.002751035397386303 3,Pimelodella_sp_Waini_T02818:0.00499575728554949):0.005723111798695196,P_modestus_SantaRosa_T
13894:0.018299972545904736):0.011036994940973793,R_quelen_UprPotaro_T12676:0.02671318708558132):0.044341810793974604):0
.020860662209423134,(Go_eques_Esequibo_River_AUFT3168:1.0000005000176948E-
6,Go_eques_Esequibo_River_AUFT3164:1.0000005000176948E-6):0.02086066220942312);

Supplementary Newick tree 5: ND2

((((((((((((L_cf_schultzi_Xingu_t5908:1.0000005000454504E-6,L_cf_schultzi_Xingu_t7907:1.0000005000454504E-
6):0.001548281716646005,(Leptorhamdia_sp1_UprVentuari_T09642:1.0000005000454504E-
6,Leptorhamdia_sp1_UprVentuari_T09653:1.0000005000454504E-6):1.0000005000176948E-
6):0.0031057564028378337,(L_cf_essequibensis_Orinoco_T09242:1.0000005000176948E-
6,L_cf_essequibensis_Orinoco_T09262:1.0000005000176948E-6):0.001551450922511854 5):1.0000005000176948E-
6,(((La_marmorata_Atabapo_AUFT3174:0.0015384916276384442,L_aspredinoides_Ventuari_T09447:1.0000005000176948E-
6):1.0000005000176948E-
6,L_aspredinoides_Orinoco_t3883:0.0016271370893973791):0.008594792265866347,(Leptorhamdia_sp2_Siapa_t5566:1.00000050004545
04E-6,Leptorhamdia_sp2_Siapa_t656:1.0000005000454504E-
6):0.013933583010814127):0.002639884381978763):1.0000005000176948E-
6,((B_nocturna_LwrVentuari_T09452:1.0000005000454504E-6,B_nocturna_Orinoco_T09302:1.0000005000454504E-
6):1.0000005000176948E-6,B_nocturna_Orinoco_T09306:1.0000005000176948E-
6):0.004657613548299244):0.004723461728698752,(My_koepckei_Ucayali_GH14201:1.0000005000454504E-
6,My_koepckei_Ucayali_GH14202:1.0000005000454504E-
6):0.022580739221347124):0.004669372973952729,(((((((Br_phalacra_LwrKuribrong_T15598:1.0000005000176948E-
6,Br_phalacra_LwrKuribrong_T15599:1.0000005000176948E-
6):0.003105247827900559,(Brachyglanis_sp1_UprKuribrong_T17250:1.0000005000454504E-
6,Brachyglanis_sp1_UprPotaro_T17164:1.0000005000454504E-6):1.0000005000176948E-6):1.0000005000176948E-
6,Brachyglanis_sp1_UprKuribrong_AUFT2043:0.0031062300800233367):0.0015397584792447572,(B_frenata_LwrKuribrong_AUFT207
1:1.0000005000176948E-6,B_frenata_LwrKuribrong_T15600:1.0000005000176948E-
6):0.0031229706311620697):0.004709400540155784,(((((B_microphthalmus_AcaraiXingu_t11497:1.0000005000176948E-
6,B_microphthalmus_AcaraiXingu_t11380:1.0000005000176948E-
6):0.003115400614059405,Brachyglanis_sp4_Siapa_t652:1.0000005000454504E-6):1.0000005000176948E-
6,Brachyglanis_sp4_Siapa_t9772:0.00167504483254191 1):0.0015474687068377235,Brachyglanis_sp5_Cuao_T09181:0.00314573545546
97003):0.009520615382465625,Brachyglanis_sp6_Cataniapo_T09914:0.004834809302447285):0.0031206551475675692):0.00155135620
62227648,(Brachyglanis_sp2_Soromoni_AUFT3180:1.0000005000176948E-
6,Brachyglanis_sp2_Soromoni_AUFT3181:1.0000005000176948E-6):0.009388407773552099):1.0000005000176948E-
6,Brachyglanis_sp3_Ventuari_T09674:0.010261897868814207):0.007842206514069111):0.0032737503453771077,(((Myoglanis_sp1_Ma
zaruni_T20576:1.0000005000315726E-6,Myoglanis_sp1_Mazaruni_T20563:1.0000005000315726E-
6):0.0030974492871738285,Myoglanis_sp1_Konawaruk_T17930:1.0000005000315726E-
6):0.006229325573686398,My_potaroensis_LwrKuribrong_T15593:0.015988771774957514):0.031573170994464994):1.00000050001769
48E-
6,Gl_machadoi_JX899765:0.04782984842921931):0.0074854601785679376,(((((A_leptos_Iguape_TEC8330:0.011318840897401289,H_
mustelinus_Uruguay_T23708:0.027200986070794853):0.007237226059080837,(I_hasemani_Takutu_T14941:0.0019025506482828747,I_
hasemani_Berbice_T18325:0.006920438455025352):0.031136355698715423):0.0046803626768188444,N_pauciradiatus_Soromoni_AUF
T3184:0.06408865884706955):0.00751019883269996,((Ch_longior_Essequibo_AUFT3167:0.007634462997454211,H_bleekeri_Marowijn
e_AUFT4772:0.01468705153699476):0.019289144049518675,(C_molinae_Suaza_T24588:1.0000005000176948E-
6,C_molinae_Suaza_T24586:0.001935494428131 2625):0.0476898859262902):0.006588808225168052):0.003660030787580648,(M_asop
os_Cataniapo_T09910:0.001633297712538062,M_asopos_Cataniapo_T09911:0.003443818160505651 7):0.0341591703643252 5):0.009060
144566895412):0.004087650277185051,(((((Pimelodella_sp_Waini_T02818:0.0031630360126857493,Pimelodella_sp_Waini_T02817:0.0
050888897797723015):0.023306013365530343,Pimelodella_sp_Parhuena_T09547:0.013015424759526037):0.003624104912593379,P_m
odestus_SantaRosa_T13894:0.008646325996863158):0.00479327073944999,R_quelen_UprPotaro_T12676:0.022453934175832677):0.01
6911787297899883,(Go_eques_Esequibo_River_AUFT3168:1.0000005000176948E-
6,Go_eques_Esequibo_River_AUFT3164:0.006859088210146025):0.013288776020512594):0.005569007046126728):0.07412197094314
432,((Phr_dracunculus_JX899763:0.00996828652351947,Phreatobius_sp_INPA_JX899762:0.01663714528047988):0.0228738257901312
53,Phr_cisternarum_JX899764:0.02354580338427137):0.051377809715969336):0.0383346445558223,Pimelodus_ornatus:0.03833464455
582231);

CAPÍTULO II: A COMPREHENSIVE MOLECULAR PHYLOGENY OF THE THREE BARBEL CATFISH (HEPTAPTERIDAE) FOCUSED ON SUBFAMILY HEPTAPTERINAE

A comprehensive molecular phylogeny of the three barbel catfish (Heptapteridae) focused on subfamily Heptapterinae

Dario R. Faustino-Fuster[1,2*], Nathan K. Lujan[3], Mark. Sabaj[4] and Luiz R. Malabarba[1]

[1]Departamento de Zoologia, Programa de Pós-Graduação em Biologia Animal, Universidade Federal do Rio Grande do Sul, Porto Alegre, Brazil

[2]Departamento de Ictiología, Museo de Historia Natural, Universidad Nacional Mayor de San Marcos, Jesús María, Perú

[3]Department of Natural History, Royal Ontario Museum, Toronto, ON M5S 2C6, Canada

[4]The Academy of Natural Sciences of Philadelphia, Philadelphia, PA, USA

ABSTRACT

The family Heptapteridae contains 23 genera and 231 valid species that are found in a wide range of freshwater habitats from southern Mexico to northern Argentina. Current phylogenetic systematics of Heptapteridae are significantly shaped by an unpublished morphology-based analysis of all extant genera and two recent, taxonomically incomplete molecular analyses. We provide a new multi-locus molecular phylogenetic hypothesis encompassing 19 of 23 valid genera in Heptapteridae, all valid Brachyglaniini genera, 11 of 14 valid Heptapterini genera, and 66% of all valid Heptapterini species (58 of 88; plus, several undescribed species). Maximum likelihood analyses of a 3,972 base alignment of five gene regions (three mitochondrial: COI, Cyt *b*, and ND2; two nuclear: RAG2, Glyt) yielded generally consistent, well-resolved, and strongly supported phylogenies. Based on these results, we provided a new suprageneric classification within Heptapterini subdivided in five clades. Dense taxonomic sampling of Heptapterini, including type species of *Acentronichthys*, *Cetopsorhamdia*, *Chasmocranus*, *Heptapterus*, *Imparfinis*, *Mastiglanis*,

Rhamdioglanis, *Rhamdiopsis*, and *Taunayia*, supports previous observations of widespread paraphyly and several new genera in the current genus-level classification.

Key words: Classification, integrated taxonomy, molecular systematics, cis-Andean, trans-Andean.

INTRODUCTION

Heptapteridae was first erected by Gill (1861) as a Pimelodidae catfish subfamily containing only the species *Heptapterus mustelinus* (Valenciennes 1835). Currently, Heptapteridae contains 23 genera and 231 valid species (Fricke et al., 2022) that are common inhabitants of a wide range of freshwater habitats from southern Mexico to northern Argentina. Although no single externally diagnostic character exists for Heptapteridae, Bockmann & Guazzelli (2003) stated that a combination of 10 homoplastic external characteristics can serve to distinguish Heptapteridae from other fishes.

Lundberg & McDade (1986) were the first to propose three synapomorphies to support the monophyly of a clade including *Brachyrhamdia* Myers 1927, *Brachyglanis* Eigenmann 1912, *Cetopsorhamdia* Eigenmann & Fisher 1916, *Goeldiella* Eigenmann & Norris 1900, *Heptapterus* Bleeker 1858, *Imparfinis* Eigenmann & Norris 1900, *Myoglanis* Eigenmann 1912, *Nannorhamdia* Regan 1913 (junior synonym of *Imparfinis*), *Pariolius* Cope 1872, *Pimelodella* Eigenmann & Eigenmann 1888, *Rhamdella* Eigenmann & Eigenmann 1888, *Rhamdia* Bleeker 1858, and *Typhlobagrus* Eigenmann & Eigenmann 1888 (junior synonym of *Pimelodella*), now placed in Heptapteridae. However, the first taxon name given to the clade diagnosed by these characters was Rhamdiinae Bleeker, 1862 by Lundberg et al. (1991), a name that was subsequently elevated to Rhamdiidae in the

unpublished cladistic analysis by de Pinna (1993) and the cytogenetic analysis of Swarça et al. (2000). Around that same time, Silfvergrip (1996) noted that the group name Heptapterinae Gill (1861) had priority over Rhamdiinae Bleeker (1862), thus cementing the former name, Heptapteridae, for the family-level clade first proposed by de Pinna (1993).

Historically, the hypotheses of relationships of Heptapteridae within Siluriformes has greatly varied according to the type and amount of data analyzed and the phylogenetic optimality criterion used. Parsimony analyses of morphological data have suggested that Heptapteridae is most closely related to Pimelodidae and Pseudopimelodidae (Lundberg & McDade, 1986; Lundberg et al., 1991), with this relationship supported by a derived lip condition in which the lower and upper lips are subdivided into two or (rarely) three fleshy ridges. Alternatively, Mo (1991) hypothesized a close relationship to Ariidae, Auchenipteridae, Doradidae, Mochokidae, and Pimelodidae based on numbers of infraorbital bones. Arratia (1992) found Heptapteridae to be paraphyletic, with species separately grouped with *Rhamdia* or *Heptapterus* and these groups related to Pimelodidae and Ariidae based on the caudal-fin skeleton and junctures between the autopalatine, metapterygoid, hyomandibula, and quadrate. Pinna (1993) found Heptapteridae to be closely related to Bagridae based on variation in the quadrate, branchial cartilages, and Weberian complex vertebrae, and Bockmann & Guazzelli (2003) found the family to be sister to large clade spanning 15 families. Recent molecular studies have confirmed the earliest morphology-based hypotheses of Lundberg et al. (1991), and consistently place Heptapteridae as sister to the clade of Pimelodidae + Pseudopimelodidae (Sullivan et al., 2006, 2013; Arcila et al., 2017; Betancur et al., 2017; Silva et al., 2021; Faustino et al., 2021).

Diagnostic characters and interrelationships of genera within Heptapteridae have been presented and discussed by several authors. Eigenmann (1912) differentiated 10 heptapterid genera, which he treated together with Neotropical catfishes now placed in Ariidae,

Pimelodidae, and Pseudopimelodidae. Gosline (1941) reworked these genera with a focus on genera lacking a free orbital rim, including mostly 12 genera now placed in Heptapteridae plus some current members of Pimelodidae and Pseudopimelodidae. Lundberg & McDade (1986) not only proposed three internal synapomorphies for Heptapteridae, but they also diagnosed a *Brachyrhamdia* subgroup (*Cetopsorhamdia*, *Goeldiella*, *Pimelodella*, *Rhamdella*, *Rhamdia* and *Typhlobagrus* (junior synonym of *Pimelodella*)) and the unnamed subgroup containing *Heptapterus*, *Nannorhamdia* (junior synonym of *Imparfinis*), *Brachyglanis*, *Myoglanis*, and *Pariolius*, based on variation of transverse process of anterior vertebrae. Ferraris (1988) also diagnosed some species of the unnamed subgroup within Heptapteridae called the *Nemuroglanis*-subclade, based in four putative synapomorphies, in which he placed *Acentronichthys* Eigenmann & Eigenmann 1889, *Cetopsorhamdia*, *Chasmocranus* Eigenmann 1912, *Heptapterus*, *Imparfinis*, *Nannorhamdia* (junior synonym of *Imparfinis*), *Nemuroglanis* Eigenmann & Eigenmann 1889, *Pariolius*, and *Rhamdiopsis* Haseman 1911.

Lundberg et al. (1991) found that lack or reduction of a free orbital rim is a synapomorphy for an unnamed "clade 1" that includes this expanded *Nemuroglanis*-subclade (all genera proposed by Ferraris (1988) plus *Horiomyzon* Stewart 1986, *Phenacorhamdia* Dahl 1961, *Phreatobius* Goeldi 1905) plus the unnamed group 1 (*Brachyglanis*, *Gladioglanis* Ferraris & Mago-Leccia 1989, *Leptorhamdia* Eigenmann 1918, and *Myoglanis* Eigenmann 1912). Also, they recognized an unnamed clade 2 that have the free orbital rim (*Brachyrhamdia*, *Goeldiella*, *Pimelodella*, *Rhamdella*, *Rhamdia*). Additionally, Lundberg et al. (1991) further suggested that *Brachyglanis*, *Leptorhamdia*, and *Myoglanis* likely form a distinct clade supported by the shared dorsal expansion of a superficial layer of the adductor mandibulae muscles over the hyomandibular articulation nearly to the midline of the skull roof.

Bockmann (1994) further expanded the Rhamdiinae/Heptapteridae (all previous species plus *Nannoglanis* Boulenger 1887, *Rhamdioglanis* Ihering 1907 and *Mastiglanis* Bockmann 1994) and diagnosed the *Nemuroglanis*-subclade by proposing 12 additional osteological characters that distinguish the *Nemuroglanis*-subclade as a whole. Also, Bockmann (1994) defined two more inclusive unnamed clades within the *Nemuroglanis*-subclade (*Mastiglanis* and *Nemuroglanis* plus all remaining *Nemuroglanis*-subclade genera) based on putative derived condition of complex centrum. Additionally, Bockmann (1994) alternatively stated two unnamed groups within the *Nemuroglanis*-subclade, based on variations of last vertebrae character (Bockmann, 1994: 774-776).

Bockmann (1998) conducted the first taxonomically comprehensive cladistic analysis of Heptapteridae, analyzing 278 morphological characters from 72 ingroup taxa and generated a partially resolved hypothesis of phylogenetic relationships within Heptapteridae (Bockmann 1998: Fig. 216). This analysis supports a monophyletic Heptapteridae including *Phreatobius* Goeldi 1905, based largely on characters previously highlighted by Lundberg & McDade (1986), Ferraris (1988), Lundberg et al. (1991), and Bockmann (1994).

Despite the richness of Heptapteridae genera and the attention that has been given to resolving intergeneric relationships, less than half of all heptapterid genera have undergone species-level taxonomic revisions. Genera that have received detailed individual treatments include *Brachyrhamdia* (Lundberg & McDade, 1986), *Heptapterus* (Buckup, 1988; Faustino-Fuster et al., 2019), *Gladioglanis* (Lundberg et al., 1991), *Mastiglanis* (Bockmann, 1994), *Nemuroglanis* (Ferraris, 1988; Bockmann & Ferraris, 2005), *Phenacorhamdia* (DoNascimiento & Milani, 2008), *Taunayia* Miranda Ribeiro 1918 (Oliveira & Britski, 2000), *Rhamdella* (Bockmann & Miquelarena, 2008), *Rhamdia* (Silfvergrip, 1996), and *Rhamdiopsis* (Bockmann & Castro, 2010). Also, the most recently phylogenetic relationship within Heptapteridae was conducted based on integrative data (Silva et al., 2021 and

Faustino-Fuster et al., 2021), and both proposing a new suprageneric classification within Heptapteridae. The first study was based on ultraconserved elements (UCEs) representing 24 described species and 18 undescribed species classifying them in Rhamdiinae + Heptapterinae (Heptapterini + Brachyglaniini); while the second work was based on multilocus analyses representing 26 described species and 15 undescribed species of the family, classifying them into Rhamdiinae (Rhamdiini + Goeldiellini) + Heptapterinae (Heptapterini + Brachyglaniini).

In the present study we examine phylogenetic relationships throughout the Heptapteridae using multi-locus molecular phylogenetic techniques with a focus on Heptapterini, representing 79 described species and 64 undescribed species. Moreover, we use the results of our phylogenetic analysis in conjunction with various previously proposed morphological characters and molecular hypothesis as the basis for a new generic classification within Heptapterini.

MATERIAL AND METHODS

Taxon Sampling and DNA sources

We generated novel sequence data for 28 genera, 145 species, and 219 samples collected in Argentina, Bolivia, Brazil, Colombia, Ecuador, Guyana, Peru, Suriname, Uruguay and Venezuela between the years 1992 and 2020. Novel data were combined with GenBank data for four outgroup species and 39 ingroup species so that sampled taxa encompassed 83% of all valid Heptapteridae genera (19 of 23); 80% of all valid Rhamdiinae genera (3 of 4); within Heptapterinae, 79% of all valid Heptapterini genera (11 of 14) and 66% of all valid Heptapterini species (58 of 88; plus several undescribed species), 100% of

all valid Brachyglaniini genera (4 of 4), and 73% of all valid species in Brachyglaniini (11 of 15; plus several undescribed species) (Table 1). Sixteen of the Heptapteridae genera examined in this study are represented by type species. Specimens examined in this study are cataloged at the following ichthyological collections: Academy of Natural Sciences of Drexel University, Philadelphia (ANSP); Auburn University Museum of Natural History, Auburn (AUM), Colección Ictiológica Fundación Miguel Lillio, Tucumán (CI-FML); Museu de Ciências e Tecnologia, Pontifícia Universidade Católica do Rio Grande do Sul, Porto Alegre (MCP); Museu Nacional, Universidade Federal do Rio de Janeiro, Rio de Janeiro (MNRJ); Museo de História Natural Universidad Nacional Mayor de San Marcos, Lima (MUSM), Royal Ontario Museum, Toronto (ROM), Universidade Federal do Rio Grande do Sul, Porto Alegre (UFRGS). Institutional abbreviations follow Sabaj (2020).

Molecular markers and DNA extraction, amplification, and sequencing

We sequenced fragments of three mitochondrial (COI: cytochrome oxidase subunit I, Cyt b: cytochrome b, and ND2: NADH dehydrogenase subunit 2), and two nuclear markers (RAG2: recombination activating genes 2, and Glyt: glycosyltransferase). Genetic markers were selected based on their ease of unambiguous amplification in Heptapteridae, with most having been used in previous phylogenetic studies of catfishes (Sullivan et al., 2006, 2013; Smith et al., 2016; Faustino et al., 2021; Supplementary Table 1).

Whole genomic DNA was extracted from fin or muscle tissues following a standard salt extraction protocol (Lujan et al., 2020) and a modified method of cetyltrimethyl ammonium bromide (CTAB; Doyle & Doyle, 1987). Fragments were amplified using a reaction as described by Faustino et al. (2019; 2021). Genes were amplified via standard polymerase chain reaction (PCR) using an Eppendorf Mastercycler pro S thermocycler

(Eppendorf Ltd., Hamburg, Germany). A 567 bp fragment of the COI gene was amplified with an initial denaturation step of 1 min at 94°C followed by 35 cycles of 94°C for 30 s, annealing at 52°C for 40 s, extension at 72°C for 1 min, and final extension at 72°C for 10 min. A 724 bp fragment of the Cyt b gene was amplified by denaturing at 95°C for 2 min followed by 35 cycles of 95°C for 30 s, annealing at 48°C for 1 min, extension at 72°C for 1 min 30 s, and final extension at 72°C for 5 min. A 1039 bp fragment of the ND2 gene was amplified by denaturing at 94°C for 2 min, followed 35 cycles of 95°C for 1 min, annealing at 58°C for 1 min, extension at 72°C for 2 min, and final extension at 72°C for 10 min. An 811 bp fragment of the Glyt gene was amplified by denaturing at 95°C for 2 min followed by 40 cycles of 95°C for 30 s, annealing at 56°C for 1 min, extension at 72°C for 1 min 30 s, and final extension at 72°C for 5 min. An 831 bp fragment of the RAG2 gene was amplified by denaturing at 94°C for 2 min followed by 31 cycles of 94°C for 30 s, annealing at 58°C for 45 s, extension at 72°C for 1 min, and final extension at 72°C for 5 min. Products of each amplification were visualized by running 3µL or 2 µL of amplicon on a 1% agarose gel. Remaining PCR product was purified using exonuclease I and calf intestine alkaline phosphatase (EXOCIAP) or exonuclease I and shrimp alkaline phosphatase (EXOSAP). Successful amplifications were bidirectionally sequenced using the dye termination method of Sanger et al. (1977).

Sequence editing, alignments, and phylogeny inference

Bidirectional sequences were assembled into contigs and manually edited using the software Geneious v6.1.7 (Biomatters Ltd., Auckland, New Zealand). Sequences for contigs having many ambiguities were reamplified and sequenced. Contigs for each gene region were aligned using the MUSCLE algorithm Edgar (2004), with the alignments being manually

edited and evaluated based on amino acid translations of consensus sequences. Individual gene alignments were concatenated to create a single matrix comprising 3.965 bp × 294 individuals (see Table 1).

Maximum likelihood (ML) phylogenetic analyses of each unpartitioned gene alignment were conducted using RAxML v8.0.0 (Stamatakis, 2014), to check for consistency in phylogenetic signal across markers. Phylogenetic analyses of the concatenated alignment were partitioned by both gene and codon position resulting in 15 data partitions (Supplementary Table 2). The RAxML analysis a GTRCAT model was selected for all 15 data partitions. All phylogenetic analyses were conducted on the CIPRES supercomputing cluster (Miller et al., 2010). The clade of (Pimelodidae (*Sorubim lima* (Bloch & Schneider 1801), *Megalonema platanum* (Günther 1880), *Pimelodus ornatus* Kner 1858, *Iheringichthys labrosus* (Lütken 1874), *Pimelodus blochii* Valenciennes 1840, *Parapimelodus nigribarbis* (Boulenger 1889), *Pimelodus pintado* Azpelicueta, Lundberg & Loureiro 2008, *Pimelodus absconditus* Azpelicueta 1995, *Pimelodus maculatus* Lacepède 1803) + Phreatobiidae (*Phreatobius cisternarum* Goeldi 1905, *Phreatobius dracunculus* Shibatta, Muriel-Cunha, and de Pinna 2007 and two *Phreatobius* sp.)) + Pseudopimelodidae (*Pseudopimelodus mangurus* (Valenciennes 1835), *Rhyacoglanis pulcher* (Boulenger 1887), *Microglanis cottoides* (Boulenger 1891), *Microglanis eurystoma* Malabarba & Mahler 1998) was designated the outgroup based on previous molecular studies finding that Heptapteridae is closely related to Pimelodidae, Phreatobiidae and Pseudopimelodidae (Sullivan et al., 2013; Faustino-Fuster et al., 2021). Maximum likelihood analysis of the concatenated alignment was conducted using RAxML programmed with workflow bootstrap and consensus, based on a 1000 generation search of tree space.

Comparative Material

All comparative material from Faustino-Fuster et al, 2019; Faustino-Fuster & Ortega, 2020; Faustino-Fuster et al, 2021; Faustino-Fuster & de Souza, 2021 and Faustino-Fuster & Malabarba in prep., see chapter II).

Acknowledgments

We thank Barbara Brown (*in memorium*), Radford Arrindell, Tom Vigliota, and Chloe Lewis (AMNH); Mark Sabaj and Mariangeles Arce (ANSP); Jonathan W. Armbruster and David C. Werneke (AUM); Dave Catania, Jon Fong, and Luiz Rocha (CAS); José I. Mojica (ICNMHN); Hernán Ortega, Max Hidalgo, Vanessa Meza-Vargas and Carla Muñoz (MUSM); Caleb McMahan, Kevin Swagel and Susan Mochel (FMNH); Carlos Lucena, (MCP); Don Stacey, Mary Burridge, Erling Holm and Marg Zur (ROM); Luiz Malabarba and Juliana Wingert (UFRG); Lynne Parenti, Jeff Clayton, and Sandra Raredon (USNM) for facilitating access to loans of type and non-type specimens and tissues. We thank Oscar Leon Mata (*in memorium*) and Donald Taphorn for facilitating fieldwork in Venezuela and the Inter-American Development Bank for facilitating fieldwork in Guyana. Research and travel by DRFF were supported by CAPES (Coordenação de Aperfeiçoamento de Pessoal de Nível Superior), by the Royal Ontario Museum E.J. Crossman Endowment Fund, by the Böhlke Award from the Academy of Natural Science of Drexel University, by the Smithsonian Visiting Student (Fellowship) at the National Museum of Natural History (NMNH), and by the Grainger Bioinformatics Center funding at the Field Museum of Natural History. NKL was supported by a Gerstner Fellowship in the Richard Gilder Graduate School at the American Museum of Natural History. Field work generating specimens for this study was funded by the National Science Foundation via NSF DEB-0315963 (All Catfish Species

Inventory) and NSF OISE-1064578 (International Research Fellowship). Field and laboratory work were supported by Coypu Foundation of New Orleans; gifts from Aquatic Critter Inc. in Nashville, TN, via Chris and Wendy Beggin; by Systematics Research Fund; by Society of Systematic Biologists Found; and by Catfish Study Group Found.

References

Arcila, D., Ortí, G., Vari, R., Armbruster, J.W., Stiassny, M.L., Ko, K.D., Sabaj MH., Lundberg J.L., Revell L.J., Betancur-R, R., 2017. Genome-wide interrogation advances resolution of recalcitrant groups in the tree of life. Nat. Ecol. Evol. 1(2), 1-10. https://doi.org/10.1038/s41559-016-0020

Arratia, G., 1992. Development and variation of the suspensorium of primitive catfishes (Teleostei: Ostariophysi) and their phylogenetic relationships. Bonner Zoologische Monographien 32, 1−149.

Betancur-R, R., Wiley, E.O., Arratia, G., Arturo, A., Bailly, N., Miya, M., Lecointre, G., Orti, G., 2017. Phylogenetic classification of bony fishes. BMC Evol. Biol. 12, 162. https://doi.org/10.1186/s12862-017-0958-3

Bockmann, F.A., 1994. Description of *Mastiglanis asopos*, a new pimelodid catfish from northern Brazil, with comments on phylogenetic relationships inside the subfamily Rhamdiinae (Siluriformes: Pimelodidae). Proc. Biol. Soc. Wash. 107, 760−777.

Bockmann, F.A., 1998. Análise filogenética da família Heptapteridae (Teleostei: Ostariophysi: Siluriformes) e redefinição de seus gêneros. Universidade de São Paulo, São Paulo. [Tese de doutorado não publicada]

Bockmann, F.A., Guazzelli, G.M., 2003. Heptapteridae (Heptapterids), p. 406–431. In: Checklist of the freshwater fishes of South and Central America. R. E. Reis, S. O. Kullander, and C. J. Ferraris, Jr. (eds.), Edipucrs, Porto Alegre, Brazil.

Bockmann, F.A., Castro, R.M.C., 2010. The blind catfish from the caves of Chapada Diamantina, Bahia, Brazil (Siluriformes: Heptapteridae): description, anatomy, phylogenetic relationships, natural history, and biogeography. Neotrop. Ichthyo. 8, 673–706. https://doi.org/10.1590/S1679-62252010000400001

Bockmann, F.A., Ferraris Jr., C.J., 2005. Systematics of the Neotropical catfish genera *Nemuroglanis* Eigenmann and Eigenmann 1889, *Imparales* Schultz 1944, and *Medemichthys* Dahl 1961 (Siluriformes: Heptapteridae). Copeia 2005, 124–137. https://doi.org/10.1643/CI-04-019R1

Bockmann, F.A., Miquelarena, A.M., 2008. Anatomy and phylogenetic relationships of a new catfish species from northeastern Argentina with comments on the phylogenetic relationships of the genus *Rhamdella* Eigenmann and Eigenmann 1888 (Siluriformes, Heptapteridae). Zootaxa 1780, 1−54. https://doi.org/10.11646/zootaxa.1780.1.1

Bockmann, F. A., & Reis, R. E. (2021). Two new, remarkably colored species of the Neotropical catfish genus *Cetopsorhamdia* Eigenmann & Fisher, 1916 (Siluriformes, Heptapteridae) from Chapada dos Parecis, western Brazil, with an assessment of the morphological characters bearing on their phylogenetic relationships. Papéis Avulsos de Zoologia, 61.

Bockmann, F.A., Slobodian V., 2013. Heptapteridae. Pages 12–71 in L. J. Queiroz, G. Torrente-Vilara, W. M. Ohara, T. H. da Silva Pires, J. Zuanon, and C. R. da Costa Doria, editors. Peixes do Rio Madeira. Dialeto, São Paulo, Brazil.

Bockmann, F.A., Slobodian, V., 2018. Family Heptapteridae – three-barbeled catfishes. In Field Guide to the Fishes of the Amazon, Orinoco & Guianas (van der Sleen, P., & Albert, J. S., eds), pp. 233–252. Princeton: Princeton University Press.

Buckup, P. A., 1988. The genus *Heptapterus* (Teleostei, Pimelodidae) in southern Brazil and Uruguay, with the description of a new species. Copeia, 641-653.

DoNascimiento, C., & Milani, N., 2008. The Venezuelan species of *Phenacorhamdia* (Siluriformes: Heptapteridae), with the description of two new species and a remarkable new tooth morphology for siluriforms. Proceedings of the Academy of Natural Sciences of Philadelphia, 157(1), 163-180.

Doyle, J. J., & Doyle, J. L., 1987. A rapid DNA isolation procedure for small quantities of fresh leaf tissue. Phytochemical Bulletin, 19, 11–15.

Edgar, R.C., 2004. MUSCLE: multiple sequence alignment with high accuracy and high throughput. Nucleic Acids Res. 32, 1792–1797. https://doi.org/10.1093/nar/gkh340

Eigenmann, C.H., 1912. The freshwater fishes of the British Guiana, including a study of the ecological grouping of species and relation of the fauna of the plateau to that of the lowlands. Mem. Carnegie Mus. 5, 1−578. https://doi.org/10.5962/bhl.title.2174

Faustino-Fuster, D. R., Bockmann, F. A., & Malabarba, L. R., 2019. Two new species of *Heptapterus* (Siluriformes: Heptapteridae) from the Uruguay River basin, Brazil. Journal of fish biology, 94(3), 352-373.

Faustino-Fuster, D. R., Meza-Vargas, V., Lovejoy, N. R., & Lujan, N. K., 2021. Multi-locus phylogeny with dense Guiana Shield sampling supports new suprageneric classification of the Neotropical three-barbeled catfishes (Siluriformes: Heptapteridae). Molecular Phylogenetics and Evolution, 162, 107186.

Ferraris Jr, C.J., 1988. Relationships of the neotropical catfish genus *Nemuroglanis*, with a description of a new species (Osteichthyes: Siluriformes: Pimelodidae). Proc. Biol. Soc. Wash. 101, 509–516.

Fricke, R., Eschmeyer, W.N., Van der Laan, R., (eds.) 2022. Eschmeyer's catalog of fishes: genera, species, references. http://researcharchive.calacademy.org/research/ichthyology/catalog/fishcatmain.asp. Electronic version accessed 01 Feb 2022.

Gill, T., 1861. Synopsis of the genera of the sub-family of Pimelodinae. Abbreviated Proc. Boston Soc. Nat. Hist. 8, 46−55.

Gosline, W.A., 1941. Synopsis of the genera of pimelodid catfishes without a free orbital rim. Stanford Ichthyological Bulletin 2, 83−88.

Instituto Chico Mendes de Conservação da Biodiversidade (ICMBio). 2021. *Heptapterus multiradiatus*. The IUCN Red List of Threatened Species 2021: e.T187180A1824319. https://dx.doi.org/10.2305/IUCN.UK.2021-1.RLTS.T187180A1824319.pt

Lujan, N.K., Weir, J.T., Noonan, B.P., Lovejoy, N.R., Mandrak., N.E., 2020. Is Niagara Falls a barrier to gene flow in riverine fishes? A test using genome-wide SNP data from seven native species. Mol. Ecol. 29, 1235−1249. https://doi.org/10.1111/mec.15406

Lundberg, J.G., McDade, L.A., 1986. On the South American catfish *Brachyrhamdia imitator* Myers (Siluriformes, Pimelodidae), with phylogenetic evidence for a large intrafamilial lineage. Not. Nat. 463, 1–24.

Lundberg, J.G., Bornbusch, A.H., Mago-Leccia, F., 1991. *Gladioglanis conquistador* n. sp., from Ecuador with diagnoses of the subfamilies Rhamdiinae Bleeker and Pseudopimelodinae n. subf. (Siluriformes, Pimelodidae). Copeia 1991, 190−209.

Miller, M.A., Pfeiffer, W., Schwartz, T. 2010. Creating the CIPRES Science Gateway for inference of large phylogenetic trees. In Gateway Computing Environments Workshop (GCE). Editora: Local.

Mo, T., 1991. Anatomy, relationships and systematics of the Bagridae (Teleostei: Siluroidei) with a hypothesis of Siluroid phylogeny. Koenigstein, Koeltz Scientific Books. 216 p.

Oliveira, J.C., Britski, H.A., 2000. Redescrição de *Taunayia bifasciata* (Eigenmann & Norris, 1900), comb. Nova, um bagre enigmático do Estado de São Paulo (Siluriformes, Pimelodidae, Heptapterinae). Pap. Avulsos de Zool. 41, 119−133.

de Pinna, M.C.C., 1993. Higher-level phylogeny of Siluriformes, with a new classification of the order (Teleostei, Ostariophysi). New York, The City University of New York. 482 p. [Tese de doutorado não publicada]

Reis, R. E., Britski, H. A., Britto, M. R., Buckup, P. A., Calegari, B. B., Camelier, P., Delapieve, M. L. S., Langeani, F., Lehmann, P., Lucinda, P. H. F., Marinho, M., Martins, F., Menezes, N. A., Moreira, C. R., de Pinna, M. C. C., Pavanelli, C. S., Rapp Py-Daniel, L. H. & Souza, L. M., 2019. Poor taxonomic sampling undermines nomenclatural stability: A reply to Roxo et al. (2019). Zootaxa, 4701(5), 497–500.

Sabaj, M.H., 2019. Standard symbolic codes for institutional resource collections in herpetology and ichthyology: an online reference. Version 7.1 (21 March 2019). Electronically accessible at http://www. asih. org/, American Society of Ichthyologists and Herpetologists, Washington, DC [Google Scholar].

Sanger, F., Nicklen, S., Coulson, A.R., 1977. DNA sequencing with chain-terminating inhibitors. Proc. Natl. Acad. Sci. U. S. A. 74, 5463–5467. https://doi.org/10.1073/pnas.74.12.5463

Silfvergrip, A.M.C., 1996. A systematic revision of the neotropical catfish genus *Rhamdia*. Department of Vertebrate Zoology, Stockholm. 156 p.

Silva, G. S., Roxo, F. F., Melo, B. F., Ochoa, L. E., Bockmann, F. A., Sabaj, M. H., Jerep F. C., Foresti F., Benine R. C., Oliveira, C., 2021. Evolutionary history of Heptapteridae catfishes using ultraconserved elements (Teleostei, Siluriformes). Zoologica Scripta, 50(5), 543-554.

Slobodian, V., Bockmann, F.A., 2013. A new Brachyrhamdia (Siluriformes: Heptapteridae) from Rio Japurá basin, Brazil, with comments on its phylogenetic affinities, biogeography and mimicry in the genus. Zootaxa 3717, 1−22. https://doi.org/10.11646/zootaxa.3717.1.1

Smith, W.L., Stern, J.H., Girard, M.G., Davis, M.P., 2016. Evolution of venomous cartilaginous and ray-finned fishes. Integr. Comp. Biol. 56, 950−961.

Stamatakis, A., 2014. RaxML version 8: a tool for phylogenetic analysis and post-analysis of large phylogenies. Bioinformatics 30, 1312–1313. https://doi.org/10.1093/bioinformatics/btu033

Stewart, D.J., 1986. A new pimelodid catfish from the deep-river channel of the Río Napo, eastern Ecuador (Pisces: Pimelodidae). Proc. Acad. Nat. Sci. Philadelphia. 38, 46−52.

Sullivan, J.P., Lundberg, J.G., Hardman, M., 2006. A phylogenetic analysis of the major groups of catfishes (Teleostei: Siluriforms) using RAG1 and RAG2 nuclear gene sequences. Mol. Biol. Evol. 41, 636–662. https://doi.org/10.1016/j.ympev.2006.05.044

Sullivan, J.P., Muriel-Cunha, J., Lundberg, J.G., 2013. Phylogenetic relationships and molecular dating of the major groups of catfishes of the Neotropical superfamily Pimelodoidea (Teleostei, Siluriformes). Proc. Acad. Nat. Sci. Philadelphia, 89−110.

Swarça, A.C., Caetano, L.G., Dias, A.L., 2000. Cytogenetics of species of the families Pimelodidae and Rhamdiidae (Siluriformes). Genet. Mol. Biol. 23, 589−593. http://dx.doi.org/10.1590/S1415-47572000000300015

Tables

Figures Captions

Figure 1. Phylogenetic hypothesis for interrelationships of Heptapteridae made by maximum likelihood of a 3,965 base pair alignment consisting of three mitochondrial (*coI*, c*ytb*, *nd2)* and two nuclear (glyt, rag2) gene regions. Node number correspond to bootstrap support values (ML).

Figure 2. Phylogenetic hypothesis for interrelationships of Heptapterina made by maximum likelihood of a 3,965 base pair alignment consisting of three mitochondrial (*coI*, c*ytb*, *nd2)* and two nuclear (glyt, rag2) gene regions. Node number correspond to bootstrap support values (ML). Specimens representing species that are types for their genus are indicated by an asterisk (*).

Figure 3. Phylogenetic hypothesis for interrelationships of Nemuroglaniina made by maximum likelihood of a 3,965 base pair alignment consisting of three mitochondrial (*coI*, c*ytb*, *nd2)* and two nuclear (glyt, rag2) gene regions. Node number correspond to bootstrap support values (ML). Specimens representing species that are types for their genus are indicated by an asterisk (*).

Figure 4. Phylogenetic hypothesis for interrelationships of Cetopsorhamdiina made by maximum likelihood of a 3,965 base pair alignment consisting of three mitochondrial (*coI*, c*ytb*, *nd2)* and two nuclear (glyt, rag2) gene regions. Node number correspond to bootstrap support values (ML). Specimens representing species that are types for their genus are indicated by an asterisk (*).

Figure 5. Phylogenetic hypothesis for interrelationships of Chasmocranina made by maximum likelihood of a 3,965 base pair alignment consisting of three mitochondrial (*coI*, c*ytb*, *nd2)* and two nuclear (glyt, rag2) gene regions. Node number correspond to bootstrap support values (ML). Specimens representing species that are types for their genus are indicated by an asterisk (*).

Figure 6. Phylogenetic hypothesis for interrelationships of Mastiglaniina made by maximum likelihood of a 3,965 base pair alignment consisting of three mitochondrial (*coI*, c*ytb*, *nd2)* and two nuclear (glyt, rag2) gene regions. Node number correspond to bootstrap support values (ML). Specimens representing species that are types for their genus are indicated by an asterisk (*).

Figures

Supplementary

Supplementary Table 1. Primers and annealing temperatures (*Ta*) for PCR for all markers.

Gene	Primers	Sequences	Ta (°C)	Reference
coI	FishF1 FishR1	TCA ACC AAC CAC AAA GAC ATT GGC AC TAG ACT TCT GGG TGG CCA AAG AAT CA	52	Ward et al. (2005)
cytb	GLUDG-L CB3-H	TGA CCT GAA RAA CCA YCG TTG GGC AAA TAG GAA RTA TCA TTC	48	Palumbi (1996)
nd2	nd2_f nd2 _r	AGC TTT TGG GCC CAT ACC CCA AGG RAC TAG GAG ATT TTC ACT CCT GCT	58	Arroyave et al. (2013)
glyt	F577 R1464	ACA TGG TAC CAG TAT GGC TTT GT GTA AGG CAT ATA SGT GTT CTC TCC	56	Li et al. (2007)
rag2	MHF1 MHR1	TGy TAT CTC CCA CCT CTG CGy TAC C TCA TCC TCC TCA TCk TCC TCw TTG TA	58	Hardman (2004)

Supplementary Table 2. Summary for each gene partitions.

Subset	Locus	Codon Position	Range in alignment	Length (bp)
1	*coI*	1		189
2	*coI*	2	1 - 567	189
3	*coI*	3		189
4	*cytb*	1		241
5	*cytb*	2	568 – 1291	241
6	*cytb*	3		242
7	*nd2*	1		346
8	*nd2*	2	1292 - 2330	346
9	*nd2*	3		347
10	glyt	1		270
11	glyt	2	2331 - 3141	270
12	glyt	3		271
13	rag2	1		277
14	rag2	2	3142 - 3972	277
15	rag2	3		277
Total			3972	3972

CAPÍTULO III: INTEGRATIVE TAXONOMY OF THE *HEPTAPTERUS* BLEEKER, 1858 (HEPTAPTERIDAE: HEPTAPTERINI) WITH DESCRIPTION OF A NEW GENUS AND TWO NEW SPECIES

Integrative taxonomy of the *Heptapterus* Bleeker, 1858 (Heptapteridae: Heptapterini) with a description of a new genus and two new species.

Dario R. Faustino-Fuster[1,2*] and Luiz R. Malabarba[1]

[1]Departamento de Zoologia, Universidade Federal do Rio Grande do Sul, Programa de Pós-Graduação em Biologia Animal, Porto Alegre, Brazil

[2]Departamento de Ictiología, Museo de Historia Natural, Universidad Nacional Mayor de San Marcos, Jesús María, Perú

ABSTRACT

The genus *Heptapterus* is revised based on molecular and morphological data, and includes only four valid species: *H. carnatus* Faustino-Fuster, Bockmann & Malabarba, 2019; *H. exilis* Faustino-Fuster, Bockmann & Malabarba, 2019; *H. mustelinus* (Valenciennes, 1835), and *H. qenqo* Aguilera, Mirande & Azpelicueta 2011. *Heptapterus eigenmanni* Steindachner, 1907, *H. ornaticeps* Ahl, 1936 NEW SYNONYM, and *H. mbya* Azpelicueta, Aguilera and Mirande, 2011 NEW SYNONYM are considered junior synonyms of *H. mustelinus*. We designate the neotype for *Heptapterus mustelinus.* The relationships of most nominal species of *Heptapterus sensu lato* are discussed based on molecular dataset. We transfer the species currently known as *Chasmocranus lopezae* to a new genus, *Leptoheptapterus* gen. n., and provide the descriptions of two new species. Morphological features are used to diagnose the genera and species.

INTRODUCTION

The family Heptapteridae comprises 231 valid species (Fricke et al., 2022) distributed throughout the Neotropics from northern Mexico to southern Argentina, including the trans-Andean region reaching southern Peru (Bockmann and Guazzelli,

2003). Heptapteridae is diagnosed exclusively by synapomorphies related to the internal anatomy (see Lundberg and McDade, 1986; Ferraris, 1988; Lundberg et al., 1991). Despite of that, externally, heptapterids can be identified by the features summarized by Bockmann and Guazzelli (2003) and Bockmann and Slobodian (2017).

Heptapterus Bleeker, 1858 has been characterized by an elongate slender body, elliptical in cross section through the dorsal-fin origin, bearing a typical eel-like aspect; and several other characters related to the external morphology, osteology, and musculature (Bockmann and Slobodian, 2017). Faustino-Fuster et al. (2019) recently described *Heptapterus carnatus* Faustino-Fuster, Bockmann and Malabarba, 2019 and *H. exilis* Faustino-Fuster, Bockmann and Malabarba, 2019 following the generic definition of Bockmann and Slobodian (2017) and further restricted the genus to include both species plus *H. mandimbusu* Aguilera, Benitez, Terán, Alonso and Mirande, 2017, *H. mbya* Azpelicueta, Aguilera and Mirande, 2011, *H. mustelinus* (Valenciennes, 1835), *H. ornaticeps* Ahl, 1936, *H. qenqo* Aguilera, Mirande and Azpelicueta, 2011, *H. stewarti* Haseman, 1911, and *H. sympterygium* Buckup, 1988. All nine valid species of *Heptapterus* considered by Faustino-Fuster et al. (2019) are distributed along the following ecoregions proposed by Abell (2008): Mar Chiquita- Salinas Grande, Chaco, Paraguay, Upper Paraná, Lower Paraná, Iguaçu, Lower Uruguay, Upper Uruguay, Laguna dos Patos, Tramandai-Mampituba, and Southeastern Mata Atlantica.

An ongoing integrative study based on morphological and molecular data revealed a new composition of *Heptapterus*, containing only four species. Seven clades tentatively classified as new genera are recognized, four of them previously proposed as new genera in an unpublished thesis (Bockmann, 1998). one of the clade is described herein as a new genus, composed by *Chasmocranus lopezae* Miranda Ribeiro, 1968 and two markedly rare new species.

MATERIAL AND METHODS

Measurements were made point to point with digital caliper and are expressed to the nearest 0.1 mm. Measurement were taken according to Lundberg and MacDade (1986), Bockmann (1994), and Faustino-Fuster et al. (2019). The position of landmarks of all measurements obtained were illustrated by Faustino-Fuster et al. (2019; fig. 1). Standard length (SL) is given in mm and other measurements are expressed in percent of standard length (LS) or, for subunits of the head, head length (HL). Principal Component Analysis (PCA) was used to compare all morphometric variables among species using the software PAST 2.17C (Hammer et al., 2001).

Paratypes and comparative material were cleared and stained (CS) according to the protocol of Taylor and Van Dyke (1985). Osteological nomenclature follows Lundberg and McDade (1986), and Bockmann and Miquelarena (2008). Branchiostegal rays, pterygiophores, ribs, and vertebrae were counted only in CS specimens, as well as the insertion of the first fins elements to vertebral number. Vertebral counts include the first five vertebrae of the Weberian apparatus and the pleural + ural centra as a single element. Nomenclature and homologies for laterosensory system follow Arratia and Huaquin (1995) with modifications provided by Schaefer and Aquino (2000). Quantitative variables were represented by Tukey box plots to provide a visual representation of the counts that differed among species using SigmaPlot (Systat Software, San Jose, CA). Such graphs better display the skewed or other nonparametric shapes of the meristic data than the mean and standard deviation. The graphs presented here display the sample median (= 50th percentile) and the 25th and 75th percentiles represented as the lateral borders of the box plots. The 10th and 90th percentiles are represented by error bars. Institutional abbreviations followed Sabaj (2020).

Comparisons with congeners were undertaken directly through examination of specimens, including types, and checking original literature of the description of species and taxonomic studies (Valenciennes, 1835, 1840; Haseman, 1911; Ahl, 1936; Buckup, 1988; Azpelicueta et al., 2011; Aguilera et al., 2011, 2017; and Faustino-Fuster et al., 2019).

Molecular analysis included a multilocus analyses for the available samples of *Heptapterus* species (*H. bleekeri*, *H. carnatus, H. exilis, H. mandimbusu, H. multiradiatus*, *H. mustelinus, H, mbya*, *H. qenqo*, *H. stewarti*, *H. panamensis*, *H. sympterygium*, *H. tapanahoniensis*) and Heptapteridae species used by Faustino-Fuster et al. (2021) and Faustino-Fuster et al. (in prep). Extraction, amplifications, sequencing, edition, alignment, and molecular analyses was conducted following the methods of Faustino-Fuster et al. (2021).

A species delimitation analysis was performed using an arbitrarily ultrametric coI gene tree for a general mixed Yule coalescent model (GMYC; Pons et al., 2006) and Poisson Tree Processes (PTP, Zhang et al., 2013) on the webserver for GMYC and PTP (Zhang et al., 2013). The ultrametric gene tree was constructed using the HKY + G (Hasegawa et al., 1985) model of molecular evolution with relaxed molecular clock using a lognormal time distribution and birth–death prior implemented in the BEAST v1.7.5. program (Drummond et al., 2012). BEAST was programmed to run for total of 10,000,000 generations, sampling every 1000 trees. For the MCMC analysis each parameter fluctuating within a stable range, the effective sample size (ESS) for all metrics exceeded 200 was checked using the program Tracer 1.6 (Rambaut et al., 2013). The first 10% of trees were discarded as burn in using TreeAnnotator 1.7.5 program (Rambaut and Drummond, 2013). Genetic distances for coI between a pair of sequences were calculated using the Kimura 2-parameter (K2P) model in MEGA6.

Conselho Nacional de Desenvolvimento Científico e Tecnológico, CNPq (Process #307890/2016-3 and 401204/2016-2 to LRM).

References

Abell R., M. L. Thieme, C. Revenga, M. Bryer, M. Kottelat, N. Bogutskaya, B. Coad, N. Mandrak, S. C. Balderas, W. Bussing, and M. L. Stiassny. 2008. Freshwater ecoregions of the world: a new map of biogeographic units for freshwater biodiversity conservation. BioScience 58(5):403–414.

Aguilera, G., M. Benitez, G. E. Téran, F. Alonso, and J. M. Mirande. 2017. A new species of *Heptapterus* Bleeker 1858 (Siluriformes: Heptapteridae) from the Uruguay river basin in Misiones, Northeastern Argentina. Zootaxa 4299: 572–580.

Aguilera, G., J. M. Mirande, and M. M. Azpelicueta. 2011. A new species of *Heptapterus* Bleeker 1858 (Siluriformes: Heptapteridae) from the Río Salí basin, north-western Argentina. Journal of Fish Biology 78: 240–250.

Ahl, E. 1936. Beschreibungen dreier neuer Welse aus Brasilien. Zoologischer Anzeiger 116: 109–111.

Arratia, G., and L. Huaquin. 1995. Morphology of the lateral line system and of the skin of diplomystid and certain primitive loricarioid catfishes and systematic and ecological considerations. Bonner Zoologische Monographien 36: 1–110.

Azpelicueta, M. M., G. Aguilera, and J. M. Mirande. 2011. *Heptapterus mbya* (Siluriformes: Heptapteridae), a new species of catfish from the Paraná River basin, in Argentina. Revue Suisse de Zoologie 118: 319–327.

Bertaco, V. A., J. Ferrer, F. R. Carvalho, and L. R. Malabarba. 2016. Inventory of the freshwater fishes from a densely collected area in South America—a case study of the current knowledge of Neotropical fish diversity. Zootaxa 4138: 401–440.

Bockmann, F. A. 1994. Description of *Mastiglanis asopos*, a new pimelodid catfish from northern Brazil, with comments on phylogenetic relationships inside the subfamily Rhamdiinae (Siluriformes: Pimelodidae). Proceedings of the Biological Society of Washington 107: 760–777.

Bockmann, F. A. 1998. Análise filogenética da família Heptapteridae (Teleostei: Ostariophysi: Siluriformes) e redefinição de seus gêneros. Unpub. PhD Diss., Universidade de São Paulo, São Paulo.

Bockmann, F. A., and G. M. Guazzelli. 2003. Family Heptapteridae (Heptapterids), p. 406–431. In *Check List of the Freshwater Fishes of South and Central America*. Reis, R. E., S. O. Kullander, and C. J. Jr. Ferraris (eds.). Porto Alegre: Editora da Pontifícia Universidade Católica do Rio Grande do Sul-EDIPUCRS.

Bockmann, F. A., and A. M. Miquelarena. 2008. Anatomy and phylogenetic relationships of a new catfish species from northeastern Argentina with comments on the phylogenetic relationships of the genus *Rhamdella* Eigenmann and Eigenmann 1888 (Siluriformes, Heptapteridae). Zootaxa, 1780(1): 1–54.

Bockmann, F. A., and R. Castro. 2010. The blind catfish from the caves of Chapada Diamantina, Bahia, Brazil (Siluriformes: Heptapteridae): description, anatomy, phylogenetic relationships, natural history, and biogeography. Neotropical Ichthyology, 8(4), 673–706.

Bockmann, F. A., and V. Slobodian. 2017. Family Heptapteridae – three-barbeled catfishes, p. 233–252. In *Field Guide to the Fishes of the Amazon, Orinoco and Guianas*. van der Sleen, P., and J. S. Albert (eds.). Princeton: Princeton University Press.

Buckup, P. A. 1988. The genus *Heptapterus* (Teleostei: Pimelodidae) in southern Brazil and Uruguay, with the description of a new species. Copeia 1988: 641–653.

Cavalheiro, L. W., and C. B. Fialho. 2020. Fishes community composition and patterns of species distribution in Neotropical streams. Biota Neotropica, 20(1): e20190828.

Drummond, A. J., M. A. Suchard, and A. Rambaut. 2012. Bayesian phylogenetics with BEAUti and the BEAST 1.7. Molecular Biology and Evolution 29: 1969–1973.

Faustino-Fuster, D. R., F. A. Bockmann, and L. R. Malabarba. 2019. Two new species of *Heptapterus* (Siluriformes: Heptapteridae) from the Uruguay River basin, Brazil. Journal of fish biology 94(3): 352–373.

Faustino-Fuster, D. R., and H. Ortega. 2020. A new species of *Mastiglanis* Bockmann 1994 (Siluriformes: Heptapteridae) from the Amazon River basin, Peru. Zootaxa, 4820(2), zootaxa-4820.

Faustino-Fuster, D. R., Meza-Vargas, V., Lovejoy, N. R., and N. K. Lujan. 2021. Multi-locus phylogeny with dense Guiana Shield sampling supports new suprageneric classification of the Neotropical three-barbeled catfishes (Siluriformes: Heptapteridae). Molecular Phylogenetics and Evolution, 162, 107186.

Faustino-Fuster, D. R., and L. S. de Souza. 2022. A new species of *Cetopsorhamdia* (Siluriformes: Heptapteridae) from the Upper Amazon River basin. Journal of fish biology, 100(1), 25–39.

Ferraris, C. J. Jr. 1988. Relationships of the neotropical catfish genus *Nemuroglanis*, with a description of a new species (Osteichthyes: Siluriformes: Pimelodidae). Proceedings of the Biological Society of Washington 101: 509–516.

Ferrer, J. and L. R. Malabarba. 2020. Systematic revision of the Neotropical catfish genus *Scleronema* (Siluriformes: Trichomycteridae), with descriptions of six new species from Pampa grasslands. Neotropical Ichthyology 18(2): e190081.

Fricke, R., W. N. Eschmeyer, and R. Van der Laan. (eds.). 2022. Eschmeyer's catalog of fishes: genera, species, references. http://researcharchive.calacademy.org/research/ichthyology/catalog/fishcatmain.asp. Electronic version accessed 06 Apr 2020.

Hammer, O., D. A. Harper, and P. D. Ryan. 2001. PAST: Paleontological statistics software package for education and data analysis. Palaeontologia electronica 4(1): 1–9.

Hasegawa, M., H. Kishino, and T. A. Yano. 1985. Dating of the human-ape splitting by a molecular clock of mitochondrial DNA. Journal of molecular evolution 22(2): 160–174.

Haseman, J. D. 1911. Some new species of fishes from the Rio Iguassú. Annals of the Carnegie Museum 7: 374–387.

Instituto Chico Mendes de Conservação da Biodiversidade (ICMBio). 2021. *Heptapterus multiradiatus*. The IUCN Red List of Threatened Species 2021: e.T187180A1824319.

Ihering, R. V. 1907. Diversas espécies novas de peixes nematognathas do Brasil. Notas preliminares do Museu Paulista, 1(1), 13-39.

Lucena, C. A. S., A. B. Zaluski, and Z. M. S. de Lucena. 2017. *Astyanax taurorum* a new species from dos Touros River, Pelotas River drainage, an upland southern Brazilian river (Characiformes: Characidae). Zoologia 34: e201174: 1–8.

Lundberg, J. G., A. H. Bornbusch, and F. Mago-Leccia. 1991. *Gladioglanis conquistador* n. sp., from Ecuador with diagnoses of the subfamilies Rhamdiinae Bleeker and Pseudopimelodinae n. subf. (Siluriformes, Pimelodidae). Copeia 1991: 190–209.

Lundberg, J. G., and L. McDade. 1986. A redescription of the rare Venezuelan catfish *Brachyrhamdia imitator* Myers (Siluriformes: Pimelodidae) with phylogenetic evidence for a large intrafamilial lineage. Notulae Naturae 463: 1–24.

Pons, J., T. G. Barraclough, J. Gomez-Zurita, A. Cardoso, D. P. Duran, S. Hazell, S. Kamoun, W. D. Sumlin, and A. P. Vogler. 2006. Sequence-based species delimitation for the DNA taxonomy of undescribed insects. Systematic Biology 55: 595–609.

Rambaut, A., and A. J. Drummond. 2013. *TreeAnnotator v1. 7.5*. Available as part of the BEAST package from http://beast.bio.ed.ac.uk.

Rambaut, A., M. Suchard, D. Xie, and A. Drummond. 2013. *Tracer v1.6*. Available from http://tree.bio.ed.ac.uk/software/tracer/.

Sabaj, M. H. 2020. Codes for Natural History Collections in Ichthyology and Herpetology. Copeia 108: 593–669.

Schaefer, S. A., and A. E. Aquino. 2000. Postotic laterosensory canal and pterotic branch homology in catfishes. Journal of Morphology 246: 212–227.

Silva, G. S., Roxo, F. F., Melo, B. F., Ochoa, L. E., Bockmann, F. A., Sabaj, M. H., Jerep, F. C., Foresti F., Benine, R. C., and C. Oliveira. 2021. Evolutionary history of Heptapteridae catfishes using ultraconserved elements (Teleostei, Siluriformes). Zoologica Scripta, 50(5), 543–554.

Stewart, D. J. 1986. Revision of Pimelodina and description of a new genus and species from the Peruvian Amazon (Pisces: Pimelodidae). Copeia, 653–672.

Sullivan, J.P., Lundberg, J.G., and M. Hardman. 2006. A phylogenetic analysis of the major groups of catfishes (Teleostei: Siluriforms) using RAG1 and RAG2 nuclear gene sequences. Mol. Biol. Evol. 41, 636–662.

Sullivan, J.P., Muriel-Cunha, J., and J.G. Lundberg. 2013. Phylogenetic relationships and molecular dating of the major groups of catfishes of the Neotropical superfamily Pimelodoidea (Teleostei, Siluriformes). Proc. Acad. Nat. Sci. Philadelphia 89–110.

Systat, S. P. 2008. Version 12.0. *Systat Software Inc., San Jose, CA*.

Taylor, W. R., and G. C. Van Dyke. 1985. Revised procedures for staining and clearing small fishes and other vertebrates for bone and cartilage study. Cybium 9: 107–119.

Tencatt, L. F. C., M. R. D. Britto, and C. S. Pavanelli. 2016. Revisionary study of the armored catfish *Corydoras paleatus* (Jenyns, 1842) (Siluriformes: Callichthyidae) over 180 years after its discovery by Darwin, with description of a new species. Neotropical Ichthyology 14(1): 75–94.

Valenciennes, A. 1835. Poissons. In *Voyage dans L'Amérique Méridionale (le Brésil, la République Orientale de l'Uruguay, la République Argentine, la Patagonie, la République du Chili, la République de Bolivia, la République du Pérou), exécuté pendant les années 1826, 1827, 1828, 1829, 1830, 1832 et 1833.* Vol. 9. d'Orbigny, A. (eds.). Paris: Bertrand et Levrault.

Valenciennes, A. 1840. Des Pimélodes, p. 123–206. In *Histoire Naturelle des Poissons.* Vol. 15. Cuvier, G., and A. Valenciennes, A., eds). Paris: Bertrand et Levrault.

Wingert, J. M., J. Ferrer, and L. R. Malabarba. 2017. Review of the *Odontesthes perugiae* species group from Río de La Plata drainage, with the description of a new species (Atherinomorpha: Atherinopsidae). Zootaxa 4250: 501–528

Zhang, J., P. Kapli, P. Pavlidis, and A. Stamatakis. 2013. A general species delimitation method with applications to phylogenetic placements. Bioinformatics 29: 2869–2876.

Tables

Figure Captions

Figure 1. Phylogenetic relationships of *Heptapterus* clade based on Maximum likelihood (ML) analysis of a 3972 bp alignment consisting of three mitochondrial loci (coI, cytb and ND2) and two nuclear loci (Glyt and Rag2). Node numbers correspond to ML support. Colour bars correspond to species delimitation methos; black barr correspond to morphological (MOR), red bar correspond to coalescent branching process of all sequences, estimated by using the Poisson Tree Processes (PTP) and blue bar correspond to General Mixed Yule Coalescent model (GMYC). *= type species of the genus.

Figure 2. *Heptapterus carnatus*, holotype, UFRGS 22840, 106.9 mm SL, Brazil, Rio Grande do Sul State, Vacaria Municipality, Passo do Portão Creek, tributary of the Pelotas River, Uruguay River basin. (A) Lateral, (B) dorsal and (C) ventral views. Scale bar 1 cm.

Figure 3. Distribution of *Heptapterus* species: *Heptapterus carnatus* (yellow circle) *Heptapterus exilis* (blue circle); *Heptapterus mustelinus* (green circle) and *H. qenqo* (red circle). Star symbol represents the type locality. Start symbol represent type localities. Each symbol may represent more than one lot.

Figure 4. *Heptapterus exilis*, holotype, UFRGS 22500, 64.0 mm SL, Brazil, Rio Grande do Sul State, Quevedos Municipality, sanga das Tunas, tributary of the Ibicuí River, Uruguay River drainage. (A) Lateral, (B) dorsal and (C) ventral views. Scale bar 1 cm.

Figure 5. *Heptapterus mustelinus*, UFRGS 21199, 117.6 mm SL, Brazil, Rio Grande do Sul, São Gabriel, tributary of creek Caiboate-Mirim, rio Jacuí drainage, Laguna dos Patos system. (A) Lateral, (B) dorsal and (C) ventral views. Scale bar 1 cm.

Figure 6. *Heptapterus qenqo*, CI-FML 3954, 182.7 mm SL, Argentina, Tucuman State, Trancas Municipality, Rearte River tributary to Sali River drainage. (A) Lateral, (B) dorsal and (C) ventral views.

Figure 7. *Leptoheptapterus lopezae*, UFRGS 24777, 82.1 mm SL, Brazil, São Paulo State, Iporanga Municipality. Betari River tributary to Ribeira do Iguape drainage. (A), dorsal (B), and ventral views (C). Scale bar = 1 cm.

Figure 8. Lateral view of the caudal skeleton of (A) *Leptoheptapterus lopezae*, UFRGS 24777, 82.1 mm SL; (B) *Leptoheptapterus longipinnis*, paratype, UFRGS 25401, 71.4 mm SL; and (C) *Leptoheptapterus robustus*, paratype, UFRGS 22597, 42.3 mm SL. Abbreviations of the anatomical parts: ep = epural; hi1 + hi2 = complex plate formed by hypurals 1 and 2; hi3 + hi4 + hi5 = complex plate formed by hypurals 3, 4, and 5; ph = parhypural; pu1 + u1 = complex centrum formed by preural centrum 1 and ural centrum 1; pu2 = preural centrum 2; ur = uroneural. Arrows = anterior processes.

Figure 9. Dorsal view of cranium of (A) *Leptoheptapterus lopezae*, UFRGS 24777, 82.1 mm SL; (B) *Leptoheptapterus longipinnis*, paratype, UFRGS 25401, 71.4 mm SL; and (C) *Leptoheptapterus robustus*, paratype, UFRGS 22597, 42.3 mm SL. Anatomical abbreviations: afo = anterior fontanel; apa = autopalatine; epo = epioccipital; exo = exoccipital; exs = extrascapula; fro = frontal; let = lateral ethmoid; max = maxilla; nas = nasal; pfo = posterior fontanel; pmx = premaxilla; pto = pterotic; soc = supraoccipital; sph = sphenotic; trp4 = transverse process 4; trp5 = transverse process 5.

Figure 10. Lateral view of suspensorium of (A) *Leptoheptapterus lopezae*, UFRGS 24777, 82.1 mm SL; (B) *Leptoheptapterus longipinnis*, paratype, UFRGS 25401, 71.4 mm SL and (B) *Leptoheptapterus robustus*, paratype, UFRGS 22597, 42.3 mm SL. Anatomical abbreviations: ent = entopterygoid; hyo = hyomandibula; iop = interopercle; met = metapterygoid; ope = opercle; pop = preopercle; and qua = quadrate.

Figure 11. Dorsal view of the branchial arch of (A) *Leptoheptapterus lopezae,* UFRGS 24777, 82.1 mm SL. (B) *Leptoheptapterus longipinnis*, paratype, UFRGS 25401, 71.4 mm SL and (C) *Heptapterus robustus*, paratype, UFRGS 22597, 42.3 mm SL. Anatomical

abbreviations: bb_{2-3} = second and third basibranchials; gr = gill rakers; cb_{1-5} = first to fifth ceratobranchials; eb_{1-4} = first to fourth epibranchials; hb_{1-3} = first to third hypobranchials.

Figure 12. Distribution of *Leptoheptapterus lopezae* (blue circle)*, Leptoheptapterus longipinnis* (green circle) and *Heptapterus robustus* (red circle). Start symbol represent type localities. Each symbol may represent more than one lot.

Figure 13. *Leptoheptapterus longipinnis*, UFRGS 11590, 61.3 mm SL, holotype. Brazil, Rio Grande do Sul State, Panambi Municipality, rio Palmeira tributary to rio Ijuí, Uruguay River basin. Lateral (A), dorsal (B), and ventral views (C). Scale bar = 1 cm.

Figure 14. *Leptoheptapterus robustus*, MCP 51365, 67.1 mm SL, holotype. Brazil, Santa Catarina State, Piratuba Municipality, rio do Peixe tributary to Upper rio Uruguai, Uruguay River basin. Lateral (A), dorsal (B), and ventral views (C). Scale bar = 1 cm.

Figure 15 (A) Principal component analysis (PCA) of the two new species, *Leptoheptapterus longipinnis* (red circle) and *L. robustus* (blue circle). Linear regression of the most discriminatory measurements between *L. longipinnis* (black circle) and *L. robustus* (white circle). (B) Body depth (M6) *vs.* standard length. (C) Caudal peduncle length (M8) *vs.* standard length. (D) Body width (M9) *vs.* standard length. Line means trend line (95%).

Figure 16. Variation of (A) number of vertebrae at dorsal fin insertion, and (B) total number of anal-fin rays for species of *Heptapterus* and *Leptoheptapterus*.

Figures

CAPITULO IV: KNOWING THE HIDDEN DIVERSITY WITHIN HEPTAPTERINI BLEEKER, 1858 GENERA (SILURIFORMES: HEPTAPTERIDAE)

Article 1: Faustino-Fuster, D. R., & Ortega, H. (2020). A new species of *Mastiglanis* Bockmann 1994 (Siluriformes: Heptapteridae) from the Amazon River basin, Peru. Zootaxa, 4820(2), zootaxa-4820.

Zootaxa 4820 (2): 323–336
https://www.mapress.com/j/zt/

Article

ISSN 1175-5326 (print edition)
ZOOTAXA
ISSN 1175-5334 (online edition)

https://doi.org/10.11646/zootaxa.4820.2.6
http://zoobank.org/urn:lsid:zoobank.org:pub:4EAC36C3-597B-404B-9AC6-2A1FD79C658F

A new species of *Mastiglanis* Bockmann 1994 (Siluriformes: Heptapteridae) from the Amazon River basin, Peru

DARIO R. FAUSTINO-FUSTER[1,2*] & HERNÁN ORTEGA[1,3]
[1]*Departamento de Ictiología, Museo de Historia Natural, Universidad Nacional Mayor de San Marcos, Av. Arenales 1256, Jesús María, Lima, Perú.*
[2]*Departamento de Zoologia, Universidade Federal do Rio Grande do Sul, Programa de Pós-Graduação em Biologia Animal Av. Bento Gonçalves, 9500, Bloco IV, Prédio 43433, Campus do Vale, Bairro Agronomia, Porto Alegre, RS, Brasil.*
[3] *https://orcid.org/0000-0002-4396-2598*
**Corresponding author. darioff36@gmail.com; https://orcid.org/0000-0002-1445-3495*

Abstract

Mastiglanis is a genus of heptapterid catfish represented by two valid species. These freshwater species are widely distributed along the Amazon, Orinoco, and Maroni River basins. However, a taxonomic review of specimens collected in the Putumayo and Nanay rivers, Amazon River basin in Peru revealed a new species of *Mastiglanis*. A morphological analysis was completed for morphometric (36 measurements) and meristic (20 counts) data. Osteological counts and descriptions were made from clear and stained specimens and X-rays images. The new species of *Mastiglanis* differs from *M. asopos* and *M. durantoni* by having a long pelvic fin, short snout, eight branched anal-fin rays, and a higher number of vertebrae and gill rakers. The distribution of the new species is restricted to the upper Amazon River basin.

Key words: small catfish, freshwater, morphology, taxonomy

Resumen

Mastiglanis es un género de bagres heptaptéridos representado por dos especies válidas. Estos peces dulceacuícolas se encuentran ampliamente distribuidos a lo largo de la cuenca de los ríos Amazonas, Orinoco y Maroni. La revisión taxonómica de ejemplares colectados en las cuencas de los ríos Putumayo y Nanay, cuenca del río Amazonas en Perú, reveló una especie nueva de *Mastiglanis*. El análisis morfológico fue realizado considerando datos morfométricos (36 medidas) y merísticos (20 conteos); algunos conteos y descripciones osteológicas fueron realizados de material diafanizado e imágenes de rayos X. La especie nueva de *Mastiglanis* se diferencia de *M. asopos* y *M. durantoni* por tener la altea pélvica larga, hocico corto, ocho radios ramificados en la aleta anal, y un mayor número de vértebras y espinas branquiales. La nueva especie se encuentra distribuida en los ríos Yaguas, tributario del rio Putumayo; y en el río Nanay, tributarios de la cuenca del rio Amazonas en Perú. La distribución de la especie nueva esta restricta a la región alta del rio Amazonas.

Palabras clave: bagre pequeño, dulceacuícola, morfología, taxonomía

Introduction

Within the order Siluriformes, Heptapteridae is the fourth most species-rich family, represented by 226 valid species and 23 genera (Fricke *et al.*, 2020). The systematic situation of Heptapteridae has been very confusing, and it was originally included as subfamily in the Pimelodidae. The first study that recognized this group as monophyletic was conducted by Lundberg & McDade (1986), who treated them as an unnamed clade within Pimelodidae. Lundberg *et al.* (1991) formally named this group as Rhamdiinae (Bleeker 1862) within Pimelodidae. Subsequently, this subfamily was raised to the family level by de Pinna (1993), in his doctoral thesis (unpublished); but the first publish usage on familial rank as Rhamdiidae was made by Swarça *et al.* (2000). Silfvergrip (1996) demonstrated the priority of the name Heptapterinae (Gill 1861) over Rhamdinae (Bleeker 1862); and Bockmann (1998), in his

Accepted by J. Armbruster: 3 Jul. 2020; published: 28 Jul. 2020

doctoral thesis (unpublished), use the new family level; but the first publish family raking was used by Bockmann & Guazelli (2003). Bockmann (1998) in his unpublished doctoral thesis; proposed the most comprehensive phylogenetic relationships, redefining the current genera and proposing new ones based on morphological data. However, none of these new genera have been formally described to date, despite being referred in other published works (*e g*. Bockmann & Slobodian, 2018).

Mastiglanis Bockmann, 1994 is considered a member of *Nemuroglanis* subclade within Heptapteridae (Bockmann, 1994) and it is the most recently defined genus for the family. It was described as monotypic, represented by *Mastiglanis asopos* Bockmann, 1994, widely distributed along the Amazon basin and Capim river in Brazil. The most recently described species, *M. durantoni* de Pinna & Keith, 2019, was described from Maroni River basin, French Guyana. *Mastiglanis* is considered a member of *Nemuroglanis* subclade based on 16 synapomorphies (Ferraris, 1988; Bockmann, 1994).

Mastiglanis is differentiated from all members of Heptapteridae based on the following diagnostic characters (Bockmann, 1994): (1) a very small amount of integument pigmentation; (2) anterior element of the dorsal fin (homologous to the spine) prolonged as a long filament; (3) first element of the pectoral fin (homologous to the pectoral-fin spine) prolonged as a filament; (4) anterior internarial width greater than the posterior internarial width; (5) narrow frontal bones in the supraorbital portion; (6) presence of a plate-like process at the anteromedial margin of the premaxilla; (7) angled mesethmoid cornu, which bends abruptly laterally at midlength; (8) elongate, roughly rectangular metapterygoid; (9) dorsal flange of the opercle in the same plane as the rest of the bone; (10) ventrally curved posterior portion of the opercle bone. Additionally, external characters are used for identification: large eye; long maxillary barbels, extending beyond the origin of the adipose fin; ventral mouth; and triangular pectoral fins. A revision of material from the Upper Amazon tributaries in Peru revealed a new form of *Mastiglanis* (Faustino-Fuster, 2019, Almeida, 2019). The new species is found in the Nanay and Yaguas rivers from Peru, sharing most of the distinctive characteristics of *Mastiglanis*, but identified by its unique morphological characteristics and pattern of coloration described here.

Material and methods

Measurements were taken with digital calipers (to 0.1 mm) following the landmarks illustrated by Faustino-Fuster *et al.* (2019, Fig. 1). The terminologies used for the measurements were following Bockmann (1994). A principal component analysis (PCA) was performed using PAST 3.x software, version 2016 (Hammer *et al.*, 2001) to reduce the dimensionality datasets and maximize morphometric variance (between all specimens in Table 1). Morphometrical variables found to better discriminate between these species are presented as linear regressions using SigmaPlot (Systat Software, San Jose, CA). Standard length (SL) was expressed in millimeters and body measurements as percentages of SL or head length (HL) for the head parts (except for barbels).

Counts of pectoral-, pelvic-, anal-, dorsal-, and caudal-fins rays, gill rakers, ribs, vertebrae (including the first five vertebrae of the Weberian apparatus and one of the hypural plate), and morphological description were taken from cleared and stained (c&s) and X-ray specimens (xr). Cleared and stained specimens were prepared according to Taylor & Van Dyke (1985); and X-rays images were taken with the AXR 110 Hotshot X-Ray System at the fish division, Field Museum of Natural History, Chicago, United States. Quantitative variations were represented by box-plot diagrams that show the median of the sample (= 50th percentile), 25th, and 75th percentiles. The 10th and 90th percentiles are represented by error bars. Nomenclature of the laterosensory cephalic system followed Bockmann & Miquelarena (2008). Geographic distribution map was made using Quantum GIS version 2.18.10 (Sherman *et al*., 2012). Institutional abbreviations follow Sabaj (2019).

Comparisons were undertaken directly through examination of specimens, including types and original descriptions of *Mastiglanis asopos* (Bockmann, 1994) and *M. durantoni* (de Pinna & Keith, 2019).

FIGURE 1. *Mastiglanis yaguas*, new species, MUSM 66612, holotype, 49.1 mm SL, (A) Lateral view of right side (image flipped), (B) Dorsal view, (C) Ventral view. Bar = 1 cm.

Results

***Mastiglanis yaguas*, new species**
(Figures 1 A–C, 2, 3, 4; Table 1)
urn:lsid:zoobank.org:act:F33BDFEC-872C-45D0-BCF8-700D28CDC999

Mastiglanis sp.: Hidalgo & Ortega-Lara, 2011: 98, 103, 106, 221, 227, 229, 324 (species list).
Mastiglanis sp1.: Faustino-Fuster, 2019: 11–17, Table 1. Fig.: 1–7 (taxonomic revision).
Mastiglanis sp5.: Almeida, 2019: 71–75. Fig. 22 (taxonomic revision).

Holotype. MUSM 66612, 49.1 mm SL. Peru, Loreto Department, Putumayo Province, Yaguas District, Putumayo River basin, Yaguas River, 2°43'5.31"S; 70°31'42.12"W, 29 November 2010, M. Hidalgo & A. Ortega-Lara.

Paratypes. All from Peru: Nanay Province, Iquitos District, Nanay River: ANSP 167653, 1, 43.1 mm SL, beach downstream from Nina Rumi community, 3°44'0.00"S; 73°19'60.00"W, 8 September 1990, Dan & Pat Fromm; ANSP 167654, 1, 37.9 mm SL, beach downstream from Nina Rumi community, 3°44'0.00"S; 73°19'60.00"W, 8 Sep. 1990, Dan & Pat Fromm; ANPS 167715, 5, 30.3–37.2 mm SL, beach downstream from Minchana community, 3°53'0.00"S; 73°27'0.00"W, 10 September. 1990, Dan & Pat Fromm; ANSP 178449, 7, 37.0–55.4 mm SL, beach in Pampachica, 3°45'9.00"S; 73°16'60.00"N, 2 August 2001, M. Sabaj, M. Littmann, N. Lovejoy, C. Skelton, K. Elkin, M. Thomas & J. Stewart; ANSP 180407, 20, 37.5–52.7 mm SL, beach upstream from Santa Clara community,

3°46'45.00"S; 73°22'6.00"W, 14 August 2003, M. Sabaj, N. Salcedo & B. Sidlauskas; ANSP 181127, 6, 40.0–43.4 mm SL, beach in Pampachica, 3°45'9.00"S; 73°16'60.00"N, 21 August 2005, M. Sabaj & C. Pérez; ANSP 182474, 7, 38.6–47.7 mm SL, beach in Pampachica, 3°45'9.00"S; 73°16'60.00"N, 7 Aug. 2005, M. Sabaj, C. Perez, M. Arce & A. Bullard; ANSP 182565, 1, 41.7 mm SL, beach in Pampachica, 3°45'9.00"S; 73°16'60.00"N, 3 August 2005, M. Sabaj, C. Pérez, A. Bullard, C. DoNascimiento, O. Castillo, S. Snyder; ANSP 182750, 1, 46.8 mm SL, beach upstream from confluence with the Amazonas River, 3°42'49.00"S; 73°16'43.00"W, 15 August 2005, M. Sabaj, C. DoNascimiento & O. Castillo; ANSP 191830, 5, 29.7–46.6 mm SL, beach upstream from Pampachica, 3°45'10.00"S; 73°16'60.00"W, 6 August 2010, M. Sabaj, B. Sidlauskas, C. Phillips, J. Tiemann & E. Correa. Loreto Department, Putumayo Province, Yaguas District: FMNH 140321, 3 (all xr), 41.5–47.1 mm SL; MCP 54155, 1, 43.3 mm SL; MUSM 61686, 5 (1 c&s), 42.7–51.3 mm SL; UFRGS 27250, 1, 38.0 mm SL, collected with the holotype. MUSM 61545, 1, 38.2 mm SL, Yaguas River, 2°43'5.31"S; 70°31'42.12"W, 27 November 2010, M. Hidalgo & A. Ortega-Lara.

Diagnosis. *Mastiglanis yaguas* differs from all its congeners by having eight branched anal-fin rays (*vs.* seven), longer pelvic fin, exceeding the origin of the adipose fin (21.2–26.1% SL) (*vs.* not exceeding the adipose-fin origin 17.7–19.1% SL in *M. asopos* and 16.0–18.4 % SL in *M. durantoni*), 39 vertebrae (*vs.* 37–38 vertebrae in *M. asopos* and 38 in *M. durantoni*), anterior process on posteriormost neural spines (*vs.* lacking of anterior process), process at symphysial region of premaxilla absent (*vs.* present), posterior fontanel two times wider than anterior fontanel (*vs.* one and a half), anterior process of premaxilla short (*vs.* long). Additionally *M. yaguas* is differentiated from *M. asopos* by having more epibranchial gill rakers (2 *vs.* 0), more ceratobranchial gill rakers (13 *vs.* 11), slender body (body width 12.9–14.9% SL *vs.* 15.6–17.2% SL), deeper head (59.5–67.9% HL *vs.* 38.5–47.8% HL), narrow head (44.7–50.9% HL *vs.* 57.9–70.9% HL), wider interorbital distance (30.3–36.4% HL *vs.* 22.3–24.6% HL), larger eye (21.4–24.7% HL *vs.* 18.6–20.5% HL), and wider posterior inter-narial distance (10.3–14.2% HL *vs.* 7.7–9.1% HL).

Description: Morphometric data presented in Table 1. Body slightly elongated, elliptical in anterior cross section at level of dorsal-fin origin, then gradually compressed along caudal peduncle (Figure 1). Dorsal profile of body more convex than ventral profile; dorsal profile convex from snout tip to last dorsal-fin ray; almost straight from last dorsal-fin ray to adipose-fin origin, and slightly convex from adipose-fin origin to caudal-fin origin. Ventral profile of head slightly convex from snout tip to gill opening. Ventral profile of body slightly convex from gill opening to pelvic-fin origin, nearly straight from pelvic-fin origin to anal-fin origin, and slightly convex to caudal peduncle. Anus and urogenital pore close to each other.

Head short, narrow, depressed, and trapezoidal in dorsal view (Figure 1B). Anterior nostril near to upper lip and posterior nostril slightly closer to anterior edge of eye than to anterior nostril. Distance between anterior nostrils greater than distance between posterior nostrils, nostrils arranged as vertices of trapezoid. Mouth subterminal, with snout projected beyond lower jaw. Barbels very long, tapering distally. Maxillary barbel origin dorsally to upper lip and lateral to anterior nostrils, reaching half of adipose fin when adpressed along body axis. Mental barbel origin between anterior edge of lower jaw and gular fold. Outer mental barbel longer than inner mental barbel, tip reaching pelvic-fin origin when adpressed along body axis. Inner mental barbel origin closer to gular fold, tip surpassing pectoral-fin origin when adpressed along body axis. Eye large; horizontally elliptical; slightly anterior at midpoint between tip of snout and edge of opercular membrane; dorsal region slightly covered by skin, lens visible and pupil rounded. Branchiostegal rays seven (1). Gill rakers on first ceratobranchial 13 (1) (including one on angle formed with epibranchial), and two (1) on first epibranchial.

Dorsal fin with i+6 (11) rays; triangular; first dorsal-fin ray unbranched, with stiffened proximal region, approximately as long as first branched ray, and distal region soft and long, surpassing half-length of adipose fin when adpressed; followed by six branched rays; dorsal-fin origin anterior to vertical through pelvic-fin origin. First pterygiophore of dorsal fin inserted between bifid neural spines of vertebrae 6–7 (4).

Pectoral fin with i+9 (11) rays; triangular; proximal region of first ray stiffened, approximately as long as first branched ray, distal region soft and filamentous, reaching vertical through half-length of adipose fin when adpressed; second ray of pectoral fin (first branched ray) almost as long as third ray (second branched ray) followed by branched rays decreasing moderately in length.

Pelvic fin with i+5 (11) rays; rounded distal margin; first pelvic-fin ray, completely flexible and slightly shorter than second and third rays (first and second branched rays, respectively); origin of pelvic-fin anterior to vertical through half-length of body standard length, and between the verticals through fourth and fifth dorsal-fin branched rays; tip of adpressed pelvic-fin reaching vertical through anal-fin origin.

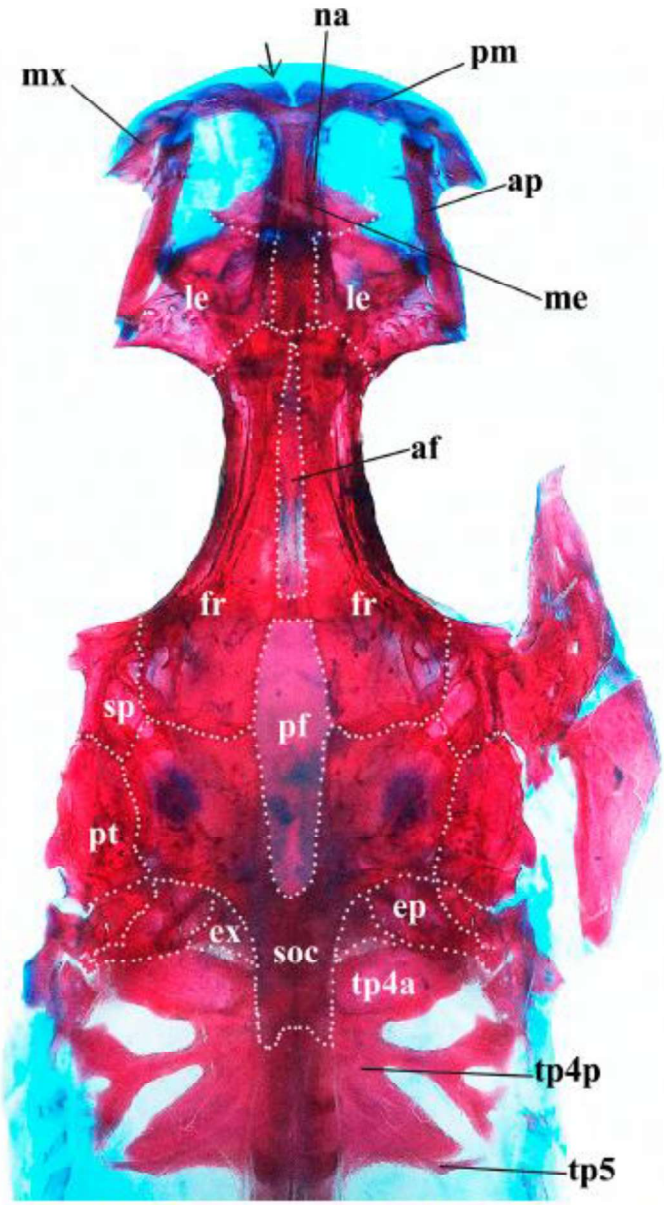

FIGURE 2. Dorsal view of cranium of *Mastiglanis yaguas*, paratype, MUSM 61686, 42.7 mm SL. Abbreviations: af = anterior fontanel; ap = autopalatine; ep = epioccipital; ex = exoccipital; fr = frontal; le = lateral ethmoid; mx = maxilla; na = nasal; pf = posterior fontanel; pm = premaxilla; pt = pterotic; soc = supraoccipital; sp = sphenotic; tp4a = anterior branch of transverse process of vertebra 4; tp4b = posterior branch of transverse process of vertebra 4; tp5 = transverse process of vertebra 5 . Arrow = symphysial region of premaxilla.

TABLE 1. Morphometric data of *Mastiglanis yaguas* and *M. asopos*. H (Holotype); N (number of specimens); Min (minimum); Max (maximum) SD (standard deviation).

	M. yaguas New species						*M. asopos* Bockmann 1994				
	H	N	Min	Max	Mean	SD	H	N	Min	Max	SD
Standard length (mm)	49.1	17	32.51	69.78	47.0	-	65.4	10	42.2	65.4	-
Percentage of SL											
M1—Predorsal length	34.0	17	31.8	35.3	33.6	0.9	34.6	10	32.8	35.2	0.7
M2—Preanal length	65.8	17	65.8	68.9	67.4	1.0	69.8	10	67.9	71.0	1.1
M3—Prepelvic length	42.4	17	39.9	42.7	41.4	1.0	42.5	10	41.1	43.6	0.7
M4—Preadipose length	59.9	17	58.5	65.4	61.5	1.6	64.7	10	62.3	66.8	1.3
M5—Caudal-peduncle length	21.3	17	20.7	23.7	22.7	0.9	20.1	10	17.7	21.8	1.1
M6—Caudal-peduncle depth	5.9	17	5.5	6.2	5.9	0.2	6.2	10	5.7	6.7	0.3
M7—Adipose-fin length	26.7	17	21.6	27.1	24.4	1.6	22.7	10	19.0	24.4	1.5
M8—Dorsal fin to adipose fin	16.0	17	15.0	19.4	17.1	1.2	17.2	10	15.9	19.3	1.0
M9—Anal-fin base length	11.7	17	9.5	11.9	10.9	0.6	10.4	10	10.4	12.0	0.4
M10—Unbranched dorsal-fin ray length	18.2	14	29.3	38.2	33.4	2.7	-	5	36.5	40.7	2.1
M11—Length of 1st branched dorsal-fin ray	27.0	17	21.6	27.1	24.6	1.7	23.9	9	22.6	26.0	1.0
M12—Length 2nd branched dorsal-fin ray	21.9	17	16.4	24.0	20.4	1.8	19.1	10	19.1	22.2	1.2
M13—Dorsal-fin base	12.2	17	11.9	14.5	13.1	0.6	13.5	10	13.1	14.8	0.5
M14—Pelvic-fin length	25.7	17	21.2	26.1	23.9	1.3	18.8	10	17.7	19.1	0.4
M15—Unbranched pectoral-fin ray length	37.1	6	49.4	59.8	54.6	7.4	65.3	9	50.6	65.3	4.6
M16—Length 1st branched pectoral-fin ray	22.1	13	18.7	25.6	21.7	1.8	20.9	10	18.0	21.4	1.0
M17—Length 2nd branched pectoral-fin ray	17.4	14	16.5	21.3	18.1	1.5	17.5	10	15.3	17.7	0.9
M18—Body depth	11.3	17	10.3	13.4	11.8	0.8	12.6	10	10.5	12.6	0.7
M19—Body width	13.4	17	12.9	14.9	13.9	0.6	17.2	10	15.6	17.2	0.5
M20—Maxillary barbel length	65.7	17	60.8	82.2	66.1	5.5	76.6	10	66.2	81.2	4.7
M21—Outer mental-barbel length	43.0	17	34.3	58.9	42.1	6.7	44.4	10	25.9	44.4	5.3
M22—Inner metal-barbel length	25.0	17	20.2	42.8	26.5	5.8	17.2	10	14.3	20.0	1.7
M23—Head length	20.6	17	19.8	23.3	21.6	0.9	22.7	10	22.7	24.7	0.8
Percentage of HL											
M24—Head depth	61.5	17	59.5	67.9	62.5	2.7	47.8	10	38.5	47.8	2.8
M25—Head width	45.8	17	44.7	50.9	47.5	2.0	70.9	10	57.9	70.9	3.8
M26—Bony Interorbital	14.0	17	13.1	15.9	14.6	0.8	11.7	10	9.6	11.7	0.6
M27—Fleshy Interorbital	34.2	17	30.3	36.4	33.8	1.8	22.5	10	22.3	24.6	0.8
M28—Eye diameter	22.7	17	21.4	24.7	22.8	0.8	19.8	10	18.6	20.5	0.6
M29—Preorbital length	48.2	17	44.2	50.7	48.1	1.7	51.6	10	46.2	53.7	2.0
M30—Snout length	37.5	17	31.9	37.5	35.6	1.6	41.9	10	36.5	43.9	2.1
M31—Internarial length	15.3	17	11.8	15.9	14.0	1.2	14.8	10	12.8	18.5	1.6
M32—Anterior internarial width	15.4	17	11.3	16.0	13.8	1.5	11.0	10	10.2	13.0	0.9
M33—Posterior internarial width	13.8	17	10.3	14.2	12.1	1.0	9.1	10	7.7	9.1	0.4

Anal fin with iii+8 (11) rays (Figure 6A–B); triangular in lateral profile; short (9.5–11.9% of SL). Anal-fin base origin anterior to vertical through adipose-fin origin, and reaching the vertical through half-length of adipose-fin when adpressed. First pterygiophore of anal-fin inserted between hemal spines of vertebrae 22–23 (3) or 23–24 (1).

Adipose fin slightly long (21.6–27.1 % of SL), convex in lateral profile; distance from last dorsal-fin ray to adipose-fin origin shorter than adipose-fin base length. Adipose-fin origin posterior to vertical through body midpoint (excluding caudal fin), posterior region of adipose fin slightly posterior to vertical through anal-fin tip.

Caudal fin bifurcated, dorsal and ventral lobes of same size. Dorsal caudal-fin lobe with seven (11) branched rays; ventral caudal-fin lobe with eight (11) branched rays. Caudal fin with 45 total rays; with 22 (1) rays on dorsal lobe and 23 (1) rays on ventral lobe. Dorsal caudal plate (hypurals 3, 4 and 5) with eight (4) rays; ventral caudal plate (parhypural plus hypurals 1 and 2) with nine (4) rays (Figure 4).

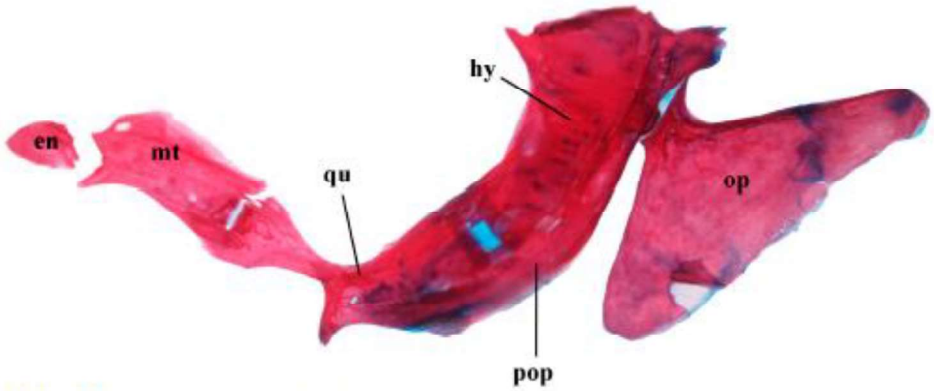

FIGURE 3. Lateral view of suspensorium of *Mastiglanis yaguas*, paratype, MUSM 61686, 42.7 mm SL. Abbreviations: en = entopterygoid; hy = hyomandibula; io = interopercle; mt = metapterygoid; op = opercle; pop = preopercle; and qu = quadrate.

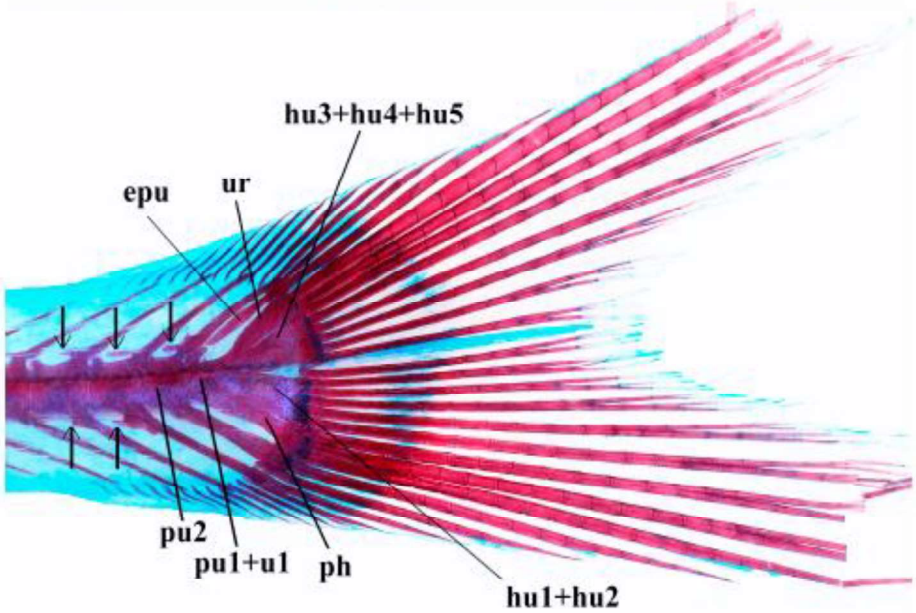

FIGURE 4. Lateral view of caudal skeleton of *Mastiglanis yaguas*, paratype, MUSM 61686, 42.7 mm SL. Abbreviations: epu = epural; hu1 + hu2 = hypurals 1 and 2; hu3 + hu4 + hu5 = hypurals 3, 4, and 5; ph = parhypural; pu1 + u1 = preural centrum 1 and ural centrum 1; pu2 = preural centrum 2; ur = uroneural. Arrows: anterior processes.

Total vertebrae 39 (4). First complete hemal spine on vertebra 14 (4). 13 (4) pre-caudal vertebrae (including five vertebrae of Weberian apparatus) followed by 26 (4) caudal vertebrae. Posteriormost vertebrae 6–9 with anterior neural process; and last 2–3 vertebrae (except on pu1 + u1) with anterior hemal process (Figure 4). Six (1) or seven (3) ribs.

Laterosensory canals of head with simple tubes ending in single pores. Supraorbital canal with seven branches: s1, s2, s3, s4, s6, s7 and s8; each one opening into its own pore, except branch s2 (fused with i2 into complex s2+i2 pore). Infraorbital canal with six branches i1, i2, i3, i4, i5 and i6; each one opening into its own pore, except branch i2 (fused with branch s2 into complex s2 + i2 pore). Preoperculomandibular canal with 10 branches; pm1, pm2, pm3, pm4, pm5, pm7, pm8, pm9, pm10 and pm11, all opening into its own pore except branch pm11, fused with branch po1 (into complex po1 + pm11 pore). Postotic canal with three branches; po1, po2 and po3, each one opening into its own pore except branch po1 (po1 + pm11 pore). Lateral line complete and continue until caudal fin base.

Color in alcohol. Body overall pale cream, with dark brown chromatophores distributed indistinctly on lateral region of body and head; ventral surface unpigmented (Figure 1). Narrow and indistinct lateral strip, dark brown, clearer on posterior region, extending from adipose-fin origin to caudal-fin base. Dorsal region with six conspicuous blotches of dark brown chromatophores: first posterior to supraoccipital process, second anterior to dorsal-fin origin, third posterior to last dorsal-fin ray, fourth between last dorsal-fin ray and adipose-fin origin, fifth at adipose-fin origin, and sixth located at end of adipose-fin base. Dorsal surface of head (supraoccipital) covered with dark brown chromatophores fading laterally, and ventral surface pale. Maxillary barbel, outer mental barbel, and inner mental barbel slightly pigmented with dark brown chromatophores dorsally; and unpigmented ventrally. Dorsal, pectoral, pelvic, anal, and caudal-fin rays lightly pigmented with light brown chromatophores, inter-radial membranes hyaline. Adipose fin with dark brown chromatophores irregularly distributed, more concentrated at proximal region than distal region (hyaline).

Geographic distribution. *Mastiglanis yaguas* is distributed in the Yaguas River, tributary of the Putumayo river basin, and in the Nanay River tributary of the western Amazon River; in Putumayo and Maynas provinces, Loreto department, Peru, Upper Amazon basin. (Figure 5).

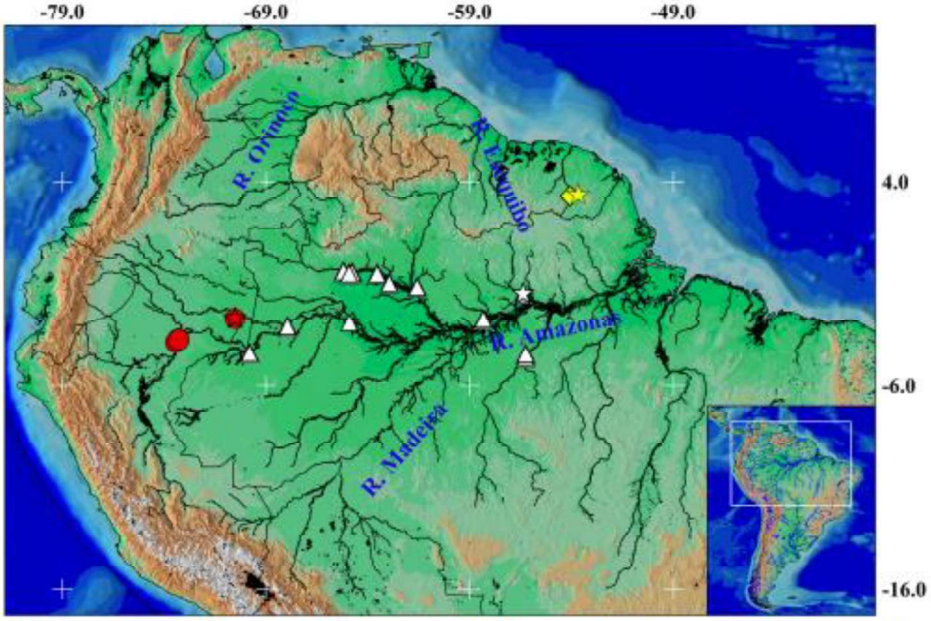

FIGURE 5. Geographical distribution of *Mastiglanis yaguas* (red circle), *M. asopos* (white triangle), and *M. durantoni* (yellow square). Stars represent the type localities of each species. Each symbol may represent more than one specimen.

Etymology. The species name, *yaguas*, is in reference to the Yaguas National Park (Parque Nacional Yaguas) in northeastern Peru; created recently as a conservation area to protect the flora and fauna, and the hidden Amazon biodiversity. The name is treated as a noun in apposition.

Identification key of *Mastiglanis*

1A. Anal fin with eight branched rays and tips of the pelvic fin reaching or surpassing the adipose fin origin ..... *Mastiglanis yaguas* (Upper Amazon basin)

1B. Anal fin with seven branched rays and tips of the pelvic fin not reaching the adipose fin origin 2

2A. Caudal-peduncle depth 5.7–6.7% of SL, 14 dorsal and 17 ventral procurrent caudal-fin rays ..... *Mastiglanis asopos* (Lower Amazon basin)

2B. Caudal peduncle depth 4.3–5.3% of SL, and 12 procurrent caudal-fin rays ..... *Mastiglanis durantoni* (Maroni basin)

Discussion

Mastiglanis belongs to the *Nemuroglanis* subclade, which is defined by 16 synapomorphies proposed by Ferraris (1988) and Bockmann (1994). All synapomorphies were found in the new species. *Mastiglanis yaguas* also presents all the synapomorphies of the genus as suggested by Bockmann (1994) with some variation in the following characters: character 5 (frontals narrow at supraorbital portion), *M. yaguas* has wider frontals than congeners, width 0.4 times of frontal length (0.3 in *M. asopos* and *M. durantoni*); character 6 (an anterodorsal oriented shelf-like process at the symphysial region of premaxilla), this structure is absent in *M. yaguas* (Figure 2); character 8 (elongated metapterygoid), *M. yaguas* has an even longer metapterygoid (Figure 3) than in *M. asopos* (Bockmann, 1994: Fig. 6) and *M. durantoni* (de Pinna & Keith, 2019: Fig. 12); character 9 (a lamina at the anterodorsal margin of the opercle), *M. yaguas* has smaller lamina (Figure 3) than in *M. asopos* (Bockmann, 1994: Fig. 6) and *M. durantoni* (de Pinna & Keith, 2019: Fig. 12); character 10 (rear portion of opercular bone tapered and curved ventrally), in *M. yaguas* the posterior region of opercle is not curved (Figure 3), while in *M. asopos* (Bockmann, 1994: Fig. 6) and *M. durantoni* (de Pinna & Keith, 2019: Fig. 12), it is curved.

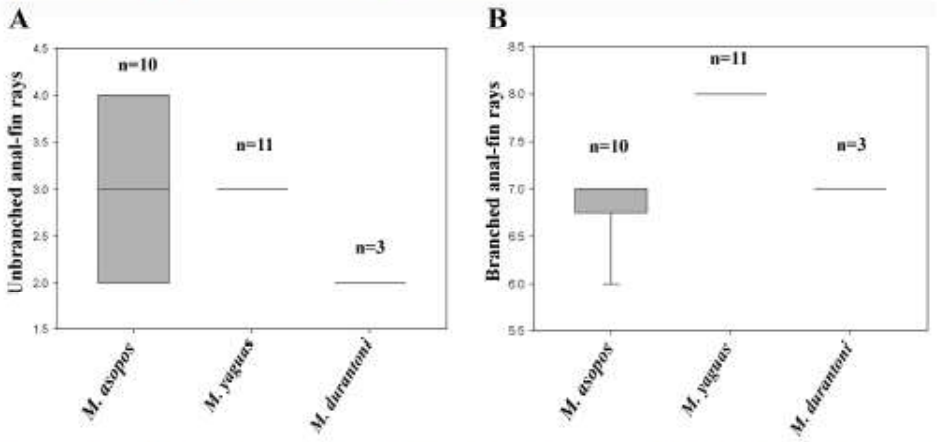

FIGURE 6. Boxplot showing meristic variation among *Mastiglanis*. (A) Total number of unbranched anal-fin rays. (B) Total number of branched anal-fin rays.

Additionally, *Mastiglanis yaguas* has osteological characteristics that differ from all congeners. Cranium: in the new species the mesethmoid is shorter (Figure 2) than in *M. asopos* and *M. durantoni* (Bockmann, 1994: Fig. 4; de Pinna & Keith, 2019: Fig. 8); the posterior region of anterior fontanel is narrower than the posterior fontanelle

(Figure 2), while in *M. asopos* and *M. durantoni* the posterior region of the anterior fontanelle has the same width as the posterior fontanelle (Bockmann, 1994: Fig. 4; de Pinna & Keith, 2019: Fig. 8); anteroposterior width of premaxilla approximately as broad as anterior portion of mesethmoid in *M. yaguas* (Figure 2), meanwhile *M. asopos* and *M. durantoni* have the anteroposterior premaxilla width larger than anterior portion of mesethmoid (Bockmann, 1994: Fig. 4; de Pinna & Keith, 2019: Fig. 11). Short nasal bone (approximately 10 times its width) in *M. yaguas* while *M. asopos* has a long nasal bone (up to 20 times its width) (Bockmann, 1994: Fig. 4). Suspensorium: ovoid entopterygoid (Figure 3), while *M. asopos* and *M. durantoni* have a quadrangular entopterygoid (Bockmann, 1994: Fig. 6 as mesopterygoid; de Pinna & Keith, 2019: Fig. 12); articular cartilage between metapterygoid and quadrate higher (seven times its length) (Figure 3) than in *M. asopos* (1.3 times its length) (Bockmann, 1994: Fig. 6); quadrate without dorsal process (Figure 3), while *M. asopos* and *M. durantoni* have a dorsal process (Bockmann, 1994: Fig. 6; de Pinna & Keith 2019: Fig. 12); pointed articular condyle of quadrate for lower jaw (Figure 3), vs. rounded in *M. asopos* (Bockmann, 1994: Fig. 6) and slightly rounded in *M. durantoni* (de Pinna & Keith, 2019: Fig. 12); and metapterygoid longer (2.3 its height) (Figure 3) than in *M. asopos* (1.8 times its height) (Bockmann, 1994: Fig. 6) and *M. durantoni* (1.9 times its height) (de Pinna & Keith, 2019: Fig. 12). Posterior caudal vertebrae: *M. yaguas* has median anterior processes nearly parallel to the vertebral column axis; at the base of neural spines of the last 6–9 vertebrae, and at the base of hemal spines of last 2–3 vertebrae (except on PU1 + U1) (Figure 4, black arrows); while *M. asopos* with any process (Bockmann, 1994: Fig. 10A).

Principal component analysis (PCA) corroborate the morphometric differences between *M. yaguas* and *M. asopos* (Figure 7). The most variable component was PC1, PC2 and PC3 with 88.4%, 7.7% and 1.8% of total variance, respectively. PC1 reflects size variation, therefore we represented the plot of PC2 vs. PC3. The most significant measurement to distinguish these species are pelvic fin length (M14), body width (M19), head depth (M24) and width (M25), interorbital width (M26), and posterior internarial width (M33). These differences are further supported for the linear regression analyses with the 95% confidence intervals not overlapping (Figure 8).

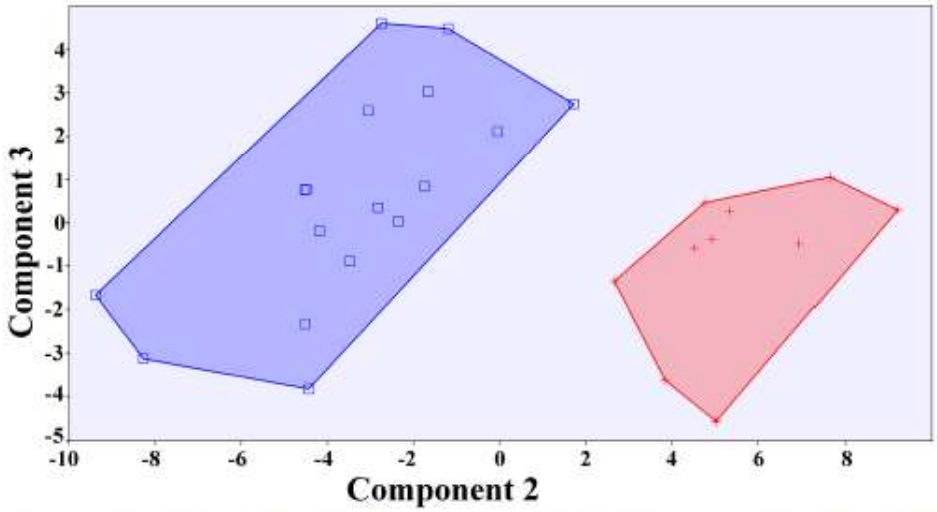

FIGURE 7. Scatter plot of Principal Component Analysis (PCA) between component 2 and component 3, of *Mastiglanis asopos* (red), and *Mastiglanis yaguas* (blue).

Mastiglanis asopos is widely distributed along the Lower Amazon basin (Bockmann, 1994; de Pinna & Keith, 2019). Meanwhile, *Mastiglanis durantoni* is restricted to the Maroni River of Eastern Guyana (de Pinna & Keith, 2019). *Mastiglanis yaguas* is distributed in the Yaguas an Nanay rivers, tributaries of the Upper Amazon basin. Despite several ichthyological expeditions being carried out along the main rivers of the Peruvian Amazon, the new species was only found in the upper Amazon River of Peru.

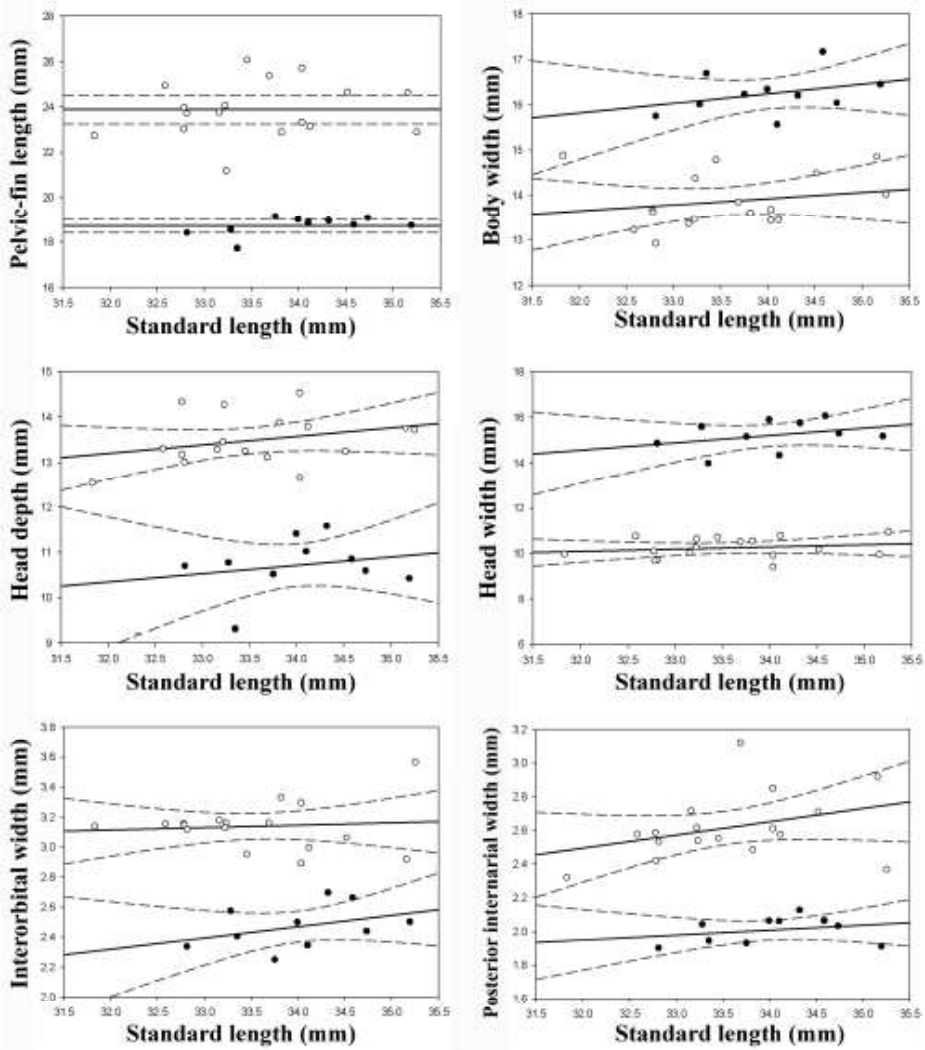

FIGURE 8. Linear regression of the main morphological measures to differentiate *Mastiglanis yaguas* (white circle), and *Mastiglanis asopos* (black circle). Dashed lines represent the 95% confidence interval.

Comparative material examined

Mastiglanis asopos

Brazil: Pará State: Holotype: MNRJ 12227, 65.4, mm SL, Igarapé Saracazinho (tributary of Trombetas River) near to Porto Trombetas, Porto Trombetas. **Paratypes:** MNRJ 12228, 9 paratypes, 42.2–53.3 mm SL, collected with the holotype. MNRJ 12229, 1 (c&s), 48.8 mm SL, collected with the holotype. **Non-Types: Pará State**: MCP

26881, 1, 49.4 mm SL, Igarapé Puraquequara, Ourém. MCP 26883, 1, 24.7 mm SL, Igarapé S/N, Concordia do Pará/BR 010 road, 10 km to east from Capim River, Concordia do Pará. MCP 26884, 1, 24.4 mm SL, Guamá River, Urucuritéua, São Miguel do Guamá. **Amazonas State**: MCP 29564, 9, 30.9–35.9 mm SL, Japurá River, Nova Colômbia community, Alvarães. MCP 35972, 62, 24.3–38.8 mm SL, Igarapé do Vinte e Dois, Recanto do Sanari, 20 km to east from Humaitá, Humaitá. MCP 35975, 112, 20.9–43.2 mm SL, Ipixuna River, balneário Porto Alegre, 7.6 km to west from BR-319, Humaitá. **Rondônia State**: MCP 35969, 1, 38.4 mm SL, Igarapé Bananeira, BR425 road to north from Guajará-Mirim, Guajará-Mirim. MCP 35973, 1, 31.2 mm SL, Da Lage River, BR-425 road, between BR-364 and Guajará-Mirim, Nova Mamoré. MCP 35978, 27, 25.8–37.8 mm SL, Jaci-Paraná River, BR-364 road between Porto Velho and Jaci-Paraná, Jaci-Paraná. **Roraima State**: MCP 46191, 1, 36.2 mm SL, Igarapé Jaburu, BR-174 road between Jundiá and Rorainópolis, Rorainópolis.

Mastiglanis* aff. *asopos

Brazil: Amazonas State: ANSP 196198, 1, 50.79 mm SL, Purús River, upstream from the confluence with the Amazon River, Beruri. ANSP 196199, 1, 32.2–34.2 mm SL, Amazonas River, upstream from the Purús River mouth, Anori. MCP 24207, 1, 47.2 mm SL, Amazon River between Madeira River mouth and Itacoatiara, Itacoatiaria. MCP 24468, 1, 49.1 mm SL, Amazon River, 30 km upstream from Itacoatiara, Itacoatiara. **Mato Grosso State:** ANSP 187247, 99, 22.9–33.7 mm SL, tributary of Cristalino River, Araguaia River, 42 km northwest from Cocalinho, MT-326 road, Corixao do Meio. MCP 33060, 1, 28.8 mm SL, arroyo Tatu, MT-423 road to a 14 km west from Cláudia, Cláudia. MCP 33692, 1, 38.7 mm SL, Ferro River, road between Novo Mato Grosso and Nova Ubiratã, 25 km to southwest from Novo Mato Grosso, Nova Ubiratã. MCP 40305, 1, 34.3 mm SL, Três stream, 30 km to south from Posto da Mata, BR 158 between Posto da Mata and Alô Brasil, Posto da Mata. **Pará State:** ANSP 194592, 2, 25.5–30.1 mm SL, Bacajái River, upstream from the confluence with Xingu River, Altamira. ANSP 198692, 4, 23.6–34.7 mm SL, Xingu River, Boa Esperança, 40 km southwest from Altamira, Altamira. ANSP 198739, 30, 25.8–47.6 mm SL, Xingu River, 45 km southwest from Altamira, Altamira. ANSP 198795, 2, 24.6–35.6 mm SL, Bacajai River, tributary to Xingu River, Altamira. ANSP 199569, 4, 29.5–39.2 mm SL, Xingu River, 44 km southwest from Altamira, Altamira. ANSP 199648, 2 25.1–31.3 mm SL, Iriri River, 8 km upstream from the confluence with the Xingu River, Altamira. MCP 26882, 1, 40.5 mm SL, Igarapé São Joaquim, road between São Domingos do Capim and Belém-Brasília (BR 010), tributary of Guamá River, São Domingos Capim. MCP 51554, 1, 52.9 mm SL, Amazon River, Sitio Pajau, Santarém. ROM 103716, 1, 35.0 mm SL, Iriri River, tributary of Xingu River, Uruará. ROM 103743, 14, 20.4–26.7 mm SL, rio Iriri, tributary from Xingu River, Uruará. **Rondônia State:** MCP 35970, 60, 22.0–46.8 mm SL, Igarapé S/N, tributary of Madeira River, BR-364 road, 51 km southwest from, Jaci Paraná.

Guyana: Potaro-Siparuni Region: ANSP 175773, 1, 45.0 mm SL, pool isolate to 40 minutes from the main channel from Essequibo River, 15 minutes upstream from Maipuri camp, Siparuni VIII-2. ANSP 175774, 2, 34.9–35.9 mm SL, Essequibo River, 1.5 hours upstream from Maipuri camp. ANSP 177253, 4, 26.1–56.8 mm SL, Essequibo River, Essequibo. ROM 91460, 3, 28.7–45.6 mm SL, Imbaima stream, Potaro River, Essequibo River basin. ROM 91488, 1, 25.4 mm SL, Little Wailang stream, Potaro River, Essequibo River basin. ROM 97143, 1, 23.7 mm SL, Konawaruk River, Konawaruk-Essequibo River basin. ROM 97198, 1, 36.9 mm SL, Konawaruk River, Konawaruk-Essequibo River basin. **Alto Demerara-Berbice Region**: ANSP 177251, 17, 21.3–60.5 mm SL, Burro Burro River, Deer stream upstream from Dogs falls, Demerara. ANSP 179730, 2, 24.7–38.8 mm SL, Essequibo River, Kurukupari. **Alto Takutu-Alto, Essequibo River**: ANSP 179731, 1, 57.9 mm LE, Ireng River, Takutu-Branco-Negro River basin, 6.9 km southwest from Karasabai village. ANSP 179732, 25, 26.6–53.7 mm SL, Rupununi River, Kwatamang, 4 km southeast from Annai. ANSP 179733, 7, 36.9–66.8 mm SL, Takutu River, Negro River, 2.75 km west from Saint Ignatius. ANSP 179734, 1, 52.0 mm SL, Ireng River, Takutu-Branco-Negro River basin, 6.9 km southwest from Karasabai village. ANSP 179735, 7, 33.5–64.0 mm SL, Rupununi River, Karanambo ranch. ANSP 180748, 5, 29.6–50.5 mm SL, Araquai stream, Rupununi River, 77.3 km southeast from Lethem. ANSP 180950, 2, 31.1–31.6 mm SL, Takutu River, Branco-Negro River basin, 3.77 km southwest from Lethem. ANSP 197720, 2, 32.8–33.3 mm SL, Manari River, Takutu-Branco River basin, 10.2 km northeast from Lethem. ANSP 202247, 14, 36.4–66.7 mm SL, Takutu River, Branco-Negro River basin, 3.77 km southeast from Lethem. **Cuyuni-Mazaruni Region, Essequibo River basin**: ROM 69508, 3, 27.0–38.3 mm SL, Mazaruni River. ROM 84034, 1, 25.6 mm SL, Semang River, Mazaruni River. ROM 84078, 1, 41.8 mm SL, Mazaruni River. ROM 86202, 26, 23.6–35.7 mm SL, Rupununi River. ROM 86402, 9, 28.8–54.3 mm SL, Rupununi River. ROM 97623, 7, 23.7–36.6 mm SL, Eping stream, Mazaruni River. ROM 97654, 2, 24.7–36.4 mm SL, Mazaruni River. ROM 101655, 3, 34.1–34.7 mm SL,

Mazaruni River. ROM 101765, 11, 25.3–43.1 mm SL, Mazaruni River. ROM 101798, 47, 25.7–44.9 mm SL, Kurupung River, tributary of Mazaruni River. ROM 101878, 1, 40.8 mm SL, Kurupung River, tributary of Mazaruni River. ROM 101900, 4, 27.0–38.1 mm SL, Mazaruni River. ROM 102059, 1, 26.5 mm SL, Mazaruni River. ROM 102095, 16, 26.9–40.7 mm SL, Mazaruni River. ROM 102141, 1, 39.0 mm SL, Meamu stream, Mazaruni River. ROM 102183, 3, 26.7–40.6 mm SL, Eping stream, Mazaruni River.

Venezuela: Bolívar State: ANSP 160405, 1, 43.1 mm SL, Orinoco River confluence with Caura River, near to Puerto Las Majadas. ANSP 166955, 1, 41.0 mm SL, caño Chuaporio confluence with Caura River, Caura River. ANSP 166956, 2, 42.2–47.2 mm SL, Caura River, 1/2 miles upstream from Jabillal. ANSP 166958, 4, 34.6–41.7 mm SL, Nichare River, La Raya beach, 15-20 minutes upstream from the confluence with the Caura River. **Amazonas State: Orinoco River basin**: ANSP 160629, 134, 28.7–55.3 mm SL, Sipapo River, 3-4 km upstream from Pendare. ANSP 182259, 2, 50.4–54.1 mm SL, Ventuari River, beach in Picua village, 34 km from Macuruco, 104 km to east from San Fernando de Atabapo. ANSP 182653, 1, 32.0 mm SL, Manapiare River, Ventuari River, 20 km northwest from San Juan de Manapiare. ANSP 182789, 3, 39.8–46.6 mm SL, Manapiare River, Ventuari River, 10 km northwest from San Juan de Manapiare. ANSP 182973, 1, 31.8 mm SL, Manapiare River, Ventuari River, 17 km northwest from San Juan de Manapiare. ANSP 191332, 1, 50.8 mm SL, Ventuari River, upstream from the end of the extensive rocky rapid, 1 km upstream from Salto Tencua, 227 km southeast from Puerto Ayacucho, Manapiare. ANSP 191406, 2, 32.1–32.7 mm SL, caño Parhuella, upstream from bridge of Ruta 12 road, 35 km northeast from Puerto Ayacucho, Atures. ANSP 202203, 2, 41.4–56.5 mm SL, Cataniapo River, bridge main crossing and downstream from confluence with Orinoco River, 5.6 km south from Puerto Ayacucho. ANSP 206024, 1, 28.3 mm SL, Guapuchi River, Ventuari River, 105.5 km to east from San Fernando de Atabapo. ROM 94413, 3, 40.3–46.3 mm SL, Cataniapo River.

Mastiglanis* aff. *durantoni

Surinam: ANSP 189106, 2, 40.8-55.2 mm SL, Litanie River, confluence with Marowini River, upstream from Konya Kondre, Sipalawini.

Acknowledegements

We would like to thank Nathan Lujan (AMNH); Mariangeles Arce and Mark Sabaj (ANSP); Caleb McMahan, Susan Mochel, and Kevin Swagel (FMNH); Carlos Lucena (MCP); Paulo Buckup (MNRJ); Max Hidalgo, Carla Muñoz, and V. Meza (MUSM); Don Stacey, Mary Burridge, Erling Holm and Marg Zur (ROM), for curatorial assistance during the senior author's visit to each fish collection. Special thanks to Kevin Swagel (FMNH) for X-ray images, and Corinthia Black for English revision. The first author was supported by a doctoral program provided by Ministry of Education of Brazil (CAPES). Additional financial support was received of the Böhlke Memorial Endowment Fund from the Academy of Natural Science of Drexel University (ANSP), Philadelphia; the Grainger Bioinformatics Center Found from the Field Museum of Natural History (FMNH), Chicago; the Royal Ontario Museum E.J. Crossman Endowment Fund; and the Smithsonian Visiting Student Fellowship from National Museum of Natural History (NMNH), Washington DC.

References

Almeida, M.A. (2019) *Revisão taxonômica e descrição da musculatura cefálica do gênero Mastiglanis Bockmann, 1994 (Siluriformes: Heptapteridae)*. Unpublished MSc Dissertation, Universidade de São Paulo, São Paulo, 130 pp.

Bleeker, P. (1862) *Atlas Ichthyologique des Indes Orientales Néêrlandaises, publié sous l'auspice du Gouvernement Colonial Néêrlandais. Tome II. Siluroïdes, Chacoïdes et Hétérobranchoïdes*. De Breuk & Smits, Amsterdan, 112 pp. https://doi.org/10.5962/bhl.title.67474

Bockmann, F.A. (1994) Description of *Mastiglanis asopos*, a new pimelodid catfish from northern Brazil, with comments on phylogenetic relationships inside the subfamily Rhamdiinae (Siluriformes: Pimelodidae). *Proceedings of the Biological Society of Washington*, 107 (4), 760–777.

Bockmann, F.A. (1998) *Análise filogenética da familia Heptapteridae (Teleostei: Ostariophysi: Siluriformes) e redefinição de seus gêneros*. Unpublished PhD Dissertation, Universidade de São Paulo, São Paulo, 599 pp.

Bockmann, F.A. & Guazzelli, G.M. (2003) Family Heptapteridae (Heptapterids). *In*: Reis, R.E., Kullander, S.O. & Ferraris Jr.,

C.J. (Eds.), *Check list of the freshwater fishes of south and central America*. Editora da Pontifícia Universidade Católica do Rio Grande do Sul-EDIPUCRS, Porto Alegre, pp. 406–431.

Bockmann, F.A. & Miquelarena, A.M. (2008) Anatomy and phylogenetic relationships of a new catfish species from northeastern Argentina with comments on the phylogenetic relationships of the genus *Rhamdella* Eigenmann and Eigenmann 1888 (Siluriformes, Heptapteridae). *Zootaxa*, 1780, 1–54.
https://doi.org/10.11646/zootaxa.1780.1.1

Bockmann, F.A. & Slobodian, V. (2018) Family Heptapteridae—threebarbeled catfishes. *In*: van der Sleen, P. & Albert, J.S. (Eds.), *Field guide to the fishes of the Amazon, Orinoco & Guianas*. Princeton University Press, Princeton, New Jersey, pp. 233–252.

Faustino-Fuster, D.R. (2019) *Revisión taxonómica del género Mastiglanis Bockmann, 1994 (Siluriformes: Heptapteridae) en Perú*. Unpublished Undergraduate Dissertation, Universidad Nacional Mayor de San Marcos, Lima, 74 pp.

Faustino-Fuster, D., Bockmann, F.A. & Malabarba, L.R. (2019) Two new species of *Heptapterus* (Siluriformes: Heptapteridae) from the Uruguay River basin, Brazil. *Journal of Fish Biology*, 94 (3), 352–373.
https://doi.org/10.1111/jfb.13908

Ferraris Jr., C.J. (1988) Relationships of the Neotropical catfish genus *Nemuroglanis*, with a description of a new species (Osteichthys: Siluriformes: Pimelodidae). *Proceedings of the Biological Society of Washington*, 101 (3), 509–516.

Fricke, R., Eschmeyer, W.N. & Van der Laan, R. (Eds.) (2020) Eschmeyer's catalog of fishes: genera, species, references. Electronic version. Available from: http://researcharchive.calacademy.org/research/ichthyology/catalog/fishcatmain.asp. (accessed 6 April 2020)

Gill, T. (1861) Synopsis of the genera of the sub-family of Pimelodinae. *Proceedings of the Boston Society of Natural History*, 8, 46–55.

Hammer, O., Harper, D.A. & Ryan, P.D. (2001) PAST: paleontological statistics software package for education and data analysis. *Palaeontologia electronica*, 4 (1), 9.

Hidalgo, M.H. & Ortega-Lara, A. (2011) Fishes. *In*: Pitman, N., Vriesendorp, C., Moskovits, D., von May, R., Alvira, D., Wachter, T., Stotz, D.F. & del Campo, Á., (Eds.), *Perú: Yaguas-Cotuhé. Rapid Biological and Social Inventories Report 23*. The Field Museum, Chicago, The Field Museum, Chicago, pp. 98–108 + 221–230 + 308–329.

Lundberg, J.G. & McDade, L.A. (1986) On the South American catfish *Brachyrhamdia imitator* Myers (Siluriformes, Pimelodidae), with phylogenetic evidence for a large intrafamilial lineage. *Notulae Naturae*, 463, 1–24.

Lundberg, J.G., Bornbusch, A.H. & Mago-Leccia, F. (1991) *Gladioglanis conquistador* n. sp., from Ecuador with diagnoses of the subfamilies Rhamdiinae Bleeker and Pseudopimelodinae n. subf. (Siluriformes, Pimelodidae). *Copeia*, 1991 (1), 190–209.
https://doi.org/10.2307/1446263

de Pinna, M.C.C. (1993) *Higher-level phylogeny of Siluriformes, with a new classification of the order (Teleostei, Ostariophysi)*. Unpublished PhD Dissertation, The City University of New York, 482 pp.

de Pinna, M.C.C. & Keith, P. (2019) *Mastiglanis durantoni* from French Guyana, a second species in the genus (Siluriformes: Heptapteridae), with a CT scan survey of phylogenetically-relevant characters. *Cybium*, 43 (2), 125–135.
https://doi.org/10.26028/cybium/2019-423-002

Sherman, G.E., Sutton, T., Blazek, R., Holl, S., Dassau, O., Morely, B., Mitchell, T. & Luthman, L. (2012) Quantum GIS User Guide. Version 1.8. "Wroclaw". Available from: http://download.osgeo.org/qgis/doc/manual/qgis-1.8.0_user_guide_en.pdf (accessed 29 June 2017)

Sabaj, M.H. (2019) Standard symbolic codes for institutional resource collections in herpetology and ichthyology: an online reference. Version 7.1. 21 March 2019. American Society of Ichthyologists and Herpetologists, Washington, D.C. Electronically accessible. Available from: http://www.asih.org/ (accessed 6 July 2020)

Silvergrip, A.M.C. (1996) *A systematic revision of the Neotropical catfish genus Rhamdia (Teleostei, Pimelodidae)*. Doctoral dissertation, Thesis in Zoology, Stockholm University, Stockholm, 156 pp.

Swarça, A.C., Caetano, L.G. & Dias, A.L. (2000) Cytogenetic of species of the families Pimelodidae and Rhamdiidae (Siluriformes). *Genetics and Molecular Biology*, 23 (3), 589–593.
https://doi.org/10.1590/S1415-47572000000300015

Taylor, W.R. & Van Dyke, G.C. (1985) Revised procedures for staining and clearing small fishes and other vertebrates for bone and cartilage study. *Cybium*, 9, 107–119.

Article 2: Faustino-Fuster, D. R., & de Souza, L. S. (2021). A new species of *Cetopsorhamdia* (Siluriformes: Heptapteridae) from the Upper Amazon River basin. Journal of Fish Biology, 1–15. https://doi.org/10.1111/jfb.14914

Received: 19 March 2021 | Accepted: 17 September 2021
DOI: 10.1111/jfb.14914

REGULAR PAPER

JOURNAL OF FISH BIOLOGY

A new species of *Cetopsorhamdia* (Siluriformes: Heptapteridae) from the Upper Amazon River basin

Dario R. Faustino-Fuster[1,2] | Lesley S. de Souza[3]

[1]Departamento de Ictiología, MUSM – Museo de Historia Natural, Universidad Nacional Mayor de San Marcos, Lima, Peru
[2]Departamento de Zoologia, UFRGS – Universidade Federal do Rio Grande do Sul, Programa de Pós-Graduação em Biologia Animal, Porto Alegre, Brazil
[3]FMNH – Keller Science Action Center, The Field Museum of Natural History, Chicago, Illinois, USA

Correspondence
Dario R. Faustino-Fuster, Departamento de Ictiología, MUSM – Museo de Historia Natural, Universidad Nacional Mayor de San Marcos (MUSM), Lima, Perú.
Email: dariorff36@gmail.com

Funding information
Smithsonian Institution

Abstract

A new species of *Cetopsorhamdia* is described from material collected on rapid inventories and ichthyological expeditions in the Amazon region of Peru, Ecuador and Colombia. The new species can be differentiated from all other species of *Cetopsorhamdia* by the colouration pattern on fins, number of vertebrae, number of ribs, level insertion of dorsal fin, number of rays on dorsal and pectoral fin, osteological characters and several other morphometric characters. The new species is distributed along tributaries of the upper Amazon River basin in Peru, Colombia and Ecuador.

KEYWORDS
fresh water, Neotropical, taxonomy, three-barbel catfish

1 | INTRODUCTION

Cetopsorhamdia Eigenmann & Fisher 1916 is a genus of Neotropical three-barbeled catfish distributed along the cis/trans Andean drainages of Magdalena, Amazon, Orinoco, São Francisco, Parana and Uruguay River basins (Bockmann & Guazzelli, 2003; Bockmann & Slobodian, 2017). This genus was previously classified with the larger bodied catfishes Siluridae within subfamily Pimelodinae by Eigemann & Fisher in Eigenmann (1922). Afterwards, Gosline (1945) and Gomes and Schubart (1958) considered *Cetopsorhamdia* a member of Pimelodidae. Stewart (1986) was the first to place *Cetopsorhamdia* within the *Heptapterus* group, which became part of the large monophyletic clade proposed by Lundberg and McDade (1986). Subsequent morphological analysis placed *Cetopsorhamdia* within the *Nemuroglanis* clade (Ferraris Jr, 1988; Lundberg *et al.*, 1991) and thus formally within Rhamdiinae (Lundberg *et al.*, 1991) but shortly thereafter raised to Rhamdiidae by de Pinna (1993) in his unpublished Ph.D. thesis. Although Bockmann (1994) corroborated *Cetopsorhamdia* as a member of the *Nemuroglanis* clade within Rhamdiinae, Silvergrip (1996) pointed out priority of Heptapterinae Gill (1861) over Rhamdiinae Bleeker (1862). Swarça *et al.* (2000) was the first to formally use Rhamdiidae based on de Pinna's thesis 1993, but has thereafter been recognized as the family Heptapteridae by Bockmann & Guazzelli (2003).

Cetopsorhamdia is a member of Heptapterini based on morphological and molecular analysis (Ferraris Jr. 1988; Bockmann, 1998; Silva *et al.*, 2021; Faustino-Fuster *et al.*, 2021. *Cetopsorhamdia* can be diagnosed from all other genera within Heptapterini by four morphological characters: (a) presence of a medial ossification over the median portion of the skull, covering the epiphyseal bar and leaving reduced anterior and posterior fontanels; (b) orbital (= optic) foramen small; (c) mouth ventral and (d) snout conical (Bockmann & Reis, 2021). In addition, the previous authors suggest a strict definition of *Cetopsorhamdia* based on two putative synapomorphies: (a) presence of a medial ossification over the median portion of the skull, covering the epiphyseal bar and leaving reduced anterior and posterior fontanels; (b) orbital (= optic) foramen small. Therefore, *Cetopsorhamdia* sensu stricto (following Bockmann & Reis, 2021) includes *Cetopsorhamdia boquillae* Eigenmann, 1922, *Cetopsorhamdia clathrata* Bockmann & Reis, 2021, *Cetopsorhamdia iheringi* Schubart & Gomes 1959, *Cetopsorhamdia insidiosa* Steindachner 1915, *Cetopsorhamdia nasus* Eigenmann & Fisher 1916, *Cetopsorhamdia picklei* Schultz 1944 and *Cetopsorhamdia spilopleura* Bockmann & Reis, 2021. Recent morphological work suggests that *Cetopsorhamdia molinae* Miles 1943, *Cetopsorhamdia orinoco*

Schultz 1944, *Cetopsorhamdia phantasia* Stewart 1985 and *Cetopsorhamdia shermani* Schultz 1944 belong to three currently unrecognized genera (Bockmann, 1998; Bockmann & Slobodian, 2017), with molecular evidence that further supports this finding for *C. molinae* (Faustino-Fuster *et al.*, 2021). *Cetopsorhamdia filamentosa* Fowler 1945 appears to be related to *Rhamdia* (Bockmann, 1998, DRFF pers. obs.). These hypotheses are not yet formally published; therefore, in this study the authors considered the following 12 valid species as *Cetopsorhamdia* (Fricke *et al.*, 2020): *C. boquillae*, *C. clathrata*, *C. spilopleura*, *C. filamentosa*, *C. iheringi*, *C. insidiosa*, *C. molinae*, *C. nasus*, *C. orinoco*, *C. phantasia*, *C. picklei* and *C. shermani*.

Recent expeditions carried out by natural history museums, governmental institutions and non-governmental organizations along the Amazon basin in Peru and Ecuador revealed one new species of *Cetopsorhamdia* herein described.

2 | MATERIALS AND METHODS

Measurements were taken with digital calipers and are expressed to the nearest 0.1 mm. All measurements were taken point to point and followed Lundberg and McDade (1986), Bockmann (1994) and Faustino-Fuster *et al.* (2019). Standard length (L_S) is given in millimetres, and the other measurements are expressed in percentage of L_S or head length (HL) (Table 1a–c). Counts of fins rays, ribs and vertebrae (including the first five vertebrae in the Weberian apparatus and one from the hypural plate) were taken from cleared and stained (c&s) specimens prepared according to Taylor and Van Dyke (1985), and digital radiographs (xr) were taken with the AXR 110 Hotshot X-Ray System in the fish division, Field Museum of Natural History, Chicago, United States. Asterisks within parenthesis (*) represent holotype count. Numbers between parenthesis () are number of specimens. Osteology analyses were done following Bockmann and Miquelarena (2008) and Ortega-Lara (2012), and Carvalho *et al.* (2013). Nomenclature of the laterosensory cephalic system followed Arratia and Huaquin (1995), Schaefer and Aquino (2000) and Bockmann and Miquelarena (2008). Geographic distribution map was prepared in the Quantum GIS version 2.18.10 software (Sherman *et al.*, 2012). Institutional abbreviations follow Sabaj (2019).

Comparisons were performed through the examination of specimens, including types, original descriptions and revisionary works on valid species of *Cetopsorhamdia*: *C. boquillae*, *C. filamentosa*, *C. iheringi*, *C. insidiosa*, *C. molinae*, *C. nasus* (Ortega-Lara, 2012), *C. orinoco*, *C. phantasia*, *C. picklei* and *C. shermani*.

2.1 | Ethical statement

This study used only ethanol-preserved specimens deposited in museums and did not involve animal experimentation.

3 | RESULTS

3.1 | *Cetopsorhamdia hidalgoi* new species

urn:lsidzoobank.org:pub:CF107813-B3A7-467E-82D0-6CDZ367B633F
urn:lsidzoobank.org:act:18608754-E7B8-400A-BD3E-2502EE5A1719

(Figures 1a–c, 2, 3, 4 and 5; Table 1a)

Cetopsorhamdia sp.: Hidalgo & Pezzi, 2006: 42, 73, 77, 79–80, 144, 173, 177–179, 254, Figure 5c (rapid biological and social inventory).

Cetopsorhamdia sp.: Hidalgo & Willink, 2007: 34, 56, 59–60, 105, 125, 127–128, 198, Figure 6c (rapid biological and social inventory).

Cetopsorhamdia sp. n. 1: Bockmann & Slobodian, 2013: 22–23 (fish inventory)

C. phantasia: Carvalho *et al.*, 2016: 417, 437 (species list).

Holotype. MUSM 69550, 30.7 mm L_S, Peru, Loreto Department, Requena Province, Tapiche River, National Park Sierra del Divisor, 7° 12′ 29.70″ S; 73° 55′ 25.57″ W, 14 August 2005, M. Hidalgo & J. Pezzi.

35 Paratypes: All from Peru, Nanay drainage. FMNH 139553, 1, 29.6 mm L_S, Loreto Department, Maynas Province, Alto Nanay, 2° 47′ 29.00″ S; 74° 49′ 36.84″ W, 22 August 2006, M. Hidalgo & P. Willink. MUSM 65034, 1, 26.22 mm L_S, collected with FMNH 139553. **Marañón drainage**, Amazonas Department, Condorcanqui Province: AUM 46744, 4, 26.3–27.2 mm L_S, Marañón River, 4° 35′ 22.45″ S; 77° 51′ 10.19″ W, 08 August 2006, N.K. Lujan, S. Flecker, A. Capps, P. German, D. Osorio. AUM 71300, 3, 24.1–26.4 mm L_S, Cenepa River, 4° 33′ 37.76″ S; 78° 11′ 7.08″, 02 August 2006, N.K. Lujan, D.C. Taphorn, S. Flecker, B. Rengifo, D. Osorio. **Ucayali drainage.** Loreto Department, Requena Province: FMNH 143004, 1, 28.9 mm L_S, Unnamed creek tributary to Tapiche River, National Park Sierra del Divisor, 7° 49′ 39.79″ S; 73° 56′ 34.10″ W, 14 August 2005, M. Hidalgo & J. Pezzi. FMNH 143018, 1, 28.3 mm L_S, collected with holotype. FMNH 143069, 2, 23.4–30.0 mm L_S, Unnamed creek tributary to Tapiche River, National Park Sierra del Divisor, 7° 12′ 21.10″ S; 73° 56′ 7.19″ W, 16 August 2005, M. Hidalgo & J. Pezzi. FMNH 143086, 2, 27.8–31.4 mm L_S, Unnamed creek tributary to Tapiche River, National Park Sierra del Divisor, 7° 11′ 38.48″ S; 73° 52′ 1.90″ W, 19 August 2005, M. Hidalgo & J. Pezzi. MUSM 62615, 2, 23.5–23.7 mm L_S, collected with FMNH 143004. MUSM 62715, 2 (1 c&s), 26.0–27.5 mm L_S, collected with FMNH 143069. MUSM 63924, 1, 28.1 mm L_S, collected with holotype. MUSM 63924, 1, 28.0 mm L_S, collected with holotype. Cusco Department, La Convención Province: MUSM 35639, 1, 23.2 mm L_S, El Dorado creek, tributary to Mishahua River, Urubamba River, 11° 22′ 35.70″ S; 72° 50′ 0.39″ W, 25 July 2009, H. Ortega et al. MUSM 54758, 1, 29.7 mm L_S, Serjali River tributary to Mishahua River, 11° 45′ 9.67″ S; 72° 30′ 24.86″ W, 10 December 2015, I. Sipión, J. Espino & P. Andia. MUSM 60687, 3 (1 c&s), 24.4–32.9 mm L_S, Megantoni District, Serjali River tributary to Mishahua River, 11° 45′ 19.34″ S; 72° 29′ 44.86″ W, 01 September 2017, I. Sipión, A. Mendoza & P. Andia. UFRGS 28665,

JOURNAL OF FISH BIOLOGY

TABLE 1 (a)–(c), Morphometric data of *Cetopsorhamdia* species

(a)

		Cetopsorhamdia hidalgoi new species						*Cetopsorhamdia boquillae* Eigenmann, 1922	*Cetopsorhamdia filamentosa* Fowler 1945		
LM	Measurement	H	N	Min	Max	Mean	SD	H	N	Min	Max
	Standard length (mm)	30.7	21	23.2	32.9	28.0	-	72.1	5	41.5	72.4
	Percentage of standard length										
1–3	Predorsal distance	39.4	22	36.7	42.7	40.3	1.4	36.9	5	**35.2**	**36.7**
1–4	Preadipose distance	71.6	22	67.4	72.8	70.1	1.4	**62.1**	5	**60.1**	**63.5**
1–5	Prepectoral distance	25.3	22	23.9	27.7	25.6	0.8	**20.1**	5	22.6	24.6
1–6	Prepelvic distance	44.7	22	42.9	48.3	45.8	1.5	43.9	5	46.6	48.7
1–7	Preanal distance	68.5	22	65.4	70.8	67.8	1.6	**64.0**	5	67.0	68.2
3–8	Body depth	16.8	22	13.0	18.1	16.0	1.5	13.7	5	14.9	17.2
9–10	Caudal peduncle depth	8.5	22	7.8	9.3	8.5	0.4	**10.2**	5	**9.4**	**11.0**
2–11	Caudal peduncle length	20.4	22	17.4	21.5	19.8	1.1	19.2	5	18.3	20.9
37–38	Body width	18.6	22	16.0	20.8	18.3	1.2	16.8	5	18.1	19.6
3–12	Dorsal-fin base length	14.8	22	11.7	15.2	13.8	0.8	**11.4**	5	14.5	16.3
7–11	Anal-fin base length	12.8	22	11.7	15.4	13.1	0.7	**15.9**	5	13.0	14.1
3–15	Unbranched dorsal-fin ray length	21.6	22	20.0	23.0	21.1	0.9	**16.1**	5	**13.9**	**17.7**
16–17	Dorsal-fin length	19.4	22	16.0	19.7	18.2	0.9	17.9	5	17.2	19.2
19–20	Adipose-fin depth	5.4	22	3.1	5.4	4.4	0.5	3.3	5	3.8	4.8
4–9	Adipose-fin base length	16.4	22	14.9	18.7	16.4	1.0	**29.9**	5	**26.7**	**29.6**
4–12	Interdorsal distance	20.3	22	14.7	20.3	17.6	1.2	15.2	5	**11.7**	**14.6**
5–18	Unbranched pectoral-fin ray length	20.9	22	18.5	21.4	19.9	0.9	**10.6**	5	**13.3**	**17.1**
5–13	Pectoral-fin length	20.6	22	15.9	20.6	18.2	1.1	16.1	5	15.4	18.3
6–14	Pelvic-fin length	15.4	22	14.5	16.8	15.5	0.6	14.6	5	14.1	17.1
5–6	Pectoral-pelvic fins distance	21.4	22	20.2	24.8	22.3	1.3	**28.4**	5	**25.1**	**27.5**
6–7	Pelvic-anal fins distance	22.4	22	20.4	23.7	22.4	0.8	**18.8**	5	20.0	21.3
3–2	Dorsal-fin insertion-hypural plate	62.9	22	59.4	64.3	62.0	1.2	**64.6**	5	**66.2**	**68.4**
6–2	Pelvic-fin insertion-hypural plate	55.4	22	52.5	56.9	54.8	1.1	55.1	5	51.3	53.6
7–2	Anal-fin insertion-hypural plate	33.1	22	30.6	35.7	33.0	1.2	35.0	5	31.3	33.7
1–21	Head length	26.8	22	26.5	29.9	27.8	0.9	**22.4**	5	25.6	27.6
Percentage of head length											
1–27	Snout length	39.3	22	34.2	42.0	38.7	1.9	35.0	5	34.2	37.3
26–27	Orbital diameter	14.1	22	9.4	14.2	11.3	1.4	12.3	5	**14.6**	**19.6**

(Continues)

TABLE 1 (Continued)

(a)

		Cetopsorhamdia hidalgoi new species						*Cetopsorhamdia boquillae* Eigenmann, 1922	*Cetopsorhamdia filamentosa* Fowler 1945		
LM	Measurement	H	N	Min	Max	Mean	SD	H	N	Min	Max
39-40	Head width	71.1	22	55.2	71.1	64.3	4.9	**74.2**	5	**64.4**	76.8
41-42	Mouth width	45.0	22	35.8	53.1	42.7	3.9	40.2	5	37.2	46.0
47-48	Mandibular isthmus-lower lip distance	20.4	22	15.6	24.9	19.7	2.1	21.5	5	**25.6**	**28.1**
47-1	Mandibular isthmus-upper lip distance	26.3	22	19.0	31.3	25.0	3.5	24.9	5	25.8	31.8
28-29	Maxillary barbel length	126.1	22	101.7	126.1	116.3	7.2	**152.8**	5	**222.5**	**276.5**
43-44	External mandibular barbel length	84.2	22	63.5	84.8	76.0	5.0	63.5	5	**89.3**	**111.2**
45-46	Internal mandibular barbel length	55.6	22	43.7	58.4	51.9	3.6	48.2	5	**58.9**	**70.4**
21-26	Postorbital distance	52.4	22	47.5	53.4	50.5	1.5	52.1	5	47.3	49.3
30-31	Interorbital width	28.6	22	25.8	31.9	28.6	1.9	28.9	5	**31.9**	**37.7**
1-32	Snout-anterior nostril distance	11.7	22	8.7	13.5	11.0	1.2	11.3	5	8.8	10.1
32-33	Internostril distance	14.9	22	9.3	15.1	12.8	1.5	12.9	5	10.6	12.9
27-33	Posterior nostril-orbit distance	7.2	22	4.2	7.2	5.5	0.8	**8.0**	5	**11.3**	**13.4**
22-23	Head depth at supra occipital	52.4	22	39.6	56.3	51.6	4.0	53.4	5	48.2	54.1
24-25	Head depth at interorbital	41.5	22	33.1	43.0	37.4	2.7	39.6	5	35.2	38.9
35-36	Head width at posterior nostril	52.9	22	45.1	60.9	52.1	4.5	52.8	5	47.8	56.7
1-34	Dorsal head length	91.7	22	86.7	96.0	92.1	2.0	89.3	5	**96.5**	**98.0**

(b)

		Cetopsorhamdia iheringi Schubart & Gomes 1959			*Cetopsorhamdia insidiosa* (Steindachner 1915)			*Cetopsorhamdia molinae* Miles 1943			*Cetopsorhamdia nasus* Eigenmann & Fisher 1916
LM	Measurement	N	Min	Max	N	Min	Max	N	Min	Max	H
	Standard length (mm)	5	56.6	75.8	2	32.7	36.8	1	36.7	36.7	54.3
Percentage of standard length											
1-3	Predorsal distance	5	38.0	40.3	2	40.0	40.3	1	38.4	38.4	38.8
1-4	Preadipose distance	5	69.8	71.7	2	67.9	69.9	1	**66.7**	**66.7**	71.1
1-5	Prepectoral distance	5	22.6	24.2	2	24.9	25.9	1	24.9	24.9	24.1
1-6	Prepelvic distance	5	44.4	46.1	2	43.1	44.0	1	45.2	45.2	46.8
1-7	Preanal distance	5	67.9	72.0	2	67.7	68.2	1	**64.8**	**64.8**	68.9
3-8	Body depth	5	15.5	17.7	2	16.2	16.3	1	17.4	17.4	13.5

TABLE 1 (Continued)

(b)

		Cetopsorhamdia iheringi Schubart & Gomes 1959			*Cetopsorhamdia insidiosa* (Steindachner 1915)			*Cetopsorhamdia molinae* Miles 1943			*Cetopsorhamdia nasus* Eigenmann & Fisher 1916
LM	Measurement	*N*	Min	Max	*N*	Min	Max	*N*	Min	Max	H
9–10	Caudal peduncle depth	5	**10.4**	**10.7**	2	8.6	9.1	1	**10.6**	**10.6**	9.3
2–11	Caudal peduncle length	5	15.0	19.3	2	19.1	20.6	1	**23.5**	**23.5**	19.3
37–38	Body width	5	17.8	20.0	2	16.5	17.5	1	**22.0**	**22.0**	16.7
3–12	Dorsal-fin base length	5	11.3	12.0	2	11.6	12.8	1	**16.2**	**16.2**	12.9
7–11	Anal-fin base length	5	13.3	14.6	2	13.5	13.7	1	12.6	12.6	14.1
3–15	Unbranched dorsal-fin ray length	5	**12.8**	**19.4**	2	**17.4**	**19.5**	1	**30.6**	**30.6**	19.9
16–17	Dorsal-fin length	5	12.5	20.3	2	16.2	18.4	1	**26.0**	**26.0**	16.6
19–20	Adipose-fin depth	5	3.8	4.7	2	2.3	4.1	1	**5.6**	**5.6**	4.6
4–9	Adipose-fin base length	5	14.3	16.4	2	15.2	15.5	1	**20.5**	**20.5**	16.9
4–12	Interdorsal distance	5	20.3	21.6	2	18.0	19.5	1	**13.4**	**13.4**	19.6
5–18	Unbranched pectoral-fin ray length	5	12.4	16.4	2	**16.3**	**17.2**	1	**23.0**	**23.0**	18.4
5–13	Pectoral-fin length	5	14.7	19.4	2	19.1	19.1	1	**21.6**	**21.6**	20.0
6–14	Pelvic-fin length	5	13.1	18.3	2	17.0	17.3	1	**19.2**	**19.2**	**17.1**
5–6	Pectoral-pelvic fins distance	5	22.8	24.9	2	20.2	20.6	1	21.9	21.9	23.9
6–7	Pelvic-anal fins distance	5	**24.3**	**26.9**	2	22.1	23.0	1	20.9	20.9	22.9
3–2	Dorsal-fin insertion-hypural plate	5	61.3	63.6	2	62.6	64.0	1	63.4	63.4	63.4
6–2	Pelvic-fin insertion-hypural plate	5	55.6	56.6	2	55.2	57.4	1	56.6	56.6	53.6
7–2	Anal-fin insertion-hypural plate	5	29.8	32.8	2	32.3	33.7	1	35.2	35.2	31.8
1–21	Head length	5	24.5	26.8	2	27.2	28.4	1	27.7	27.7	**25.7**
Percentage of head length											
1–27	Snout length	5	36.4	41.1	2	35.4	36.2	1	38.2	38.2	-
26–27	Orbital diameter	5	10.0	13.9	2	10.7	11.1	1	11.0	11.0	13.2
39–40	Head width	5	66.5	81.7	2	61.9	63.3	1	**73.9**	**73.9**	62.6
41–42	Mouth width	5	35.0	40.2	2	**30.5**	**32.6**	1	45.0	45.0	**32.0**
47–48	Mandibular isthmus-lower lip distance	5	21.5	24.0	2	22.4	23.5	1	20.9	20.9	24.4
47–1	Mandibular isthmus-upper lip distance	5	28.0	32.7	2	**32.5**	**32.6**	1	25.8	25.8	**35.5**
28–29	Maxillary barbel length	5	62.4	134.6	2	**79.6**	**85.5**	1	121.5	121.5	**94.1**
43–44	External mandibular barbel length	5	**35.9**	**59.8**	2	**47.4**	**52.0**	1	63.5	63.5	**49.5**
45–46	Internal mandibular barbel length	5	**29.8**	**38.9**	2	**35.4**	**39.4**	1	43.6	43.6	52.5

(Continues)

TABLE 1 (Continued)

(b)

LM	Measurement	*Cetopsorhamdia iheringi* Schubart & Gomes 1959			*Cetopsorhamdia insidiosa* (Steindachner 1915)			*Cetopsorhamdia molinae* Miles 1943			*Cetopsorhamdia nasus* Eigenmann & Fisher 1916
		N	Min	Max	*N*	Min	Max	*N*	Min	Max	H
21–26	Postorbital distance	5	47.8	52.6	2	52.0	54.2	1	48.1	48.1	**31.5**
30–31	Interorbital width	5	25.1	28.4	2	25.7	26.8	1	26.6	26.6	**47.8**
1–32	Snout-anterior nostril distance	5	10.8	12.5	2	8.9	11.6	1	**15.3**	**15.3**	11.5
32–33	Internostril distance	5	12.1	13.4	2	8.3	11.1	1	12.0	12.0	13.6
27–33	Posterior nostril-orbit distance	5	6.1	7.6	2	**7.8**	**8.6**	1	7.1	7.1	5.0
22–23	Head depth at supra occipital	5	47.7	52.8	2	52.9	59.1	1	53.5	53.5	54.1
24–25	Head depth at interorbital	5	32.9	39.6	2	36.5	36.7	1	42.6	42.6	41.8
35–36	Head width at posterior nostril	5	52.8	58.3	2	46.7	47.2	1	**61.9**	**61.9**	47.6
1–34	Dorsal head length	5	88.8	93.3	2	94.7	94.9	1	87.5	87.5	91.6

(c)

LM	Measurement	*Cetopsorhamdia orinoco* Schultz 1944				*Cetopsorhamdia phantasia* Stewart 1985				*Cetopsorhamdia picklei* Schultz 1944				*Cetopsorhamdia shermani* Schultz 1944
		H	*N*	Min	Max	H	*N*	Min	Max	H	*N*	Min	Max	H
	Standard length (mm)	54.3	6	32.3	71.0	38.8	2	38.8	39.0	88.4	17	42.2	89.3	30.5
Percentage of standard length														
1–3	Predorsal distance	36.2	6	32.4	38.8	42.5	2	41.4	42.5	35.4	17	34.8	40.4	38.7
1–4	Preadipose distance	68.2	6	64.6	69.7	67.2	2	67.2	67.8	69.5	17	65.7	71.9	67.8
1–5	Prepectoral distance	23.2	6	18.9	24.5	24.9	2	22.8	24.9	23.1	17	21.2	26.7	24.4
1–6	Prepelvic distance	44.5	6	38.0	44.7	45.1	2	45.1	46.3	45.5	17	44.4	47.3	45.6
1–7	Preanal distance	64.8	6	62.0	66.3	67.1	2	67.1	67.2	69.5	17	67.0	70.8	**65.0**
3–8	Body depth	11.6	6	8.7	13.5	19.8	2	**19.0**	**19.8**	20.5	17	15.3	23.3	17.4
9–10	Caudal peduncle depth	8.7	6	5.9	9.9	9.3	2	9.2	9.3	12.5	17	**11.1**	**14.1**	**10.4**
2–11	Caudal peduncle length	22.8	6	20.7	25.1	21.2	2	21.0	21.2	19.0	17	18.2	22.6	19.4
37–38	Body width	19.8	6	16.1	19.8	17.2	2	17.1	17.2	18.9	17	17.4	20.4	20.7
3–12	Dorsal-fin base length	13.7	6	12.2	14.2	22.8	2	**22.6**	**22.8**	12.4	17	11.1	13.2	**16.6**
7–11	Anal-fin base length	13.7	6	12.1	14.4	12.7	2	12.7	15.2	13.8	17	11.9	13.8	14.2
3–15	Unbranched dorsal-fin ray length	16.7	6	16.7	21.7	26.1	2	**25.6**	**26.1**	21.1	17	19.5	22.8	**24.7**

JOURNAL OF FISH BIOLOGY

TABLE 1 (Continued)

(c)

		Cetopsorhamdia orinoco Schultz 1944				*Cetopsorhamdia phantasia* Stewart 1985				*Cetopsorhamdia picklei* Schultz 1944				*Cetopsorhamdia sherman*i Schultz 1944
LM	Measurement	H	*N*	Min	Max	H	*N*	Min	Max	H	*N*	Min	Max	H
16–17	Dorsal-fin length	16.2	6	14.2	20.4	18.8	2	18.8	21.7	20.6	17	18.3	22.3	**21.3**
19–20	Adipose-fin depth	4.0	6	3.1	4.5	4.8	2	4.8	5.2	5.5	17	3.6	6.4	**6.3**
4–9	Adipose-fin base length	22.8	6	**21.6**	**23.4**	21.4	2	**20.4**	**21.4**	17.4	17	14.8	18.5	**19.6**
4–12	Interdorsal distance	18.5	6	16.5	20.1	5.9	2	**5.5**	**5.9**	22.0	17	17.7	23.1	**13.9**
5–18	Unbranched pectoral-fin ray length	17.7	6	17.4	20.7	31.4	2	**28.3**	**31.4**	17.6	17	14.2	19.8	22.1
5–13	Pectoral-fin length	17.6	6	14.8	21.8	22.2	2	**22.2**	**23.4**	20.1	17	17.7	21.7	**20.9**
6–14	Pelvic-fin length	16.2	6	13.9	17.3	25.0	2	**21.1**	**25.0**	19.1	17	**17.3**	**20.3**	**18.3**
5–6	Pectoral-pelvic fins distance	24.7	6	19.7	24.7	24.3	2	24.3	25.1	24.0	17	21.7	27.5	22.6
6–7	Pelvic-anal fins distance	22.4	6	21.6	24.6	24.0	2	20.9	24.0	24.1	17	22.5	26.7	**19.6**
3–2	Dorsal-fin insertion-hypural plate	64.7	6	**64.3**	**66.9**	61.8	2	61.6	61.8	65.2	17	61.9	66.7	64.4
6–2	Pelvic-fin insertion-hypural plate	57.8	6	55.1	61.3	55.7	2	55.7	56.9	55.3	17	54.5	58.2	54.7
7–2	Anal-fin insertion-hypural plate	35.9	6	34.3	37.5	34.3	2	34.3	35.2	31.7	17	30.0	34.6	35.4
1–21	Head length	23.5	6	21.7	27.3	25.4	2	**24.9**	**25.4**	25.6	17	24.4	27.4	27.3
1–27	Snout length	36.2	6	32.4	38.8	34.9	2	34.3	34.9	38.0	17	34.5	40.3	41.9
26–27	Orbital diameter	68.2	6	64.6	69.7	22.1	2	**20.4**	**22.1**	10.6	17	7.7	13.8	10.1
39–40	Head width	23.2	6	**18.9**	**24.5**	58.4	2	58.4	60.8	76.5	17	62.4	76.5	70.4
Percentage of head length														
41–42	Mouth width	40.5	6	35.2	40.5	45.4	2	45.4	45.8	34.8	17	27.6	41.0	41.4
47–48	Mandibular isthmus-lower lip distance	9.0	6	8.4	10.4	19.0	2	19.0	20.9	18.5	17	17.8	23.3	16.6
47–1	Mandibular isthmus-upper lip distance	86.3	6	73.4	86.3	24.7	2	24.7	25.2	31.6	17	27.1	35.8	21.1
28–29	Maxillary barbel length	40.5	6	**40.0**	**44.8**	430.3	2	**403.1**	**430.3**	119.9	17	104.2	135.2	**172.4**
43–44	External mandibular barbel length	21.5	6	20.9	26.1	137.8	2	**137.8**	**140.5**	56.4	17	51.8	68.5	**85.8**
45–46	Internal mandibular barbel length	33.3	6	25.2	33.3	57.8	2	57.8	66.8	34.3	17	**33.5**	**42.2**	51.4
21–26	Postorbital distance	128.5	6	128.5	144.7	46.6	2	**46.6**	**46.8**	49.1	17	47.8	52.9	47.4
30–31	Interorbital width	74.8	6	66.5	84.6	22.7	2	**22.7**	**22.7**	20.2	17	20.2	25.9	31.0
1–32	Snout-anterior nostril distance	49.0	6	43.1	50.2	10.5	2	10.5	11.1	11.8	17	9.9	12.8	13.1
32–33	Internostril distance	51.2	6	49.1	53.7	19.1	2	**19.1**	**19.1**	14.0	17	9.2	15.2	14.9
27–33	Posterior nostril-orbit distance	26.9	6	23.7	28.0	1.9	2	**1.9**	**2.4**	7.1	17	4.5	7.9	5.4
22–23	Head depth at supra occipital	13.9	6	11.8	13.9	57.7	2	54.4	57.7	57.8	17	47.9	60.1	52.9

(Continues)

TABLE 1 (Continued)

(c)

LM	Measurement	*Cetopsorhamdia orinoco* Schultz 1944				*Cetopsorhamdia phantasia* Stewart 1985				*Cetopsorhamdia picklei* Schultz 1944				*Cetopsorhamdia shermani* Schultz 1944
		H	N	Min	Max	H	N	Min	Max	H	N	Min	Max	H
24–25	Head depth at interorbital	11.9	6	8.0	12.1	43.2	2	43.2	**43.4**	38.5	17	34.5	43.7	41.4
35–36	Head width at posterior nostril	7.4	6	4.6	7.4	47.4	2	47.4	48.6	50.2	17	46.8	52.0	52.6
1–34	Dorsal head length	52.2	6	43.0	52.5	100.0	2	**97.1**	**100.0**	90.8	17	88.6	97.0	93.3

Note: Highlighted areas indicate measurements that differ from those of new species.

Abbreviations: H: holotype; LM: landmark; Max: maximum; Min: minimum; N: number of specimens; SD: standard deviation.

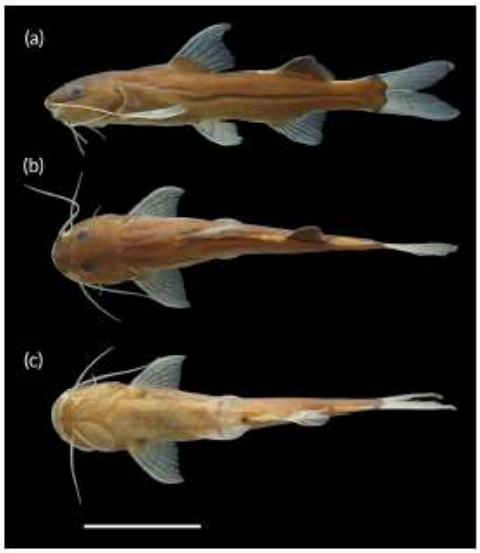

FIGURE 1 *Cetopsorhamdia hidalgoi*. MUSM 69550, holotype, 30.7 mm L_S, Peru, Loreto, Requena, Tapiche River tributary to Ucayali River basin. (a) Lateral view, (b) dorsal view and (c) ventral view. Black arrow indicates the urogenital papillae. Scale bar = 1 cm

2, 28.9–30.7, collected with MUSM 60687. **Madre de Dios drainage.** Madre de Dios Department, Manu Province: MUSM 23696, 1, 28.3 mm L_S, Amiguillos Boca creek, tributary to Amiguillos River, Amigos River, 12° 22′ 15.91″ S; 70° 22′ 13.83″ W, 21 June 2004, M. Hidalgo et al. **All from Ecuador, Napo drainage.** All from Sucumbios Province, Shushufundi Canton: FMNH 103260, 1, 27.0 mm L_S, Napo River, 0° 10′ 59.88″ S; 76° 30′ 0.00″ W, 25 November 1985, D. J. Stewart, M. C. Ibarra, R. Barriga-Salazar. FMNH 103261, 1, 28.8 mm L_S, Napo River, 0° 10′ 54.12″ S; 76° 50′ 35.88″ W, 27 September 1981, D. J. Stewart, M. C. Ibarra, R. Barriga-Salazar. All from Orellana Province, Francisco de Orellana Canton: FMNH 103262, 2, 28.9–28.9 mm L_S, Napo River, 0° 40′ 0.12″ S; 76° 53′ 42.00″ W, 04 November 1981, D. J. Stewart, M. C. Ibarra, R. Barriga-Salazar. **Colombia:** ROM 107277, 2, 29.6–31.5 mm L_S, Caqueta Department, Florencia, Orteguaza River, 1° 39′ 29.70″ N; 75° 32′ 31.06″ W, 08 July 2017, N. K. Lujan, A. Ortega-Lara, G. C. Sanchez, C. Conde, V. Meza-Vargas.

Diagnosis

C. hidalgoi new species is distinguished from all congeners by having one or two dark brown stripes on dorsal, pelvic and anal fins (*vs.* stripes on previous fins absent). In addition, *C. hidalgoi* can be distinguished from all congeners except from *C. molinae* by having fewer vertebrae (34–35 vertebrae *vs.* 36 in *C. shermani*; 36–37 in *C. phantasia*; 36–38 in *C. picklei*; 36–39 in *C. nasus*; 37 in *C. boquillae* and *C. insidiosa*; 37–39 in *C. iheringi*; 38–40 in *C. orinoco*; 39–40 in

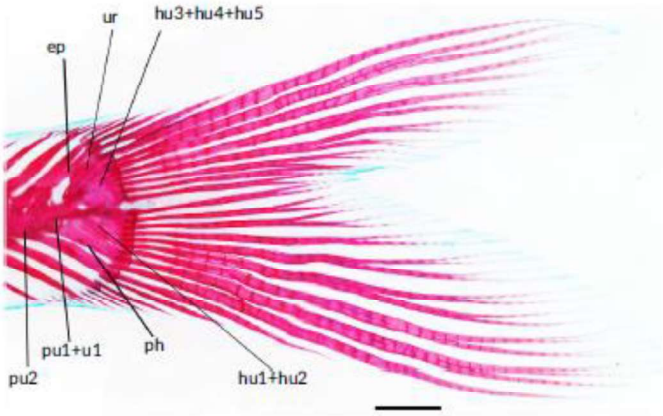

FIGURE 2 Left lateral view of the caudal skeleton of *Cetopsorhamdia hidalgoi*, MUSM 60687, paratype, 28.7 mm L_S. Abbreviations of the anatomical parts: ep: epural; hu1 + hu2: complex plate formed by hypurals 1 and 2; hu3 + hu4 + hu5: complex plate formed by hypurals 3, 4 and 5; ph: parhypural; pu1 + u1: complex centrum formed by preural centrum 1 and ural centrum 1; pu2: preural centrum 2; ur: uroneural. Scale bar = 1 mm

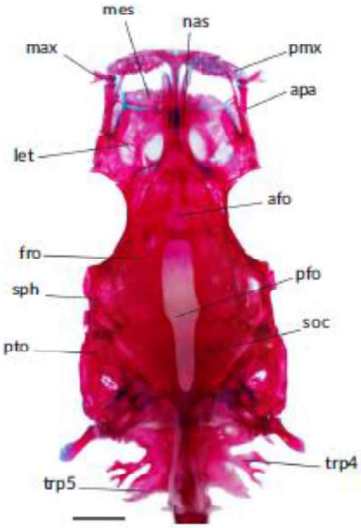

FIGURE 3 Dorsal view of cranium of *Cetopsorhamdia hidalgoi*, MUSM 60687, paratype, 28.7 mm L_S. Abbreviations of the anatomical parts: afo: anterior fontanel; apa: autopalatine; fro: frontal; let: lateral ethmoid; max: maxilla; mes: mesethmoid; nas: nasal; pfo: posterior fontanel; pmx: premaxilla; pto: pterotic; soc: supraoccipital; sph: sphenotic; trp4: transverse process 4; trp5: transverse process 5. Scale bar = 1 mm

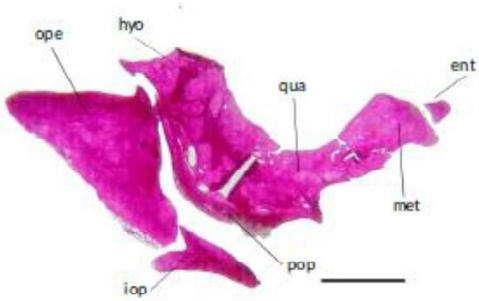

FIGURE 4 Right lateral view of suspensorium of *Cetopsorhamdia hidalgoi*, MUSM 62715, paratype, 27.8 mm L_S. Abbreviations of the anatomical parts: ent: entopterygoid; hyo: hyomandibula; iop: interopercle; met: metapterygoid; ope: opercle; pop: preopercle; qua: quadrate. Scale bar = 1 mm

C. spilopleura; 40–42 in *C. clathrata* and 45 in *C. filamentosa*). *C. hidalgoi* can be distinguished from all *Cetopsorhamdia* except from *C. boquillae* and *C. spilopleura* by having fewer number of paired ribs (7 ribs vs. 8 ribs in *C. molinae*, *C. phantasia* and *C. filamentosa*; 8–9 ribs in *C. orinoco* and *C. clathrata*; 9 ribs in *C. insidiosa*, *C. picklei* and *C. shermani*; 10 ribs in *C. nasus*; and 9–12 ribs in *C. iheringi*). Moreover, *C. hidalgoi* can be distinguished from all congeners except from *C. molinae* and *C. shermani* by having the first anal fin pterygiophore inserted on vertebrae 18–19 and 19–20 (vs. inserted on vertebrae 21 in *C. boquillae*, *C. insidiosa*, *C. orinoco*, *C. phantasia* and *C. picklei*; 21–22 in *C. iheringi*; 22–24 in *C. spilopleura*; 22–25 in *C. clathrata*; 23 in *C. nasus* and *C. filamentosa*). It is further distinguished from all *Cetopsorhamdia* species except from *C. molinae*, *C. picklei* and *C. shermani* by having the first dorsal fin pterygiophore inserted on vertebra 7 (vs. inserted on vertebrae 4 in *C. filamentosa*; 8 in *C. boquillae*, *C. iheringi*, *C. insidiosa*, *C. orinoco*; 9 in *C. nasus*; 10 in *C. phantasia*; 11–12 in *C. clathrata* and *C. spilopleura*). It is further distinguished from *C. clathrata*, *C. spilopleura*, *C. molinae* and *C. shermani* by having homogeneous dark brown colouration on body sides with

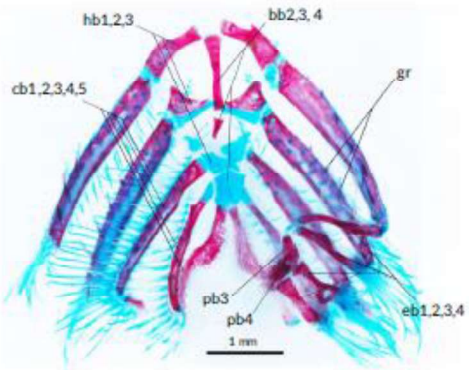

FIGURE 5 Dorsal view of the branchial arch of *Cetopsorhamdia hidalgoi*, MUSM 60687, paratype, 28.7 mm L_S. Abbreviations of the anatomical parts: bb_{2-4}: basibranchial 2 to 4; cb_{1-5}: ceratobranchial 1–5; eb_{1-4}: epibranchial 1–4; gr: gill rakers; hb_{1-3}: hypobranchial 1–3; pb_{3-4}: pharyngo-branchial 3–4. Scale bar = 1 mm

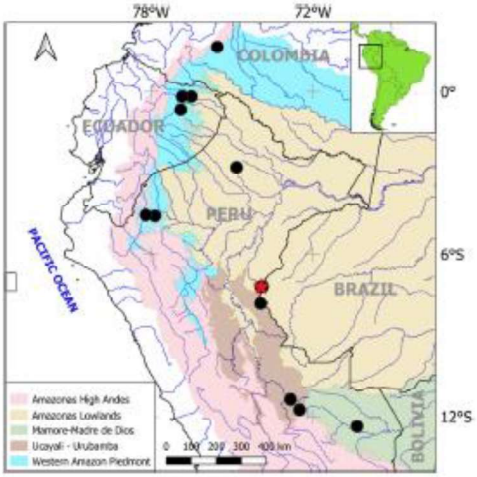

FIGURE 6 Geographical distribution of *Cetopsorhamdia hidalgoi*. Red star symbol represents the type locality. Each symbol may represent more than one collection lot

two more intense dark brown bars, first one ventral to adipose fin and second one at the caudal-fin base (vs. two longitudinal rows of 10–12 quadrangular dark brown marks in *C. clathrata*; 18–22 irregular, vertical brown bars in *C. spilopleura*; four well-defined vertical dark brown bars, first anterior to dorsal-fin, second posterior to dorsal-fin, third below adipose fin and a last one at the caudal-fin base in *C. molinae* and *C. shermani*). Furthermore, *C. hidalgoi* can be distinguished from *C. phantasia* by having six branched rays on dorsal-fin (vs. 10 branched rays on dorsal-fin). In addition, other proportional measurements distinguish *C. hidalgoi* from all congeners (except *C. clathrata* and *C. spilopleura*) as highlighted in Table 1a–c.

Description. Morphometric data presented in Table 1a.

Body elongate, cylindrical in cross section until adipose-fin and becoming progressively compressed posteriorly. Body depth at dorsal-fin origin *c.* 0.12–0.18 of L_S, and less than HL. Lateral line on body complete until anterior edge of the hypural plate. Dorsal profile of body slightly convex, mildly straight from nape to adipose fin insertion, slightly convex from insertion to end of adipose-fin and slightly straight from end of adipose-fin to caudal-fin base. Ventral profile of body slightly convex from opercle opening to pelvic girdle, mildly straight from that point to anal-fin origin, slightly convex from anal-fin insertion to caudal-fin origin. Caudal-peduncle depth approximately twice of caudal-peduncle length.

Head small, slightly depressed with conical snout in dorsal view. Dorsal profile of head forming convex arch from snout tip to supraoccipital, and ventral profile of head slightly convex from tip of lower lip to opercle opening. Anterior nostril tubular and closer to upper lip. Posterior nostril opening nearly round and with flap of skin extending along aperture, closer to anterior margin of eye than to anterior nostril. Four nostrils arranged as in vertices of a trapezoid; anterior nostril

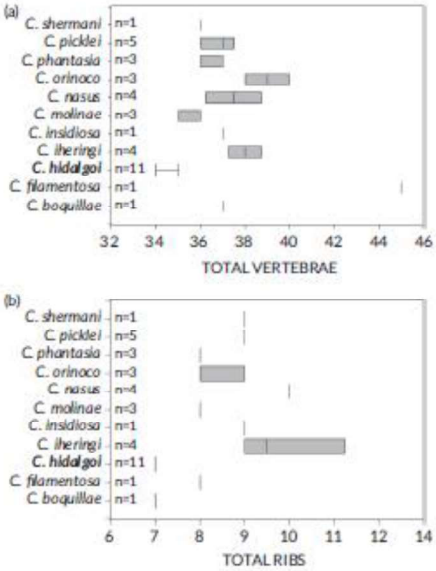

FIGURE 7 Boxplot showing meristic variation among *Cetopsorhamdia*. (a) Number of total vertebrae. (b) Number of ribs. | median; □ 25th to 75th percentiles; T, 95% range; *n*, sample size

distance narrower than posterior nostril distance; all nostrils lacking barbels. Eye diameter similar to internostril distance.

Mouth wide, subterminal (approximately half of HL); margin of lower jaw slightly convex, lateral commissure reaching to vertical through middle of internostril region. Premaxillary rectangular, length approximately four times its width; teeth on premaxilla small, conical and sharply pointed and arranged in five or six nearly regular rows. Maxillary, inner and outer mental barbels short, slender and tapering distally. Maxillary barbel reaching pectoral-fin origin when adpressed (more than one time its HL), inserted posterior to upper lip. Outer mental barbel inserted at middle of vertical through region between maxillary barbel insertion and anterior eye margin, its tip reaching pectoral-fin insertion when adpressed (one-sixth to one-eighth of HL). Inner mental barbel inserted anterior to vertical through insertion of mental barbel, its tip reaching inner border of branchiostegal membrane when adpressed.

Dorsal fin moderately large, with length of dorsal-fin base 0.4–0.5 of HL, distally triangular in lateral profile. Dorsal-fin spinelet absent, first dorsal fin ray unbranched with proximal one-fifth rigid and remainder flexible, lacking distal filament in all examined specimens, six branched rays (18), first pterygiophore inserted on bifid neural spine of vertebrae 7 (12).

Pectoral fin length approximately four-fifths of HL, with i + 8 (16*) or i + 9 (2) rays, and distal margin triangular; first pectoral fin ray slightly longer than other fin rays, proximal portion of first pectoral-fin ray slightly rigid and distal portion soft, and not prolonged as filament in any examined specimens, tip of pectoral-fin close to pelvic-fin insertion.

Pelvic fin small, approximately half of HL, with i + 6 (21), all rays completely soft, distal margin slightly convex. Pelvic fin insertion located halfway between pectoral and anal fin insertions, tip of pelvic fin surpassing anus and urogenital papillae.

Anal fin iii + 7 (1), iii + 8 (2), iv + 7 (13) and iv + 8 (2*); triangular margin on lateral profile, small fin base (0.11–0.15 of L_S). Anal-fin base insertion anterior to vertical through the adipose fin insertion. First anterior pterygiophore of anal fin inserted between 18 and 19 (8) or 19 and 20 (3) vertebrae.

Adipose fin short (0.15–0.19 of L_S), distal margin triangular in lateral profile. Adipose fin insertion slightly posterior to body midpoint and posterior to vertical through anal fin insertion. Adipose fin insertion between vertebrae 20 and 21 (9) and 21 and 22 (2).

Caudal fin deeply forked, with ventral lobe slightly longer than dorsal lobe and tips of lobes rounded. Total caudal fin rays 40 (2), 41 (5), 42 (2), 43 (1) and 44 (2); 19 (1), 20 (4), 21 (5) and 22 (2) on dorsal caudal lobe and 20 (4), 21 (5), 22 (2) and 23 (1) on ventral caudal lobe. Dorsal caudal lobe with 7 (19*) branched rays and ventral caudal lobe with 8 (19*) branched rays. Caudal fin (Figure 2) with five hypurals series: hu1, hu2, hu3, hu4 and hu5. Ventral caudal plate (hu1 and hu2) and dorsal caudal plate (hu3, hu4 and hu5) separated distally. Hypurals 1 and 2 completely fused into single ventral caudal plate, without any vestige of suture line. Parhypural very close to ventral margin of hu1 with some proximal suture region. Third and fourth hypurals completely fused into single dorsal caudal plate. Fifth hypural and hu3 + hu4 with proximal region suture, medial and distal region free. Uroneural present and fused to hypural five, with vestige of suture. Epural rod-like and connected to dorsal region of preural centrum 1 and ural centrum 1 (pu1 + u1). Hypurapophysis complex with foramen (passage of dorsal branch of caudal artery) posterior to pu1 + u1 centrum. Posteriormost neural spines without any process. Dorsal caudal plate (hypural 3, 4 and 5) with 8 (12) rays. Ventral caudal plate (hypural 1 and 2) with 9 (12) rays. Total vertebrae 34 (2) or 35 (9). 12 (1) or 13 (10) precaudal vertebrae and 21 (2), 22 (8) or 24 (1) caudal vertebrae (complete haemal spine). Ribs 8 (11) pairs.

Cranial skeleton (Figure 3). Cranial roof bones lacking ornamentation; dorsal surface slightly convex and without crests; orbital region well defined dorsally; concave and limited anteriorly by lateral ethmoid, laterally by frontal and posteriorly by sphenotic; interorbital wider than its length; two cranial fontanels separated by epiphyseal bar; posterior fontanel longer than anterior fontanel (more than thrice of anterior fontanel length), anterior region of posterior fontanel twice the width of its posterior region, anterior region of anterior fontanel elongated, posterior region of anterior fontanel rounded; epiphyseal bar located anterior to midpoint of frontals length. Mesethmoid in dorsal and ventral plane; anterolateral mesethmoid in dorsal horizontal plane, anterolateral mesethmoid *cornu* short, thick, blunt-tipped and anterolaterally directed; posterolateral mesethmoid in ventral horizontal plane, laterally projected; region between posterior border of posterolateral mesethmoid and anterior border of lateral ethmoid separated (connected only by ethmoidean cartilage). Lateral ethmoid slightly rectangular; anterior and lateral margins slightly concave; posterior portion longer than anterior portion; lateral region of posterior portion pointed. Vomer arrow-shaped, small (half size of posterolateral mesethmoid). Premaxilla rectangular, width more than thrice its length; anterior margin continuous, posterolateral edge similar to posteromedial angle; five or six irregular rows of villiform teeth. Maxilla small and trapezoidal (distal longer than mesial region), distal region forming bony tubule around maxillary barbel base. Autopalatine rod-like; size longer than orbital region; small cartilages at anterior and posterior margins, anterior slightly longer than posterior cartilage. Nasal shorter than autopalatine, slightly wider than autopalatine, and poorly ossified. Frontal smooth and lacking processes; anteriorly limited by lateral ethmoid, posterolaterally limited by sphenotic and posteriorly limited by supraoccipital; posterior and anterior portion with similar width. Sphenotic smaller than pterotic; sphenotic slightly narrower than pterotic, anterior and posterior portions with similar width. Pterotic longer than sphenotic; anterior portion narrower than posterior portion. Supraoccipital limited laterally by sphenoid, and anteriorly by posterior margin of sphenotic and frontals; supraoccipital process narrow, bifid and medium-sized (similar size of anterior fontanel length), reaching midpoint of complex *centra* (in dorsal view).

Complex anterior vertebra (Figure 3). Composed of vertebrae 1, 2, 3, 4 and 5; vertebrae 1 disc-like element and attached to complex vertebra; complex vertebra (vertebrae 2–4) attached to vertebra 5 with suture ventrally; neural spine of vertebra 4 not covering neural spine of vertebra 5. Transverse process of vertebra 4 divided into anterior and posterior branches. Anterior branch of transverse process of vertebra 4 wide, laminar and expanded laterally; proximal portion

wider than distal portion. Posterior branch divided in anterior and posterior portion; anterior portion arborescent, divided into two main arms (anterior and posterior arms), posterior arms with conspicuous notch; posterior portion triangular and expanded laterally one-third length of anterior portions. Transverse process of vertebra 5 is expanded and not branched.

Suspensory (Figure 4). Entopterygoid small and slightly quadrangular; anterodorsal and posteroventral margins pointed and anterior margin attached to lateral process of vomer; posterior margin slightly concave and attached to anterodorsal margin of metapterygoid. Metapterygoid quadrangular, smooth and approximately four times entopterygoid size; dorsal, anterior and ventral margins slightly concave; posterodorsal and posteroventral margin of metapterygoid attached with dentate suture and small cartilaginous bar to anterodorsal margin of quadrate; and ventral margin joint with anterodorsal process of quadrate. Quadrate approximately rectangular, smaller than hyomandibula; anterior and posterior portions separate each other; anterior margin of quadrate with long anterodorsal process covering ventrolateral margin of metapterygoid; dorsal margin slightly concave; posterodorsal and posteroventral margins connected to hyomandibula with dentate sutures and large cartilaginous bar; anterior portion of quadrate with robust triangular process to articulate with angulo-articulo-retroarticular. Hyomandibula rectangular and slightly smooth (with crest for the insertion of the *levator arcus palatini* muscle); anterodorsal margin concave; dorsal margin with wide processes to connect to neurocranium; posterodorsal hyomandibular process slender and triangular (insertion of *levator operculi* muscle) with posterior margin pointed; medial face of hyomandibula with slender elliptical foramen for hyoideomandibular nerve trunk passage. Opercle triangular and longer than hyomandibula; anterior and posteroventral margins slightly convex; dorsal margin mostly straight; posterior and ventral margins rounded, with posterior margin oriented ventrally; lateral surface flat with conspicuous crest and fossae for accommodation of *levator operculi* muscle. Interopercle triangular; anterior, posterior and dorsal margin pointed; ventral margin and posterodorsal region concave; anterodorsal region slightly concave. Preopercle rod-shape; anterior margin wider than posterior margin; anterodorsal border articulating with ventral margin of quadrate and posterodorsal border articulating with anteroventral border of hyomandibula.

Branchial arches (Figure 5). Three basibranchial series: bb2, bb3 and bb4 (basibranchial 1 absent). Basibranchial 2 and 3 anteroposteriorly elongate, largely ossified, anterior portion wider than posterior portion, bb2 four times longer than bb3. Basibranchial 4 completely cartilaginous, hexagonal shape, anterior and posterior portions pointed and lateral portions slightly concave; bordered by cartilaginous heads, hypobranchial 3 anteriorly, ceratobranchial 5 posteriorly and ceratobranchial 4 laterally. Three hypobranchial series: hb1, hb2 and hb3. Hypobranchial 1 laterally elongate, largely ossified, size more than twice its greatest width, largely ossified, cartilage just in proximal and distal extremities, anterior portion with uncinate process. Hypobranchial 2 slightly elongate, triangular with medial portion more pointed than lateral portion, anterior portion ossified and posterior portion cartilaginous, ossified portion twice longer than cartilaginous portion. Hypobranchial 3 completely cartilaginous, rectangular and elongate anterolaterally; hypobranchial 4 absent. Five ceratobranchial series: cb1, cb2, cb3, cb4 and cb5; fully ossified with cartilage only at their distal and proximal extremities; ceratobranchial 1 and 2 similar size, longer and wider than ceratobranchial 3, 4 and 5. Ceratobranchial 3 longer and wider than ceratobranchial 4. Ceratobranchial 4 and 5 with similar length but cb5 expanded anteromedially to support one patch of conical teeth, teeth with similar size and covering more than half of cb5 length. Four epibranchial series plus accessory element of ceratobranchial 4: eb1, eb2, eb3, eb4 and aecb4; first four rod-shaped, anteromedially narrower than posterolaterally portion; mostly ossified; eb1, eb2, eb3 and eb4 extremities and aecb4 cartilaginous; epibranchial 1 and 2 with similar size, eb1 and eb2 longer than eb3 and eb4. Epibranchial 3 with triangular posterior uncinate process united to medial portion to itself (looks like foramen on posterior portion of cb3). Epibranchial 4 expanded at anterior and posterior portion. Two pharyngobranchial series: pb3 and pb4; pharyngobranchial 1 and 2 absent. Pharyngobranchial 3 rectangular, ossified and anterior portion narrower than posterior portion. Pharyngobranchial 4 ossified, semicircular with patch of conical teeth.

3.2 | Colour in alcohol

Dorsal and lateral body surfaces mostly dark brown with cream details and ventral surface cream (Figure 1). Dorsal region of head and cheeks covered by dark brown pigment, ventral region cream with scattered dark brown chromatophores fading ventrally and cream blotches anterior to adipose fin insertion and on dorsal region of caudal peduncle. Distal portion of maxillary barbel with dark brown pigment dorsally and proximal portion unpigmented. Outer mental barbel dark brown dorsally only on distal portion and proximal portion unpigmented. Inner mental barbel dark brown pigment only on insertion, and proximal portion unpigmented.

Base of caudal fin with "W" shape dark brown blotch. Caudal-fin rays grey and inter-radial caudal-fin membrane translucid with one well-defined dark brown vertical "V" shape stripe and one diffuses dark brown vertical "V" shape stripe. Dorsal, anal, pectoral and pelvic fins with two dark brown stripes, with concentration of grey chromatophores along rays and interradial membranes translucent; fin bases with concentration of dark brown chromatophores. Adipose fin with distal grey pigmentation, base with concentration of dark brown chromatophores reaching more than half its depth. Black and narrow stripe along lateral line, slightly convex above pectoral fin and straight along midbody line from that point to caudal-fin base.

3.3 | Sexual dimorphism

Urogenital region triangular and slightly elongate in males (Figure 1c, black arrow), trapezoidal and short in females.

3.4 | Etymology

Named in honour of the authors' colleague and friend Max Hidalgo, professor, and curator of the Ichthyology Department at the Museo de Historia Natural in the Universidad Nacional Mayor de San Marcos (MUSM) for his devotion and dedication to Peru Ichthyology. Hidalgo collected the holotype, in addition to many specimens of the type series on expeditions including several rapid inventories in Peru that have led to the creation of multiple conservation areas.

3.5 | Geographic distribution

C. hidalgoi is known from the Ucayali, Marañón, Napo and Orteguaza rivers tributaries of the Upper Amazon River in Peru, Ecuador and Colombia and from the Madre de Dios River tributary of the Madeira River basin in Peru (Figure 6).

3.6 | Ecology

Found in clearwater streams with modest flow, substrate often with submerged leaves and sand.

4 | DISCUSSION

Cetopsorhamdia belongs to Heptapterini which is based on 12 synapomorphies (Bockmann, 1998; Ferraris Jr, 1988; Silva *et al.*, 2021). All these synapomorphies were found in the new species *C. hidalgoi*, most of them shown in Figures 1–5.

Based on morphological (Bockmann, 1998) and molecular (Faustino-Fuster *et al.*, 2021) phylogenies, *Cetopsorhamdia* do not form a monophyletic genus, and some species are to be moved to different genera not yet formally described (Bockmann & Slobodian, 2017).

Bockmann and Reis (2021) (based on Bockmann, 1998) diagnosed the genus *Cetopsorhamdia* by having four synapomorphies: (a) presence of a medial ossification over the median portion of the skull, covering the epiphyseal bar and leaving reduced anterior and posterior fontanels; (b) orbital (= optic) foramen small; (c) mouth ventral and (d) snout conical. According to morphological data (Figures 1 and 2) *C. hidalgoi* does not contain the first previous synapomorphy of the four morphological characters to diagnosis *Cetopsorhamdia*. It is more similar to *C. molinae*, *C. orinoco*, *C. phantasia* and *C. shermani* by the absence of a medial ossification over the medial portion of the skull, covering the epiphyseal bar and leaving reduced anterior and posterior fontanels. This character is present in *C. boquillae*, *C. clathrata*, *C. spilopleura*, *C. nasus*, *C. iheringi* and *C. insidiosa* (Bockmann, 1998; Ortega-Lara, 2012; Bockmann & Reis, 2021; DRFF pers. obs.).

The morphometric data of this study (Table 1a) indicate that *C. hidalgoi* is most similar to *C. nasus*, *C. insidiosa*, *C. orinoco* and *C. pinkdei*, whereas the vertebrae and ribs count data suggest that *C. hidalgoi* is more similar to *C. molinae* (Figure 7a) or *C. boquillae*. Despite this difference all previous *C. hidalgoi* morphological data are most congruent with the phylogenetic hypothesis of *Cetopsorhamdia* proposed by Bockmann (1998) and Faustino-Fuster et al., (2021).

Distributional patterns of *C. hidalgoi* suggest that the new species is found in the piedmont region of the Amazon basin in Ecuador, Colombia and Peru and the lowlands in tributaries of the Upper Madeira River. Bockmann and Slobodian (2013) recorded a similar morphotype distributed in the Beni River (Bolivia), Guapore River (Brazil) and Madeira River (Brazil) but the authors of this study could not access this material to include them in the analyses of this study. Based on photographic and morphological information provided by these authors, the authors of this study found colouration patterns and some meristic data similar to *C. hidalgo*, thus possibly expanding the distribution of *C. hidalgoi* to Bolivia and Brazil.

4.1 | Comparative material examined

In addition to the comparative material listed by Faustino-Fuster *et al.* (2019), the following lots were examined:

C. boquillae. All from Colombia: **Holotype**: FMNH 55212, xr, 72.1 mm L_S, Boquilla, Cauca River. **Paratype**: FMNH 55213, 6, 44.9–60.2 mm L_S, Boquilla, Cauca River.

C. filamentosa. All from Peru, Junín Department: **Non-type:** Perene River basin: MUSM 15606, 3, 62.1–72.4 mm L_S, Tulumayo River, San Ramon. MUSM 12667, 6, 25.4–42.2 mm L_S, creek tributary to Chanchamayo River, Chanchamayo.

C. iheringi. All from Brazil. **Non-type:** MCP 47191, 4 (1c&s), 43.7–64.8 mm L_S, Paraná River, Pratinha, Minas Gerais. MCP 49058, 5 (1c&s), 36.8–56.0 mm L_S, São Francisco River, Jaboticatubas, Minas Gerais. UFRGS 11277, 3 (c&s), 56.0–72.9 mm L_S, Paraná River, Planaltina, Distrito Federal. UFRGS 25409, 10 (1c&s), 35.3–78.1 mm L_S, Uruguai River, Ijuí, Rio Grande do Sul. USNM 313192, 4, 56.6–75.8 mm L_S, Cubatao River, Upper Parana River, Near Cajuru, São Paulo State. USNM 345663, 1, 63.2 mm L_S, Pedro Leopoldo creek, tributary to Das Velhas River, Jaguara, Minas Gerais State.

C. insidiosa. All from Venezuela, Amazonas State. **Non-type:** ANSP 160596, 1, 32.7 mm L_S, Orinoco River, Puerto Ayacucho. ANSP 165534, 1, 36.8 mm L_S, Cataniapo River, Puerto Ayacucho.

C. molinae. All from Colombia, Magdalena Basin. **Non-type:** Huilla Department. ICN-MNH 5719, 1, 35.7 mm L_S, Magdalena River. ICN-MNH 20207, 5, 33.7–40.1 mm L_S, Suaza River, Garzon Municipality. ICN-MNH 23039, 1, 31.2 mm L_S, Suaza River, Garzon Municipality. ICN-MNH 23049, 5, 23.2–23.9 mm L_S, Magdalena River confluence with Páez River, Gigante Municipality. ICN-MNH 23131, 1, 34.8 mm L_S, Suaza River, Garzón Municipality. ICN-MNH 23154, 10, 22.6–24.6 mm L_S, Magdalena River near to Betania, Gigante Municipality. ICN-MNH 23317, 2, 26.2–26.8 mm L_S, Paéz River, Tesalia Municipality. Caldas Department. ICN-MNH 13829, 1, 33.0 mm L_S, Magdalena River.

C. nasus. **Holotype:** FMNH 58126, xr, 54.3 mm L_S, Honda, Colombia.

C. orinoco. **Holotype:** USNM 121214, xr, 54.3 mm L_S, Torbes River, Orinoco River basin, Tariba, Venezuela. **Paratype:** USNM 121215, 3, 32.3–52.3 mm L_S, same data of holotype. **Non-type:** ICN-13391, 1, 69.9 mm L_S, Colombia. ICN-16983, 1, 71.4 mm L_S, Colombia.

C. phantasia. All from Ecuador, Orellana Province. **Holotype:** FMNH 94601, xr, 38.8 mm L_S, Jivino River. **Paratype:** FMNH 94602, 1, 39.0 mm L_S, Jivino River.

C. picklei. All from Venezuela. **Holotype:** USNM 121217, xr, 88.4 mm L_S, Motatan River, Motatan, Maracaibo Basin. **Paratype:** USNM 121218, 28, 45.3–116.9 mm L_S, same data of holotype. USNM 121219, 22, 37.0–79.8 mm L_S, San Juan River, tributary to Motatan River, Mene Grande, Maracaibo Basin. USNM 121220, 7, 51.6–94.4 mm L_S, Motatan River, Motatan, Maracaibo Basin. USNM 121221, 17, 36.9–70.2 mm L_S, Palmar River, Totuma, southwest of Maracaibo, Zulia Province. USNM 121222, 24, 46.0–95.7 mm L_S, Jimellas River, Motatan, tributary of Motatan River, Maraicaibo Basin. UMMZ 141935, 5, 50.4–77.5 mm L_S, Jimelles River, tributary to Motatan River, Motatan.

C. shermani. **Holotype:** USNM 121216, xr, 30.5 mm L_S, Guarico River, Aragua State, Venezuela.

ACKNOWLEDGEMENTS

We give special thanks to Mariangeles Arce and Mark Sabaj (ANSP); Caleb McMahan, Kevin Swagel and Susan Mochel (FMNH); José I. Mojica (ICNMHN); Hernán Ortega, Max Hidalgo, Omar Loyola, Alessandra Escurra and Carla Muñoz (MUSM); and Lynne Parenti, Jeff Clayton and Sandra Raredon (USNM) for curatorial assistance during their visit to these fish collections. Special thanks to Kevin Swagel (FMNH) and Sanda Raredon (USNM) for assistance with the X-ray images. Thanks to Vanessa Meza for providing the map. The first author was supported by a doctoral programme provided by Ministry of Education of Brazil (CAPES). Additional financial support was received from Böhlke Award from the Academy of Natural Science of Drexel University, Philadelphia; Smithsonian Visiting Student (Fellowship) at the National Museum of Natural History (NMNH), Washington; and funding from the Grainger Bioinformatics Center at the Field Museum of Natural History, Chicago.

AUTHOR CONTRIBUTIONS

Dario R. Faustino-Fuster examined the specimens and performed the morphometric, meristic and osteological examinations. Dario R. Faustino-Fuster and Lesley S. de Souza analysed, discussed and prepared the manuscript. Lesley S. de Souza provided project funding and laboratory resources.

ORCID

Dario R. Faustino-Fuster https://orcid.org/0000-0002-1445-3495
Lesley S. de Souza https://orcid.org/0000-0002-1669-8074

REFERENCES

Arratia, G., & Huaquin, L. (1995). Morphology of the lateral line system and of the skin of diplomystid and certain primitive loricarioid catfishes and systematic and ecological considerations. *Bonner Zoologische Monographien*, *36*, 1–110.

Bockmann, F. A. (1994). Description of *Mastiglanis asopos*, a new pimelodid catfish from northern Brazil, with comments on phylogenetic relationships inside the subfamily Rhamdiinae (Siluriformes: Pimelodidae). *Proceedings of the Biological Society of Washington*, *107*, 760–777.

Bockmann, F.A. (1998). *Análise filogenética da família Heptapteridae (Teleostei: Ostariophysi: Siluriformes) e redefinição de seus gêneros* (Unpublished Doctoral Dissertation). Universidade de São Paulo, São Paulo, p. 599.

Bockmann, F. A., & Guazzelli, G. M. (2003). Family Heptapteridae (Heptapterids). In R. E. Reis, S. O. Kullander, & C. J. Ferraris, Jr. (Eds.), *Check list of the freshwater fishes of South and Central America* (pp. 406–431). Porto Alegre: Editora da Pontifícia Universidade Católica do Rio Grande do Sul-EDIPUCRS.

Bockmann, F. A., & Miquelarena, A. M. (2008). Anatomy and phylogenetic relationships of a new catfish species from northeastern Argentina with comments on the phylogenetic relationships of the genus *Rhamdella* Eigenmann and Eigenmann 1888 (Siluriformes, Heptapteridae). *Zootaxa*, *1780*(1), 1–54.

Bockmann, F. A., & Reis, R. E. (2021). Two new, remarkably colored species of the Neotropical catfish genus *Cetopsorhamdia* Eigenmann & Fisher, 1916 (Siluriformes, Heptapteridae) from Chapada dos Paredes, western Brazil, with an assessment of the morphological characters bearing on their phylogenetic relationships. *Papéis Avulsos de Zoologia*, *61*, e20216156.

Bockmann, F. A., & Slobodian, V. (2013). Heptapteridae. In L. J. Queiroz, G. Torrente-Vilara, W. M. Ohara, T. H. da Silva Pires, J. Zuanon, & C. R. da Costa Doria (Eds.), *Peixes do Rio Madeira* (pp. 12–71). São Paulo, Brazil: Dialeto.

Bockmann, F. A., & Slobodian, V. (2017). Family Heptapteridae – three-barbeled catfishes. In P. van der Sleen & J. S. Albert (Eds.), *Field guide to the fishes of the Amazon, Orinoco & Guianas* (pp. 233–252). Princeton: Princeton University Press.

Carvalho, M., Bockmann, F. A., & de Carvalho, M. R. (2013). Homology of the fifth epibranchial and accessory elements of the ceratobranchials among Gnathostomes: Insights from the development of ostariophysans. *PloS One*, *8*(4), e62389.

Carvalho, T. P., Espino, J., Máxime, E., Quispe, R., Rengifo, B., Ortega, H., & Albert, J. S. (2016). Fishes from the lower urubamba river near sepahua, Amazon Basin, Peru. *Check List*, *7*(4), 413–442.

de Pinna, M. C. C. (1993). Higher-level phylogeny of Siluriformes, with a new classification of the order (Teleostei, Ostariophysi). New York, The City University of New York. 482 p. [Tese de doutorado não publicada]

Eigenmann, C. H. (1922). The fishes of Western South America [Part I]: The fresh-water fishes of Northwestern South America, includind Colombia, Panama, and the Pacific slopes of Ecuador and Peru, together with and appendix upon the fishes of the río Meta in Colombia. *Memoirs of the Carnegie Museum*, *9*(1), 1–346.

Faustino-Fuster, D. R., Bockmann, F. A., & Malabarba, L. R. (2019). Two new species of *Heptapterus* (Siluriformes: Heptapteridae) from the Uruguay River basin, Brazil. *Journal of Fish Biology*, *94*(3), 352–373.

Faustino-Fuster, D. R., Meza-Vargas, V., Lovejoy, N. R., & Lujan, N. K. (2021). Multi-locus phylogeny with dense Guiana Shield sampling supports new suprageneric classification of the neotropical three-barbeled catfishes (Siluriformes: Heptapteridae). *Molecular Phylogenetics and Evolution*, *162*, 107186.

Ferraris, C. J., Jr. (1988). Relationships of the neotropical catfish genus *Nemuroglanis*, with a description of a new species (Osteichthys: Siluriformes: Pimelodidae). *Proceedings of the Biological Society of Washington*, *101*(3), 509–516.

Fricke, R., Eschmeyer, W. N. & Van der Laan, R. (eds) (2020). *Eschmeyer's catalog of fishes: Genera, species, references*. http://researcharchive.calacademy.org/research/ichthyology/catalog/fishcatmain.asp.

Gomes, A. L. & Schubart, O. (1958). Descrição de" Chasmocranus brachynema" sp. n., novo" Luciopimelodinae" da Bacia do Rio Mogi Guaçu, estado de São Paulo (Pisces, Nematognathi, Pimelodidae). *Revista Brasileira de Biologia*, *18*(4), 413–416.

Gosline, W. A. (1945). Catálogo dos nematognatos de água-doce da América do Sul e Central. *Boletim do Museu Nacional, Nova Série, Zoologia*, *33*, 1–138.

Hidalgo, M., & Willink, P. W. (2007). Peces. In C. Vriesendorp, J. A. Álvarez, N. Barbagelata, W. S. Alverson, & D. Moskovits (Eds.), *Perú: Nanay-Mazán-Arabela. Rapid biological inventories report 18* (pp. 56–62). Chicago: The Field Museum.

Hidalgo, M. H., & Pezzi, J. F. (2006). Peces. In C. Vriesendorp, T. S. Schulenberg, W. S. Alverson, D. K. Moskovits, & J.-I. Rojas Moscoso (Eds.), *Perú: Sierra del Divisor. Rapid biological inventories report 17* (pp. 13–83). Chicago: The Field Museum.

Lundberg, J. G., Bornbusch, A. H., & Mago-Leccia, F. (1991). *Gladioglanis conquistador* n. sp., from Ecuador with diagnoses of the subfamilies Rhamdiinae Bleeker and Pseudopimelodinae n. subf. (Siluriformes, Pimelodidae). *Copeia*, *1991*(1), 190–209.

Lundberg, J. G., & McDade, L. A. (1986). On the South American catfish *Brachyrhamdia imitator* Myers (Siluriformes, Pimelodidae), with phylogenetic evidence for a large intrafamilial lineage. *Notulae Naturae*, *463*, 1–24.

Ortega-Lara, A. (2012). Redescripción de *Cetopsorhamdia nasus* Eigenmann y Fisher, 1916 (Siluriformes: Heptapteridae). *Biota Colombiana*, *13*(1), 47–70.

Sabaj, M. H. (2019). *Standard symbolic codes for institutional resource collections in herpetology and ichthyology: An online reference. Version 7.1 (21 March 2019)*. Washington, DC: American Society of Ichthyologists and Herpetologists. Retrieved from http://www.asih.org/

Schaefer, S. A., & Aquino, A. E. (2000). Postotic laterosensory canal and pterotic branch homology in catfishes. *Journal of Morphology*, *246*, 212–227.

Sherman, G. E., Sutton, T., Blazek, R., Holl, S., Dassau, O., Morely, B., Mitchell, T., & Luthman, L. (2012). *Quantum GIS user guide - Version 1.8 "Wroclaw"*. Retrieved from http://download.osgeo.org/qgis/doc/manual/qgis-1.8.0_user_guide_en.pdf.

Silva, G. S. C., Roxo, F. F., Melo, B. F., Ochoa, L. E., Bockmann, F. A., Sabaj, M. H., … Oliveira, C. (2021). Evolutionary history of Heptapteridae catfishes using ultraconserved elements (Teleostei, Siluriformes). *Zoologica Scripta*, *50*, 1–12.

Silvergrip, A. M. C. (1996). *A systematic revision of the neotropical catfish genus Rhamdia (Teleostei, Pimelodidae)* (Doctoral dissertation, Thesis in Zoology). Stockholm University, Stockholm.

Stewart, D. J. (1986). A new pimelodid catfish from the deep-river channel of the Rio Napo, eastern Ecuador (Pisces: Pimelodidae). *Proceedings of the Academy of Natural Sciences of Philadelphia*, *138*, 46–52.

Swarça, A. C., Caetano, L. G., & Dias, A. L. (2000). Cytogenetic of species of the families Pimelodidae and Rhamdiidae (Silurifores). *Genetics and Molecular Biology*, *23*(3), 589–593.

Taylor, W. R., & Van Dyke, G. C. (1985). Revised procedures for staining and clearing small fishes and other vertebrates for bone and cartilage study. *Cybium*, *9*, 107–119.

How to cite this article: Faustino-Fuster, D. R., & de Souza, L. S. (2021). A new species of *Cetopsorhamdia* (Siluriformes: Heptapteridae) from the Upper Amazon River basin. *Journal of Fish Biology*, 1–15. https://doi.org/10.1111/jfb.14914

Two new species of *Pariolius* Cope 1872 (Siluriformes: Heptapteridae) from the Orinoco and Amazon River basin, Colombia

Dario R. Faustino-Fuster[1,2] Jeisson A. López-Castaño[3] Jhonatan M. Quiñones Montiel[3]

[1]Departamento de Ictiología, Museo de Historia Natural, Universidad Nacional Mayor de San Marcos, Av. Arenales 1256, Jesús María, Lima, Perú.

[2]Departamento de Zoologia, Universidade Federal do Rio Grande do Sul, Programa de Pós-Graduação em Biologia Animal, Porto Alegre, Brasil.

[3] Grupo de Investigación en Recursos Hidrobiológicos y Pesqueros GIREPHES, Universidad de los Llanos, vereda Barcelona, Km 4 Vía Puerto López

Correspondence: Dario R. Faustino-Fuster, Departamento de Ictiología, Museo de Historia Natural, Universidad Nacional Mayor de San Marcos, Av. Arenales 1256, Jesús María, Lima, Perú. Email: dariorff36@gmail.com

ABSTRACT

The genus *Pariolius* is monotypic heptapterid genus represented by *P. armillatus* distributed along the upper Amazon River basin. A taxonomic revision of *Pariolius* from Colombian Rivers revealed two new species. A morphological, morphometric, and meristic data were used to distinguished between congeners. Osteological descriptions and counts were conducted from clear and stained specimens and X-rays images. The two new species are distinguished from congeners by the caudal-fin shape and numbers of rays, colorations patterns and several morphometric characters. The two new species of *Pariolius* are restricted from tributaries of the Upper Orinoco and Upper Negro River in Colombia.

Key words: endemic, freshwater, Heptapterini, morphology, taxonomy.

INTRODUCTION

Pariolius is a monotypic genus represented by *Pariolius armillatus* Cope 1872. This species was described within the current Trichomycteridae, but reassigned to Pimelodidae by Gosline in 1940. Mees (1974) considered *Pariolius* Cope 1872 as junior synonym of *Heptapterus* Bleeker 1858 and listed as *Heptapterus armillatus* by Ortega & Vari (1986) and Burgess (1989). After previous studies, *Pariolius* was considered as a valid genera by several authors (Ferraris, 1988; Lundberg et al., 1988; Lundberg et al. 1991; Bockmann, 1994; Bockmann & Guazzelli, 2003; Bockmann & Ferraris, 2005; Ferraris, 2007; Bockmann & Miquelarena, 2008; Bockmann & Castro, 2010; Bockmann & Slobodian, 2017) and assigned within *Nemuroglanis* subclade (Ferraris, 1988; Lundberg et al., 1991; Bockmann, 1994; Bockmann & Ferraris, 2005, Bockmann & Castro 2010). Currently, *Pariolius armillatus* is included in Heptapterini (Silva et al. 2021 and Faustino-Fuster et al. 2021) and mostly restricted to the upper of the Amazon River basin along Brazil, Ecuador, Colombia, and Peru (Fricke et al. 2022).

Previous studies about *Pariolius* were just to compare with others heptapterids (Bockmann & Ferraris, 2005; Bockmann & Miquelarena, 2008; Bockmann & Castro, 2010, Silva et al, 2021) since the original description by Cope (1872). Among heptapterids *Pariolius* Cope 1872 is characterized by the following features: mouth dorsal, posterior portion of the head with unpigmented collar, region anterior to dorsal fin with unpigmented mark, dorsal lobe of caudal fin slightly longer than ventral lobe, (Bockmann & Slobodian, 2017). An ongoing taxonomic study of *Pariolius* from the Orinoco and Amazon River basin in Colombia, reveal two species new to science, and are described herein.

MATERIALS AND METHODS

Measurements were taken with a digital caliper (to 0.01 mm) on the left side of specimens following landmarks proposed by Faustino-Fuster et al. (2019, fig. 1), adding length of dorsal and ventral lobes of caudal fin. Standard length (SL) is given in mm and other measurements were expressed as percentages of standard (SL) or head length (HL) for subunits of the head. Principal Component Analysis (PCA) was used to compare all morphometric variables among species using the software PAST 2.17C (Hammer et al., 2001), the statistical analyses were for all specimens provided in Table 1.

Pectoral, pelvic, dorsal, anal, and caudal fin rays were counted in preserved specimens. Six paratypes were clear and stained (c&s) following Taylor & van Dyke (1985) using ethanol with the alizarin red as were proposed by Springer & Johnson (2000). Pterygiophores, branchiostegal rays, branchial rakers, ribs, and vertebrae were counted in c&s specimens, as well as the insertion of the first fins elements related to vertebral number. Vertebral counts include the five vertebrae of the Weber apparatus and the caudal compound centrum (PU1+U1) counted as one. Osteological nomenclature and laterosensory canals system follows Bockmann & Miquelarena, 2008 and Bockmann & Castro (2010), Carvalho et al, 2013. Institutional codes followed Sabaj (2020).

RESULTS

Pariolius pax new species

Figure 1 a-c, and Table 1, 2.

Holotype

MHNU-I, 3258, 38.8 mm SL, Colombia, Meta, Mapiripán Municipality, vereda San Jorge, Caño Ovejas, tributary of the Guaviare River, 03°5'26.82"N; 72°42'33.14"W, 28 February 2021, J. M. Vásquez-Ramos, M. A. Cortés-Hernández, J. M. Quiñones-Montiel, Y. A. Rojas-Molina, J. A. López-Castaño.

Paratypes

Twelve specimens, all from Colombia, **Orinoco basin**, IAvH-P 11228, 4, 25.8-27.3 mm SL (1C&S), Puerto Gaitán municipality, vereda Alto Neblinas, Finca Unillanos, Caño La Insula, 4°18'59.8"N; 72°03'57.6"W, 5 March 2008, E. Aya-Baquero, Rincón M. Meta: MPUJ 10047, 5 (2 C&S), 26.9−36.7 mm SL, Mapiripán Municipality, Caño Claro, tributary of the Guaviare River, 03°7'5.1"N; 72°30'14.8"W, 16 September 2013, J. E. Zamudio. MPUJ 10048, 3 (1 C&S), 24.5−29.1 mm SL, Mapiripán Municipality, Caño La División, 3°7'26.60"N; 72°32'18.50"W, 17 September 2013, J. E. Zamudio. MPUJ 10790, 2, 36.1−37.0 mm SL, Vista Hermosa municipality, Sardinata River, 3°1'7.10"N; 73°50'27.40"W, 25 January 2014, J. E. Zamudio. MPUJ 11256, 2, 31.8−32.6 mm SL, Mapiripán Municipality, 3°5'19.86"N; 72°35'2.31"W, 6 June 2011, J. E. Zamudio. MHNU-I 3256, 6, 27.2-33.4 mm SL. Same data as holotype. MHNU-I XXX, 5, 17.2-34.8 mm SL, Puerto Gaitán municipality,

11 March 2021. MHNU-I XXXX, 4, 20.8-25.6 mm SL, Puerto Gaitán Municipality, 24 March 2021.

Diagnosis

Pariolius pax is distinguished from all congeners by absent of well-defined white nuchal collar (*vs.* present), absent of white spot anterior to dorsal and adipose-fin origin (*vs.* present), six branched caudal fin rays on dorsal lobe (*vs.* 4−5 in *P. maldonadoi* sp. nov. and five in *P. armillatus*), deeper body (13.3−17.0% SL *vs.* 8.8−13.2% SL), wider head (70.6−73.0% SL *vs.* 64.3−68.3%SL in *P. maldonadoi* and 68.3−69.7% SL in *P. armillatus*), and shorter outer mandibular barbel (66.4−76.9% SL *vs.* 77.5−88.2% SL in *P. maldonadoi* and 83.4−102.4% in *P. armillatus*) deeper head at supraoccipital (48.0−51.5% SL *vs.* 35.7−42.1% SL in *P. maldonadoi* and 37.7−45.1% SL in *P. armillatus*), deeper head at interorbital (34.5−38.8% SL *vs.* 26.3−29.9% SL in *P. maldonadoi* and 23.7−30.3% in *P. armillatus*), and wider head at posterior nostril (60.8−64.7% SL *vs.* 54.2−59.4% SL in *P. maldonadoi* and 53.3−60.3% SL in *P. armillatus*). Additionally, it is further distinguished from *P. maldonadoi* by having shorter caudal fin lobe (20.7−24.0% SL *vs.* 24.4−34.8% SL). It is further distinguished from *P. armillatus* by having shorter preadipose distance (70.2−73.3% SL *vs.* 74.0−76.7% SL), deeper adipose fin (3.1−4.6% SL *vs.* 2.1−2.2% SL), bigger eye (8.5−11.5% SL *vs.* 6.8−7.3% SL), wider internostril distance (9.5−11.5% SL *vs.* 6.3−9.0% SL).

Description

Morphometric data present in Table 1. Body moderately elongated. Cylindrical in cross section at dorsal-fin origin and compressed on caudal peduncle. Dorsal body profile nearly straight from snout tip to supraoccipital, slightly convex from supraoccipital to dorsal-fin origin, straight from dorsal-fin origin to adipose-fin origin, slightly convex from adipose-fin origin to posterior base of adipose-fin, straight from posterior adipose-fin base to caudal-fin origin. Ventral profile of head slightly convex from snout tip to pectoral-fin origin, nearly convex from pectoral-fin origin to pelvic-fin origin, straight descending from pelvic-fin to anal-fin origin, and slightly convex from anal-fin origin to caudal-fin origin. Anus pore localized at level of one third of pelvic fin length, urogenital papilla close to anus pore (approximately eye diameter).

Head small, depressed ascending to supraoccipital, and trapezoidal in dorsal view (Figure 1). Mouth wide and subterminal. Snout short and rounded in dorsal view. Barbels shorts, slender, flatted. Maxillary barbel longest; inserted dorsal to upper lip, lateral and nearly posterior to anterior nostrils; anterior portion extending in superficial groove under anterior- and posterior-nostril region; tip of maxillary barbel surpassing pectoral-fin origin (one third pectoral-fin length). Mental barbels inserted midway between the anterior border of lower jaw and gular fold. Inner mental barbel shorter than outer barbel and inserted approximately posterior to third pore of preoperculomandibular laterosensory canal (pm3); tip of inner mental barbel surpassing the inner margin of branchiostegal membrane. Outer mental barbel inserted posterior to fourth pore of preoperculomandibular laterosensory canal (pm4); tip of outer mental barbel surpassing the pectoral-fin origin. Eye small, elliptical horizontally, slightly dorsal, and anterior to midpoint of head length. Orbital margin not free and pupil rounded. Nostrils arranged as in vertices of squared, anterior internostril distance similar than posterior internostril distance. Anterior nostril tubular, closer to upper lip than

posterior nostril. Posterior nostril closer to anterior margin of eye than anterior nostril, anterior margin with flap.

Pectoral fin rays i + 7 (7), distal margin rounded; unbranched pectoral-fin ray soft and short (0.8−0.9 times length of pectoral-fin ray); second pectoral-fin ray (first branched rays) as long as third ray (second branched ray); last branched rays short and decreasing gradually; tip of pectoral fin not reaching pelvic-fin origin. Pelvic fin rays i + 5 (7), distal margin rounded; unbranched pectoral -fin rays soft and short (0.8 times length of pelvic-fin ray); second pelvic-fin ray (first unbranched ray) shorter than third ray (second branched rays); third pelvic-fin ray (second branched ray) as long as and fourth ray (third branched ray);last two branched rays short and decreasing gradually; pelvic-fin origin anterior to midpoint body (excluding caudal fin) and anterior to vertical through dorsal-fin origin; tip of pelvic fin surpassing the urogenital papilla (one half its length). Insertion of first pelvic-fin ray on basipterygium at vertical through between centra 13−14.

Dorsal fin rays i + 6 (7), distally rounded in lateral profile, unbranched dorsal-fin soft and short (0.7−0.8 times length of longest dorsal-fin rays) followed by six branched rays decreasing gradually in length; dorsal-fin origin anterior to vertical through pelvic-fin origin; First dorsal-fin pterygiophore inserted on bifid neural spine of vertebrae 13 (2). Last dorsal-fin pterygiophore inserted between space of neural spine of vertebrae 15−16 (1) or 16−17 (1). Anal fin rays iv + 7 (1), v + 7 (1), iii + 8 (1), iii +9 (3), v + 9 (1). Anal fin convex and short (0.2 times its standard length). Anal-fin origin anterior to vertical through adipose-fin origin, and last anal-fin ray slightly posterior to half adipose-fin base length. First anal-fin pterygiophore inserted between hemal spines of vertebrae 22−23 (2). Last anal-fin pterygiophore inserted between haemal spines of vertebrae 29−30(1) or 30−31 (1). Anal fin with 11 (1) and 12 (1) pterygiophores. Adipose fin short (0.2 times of standard length),

rectangular and gently convex in lateral profile (Figure 1a); adipose-fin base longer than dorsal to adipose fin distance (1.3−2.1 times its length) and anal-fin base (1.3−1.5 times its length). Adipose-fin origin posterior of anal-fin origin and posteriorly not continuous with dorsal procurrent caudal-fin rays. Insertion of adipose fin at vertical through vertebrae centra 27−28; and terminus of adipose fin at vertebrae 38−39.

Caudal fin gently emarginate with rounded border, dorsal lobe slightly longer than ventral lobe; dorsal caudal lobe with six (15) branched rays; ventral lobe with five (9) or six (6) branched rays. Total caudal-fin rays 40 (2) or 42 (1); with 20 (1) or 21(2) rays on dorsal lobe and 19 (1), 20 (1) or 21(1) rays on ventral lobe. Five hypural series: hi1, hi2, hi3, hi4, and hi5. Ventral caudal plate (hi1 and hi2) free from parhypural, and dorsal caudal plate hi3, hi4 separated from h5 or fused (Figure 2A).

Canals of laterosensory system with simple pores and arrangement according to Figure 3. Supraorbital canal with four branches: s1, s2, s3 and s8; each supraorbital laterosensory opening into a single pore, except branch s2 fused with antorbital branch (s2+i2). Infraorbital canals with six branches: i1, i2, i3, i4, i5 and i6; all opening into its own, except branch i2 fused with s2 opening into a single pore (s2+i2). Preoperculomandibular canal with 11 branches: pm1, pm2, pm3, pm4, pm5, pm6, pm7, pm8, pm9, pm10 and pm11; all opening into its own pore except branch pm11, fused with branch po1 (pm11+po1). Postotic canal with three branch: po1, po2 and po3; all opening into its own pore except branch po1 fused with pm11 opening into a single pore (pm11+po1). Lateral line incomplete, last pore approximately at vertical through the end of anal-fin base.

Total of vertebrae 40 (1) or 41 (2). 14 (2) or 15 (1) vertebrae with incomplete haemal spine on vertebrae. 26 (2) or 27 (1) vertebrae with complete haemal spine. Six (3) pair ribs.

Osteology

Cranial skeleton (Figure 4) not ornamented; dorsal surface straight or slightly convex and without crests; orbital region well defined dorsally; slightly concave and limited by lateral ethmoid anteriorly, frontal laterally, and sphenotic posteriorly; interorbital approximately half its length; two cranial fontanels separated by epiphyseal bar; posterior and anterior fontanels similar width; posterior fontanel longer than anterior in length; anterior and posterior region of anterior fontanel rounded; anterior region of posterior fontanel triangular and posterior region rounded; epiphyseal bar located to midpoint of frontal length. Mesethmoid with dorsal and ventral horizontal plane; anterolateral mesethmoid in dorsal horizontal plane, anterolateral mesethmoid ramus shorter, thicker, and more blunt-tipped than posterolateral mesethmoid, and anterolaterally directed; posterolateral mesethmoid anterolaterally projected forming a conspicuous cornu; region between posterior border of posterolateral mesethmoid and anterior border of lateral ethmoid filled by ethmoidean cartilage. Vomer arrow-shape, posterior portion longer than lateral arms, anterior margin of vomer anterior of posterolateral mesethmoid cornu. Lateral ethmoid slightly quadrangular; posterior and anterior face straight and lateral face concave; posterior portion longer than anterior portion; posterolateral angle more pointed than anterolateral angle. Premaxilla rectangular, size three times its width, anterior margin continuous and without process, posterolateral angle not pronounced; six or seven irregular rows of villiform teeth. Maxilla small and trapezoidal (distal margin longer than proximal margin), distal region forming bony tubule attached to maxillary barbel. Autopalatine rod-like, shorter than orbital region; small cartilages at extremities, anterior cartilage longer than posterior one. Nasal bone poorly ossified, shorter and narrower than autopalatine. Antorbital poorly ossified triangular, and shorter than autopalatine. Frontal smooth and lacking any process; anteriorly limited by lateral ethmoid, posterolaterally limited by sphenotic and posteriorly limited by supraoccipital; posterior portion slightly wider than anterior portion; orbital face straight.

Sphenotic longer and gently narrower than pterotic length; anterior portion with anterior and lateral process. Pterotic shorter and wider than pterotic; anterior and posterior portion with similar width. Supraoccipital limited laterally by posterior portion of sphenoid and the pterotic; supraoccipital process thin and not reaching the anterior region of complex *centra* (in dorsal view).

Complex anterior vertebra (Figure 5A). Composed by vertebrae 1, 2, 3, 4 and 5; vertebrae 1 disc-like element and attached to complex vertebra with tissues ventrally; complex vertebra (vertebrae 2 to 4) attached to vertebra 5 with suture ventrally; neural spine of vertebra 4 not covering neural spine of vertebra 5. Transverse process of vertebra 4 divided in anterior and posterior branches. Anterior branch of transverse process of vertebra 4 wide, laminar, and expanded laterally; proximal portion wider than distal portion. Posterior branch of transverse process of vertebrae 4 arborescent; proximal region wider than distal region; distal region divided in anterior and posterior portion; anterior portion laminar, rectangular, notched and joined to distal region of the posterior portion; posterior portion triangular. Transverse process of vertebra 5 is expanded and not branched.

Suspensory (Figure 6A). Entopterygoid small and slightly triangular; posterior edge concave and attached to anterior margin of metapterygoid. Metapterygoid quadrangular, smooth, and approximately three times entopterygoid size; dorsal margin convex; posteroventral and medial margin of metapterygoid attached with dentate suture and cartilaginous bar to dorsal margin of quadrate; and ventral margin joint with anterodorsal process of quadrate. Quadrate approximately quadrangular and slightly shorter than hyomandibula; anterior and posterior portion separates; anterior margin of quadrate with long anterodorsal process covering ventrolateral margin of metapterygoid; dorsal margin gently

concave along its free dorsal margin; posterior and ventral margin join to hyomandibula with denticulate suture and cartilaginous bar; antero-ventral portion of quadrate with robust quadrangular process to articulate to angulo- retroarticular. Hyomandibula quadrangular; mostly smooth; anterodorsal margin slightly concave; posterodorsal hyomandibular process slightly rectangular with posterior margin gently pointed. Opercle triangular and two times interopercle length; anterior and posterior margins convex, ventral-posterior margin slightly convex, and dorsal margin straight; Interopercle triangular; anterior, posterior, and dorsal margin pointed; ventral margin slightly convex, anterodorsal and posterodorsal region concave.

Branchial arches (Figure 7A). Three basibranchial series: bb2, bb3, and bb4 (basibranchial 1 absent). Basibranchial 2 ante-posteriorly elongate, largely ossified, size is three times bb3 length, anterior portion wider than posterior portion. Basibranchial 4 completely cartilaginous, quadrangular shape; bordered by cartilaginous heads of hb3 anteriorly, cb5 posteriorly and cb4 laterally. Three hypobranchial series: hb1, hb2, hb3. Hypobranchial 1 laterally elongate, largely ossified, size more than three times its greatest width, cartilage in extremities, anterior portion with uncinate process. Hypobranchial 2 slightly elongate, L-shape, anterior portion ossified and posterior portion cartilaginous with similar size. Hypobranchial 3 completely cartilaginous, rectangular, elongate anterolaterally. Five ceratobranchial series: cb1, cb2, cb3, cb4, cb5; fully ossified with cartilage only at their distal and proximal extremities; ceratobranchial 1, 2 and 3 similar size and longer than ceratobranchial 4 and 5. Ceratobranchial 1 to 4 with similar width along its length. Ceratobranchial 5 expanded anteromedially to support patch of conical teeth, teeth with similar size and covering more than two-thirds of cb5 length. Four epibranchial series plus accessory element of ceratobranchial 4: eb1, eb2, eb3, eb4, and aecb4; first four rod-shaped, anteromedial narrower than posterolateral portion; eb1, eb2, eb3 and eb4 mostly ossified;

aecb4 cartilaginous; epibranchial 1 and 2 similar size and longer than epibranchial 3 and 4. Epibranchial 3 with triangular posterior uncinate process close to epibranchial 4. Epibranchial 4 expanded at anterior and posterior portion. Two pharyngobranchial series: pb3 and pb4; pharyngobranchial 1 and 2 absent. Pharyngobranchial 3 rod-like, ossified, anterior portion narrower than posterior portion; posterior margin mostly expanded. Pharyngobranchial 4 ossified; quadrangular and ante-posteriorly elongate.

Color in alcohol

Dorsal and lateral surface of body cream covered by brown marbled melanophores in preserved specimens and rosy light in life specimens (Figure 8A). Ventral surface of head cream. Upper portion of head covered by brown pigment; checks with brown scattered melanophores fading ventrally. Dorsal surface of head between eyes and supraoccipital with dark brown quadrate spot. Very faint cream bar (collar) above pectoral fins contacting each other dorsally. Region between posterior margin of eye and maxillary barbel insertion with dark brown bar. Maxillary barbel pigmented with dark brown dorsally (until one half its length) and ventrally unpigmented. Outer mental barbel pigmented with dark brown dorsally (until one half its length) and ventrally unpigmented. Inner mental barbel unpigmented (some brown melanophores at base). At least seventeen brown chevron-shape lines marking the myosepta, progressively narrower, more angled, and intense posteriorly. Dorsal, anal, caudal, pectoral, and pelvic fins with dispersal brown melanophores along rays and inter-radial membranes devoid of melanophores. Base of caudal fin with dark brown semilunar spot. Base of dorsal and anal fins with concentration of dark brown melanophores. Adipose fin with concentration of brown melanophores (half its height) and distal region unpigmented. Lateral line with dark brown and narrow stripe, nearly convex above pectoral fin and straight along midbody from that point to caudal-fin base and more intense anteriormost (Figure 2), lateral stripe more intense in life (Figure 8A).

Geographic distribution

Pariolius pax is distributed along small creeks tributaries to the Guaviare River and Meta River in the Orinoco River basin, Meta State, Colombia (Figure 9).

Etymology

The specific epithet is given in allusion to the PAX, peace movement from the Netherlands, which since the early nineties has been working to protect human security, prevent armed conflicts and build societies with peace and justice in Colombia. A noun in apposition.

Pariolius maldonadoi **new species**

Figure 10 a-c, Table 1, 2

Holotype

MHNU-I 3257, 32.6 mm SL, Colombia, Guaviare State, Retorno Municipality, Caño Potosí, tributary of the Inírida River, Orinoco River basin, 2°10'50.8"N; 72°38'48.8"W, 27 February 2021, J. M. Vásquez-Ramos, M. A. Cortés-Hernández, J. M. Quiñones-Montiel, Y. A. Rojas-Molina, J. A. López-Castaño.

Paratype

Thirty specimens, **all from Colombia: Amazon River basin:** Guaviare State: MPUJ 13074, 11, 19.3−38.8 mm SL, Calamar Municipality, Caño Bálsamo, tributary of the Unilla River,

Upper Negro River, 1°57'59.0"N; 72°37'16.5"W, 11 January 2017, C. Moreno-Arias. **Orinoco River basin:** Meta State: IAvH-P-16263, 1, 22.5 mm SL, La Macarena Municipality, unnamed creek tributary to El Silencio Lake, Guayabero River, 02°14'57.5"N; 73°45'33.8"W, 28 October 2016, L. Mesa Salazar, C. A. Lasso, P. Herrera. IAvH-P-16293, 1, 26.6 mm SL, La Macarena Municipality, Canoas creek, tributary to Guayabero River, 02°28'29.8"N; 73°44'33.2"W, 31 October 2016, C. A. Lasso, M. Morales-Betancourt, P. Herrera. Guaviare State: MPUJ 13075, 1, 33.5 mm SL, El Retorno Municipality, Caño Platanales, tributary of Inírida river, 2°10'50.81"N; 72°38'48.80"W, 11 January 2011, C. Moreno-Arias. MPUJ 13076, 5, 23.2−35.4 mm SL, El Retorno Municipality, Caño Blanco, tributary of the Inírida river, 2°11'1.72"N; 72°41'26.99"W, 12 January 2017, C. Moreno-Arias. MPUJ 13077, 5, 17.8−27.3 mm SL, El Retorno Municipality, Caño Potosí, tributary of the Inírida river, 2°12'18.40"N; 72°38'14.71"W, 12 January 2017, C. Moreno-Arias. EX-MHNU-I 3257, 6, 20.7-29.9 mm SL, same data as holotype.

Diagnosis

Pariolius maldonadoi is distinguished from all congeners by having six branched pectoral fin rays (*vs.* seven branched rays) and longer dorsal caudal lobe (24.4−34.8 % SL *vs.* 20.7−24.0% in *P. pax* and 18.5−23.1% SL in *P. armillatus*). Additionally, *Pariolius maldonadoi* can be distinguished from *P. pax* by having well-defined white nuchal collar (*vs.* undistinguishable white nuchal collar), white spot anterior to dorsal and adipose-fin origin (*vs.* absent), five branched caudal fin rays on dorsal lobe (*vs.* six branched rays), deeper body (9.5−13.2% SL *vs.* 13.3−17.0% SL), narrow head (64.3−68.3% SL *vs.* 70.6−73.0% SL), longer outer mandibular barbel (77.5−88.2% SL *vs.* 66.4−76.9% SL), deeper head at supraoccipital (35.7−42.1% SL *vs.* 48.0−51.5% SL), deeper head at interorbital (26.3−29.9%

SL *vs.* 34.5−38.8% SL), narrow head at posterior nostril (54.2−59.4% SL). It is further distinguished from *P. armillatus* by having longer adipose fin (22.7−25.1% SL *vs.* 18.2% SL *vs.* 20.7% SL), and shorter snout to anterior nostril distance (7.7−12.0% SL *vs.* 12.8−13.3% SL).

Description

Morphometric data present in Table 1. Body moderately elongated. Cylindrical in cross section at dorsal-fin origin and compressed on caudal peduncle. Dorsal body profile straight from snout tip to supraoccipital, nearly convex from supraoccipital to dorsal-fin origin, straight from dorsal-fin origin to adipose-fin origin, slightly convex from adipose-fin origin to caudal-fin origin. Ventral profile of head gently convex from snout tip to pectoral-fin origin, convex from pectoral-fin origin to pelvic-fin origin, straight from pelvic-fin to anal-fin origin, and from anal-fin origin to caudal-fin origin. Anus pore localized at level of one third of pelvic fin length, urogenital papilla close to anus pore (separated approximately eye diameter).

Head small (0.2−0.3 times of SL), depressed (ascending to supraoccipital), and trapezoidal in dorsal view (Figure 10). Mouth wide and subterminal. Snout short and rounded in dorsal view. Barbels shorts, slender, flatted. Maxillary barbel longest; inserted dorsal to upper lip, lateral and gently posterior to anterior nostrils; anterior portion extending in superficial groove under anterior- and posterior-nostril region; tip of maxillary barbel surpassing pectoral-fin origin (one third pectoral-fin length). Mental barbels inserted midway between the anterior border of lower jaw and gular fold. Inner mental barbel shorter than outer barbel and inserted posterior to third pore of preoperculomandibular laterosensory canal (pm3); tip of inner mental barbel reaching pectoral-fin origin. Outer mental barbel inserted

approximately posterior to midway between fourth and five pore of preoperculomandibular laterosensory canal; tip of outer mental barbel surpassing the pectoral-fin origin. Eye small, elliptical horizontally, slightly dorsal, and anterior to midpoint of head length. Orbital margin not free and pupil rounded. Nostrils arranged as in vertices of squared, anterior internostril distance similar than posterior internostril distance. Anterior nostril tubular, closer to upper lip than posterior nostril. Posterior nostril closer to anterior margin of eye than anterior nostril, anterior margin with flap.

Pectoral fin rays i +6 (9), distal margin rounded; unbranched pectoral-fin ray soft and short (0.8−0.9 times length of pectoral-fin ray); second pectoral-fin ray (first branched rays) as long as third ray (second branched ray); last branched rays short and decreasing gradually; tip of pectoral fin behind vertical through pelvic-fin origin. Pelvic fin rays i + 5 (9), distal margin rounded; unbranched pectoral -fin rays soft and short (0.7 times length of pelvic-fin ray); second pelvic-fin ray (first unbranched ray) shorter than third ray (second branched rays); third pelvic-fin ray (second branched ray) as long as and fourth ray (third branched ray);last two branched rays short and decreasing gradually; pelvic-fin origin anterior to midpoint body (excluding caudal fin) and anterior to vertical through dorsal-fin origin; tip of pelvic fin surpassing the urogenital papilla (one half its length). Insertion of first pelvic-fin ray on basipterygium at vertical through between centra 13−14.

Dorsal fin rays i + 6 (9), distally rounded in lateral profile, unbranched dorsal-fin soft and short (0.8−.96 times length of longest dorsal-fin rays) followed by six branched rays; dorsal-fin origin anterior to vertical through pelvic-fin origin; First dorsal-fin pterygiophore inserted on bifid neural spine of vertebrae 13 (2). Last dorsal-fin pterygiophore inserted between space of neural spine of vertebrae 16−17 (2) or 17−18 (1). Anal fin rays iv + 7 (1), iii + 8 (2), iv +8 (4), v + 8 (2). Anal fin convex and short (0.1−0.2 times its standard). Anal-

fin origin anterior to vertical through adipose-fin origin, and last anal-fin ray slightly anterior to half adipose-fin base length. First anal-fin pterygiophore inserted between hemal spines of vertebrae 24−25 (3). Last anal-fin pterygiophore inserted between haemal spines of vertebrae 31−32(3). Anal fin with 12 (2) pterygiophores. Adipose fin short (0.2−0.25 times its standard length), rectangular and slightly convex in lateral profile (Figure 1a); adipose-fin base longer than dorsal to adipose fin distance (1.1−1.5 times its length) and anal-fin base (1.2−1.6 times its length). Adipose-fin origin posterior of anal-fin origin and terminus not continuous with dorsal procurrent caudal-fin rays. Insertion of adipose fin at vertical through vertebrae centra 28−29 (2); and terminus of adipose fin at vertebrae 39−40 (2). Caudal fin gently emarginate, dorsal lobe longer and pointed than ventral lobe; dorsal caudal lobe with rarely four (2) or usually with five (12) branched rays; ventral lobe with rarely four (4) or usually five (10) branched rays. Total caudal-fin rays 36 (2) or 37 (1); with 18 (2) or 19 (1) rays on dorsal lobe and 18 (3) rays on ventral lobe (Figure 2B).

Canals of laterosensory system with simple pores and arrangement according to Figure 11. Supraorbital canal with four branches: s1, s2, s3 and s8; each supraorbital laterosensory opening into a single pore, except branch s2 fused with antorbital branch (s2+i2). Infraorbital canals with six branches: i1, i2, i3, i4, i5 and i6; all opening into its own, except branch i2 fused with s2 opening into a single pore (s2+i2). Preoperculomandibular canal with 11 branches: pm1, pm2, pm3, pm4, pm5, pm6, pm7, pm8, pm9, pm10 and pm11; all opening into its own pore except branch pm11, fused with branch po1 (pm11+po1). Postotic canal with three branches: po1, po2 and po3; all opening into its own pore except branch po1 fused with pm11 opening into a single pore (pm11+po1). Lateral line incomplete, last pore approximately at vertical through end of dorsal-fin base.

Total of vertebrae 41 (1) or 41 (2). 14 (1) or 15 (1) vertebrae with incomplete haemal spine. 27 (1) or 28 (2) vertebrae with complete haemal spine. Six (3) pair ribs.

Osteology

Cranial skeleton (Figure 12) not ornamented; dorsal surface straight or slightly convex and without crests; orbital region well defined dorsally; slightly concave and limited by lateral ethmoid anteriorly, frontal laterally, and sphenotic posteriorly; interorbital region similar its length; two cranial fontanels separated by epiphyseal bar; anterior fontanel wider than anterior one; posterior fontanel longer than anterior in length; anterior and posterior edge of anterior fontanel slightly rounded; anterior region of posterior fontanel triangular and posterior region rounded; epiphyseal bar located to anterior to midpoint of frontal length. Mesethmoid with dorsal and ventral horizontal plane; anterolateral mesethmoid in dorsal horizontal plane, anterolateral mesethmoid ramus shorter, narrower, and more blunt-tipped than posterolateral mesethmoid, and anterolaterally directed; posterolateral mesethmoid anterolaterally projected forming a conspicuous cornu. Vomer arrow-shape, posterior portion longer than lateral arms, anterior margin of vomer at same level of posterolateral mesethmoid cornu. Lateral ethmoid slightly quadrangular; posterior and anterior face straight and lateral face concave; posterior portion longer than anterior portion; posterolateral angle more pointed than anterolateral angle. Premaxilla rectangular, size three times its width, anterior margin continuous and without process, posterolateral angle not pronounced; five or six rows of villiform teeth on premaxilla. Maxilla small and trapezoidal (distal margin longer than proximal margin), distal region forming bony tubule attached to maxillary barbel. Autopalatine rod-like, shorter than orbital region. Nasal bone poorly ossified, and shorter and narrower than autopalatine. Antorbital poorly ossified

triangular, and shorter than autopalatine. Frontal smooth and lacking any process; anteriorly limited by lateral ethmoid, posterolaterally limited by sphenotic and posteriorly limited by supraoccipital; posterior portion slightly wider than anterior portion; orbital face straight. Sphenotic longer and gently narrower than pterotic length; anterior portion with anterior and lateral process. Pterotic shorter and wider than pterotic; anterior and posterior portion with similar width. Supraoccipital limited laterally by posterior portion of sphenoid and the pterotic; supraoccipital process thin and not reaching the anterior region of complex *centra* (in dorsal view).

Complex anterior vertebra (Figure 5B). Composed by vertebrae 1, 2, 3, 4 and 5; vertebrae 1 disc-like element and attached to complex vertebra with tissues ventrally; complex vertebra (vertebrae 2 to 4) attached to vertebra 5 with suture ventrally; neural spine of vertebra 4 not covering neural spine of vertebra 5. Transverse process of vertebra 4 divided in anterior and posterior branches. Anterior branch of transverse process of vertebra 4 wide, laminar, and expanded laterally; proximal portion wider than distal portion. Posterior branch of transverse process of vertebrae 4 arborescent; proximal region wider than distal region; distal region divided in anterior and posterior portion; anterior portion laminar, rectangular, notched and joined to distal region of the posterior portion; posterior portion triangular. Transverse process of vertebra 5 is expanded and not branched.

Suspensory (Figure 6B). Entopterygoid small and rectangular; posterior edge concave and attached to anterior margin of metapterygoid. Metapterygoid rectangular, smooth, and approximately three times entopterygoid size; dorsal margin convex; posteroventral and medial margin of metapterygoid attached with dentate suture and cartilaginous bar to dorsal margin of quadrate; posterodorsal margin joint with dentate suture to anterodorsal margin of hyomandibula and ventral margin joint with anterodorsal process of quadrate. Quadrate approximately rectangular and similar size than hyomandibula; anterior and posterior portion

separates; anterior margin of quadrate with long and strong anterodorsal process covering ventrolateral margin of metapterygoid; dorsal margin straight along its free dorsal margin; posterior and ventral margin join to hyomandibula with denticulate suture and cartilaginous bar; dorsal margin joint to posterodorsal margin of metapterygoid and anteroventral margin of hyomandibula; anteroventral portion of quadrate with rectangular process to articulate to angulo- retroarticular. Hyomandibula quadrangular; mostly smooth; anterodorsal margin slightly concave; posterodorsal hyomandibular process triangular with posterior margin very pointed. Opercle triangular and less than two times interopercle size; anterior and posterior margins rounded, ventral margin slightly convex, posterior and dorsal margin slightly concave. Interopercle triangular; anterior, posterior, and dorsal margin pointed; ventral margin convex, anterodorsal straight and posterodorsal margin concave.

Branchial arches (Figure 7B). Three basibranchial series: bb2, bb3, and bb4 (basibranchial 1 absent). Basibranchial 2 ante-posteriorly elongate, largely ossified, anterior portion wider than posterior, size is three times bigger than bb3 length, anterior portion wider than posterior portion. Basibranchial 3, completely cartilaginous, size two times its anterior width size, anterior portion wider than posterior region. Basibranchial 4 completely cartilaginous, rectangular shape; bordered by cartilaginous heads of hb3 anteriorly, cb5 posteriorly and cb4 laterally. Three hypobranchial series: hb1, hb2, hb3. Hypobranchial 1 laterally elongate, largely ossified, size three times its greatest width, cartilage just in proximal and distal extremities, anterior portion with uncinate process. Hypobranchial 2 slightly elongate, L-shape, anterior portion ossified and posterior portion cartilaginous with two times ossified size. Hypobranchial 3 completely cartilaginous, triangular, elongate laterally. Five ceratobranchial series: cb1, cb2, cb3, cb4, cb5; fully ossified with cartilage at their extremities; ceratobranchial 1, 2 and 3 similar size and longer than ceratobranchial 4 and 5. Ceratobranchial 1 to 4 with similar width along its length. Ceratobranchial 5 expanded

anteromedially to support patch of conical teeth, teeth with similar size and covering one-half of cb5 length. Four epibranchial series plus accessory element of ceratobranchial 4: eb1, eb2, eb3, eb4, and plus accessory element of ceratobranchial 4; first four epibranchials rod-shaped, anteromedial narrower than posterolateral portion; eb1, eb2, eb3 and eb4 mostly ossified; aecb4 cartilaginous; epibranchial 1 and 2 similar size and longer than epibranchial 3 and 4. Epibranchial 3 with rectangular posterior uncinate process. Epibranchial 4 expanded at anterior and posterior portion. Two pharyngobranchial series: pb3 and pb4; pharyngobranchial 1 and 2 absent. Pharyngobranchial 3 rod-like, ossified, anterior portion narrower than posterior portion; posterior margin mostly expanded. Pharyngobranchial 4 ossified; rectangular and ante-posteriorly elongate.

Colour in alcohol

Dorsal and lateral surface of body dark brown (Figure 9) and dark grey in life (Figure 8B). Ventral body surface cream. Upper portion of head covered by brown pigment, surface between posterior eye margins and supraoccipital more intense; checks with brown melanophores fading ventrally. Cream bar (collar) above pectoral fins contacting each other dorsally. Region between posterior margin of eye and maxillary barbel insertion with dark brown bar. Maxillary barbel pigmented with dark brown dorsally (one half its length) and ventrally unpigmented. Outer mental barbel pigmented with dark brown dorsally (until one third its length) and ventrally unpigmented. Inner mental barbel unpigmented (some brown melanophores at base). At least twenty four brown chevron-shape lines marking the myosepta at the posterior region of the body, progressively narrower, more angled, and intense posteriorly. Dorsal-, anal-, pectoral-, and pelvic-fin with some dispersal brown (preserved) and grey (life) melanophores along rays and inter-radial membranes devoid of melanophores.

Caudal- and adipose-fin with marbled. Caudal-fin base with triangular spot dark brown (preserved) and dark grey (life). Lateral line with dark brown and narrow stripe; nearly convex above pectoral fin and straight along midbody from that point to caudal-fin base and more intense anteriormost.

Geographic distribution

Pariolius maldonadoi is distributed along small creeks tributaries to Inírida River and Guayabero River in the Orinoco River basin, Meta State and Vaupes River in the Rio Negro basin, Guaviare State, Colombia (Figure 9).

Etymology

The specific name in honour of the authors' colleague and friend *in memoriam* to Javier Maldonado-Ocampo, professor of the Pontificia Universidad Javeriana in Bogotá, Colombia for his great contribution and devotions to the Colombian and Neotropical Ichthyology. A noun in apposition.

Identification key of *Pariolius*

1A. Body of color light brown; caudal-fin base with a triangular dark brown spot; indistinguishable white nuchal collar; head wide, 70.6−73.0 % of HL; head depth, 48.0−51.5 % of HL. *P. pax* sp. nov.

1B. Body of color dark brown; caudal-fin base with a semilunar dark brown spot; well-defined white nuchal collar; head narrow, 64.3−69.7% of SL; head depth, 35.7−45.1 % of HL. **2**

2A. Six branched rays in pectoral fin; dorsal caudal-fin lobe longest, 24.4−42.6% of SL; subterminal mouth, upper jaw longer than lower jaw; long adipose-fin base, 22.7−25.1 % of SL. *P. maldonadoi* sp. nov**.**

2B. Seven branched rays in pectoral fin; dorsal caudal-fin lobe shortest, 18.5−23.1% of SL; upper mouth, lower jaw longer than upper jaw; short adipose-fin base, 18.2−21.0 % of SL.*P. armillatus*

DISCUSSION

Bockmann & Slobodian, 2017 propose some features to distinguished *Pariolius* from all Heptapteridae (see above), according to our analysis and inclusion of the new species we found most of them no exclusive to *Pariolius*. Posterior portion of the head with unpigmented collar and region anterior to dorsal fin with unpigmented mark; those feature is present in most species of *Cetopsorhamdia,* and *Chasmocranus* too. Dorsal lobe of caudal fin slightly longer than ventral lobe, most of Heptapterinae have this character. Mouth dorsal, present in *Phenacorhamdia* too.

The most recent phylogenetic study which include *Pariolius* was done by Silva et al. (2021). The previous study found *Pariolius* sister to *Phenacorhamdia*, and all previous species sister to *Cetopsorhamdia* species.

Based on previous studies and our result *Pariolius* is distinguished from all Heptapterini genera by having the apomorphic character, distal region of anterior and the

posterior portion of posterior branch of trp4 joined (Figure 5 A-B) and absent. Additionally, it can be distinguished from its sister genera *Phenacorhamdia* and *Cetopsorhamdia* by having the dorsal caudal-fin lobe longer than ventral lobe.

Principal component analysis (PCA) corroborates the morphometric differences between *Pariolius* species (Figure 13). The most significant measurement to distinguish those species are body width, head width, and head depth (Table 1).

Pariolius armillatus is widely distributed along Upper Amazon River basin in Brazil, Colombia, Ecuador, and Peru (Ortega & Vari 1986; Bockmann & Guazzelli 2003; Ferraris 2007; Barriga Salazar 2014; Donascimiento et al. 2017). Despite several ichthyological expeditions being carried out along the main rivers of the Colombian River and well recorded Heptapteridae species in literature (Donascimiento et al, 2017); *Pariolius pax* was found only small creeks tributaries of the upper Orinoco River basin; while *P. maldonadoi* was found in small creeks tributaries of the Upper Orinoco and Negro Rivers; thus, making the two new species very restricted to these two Colombian basins.

Comparative Material Examined

In addition to the comparative material listed by Faustino-Fuster et al. (2019), Faustino-Fuster & Ortega (2020) and Faustino-Fuster & de Souza (2021) the following lots were examined:

Pariolius armillatus Cope, 1872: **Colombia:** *Amazonas State*: IAvH-P 08680, 3, 27.1-27.8 mm SL, Tucuchira creek, Leticia. IAvH-P 08935, 1, 32.3 mm SL, Sufragio creek, Leticia. IAvH-P 09003, 3, 30.3-31.4 mm SL, Sufragio creek, Leticia. IAvH-P 09087, 1, 30.5 mm SL,

Unnamed creek tributary to Calderón, Leticia. IAvH-P 09113, 1, 32.0 mm SL, unnamed creek tributary to Calderón, Leticia. IAvH-P 09389, 1, 28.5 mm SL, unnamed creek tributary to Purité River, Leticia. IAvH-P 09433, 1, 21.8 mm SL, unnamed creek tributary to Purité River, Leticia. MPUJ 3460, 1, 24.5 mm SL, Leticia. **Peru**: Loreto State: FMNH 139554, 1, 29.2 mm SL, Maynas. FMNH 140844, 1, 32.1 mm SL, Putumayo. FMNH 140850, 1, 27.8 mm SL, Putumayo. FMNH 142189, 2, 26.7-29.3 mm SL, Putumayo. FMNH 142297, 1, 30.2 mm SL, Putumayo. MCP 35607, 1, 21.7 mm SL, Parnayari creek, Jenaro Herrera. MCP 37408, 3, 12.3-27.2 mm SL, Chica creek, Jenaro Herrera. MCP 37496, 4, 14.2-28.9 mm SL, unnamed creek tributary to Parnayari cree, Jenaro Herrera. USNM 176001, 1, 31.3 mm SL, Peru, Mariscal Ramon Castilla, Pebas, Shansho Caño tributary to Río Amazon.

Pariolius cf. *armillatus*: All from Ecuador: All from Napo: FMNH 98303, 1, 26.5 mm SL, Sucumbios. FMNH 98304, 5, 14.9-39.6 mm SL, Sucumbios. FMNH 103238, 5, 27.1-36.5 mm SL, Sucumbios. FMNH 103237, 3, 13.1-20.5 mm SL, Sucumbios. FMNH 103239, 1, 19.4 mm SL, Palma Roja. FMNH 103240, 1, 24.1 mm SL, Palma Roja. FMNH 103241, 2, 25.2-26.7 mm SL, Orellana, San Sebastian del Coca. FMNH 103242, 9, 17.9-34.2 mm SL, Sucumbios, Palma Roja.

Pariolius sp: **All from Ecuador: Napo State:** ANSP 130595, 3, 24.1-34.2 mm SL, unnamed stream tributary to Conejo River, Santa Cecilia. ANSP 130596, 6, 16.0-35.8 mm SL, unnamed stream tributary to Aguarico River, Santa Cecilia. ANSP 130597, 3, 20.5-31.2 mm SL, unnamed stream tributary to Aguarico River, Santa Cecilia. ANSP 130598, 3, 33.5-35.1 mm SL, effluent to unnamed Lake, Santa Cecilia. ANSP 170611, 1, 34.4 mm SL, unnamed stream tributary to Aguarico River, Santa Cecilia. **All from Peru: Loreto:** FMNH 142750, 5,

28.5-44.4 mm SL, Contamana. FMNH 142855, 1, 32.8 mm SL, Yaquerana. FMNH 142905, 5, 31.2-37.1 mm SL, Contamana. FMNH 142912, 3, 30.7-40.2 mm SL, Contamana. FMNH 142916, 2, 36.8-38.2 mm SL, Contamana. FMNH 142925, 3, 37.1-41.1 mm SL, Contamana. FMNH 142986, 1, 39.2 mm SL, Contamana. FMNH 142988, 2, 36.0-37.7 mm SL, Contamana. FMNH 143087, 2, 19.4-24.9 mm SL, Contamana.

Acknowledgements

We give special thanks to Mariangeles Arce and Mark Sabaj (ANSP); Caleb McMahan, Kevin Swagel and Susan Mochel (FMNH); Carlos Donacimento (IAvH); José I. Mojica (ICNMHN); Carlos Lucena, (MCP); Miguel A. Cortés-Hernández (MHNU); Hernán Ortega, Max Hidalgo, and Carla Muñoz (MUSM); and Lynne Parenti, Jeff Clayton and Sandra Raredon (USNM) for curatorial assistance during their visit to these fish collections. Special thanks to Kevin Swagel (FMNH) and Sanda Raredon (USNM) for assistance with the X-ray images. The first author was supported by a doctoral programme provided by Ministry of Education of Brazil (CAPES). Additional financial support was received from Böhlke Award from the Academy of Natural Science of Drexel University, Philadelphia; Smithsonian Visiting Student (Fellowship) at the National Museum of Natural History (NMNH), Washington; and funding from the Grainger Bioinformatics Center at the Field Museum of Natural History, Chicago. Systematics Research Fund and the Society of Systematic Biologists Found for field work support.

References

Barriga Salazar, R. E. 2014. Lista de peces de agua dulce e intermareales del Ecuador. Revista Politécnica v. 30 (no. 3) (for Sept. 2012): 83-119.

Bockmann, F. A. 1994. Description of *Mastiglanis asopos*, a new pimelodid catfish from northern Brazil, with comments on phylogenetic relationships inside the subfamily Rhamdiinae (Siluriformes: Pimelodidae). Proceedings of the Biological Society of Washington 107: 760–777.

Bockmann, F. A., & Ferraris Jr, C. J. 2005. Systematics of the Neotropical catfish genera Nemuroglanis Eigenmann and Eigenmann 1889, Imparales Schultz 1944, and Medemichthys Dahl 1961 (Siluriformes: Heptapteridae). Copeia, 124-137.

Bockmann, F. A., and G. M. Guazzelli. 2003. Family Heptapteridae (Heptapterids), p. 406–431. In *Check List of the Freshwater Fishes of South and Central America*. Reis, R. E., S. O. Kullander, and C. J. Jr. Ferraris (eds.). Porto Alegre: Editora da Pontifícia Universidade Católica do Rio Grande do Sul-EDIPUCRS.

Bockmann, F. A., and A. M. Miquelarena. 2008. Anatomy and phylogenetic relationships of a new catfish species from northeastern Argentina with comments on the phylogenetic relationships of the genus *Rhamdella* Eigenmann and Eigenmann 1888 (Siluriformes, Heptapteridae). Zootaxa, 1780(1): 1–54.

Bockmann, F. A., and R. Castro. 2010. The blind catfish from the caves of Chapada Diamantina, Bahia, Brazil (Siluriformes: Heptapteridae): description, anatomy, phylogenetic relationships, natural history, and biogeography. Neotropical Ichthyology, 8(4), 673–706.

Bockmann, F. A., and V. Slobodian. 2017. Family Heptapteridae – three-barbeled catfishes, p. 233–252. In *Field Guide to the Fishes of the Amazon, Orinoco and Guianas*. van der Sleen, P., and J. S. Albert (eds.). Princeton: Princeton University Press.

Burgess, W. E. 1989. An atlas of freshwater and marine catfishes. A preliminary survey of the Siluriformes. TFH Publication, Neptune City, Canada, 28, 305-325.

Carvalho, M., Bockmann, F. A., & de Carvalho, M. R. 2013. Homology of the fifth epibranchial and accessory elements of the ceratobranchials among Gnathostomes: insights from the development of ostariophysans. *PloS One*, *8*(4), e62389.

Cope, E. D. 1871. On the fishes of the Ambyiacu River. Proceedings of the Academy of Natural Sciences of Philadelphia, 250-294.

DoNascimiento, C., Herrera-Collazos, E. E., Herrera-R, G. A., Ortega-Lara, A., Villa-Navarro, F. A., Oviedo, J. S. U., & Maldonado-Ocampo, J. A. 2017. Checklist of the freshwater fishes of Colombia: a Darwin Core alternative to the updating problem. ZooKeys, (708), 25.

Faustino-Fuster, D. R., F. A. Bockmann, and L. R. Malabarba. 2019. Two new species of *Heptapterus* (Siluriformes: Heptapteridae) from the Uruguay River basin, Brazil. Journal of fish biology 94(3): 352–373.

Faustino-Fuster, D. R., and H. Ortega. 2020. A new species of *Mastiglanis* Bockmann 1994 (Siluriformes: Heptapteridae) from the Amazon River basin, Peru. Zootaxa, 4820(2), zootaxa-4820.

Faustino-Fuster, D. R., Meza-Vargas, V., Lovejoy, N. R., and N. K. Lujan. 2021. Multi-locus phylogeny with dense Guiana Shield sampling supports new suprageneric classification of the Neotropical three-barbeled catfishes (Siluriformes: Heptapteridae). Molecular Phylogenetics and Evolution, 162, 107186.

Faustino-Fuster, D. R., and L. S. de Souza. 2022. A new species of *Cetopsorhamdia* (Siluriformes: Heptapteridae) from the Upper Amazon River basin. Journal of fish biology, 100(1), 25–39.

Ferraris, C. J. Jr. 1988. Relationships of the neotropical catfish genus *Nemuroglanis*, with a description of a new species (Osteichthyes: Siluriformes: Pimelodidae). Proceedings of the Biological Society of Washington 101: 509–516.

Ferraris, C. J. 2007. Checklist of catfishes, recent and fossil (Osteichthyes: Siluriformes), and catalogue of siluriform primary types. Zootaxa, 1418(1), 1-628.

Fricke, R., W. N. Eschmeyer, and R. Van der Laan. (eds.). 2022. Eschmeyer's catalog of fishes: genera, species, references. http://researcharchive.calacademy.org/research/ichthyology/catalog/fishcatmain.asp. Electronic version accessed 06 Apr 2020.

Gosline, W. A. 1940. Rediscovery and redescription of Pariolius armillatus, a genus and species of pimelodid catfishes described by ED Cope from the Peruvian Amazon in 1872. Copeia, 1940(2), 78-80.

Hammer, O., D. A. Harper, and P. D. Ryan. 2001. PAST: Paleontological statistics software package for education and data analysis. Palaeontologia electronica 4(1): 1–9.

Lundberg, J. G., Linares, O. J., Antonio, M. E., & Nass, P. 1988. Phractocephalus hemiliopterus (Pimelodidae, Siluriformes) from the upper Miocene Urumaco Formation, Venezuela: a further case of evolutionary stasis and local extinction among South American fishes. Journal of Vertebrate Paleontology, 8(2), 131-138.

Lundberg, J. G., A. H. Bornbusch, and F. Mago-Leccia. 1991. *Gladioglanis conquistador* n. sp., from Ecuador with diagnoses of the subfamilies Rhamdiinae Bleeker and Pseudopimelodinae n. subf. (Siluriformes, Pimelodidae). Copeia 1991: 190–209.

Mees, G. F. 1974. The Auchenipteridae and Pimelodidae of Suriname (Pisces, Nematognathi). Zoologische Verhandelingen (Leiden) No. 132: 1-256, Pls. 1-15.

Ortega, H. and R. P. Vari. 1986. Annotated checklist of the freshwater fishes of Peru. Smithsonian Contributions to Zoology No. 437: iii + 25 p.

Sabaj, M. H. 2020. Codes for Natural History Collections in Ichthyology and Herpetology. Copeia 108: 593–669.

Silva, G. S., Roxo, F. F., Melo, B. F., Ochoa, L. E., Bockmann, F. A., Sabaj, M. H., Jerep, F. C., Foresti F., Benine, R. C., and C. Oliveira. 2021. Evolutionary history of Heptapteridae catfishes using ultraconserved elements (Teleostei, Siluriformes). Zoologica Scripta, 50(5), 543–554.

Springer, V. G., & David Johnson, G. 2000. Use and advantages of ethanol solution of alizarin red S dye for staining bone in fishes. Copeia, 2000(1), 300-301.

Taylor, W. R., and G. C. Van Dyke. 1985. Revised procedures for staining and clearing small fishes and other vertebrates for bone and cartilage study. Cybium 9: 107–119.

Tables

Table 1. Morphometric data of *Pariolius* species. H (Holotype); Min (minimum); Max (maximum); SD (standard deviation); n= individuals; LM (landmarks).

	Pariolius pax **new species**						***Pariolius maldonadoi*** **new species**					
	H	n	Min	Max	Mean	SD	H	n	Min	Max	Mean	SD
Standard length (mm)	38.8	14	26.9	39.7	32.1	-	34.2	16	17.8	38.8	27.8	-
Percent of Standard Length												
Predorsal distance	45.4	14	44.1	48.6	46.1	1.3	44.1	16	42.2	46.0	44.2	1.0
Preadipose distance	71.8	14	70.2	73.3	71.4	0.9	73.1	16	70.8	74.4	72.7	0.8
Prepectoral distance	21.4	14	19.2	24.8	22.9	1.4	21.9	16	19.6	26.2	23.0	1.6
Prepelvic distance	41.0	14	40.7	44.8	42.6	1.3	41.6	16	36.7	42.4	40.5	1.5
Preanal distance	69.1	14	64.1	69.1	67.3	1.3	67.6	16	61.8	70.1	67.2	1.8
Body depth	13.5	14	13.3	17.0	14.2	1.0	12.2	16	9.5	13.2	11.6	0.9
Caudal peduncle depth	9.8	14	8.5	10.1	9.4	0.5	8.7	16	7.6	9.0	8.4	0.4
Caudal peduncle length	15.6	14	13.2	16.3	14.9	0.9	16.6	16	14.3	17.2	15.6	0.8
Body width	17.1	14	15.9	18.9	17.5	0.8	15.8	16	13.7	17.9	16.3	1.0
Dorsal-fin base length	10.6	14	10.3	12.8	11.4	0.7	12.2	16	11.0	12.4	11.6	0.4
Anal-fin base length	18.1	14	16.9	18.7	18.2	0.4	18.1	16	14.7	20.8	18.1	1.3
Unbranched dorsal-fin ray length	9.9	14	9.3	13.6	12.2	1.5	12.0	16	9.2	14.1	12.8	1.2
Dorsal-fin length	15.6	14	14.3	16.6	15.4	0.7	15.5	16	11.8	18.0	15.3	1.3

Adipose-fin depth	3.1	14	3.1	4.6	3.8	0.5	3.4	16	1.9	4.7	3.2	0.8
Adipose-fin base length	23.6	14	22.1	25.1	23.8	0.8	23.7	15	22.7	25.1	24.0	0.7
Interdorsal distance	17.1	14	12.4	18.0	15.7	1.6	17.2	16	16.7	18.5	17.4	0.5
Unbranched pectoral-fin ray length	11.9	14	10.3	14.0	12.0	1.0	13.4	16	9.8	13.8	12.9	0.9
Pectoral-fin length	15.6	14	13.0	15.9	14.7	0.8	14.1	16	11.4	16.5	15.2	1.2
Pelvic-fin length	13.4	14	12.5	16.2	14.2	1.1	14.5	16	13.9	17.0	15.1	1.0
Pectoral-pelvic fins distance	20.6	14	20.6	24.6	22.0	1.3	20.6	16	17.3	23.0	20.0	1.2
Pelvic-anal fins distance	25.5	14	24.3	26.3	25.2	0.6	27.1	16	26.0	28.1	27.1	0.7
Dorsal-fin insertion-hypural plate	55.8	14	53.5	58.3	55.8	1.0	56.8	16	55.1	58.9	56.7	1.0
Pelvic-fin insertion-hypural plate	60.2	14	57.4	60.2	58.9	0.8	60.4	16	58.1	62.6	60.8	1.1
Anal-fin insertion-hypural plate	33.2	14	32.7	35.0	33.8	0.8	34.2	16	31.9	36.1	33.5	1.2
Ventral caudal-fin lobe length	18.3	14	17.4	21.2	19.7	1.1	18.0	16	18.0	25.8	22.5	1.8
Dorsal caudal-fin lobe length	45.4	14	20.7	25.7	23.0	1.2	30.0	14	24.4	42.6	29.6	4.2
Head length	71.8	14	22.5	26.1	24.8	1.0	23.0	16	21.7	26.7	24.0	1.2
Percent of Head Length												
Snout length	21.9	14	32.9	37.2	35.0	1.4	33.8	9	31.4	37.8	35.3	2.1
Orbital diameter	22.5	14	8.5	11.5	9.9	0.8	10.2	9	3.7	12.0	10.6	1.9
Head width	33.2	14	70.6	73.0	71.8	0.7	68.1	9	64.3	68.3	66.3	1.2
Mouth width	10.0	14	45.4	50.9	46.8	1.5	47.3	9	44.3	47.7	46.0	1.1
Mandibular isthmus-lower lip distance	72.0	14	18.7	26.2	22.4	2.0	22.0	9	20.6	28.6	22.9	1.9

Mandibular isthmus-upper lip distance	46.0	14	22.7	27.0	24.5	1.2	23.0	9	21.4	32.6	24.5	2.5
Maxillary barbel length	23.9	14	83.5	104.9	94.2	7.7	102.9	9	91.9	119.4	107.8	6.5
External mandibular barbel length	25.9	14	66.4	79.0	74.3	3.4	83.4	9	77.5	88.2	82.7	3.4
Internal mandibular barbel length	93.7	14	55.7	62.0	59.3	1.8	60.2	9	55.4	66.3	59.3	3.4
Postorbital distance	74.9	14	56.9	60.4	58.5	1.1	56.0	9	55.3	59.7	56.9	1.2
Interorbital width	59.5	14	23.4	26.3	25.2	0.8	25.5	9	20.1	27.7	24.0	1.8
Snout-anterior nostril distance	57.8	14	8.9	12.9	10.5	1.1	12.9	9	7.7	12.9	10.7	1.3
Internostril distance	25.9	14	9.5	11.5	10.5	0.6	10.7	9	6.6	10.7	9.1	1.0
Posterior nostril-orbit distance	11.0	14	4.3	7.0	6.1	0.7	7.5	9	4.4	9.6	7.5	1.5
Head depth at supra occipital	11.1	14	48.0	51.5	49.4	1.2	40.5	9	35.7	41.6	38.9	1.7
Head depth at interorbital	5.8	14	34.5	38.8	37.2	1.3	28.6	9	26.3	29.9	28.2	1.1
Head width at posterior nostril	49.9	14	60.8	64.7	62.3	1.0	58.2	9	54.2	59.4	57.5	1.4
Dorsal head length	38.1	14	83.7	87.9	85.5	1.1	87.2	9	85.4	90.9	87.7	1.4

Figures Captions

Figure 1. *Pariolius pax*, new species, MHNU-I, 3258, holotype, 38.8 mm SL, Ovejas creek tributary to Guaviare River, Meta State. (A) Lateral view. (B) Dorsal view. (C) Ventral view. Bar = 1 cm.

Figure 2. Lateral view of the caudal skeleton of (A) *Pariolius pax*, MPUJ 10047, paratype, 34.0 mm SL (B) *Pariolius maldonadoi*, MPUJ 13076, paratype, 28.4 mm SL. Abbreviations of the anatomical parts: ep = epural; hi1 + hi2 = complex plate formed by hypurals 1 and 2; hi3+hi4 = complex plate formed by hypurals 3, 4; hi5 = hypural 5; ph = parhypural; pu1 + u1 = complex centrum formed by preural centrum 1 and ural centrum 1; pu2 = preural centrum 2; ur = uroneural.

Figure 3. Laterosensory pores of *Pariolius pax* MPUJ 10047, paratype, 34.0 mm SL. (A) Lateral view. (B) Dorsal view. (C) Ventral view. Abbreviations of the anatomical parts: i1 = infraorbital sensory pore 1; i3-6 = infraorbital sensory pores 3–6; ll1-3 = lateral line sensory pores 1–3; pm1–10 = preoperculomandibular sensory pores 1–10; po1 + pm11 = postotic sensory pore 1 + preoperculomandibular sensory pore 11; po2 = postotic sensory pore 2; po3 = postotic sensory pore 3; s1 = supraorbital sensory pore 1; s2 + i2 = supraorbital sensory pore 2 + infraorbital sensory pore 2; s3 = supraorbital sensory pore 3; s8 = supraorbital sensory pore 8.

Figure 4. (A) Dorsal view and (B) Ventral view of cranium of *Pariolius pax*, MPUJ 10047, paratype, 34.0 mm SL. Abbreviations of the anatomical parts: afo = anterior fontanel; apa = autopalatine; boc: basioccipital; epo = epioccipital; exo = exoccipital; exs = extrascapula; fro

= frontal; let = lateral ethmoid; max = maxilla; mes = mesethmoid; nas = nasal; opf: optic foramen; osp: orbitosphenoid; par: parasphenoid; pfo = posterior fontanel; pmx = premaxilla; pro: prootic; pto = pterotic; pts: pterosphenoid; soc = supraoccipital; and sph = sphenotic; tff: trigeminofacial foramen; vom = vomer.

Figure 5. Dorsal view of the complex anterior vertebra of (A) *Pariolius pax*, MPUJ 10047, paratype, 34.0 mm SL and (B) *Pariolius maldonadoi*, MPUJ 13077, paratype, 27.3 mm SL. Abbreviations of the anatomical parts: scl = supracleithrum; tri = *tripus*; trp4 = transverse process 4; trp5: transverse process 5 and vc6: sixth vertebral centrum.

Figure 6. Lateral view of suspensorium (A) *Pariolius pax*, MPUJ 10047, paratype, 34.0 mm SL. (B) *Pariolius maldonadoi*, MPUJ 13076, paratype, 28.4 mm SL. Abbreviations of the anatomical parts: hyo = hyomandibula; ent = entopterygoid; iop = interopercle; met = metapterygoid; ope = opercle; pop = preopercle; qua = quadrate and spo = subpreopercle.

Figure 7. Dorsal view of the branchial arch of (A) *Pariolius pax*, MPUJ 10047, paratype, 36.7 mm SL. (B0 *Pariolius maldonadoi*, MPUJ 13076, paratype, 28.4 mm SL. Abbreviations of the anatomical parts: bb_{2-4} = basibranchial 2 a 4; cb_{1-5} = ceratobranchial 1 to 5; eb_{1-4} = epibranchial 1 to 4; pb_{3-4} = pharyngo- branchial 3 to 4; hb_{1-3} = hypobranchial 1 to 3.

Figure 8. Live specimen of (A) *Pariolius pax* collected in Mapiripán Municipality, vereda San Jorge, Caño Ovejas tributary of the Guaviare River, Orinoco River basin, Meta,

Colombia (not preserved) and (B) *P. maldonadoi* collected in Retorno Municipality, Caño Potosí tributary of the Inírida River, Orinoco River basin, Guaviare, Colombia.

Figure 9. Geographical distribution of *Pariolius pax* (yellow) and *Pariolius maldonadoi* (red) from Colombia. Star represents the type localities. Each symbol may represent more than one specimen.

Figure 10. *Pariolius maldonadoi*, MHNU-I 3257, holotype, 32.6 mm SL, Potosí creek tributary to Inírida River, Guaviare State. (A) Lateral view. (B) Dorsal view. (C) Ventral view. Bar = 1 cm.

Figure 11. Laterosensory pores of *Pariolius maldonadoi*, MPUJ 13077, paratype, 27.3 mm SL. (A) Lateral view. (B) Dorsal view. (C) Ventral view. Abbreviations of the anatomical parts: i1 = infraorbital sensory pore 1; i3-6 = infraorbital sensory pores 3–6; ll1-3 = lateral line sensory pores 1–3; pm1–10 = preoperculomandibular sensory pores 1–10; po1 + pm11 = postotic sensory pore 1 + preoperculomandibular sensory pore 11; po2 = postotic sensory pore 2; po3 = postotic sensory pore 3; s1 = supraorbital sensory pore 1; s2 + i2 = supraorbital sensory pore 2 + infraorbital sensory pore 2; s3 = supraorbital sensory pore 3; s8 = supraorbital sensory pore 8.

Figure 12. (A) Dorsal view and (B) Ventral view of cranium of *Pariolius maldonadoi*, MPUJ 13076, paratype, 28.4 mm SL. Abbreviations of the anatomical parts: afo = anterior fontanel;

apa = autopalatine; boc: basioccipital; epo = epioccipital; exo = exoccipital; exs = extrascapula; fro = frontal; let = lateral ethmoid; max = maxilla; mes = mesethmoid; nas = nasal; opf: optic foramen; osp: orbitosphenoid; par: parasphenoid; pfo = posterior fontanel; pmx = premaxilla; pro: prootic; pto = pterotic; pts: pterosphenoid; soc = supraoccipital; and sph = sphenotic; tff: trigeminofacial foramen; vom = vomer.

Figure 13. Scatter plot of Principal Component Analysis (PCA) between component 2 and component 3 of *Pariolius armillatus* (black), *P. maldonadoi* (red), and *P. pax* spB (blue).

Figures

Figure 1.

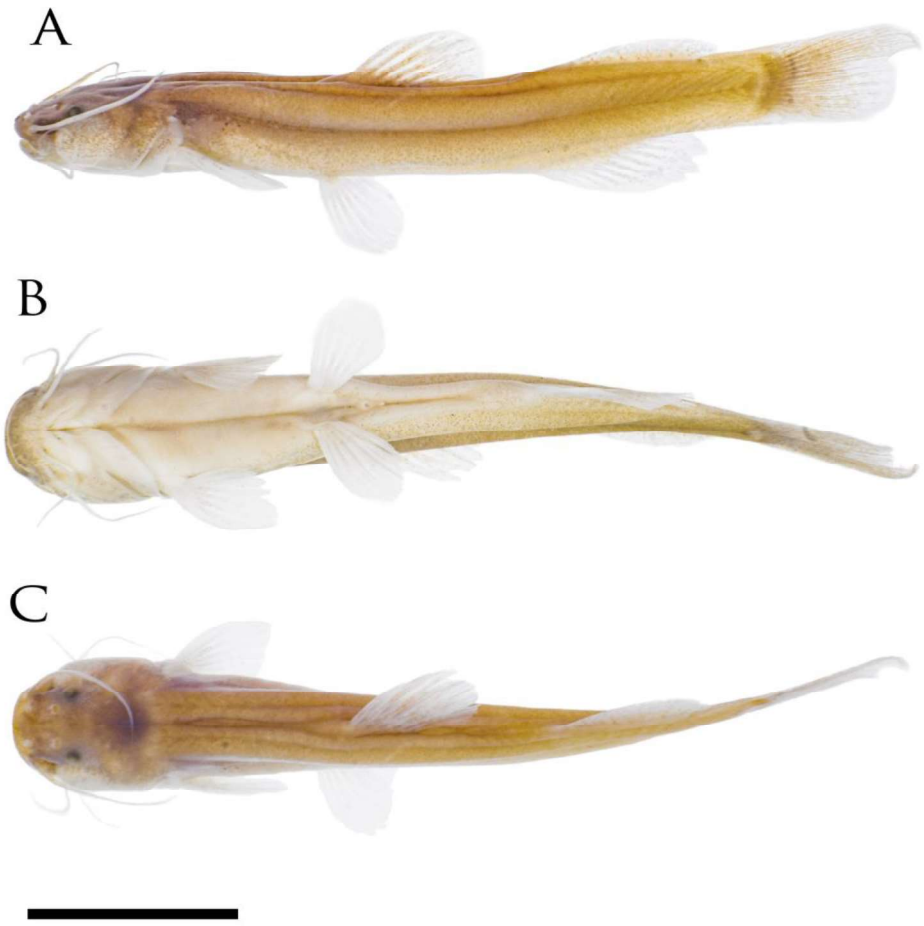

Figure 2.

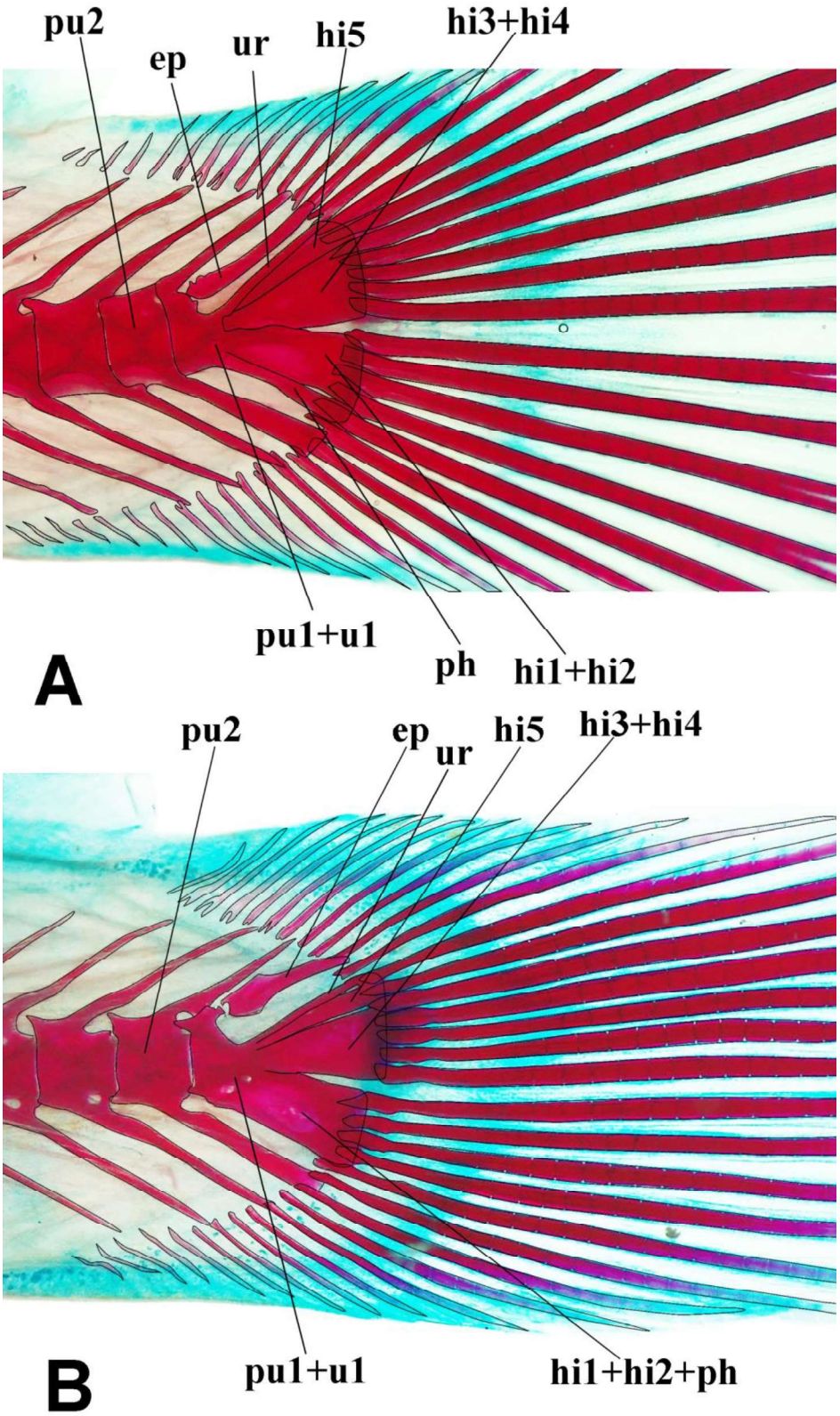
pu2
ep
ur
hi5
hi3+hi4
pu1+u1
ph
hi1+hi2
A
pu2
ep
ur
hi5
hi3+hi4
pu1+u1
hi1+hi2+ph
B

Figure 3.

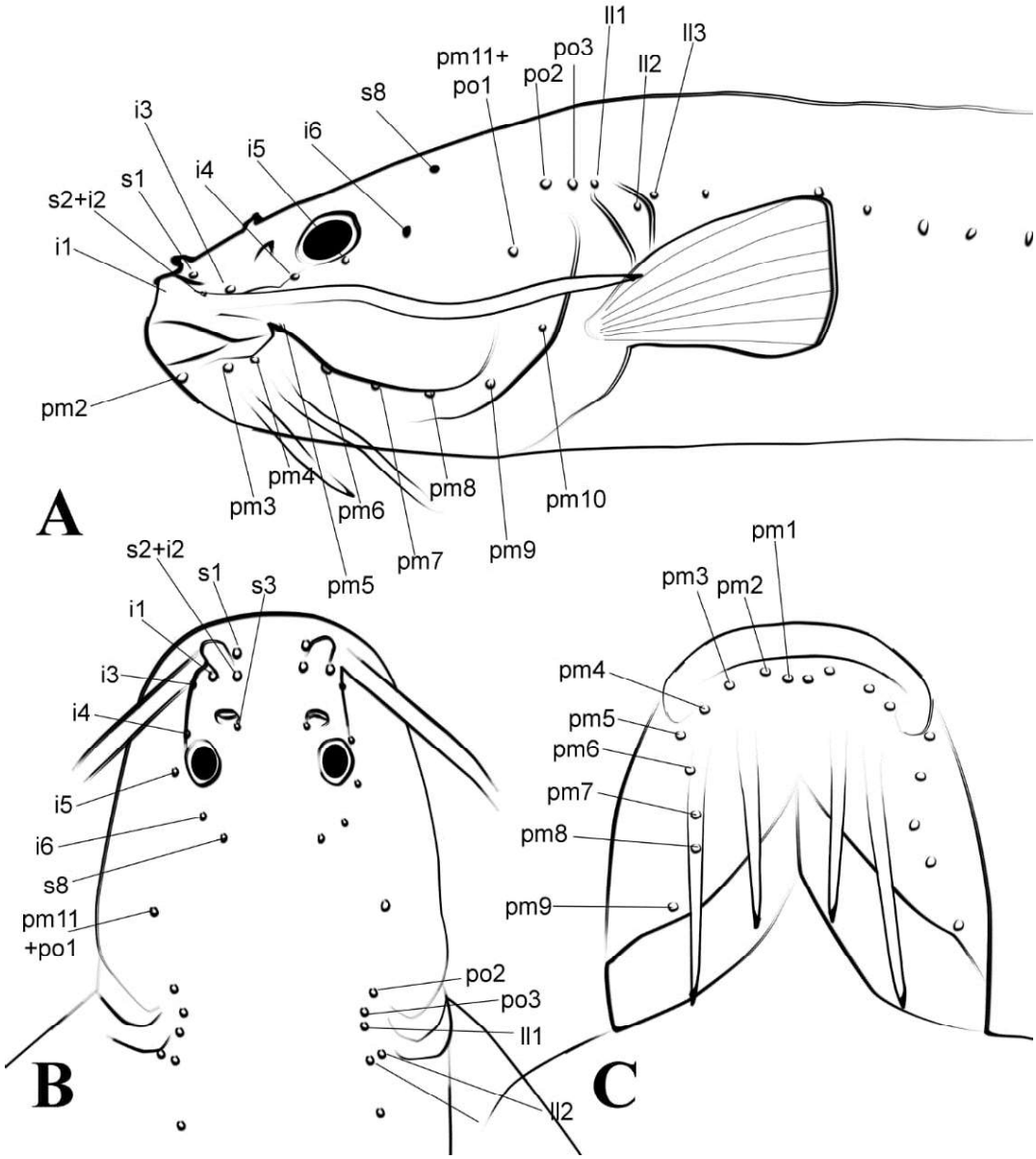
A
s2+i2
s1
i1
i3
i4
i5
i6
s8
pm11+
po1
po2
po3
ll1
ll2
ll3
pm2
pm3
pm4
pm5
pm6
pm7
pm8
pm9
pm10
B
s2+i2
s1
s3
i1
i3
i4
i5
i6
s8
pm11
+po1
po2
po3
ll1
ll2
C
pm1
pm3
pm2
pm4
pm5
pm6
pm7
pm8
pm9

Figure 4.

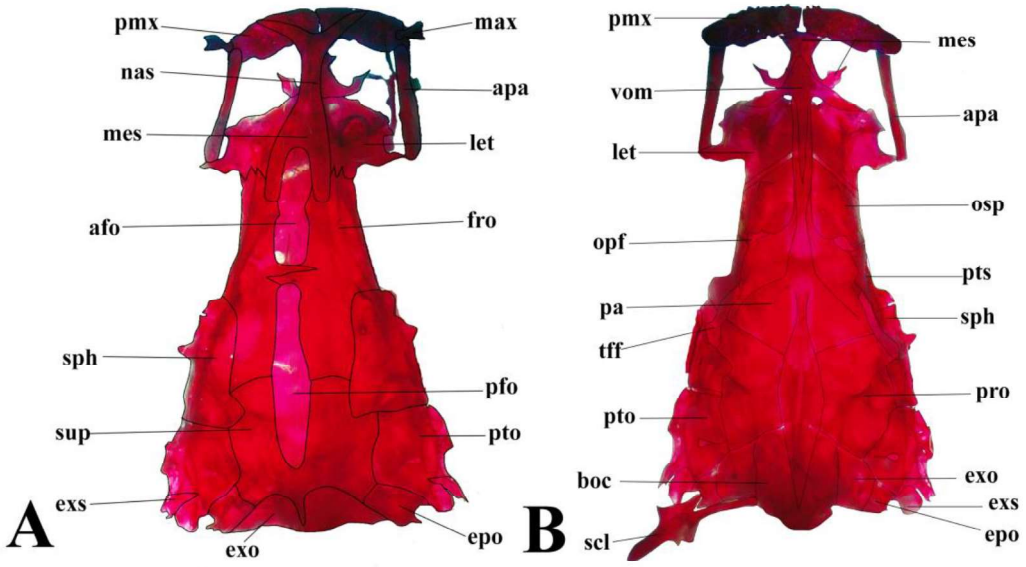
pmx
max
nas
apa
mes
let
afo
fro
sph
pfo
sup
pto
exs
epo
exo
A
pmx
mes
vom
apa
let
osp
opf
pts
pa
sph
tff
pro
pto
boc
exo
exs
epo
scl
B

Figure 5.

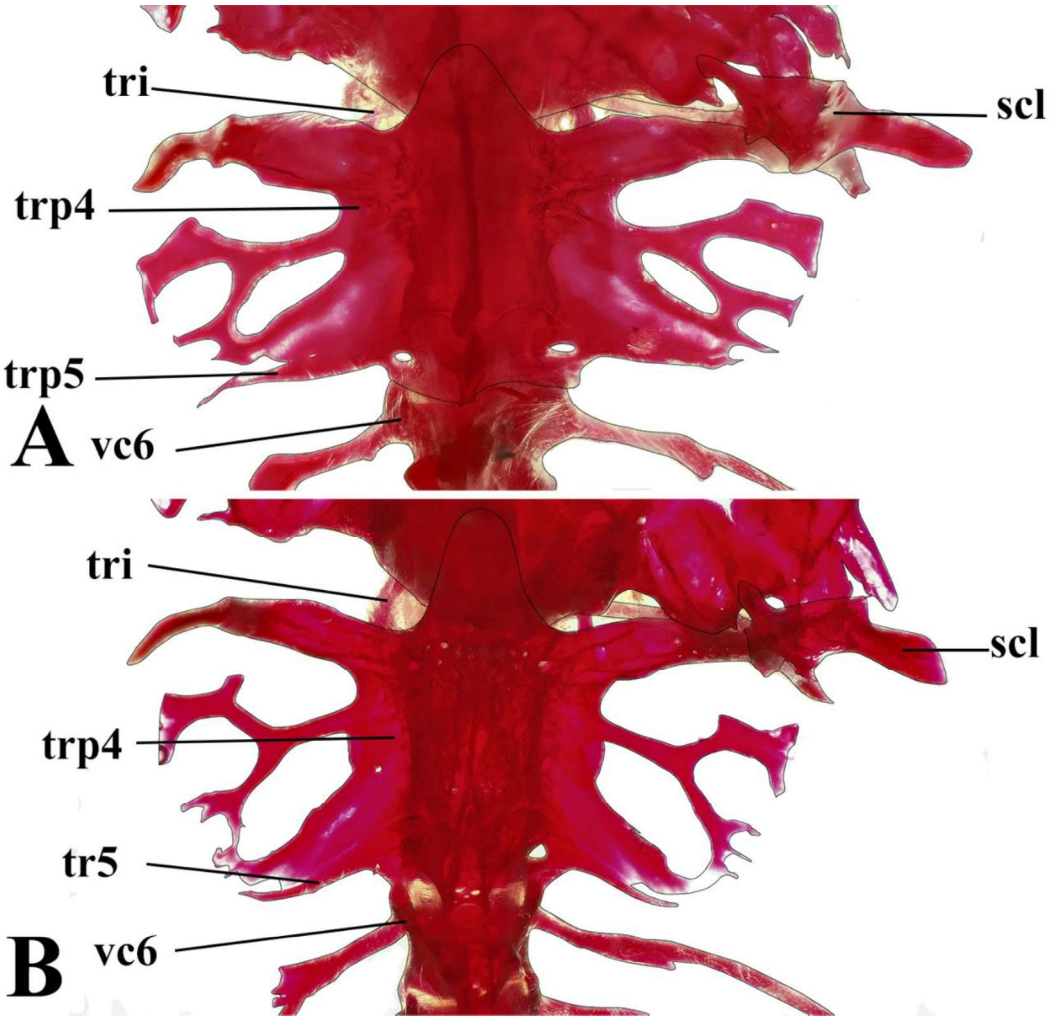

Figure 6.

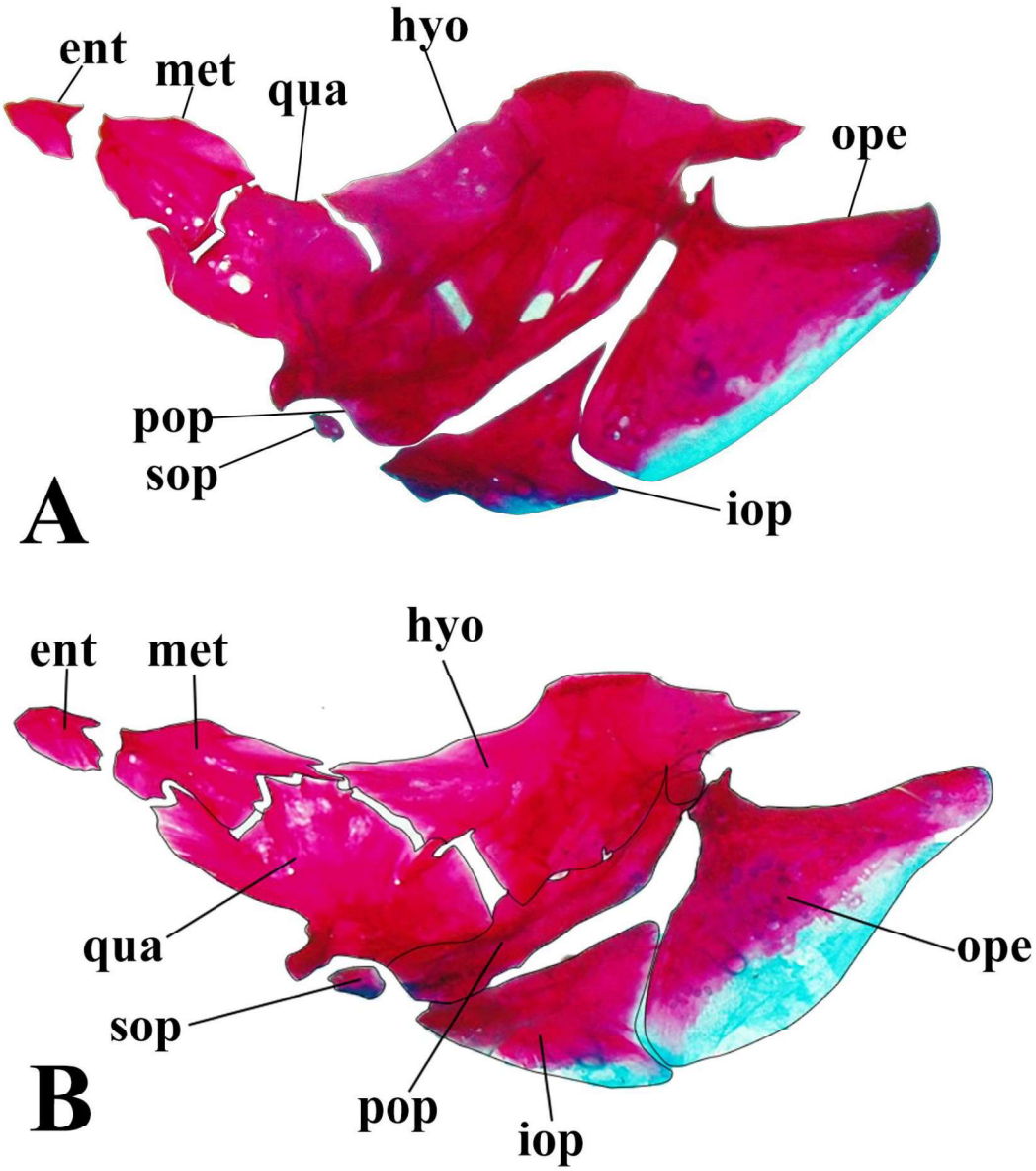
ent
met
qua
hyo
ope
pop
sop
iop
A
ent
met
hyo
qua
ope
sop
pop
iop
B

Figure 7.

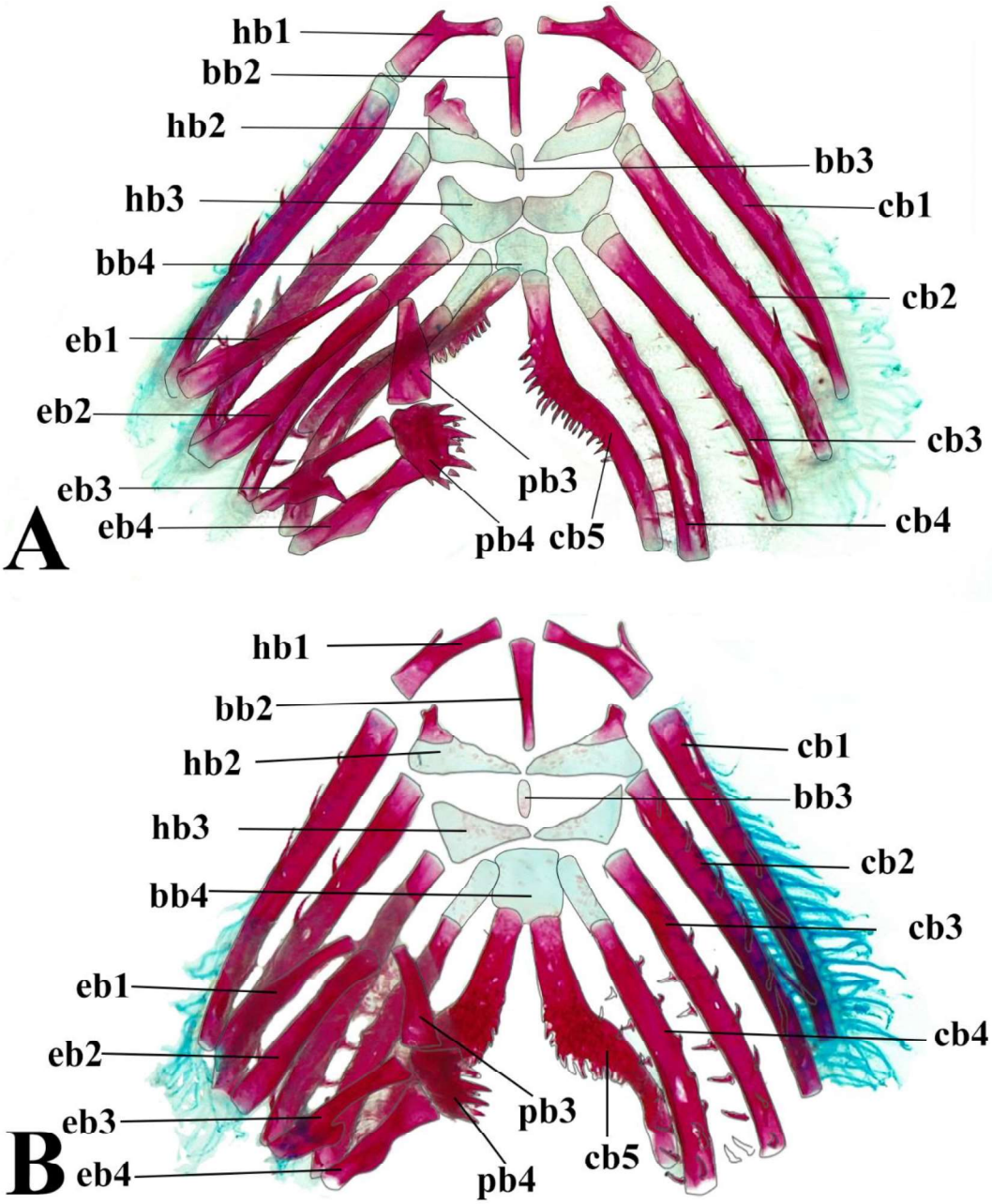
hb1
bb2
hb2
hb3
bb4
eb1
eb2
eb3
eb4
bb3
cb1
cb2
cb3
cb4
pb3
pb4
cb5
A
hb1
bb2
hb2
hb3
bb4
eb1
eb2
eb3
eb4
cb1
bb3
cb2
cb3
cb4
pb3
pb4
cb5
B

Figure 8.

Figure 9.

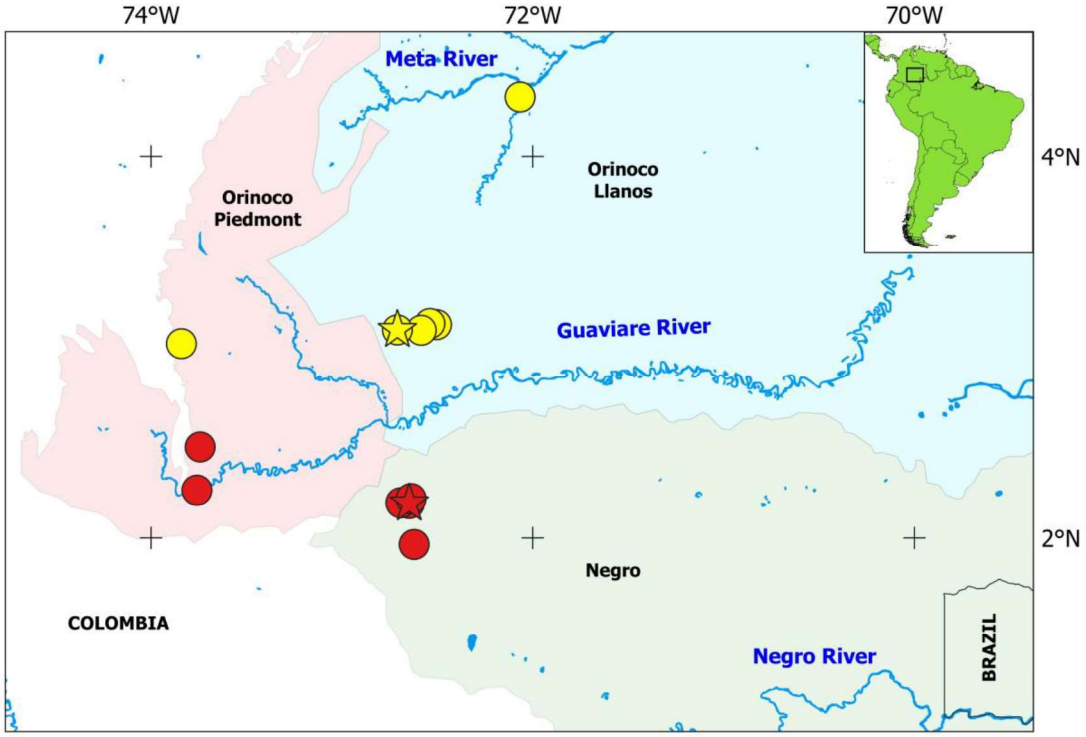
74°W
72°W
70°W
4°N
2°N
Meta River
Orinoco
Llanos
Orinoco
Piedmont
Guaviare River
Negro
COLOMBIA
Negro River
BRAZIL

Figure 9.

Figure 11.

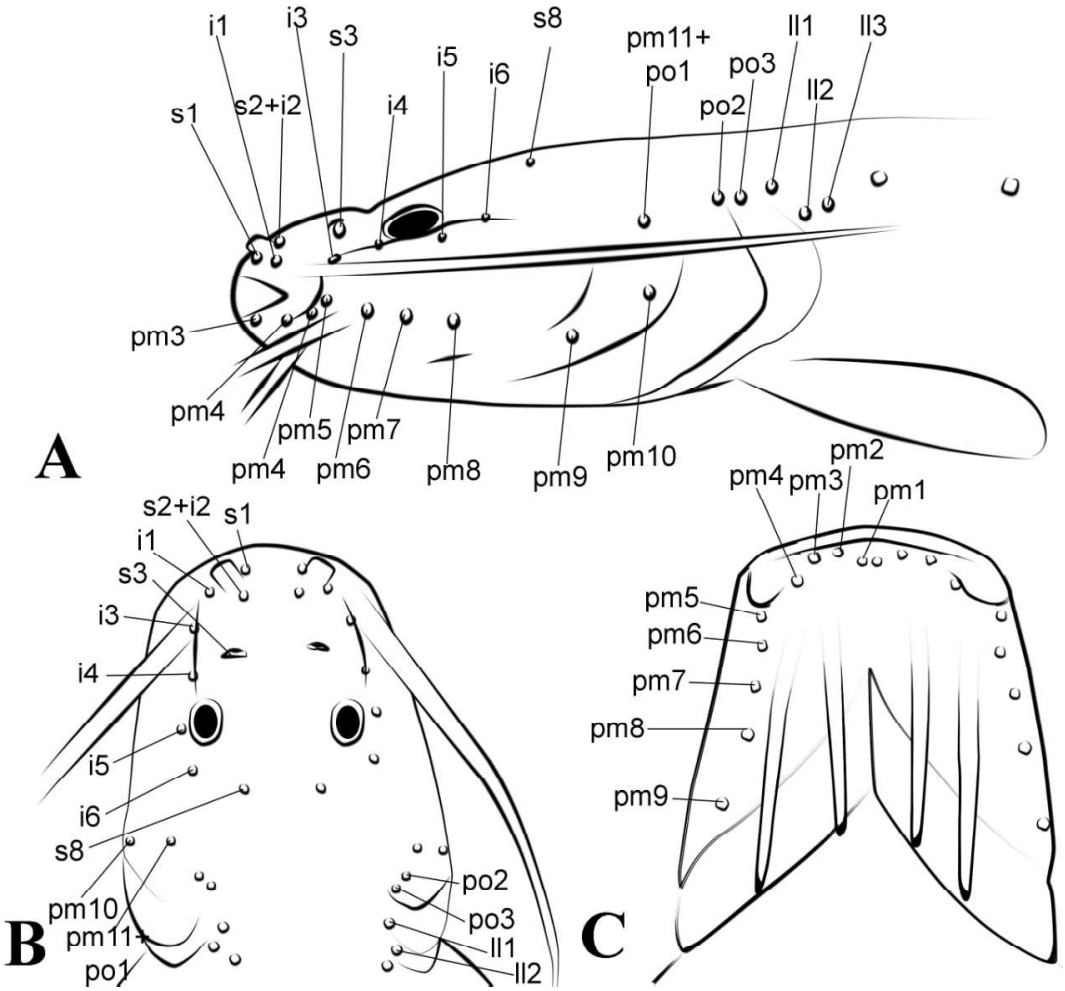
A
i1
i3
s3
s8
pm11+
po1
ll1
ll3
i5
i6
po3
ll2
s1
s2+i2
i4
po2
pm3
pm4
pm5
pm7
pm4
pm6
pm8
pm9
pm10
B
s2+i2
s1
i1
s3
i3
i4
i5
i6
s8
pm10
pm11+
po1
po2
po3
ll1
ll2
C
pm4
pm3
pm2
pm1
pm5
pm6
pm7
pm8
pm9

Figure 12.

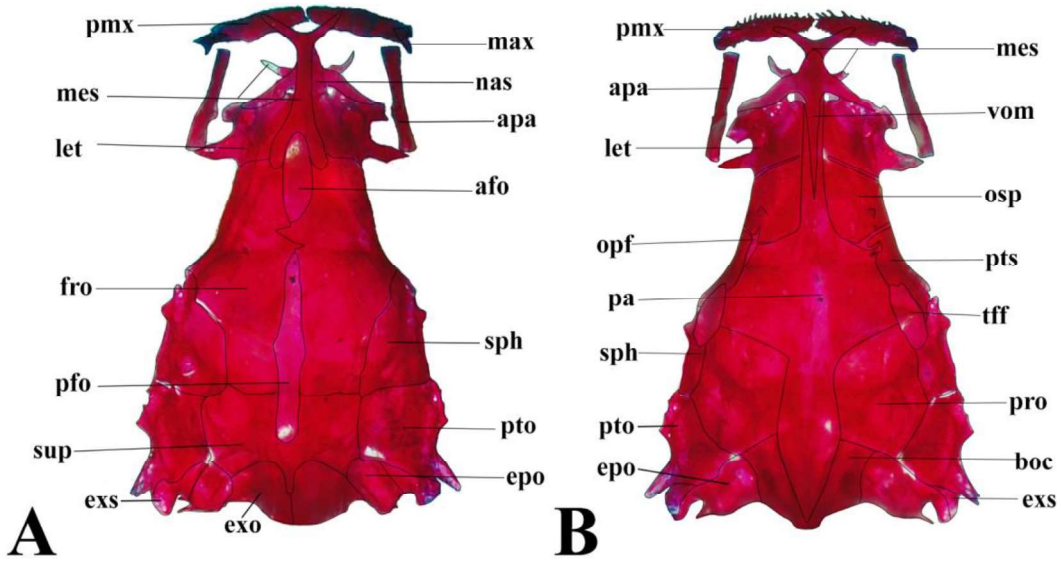
pmx
max
mes
nas
apa
let
afo
fro
sph
pfo
pto
sup
epo
exs
exo
A
pmx
mes
apa
vom
let
osp
opf
pts
pa
tff
sph
pro
pto
boc
epo
exs
B

Figure 13.

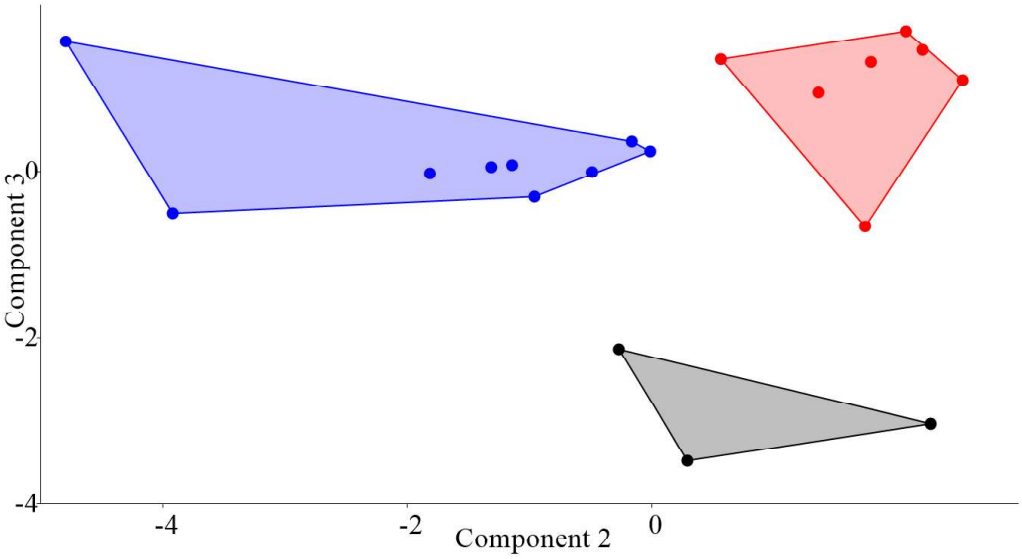

CONCLUSÕES GERAIS

A monofilia de Heptapteridae e confirmada baseado em uma análise filogenética multilocus incluindo 142 espécies (82 espécies nominais mais 60 espécies novas) e 3965 caracteres. A monofilia da subfamília Rhamdiinae contendo as tribos Goeldiellini e Rhamdiini foram fortemente suportadas. A subfamília Heptapterinae foi a mais densamente representada e dentro dela as tribos Brachyglaniini e Heptapterini também foram suportados como monofiléticos. Brachyglaniini agora contém aos gêneros *Brachyglanis* Eigenmann 1912, com cinco espécies mais oito espécies novas; *Gladioglanis* Ferraris and Mago-Leccia 1989, com três espécies; *Leptorhamdia* Eigenmann 1918, com três espécies mais uma espécie nova; e *Myoglanis* Eigenmann 1912, com uma espécie mais uma espécie nova; mais 3 gêneros novos contendo duas espécies mais duas espécies novas.

Enquanto as relações filogenéticas dentro de Heptapterini agora se encontram representada por 5 novas subtribos: Heptapterina a subtribo mais diversa representados por os gêneros *Heptapterus* Bleeker 1858, com quatro espécies; *Rhamdioglanis* Ihering 1907, monotípico; *Acentronichthys* Eigenmann & Eigenmann 1889, com uma espécie mais três espécies novas; *Rhamdiopsis* Haseman 1911, com duas espécies; *Taunayia* Miranda Ribeiro 1918, monotípico; mais 8 novos gêneros. Nemuroglaniina representada por os gêneros *Imparfinis* Eigenmann & Norris 1900, com 14 espécies mais seis espécies novas; *Nemuroglanis* Eigenmann & Eigenmann 1889, com quatro espécies; mais um gênero novo, com duas espécies mais duas espécies novas. Cetopsorhamdiina contendo os gêneros *Cetopsorhamdia* Eigenmann & Fisher 1916, com sete espécies mais uma espécie nova; *Phenacorhamdia* Dahl 1961, com 12 espécies mais seis espécies novas; *Pariolius* Cope 1872, com uma espécie mais duas espécies novas; mais 3 gêneros novos. Chasmocranina contendo

o gênero *Chasmocranus* Eigenmann 1912, com seis espécies. E Mastiglaniina contendo *Mastiglanis* Bockmann 1994, com três espécies mais nove espécies novas; mais um gênero novo, monotípico.

A análise integrativa do gênero tipo da família delimitou *Heptapterus* a quatro espécies, e as outras espécies nominais descritas no gênero foram realocadas nos respetivos gêneros ou colocados como *incertae sedis* in Heptapteridae aguardando a descrição formal dos gêneros novos a onde eles pertenceriam, baseado na nossa análise molecular. Além da limitação do genro tipo um novo gênero irmão foi descrito contendo três espécies, sendo dois de elas espécies novas.

A análise morfológica do material examinado dos Heptapterinae permitiu registrar muitas novas espécies novas, sendo algumas delas publicado neste trabalho e muitas outras sendo descritas assim como aguardando ser divulgados para a comunidade cientifica.